POLITECNICO DI TORINO

MASTER'S DEGREE IN ENERGY AND NUCLEAR ENGINEERING
(LM-30)

MASTER'S DEGREE THESIS

Simulation-Based Optimization Method on Buildings' Early Design Stages

A comparison between Sequential and Integrated Approaches on a Non-Residential Case Study

Supervisors

Prof. ENRICO FABRIZIO

Candidate

ALESSIA CURRERI

Advisors

Arch. ELISA SIROMBO

Eng. TEODORO MAIORANO

ACADEMIC YEAR 2024/2025

A mamma, papà e Nicolò,

per essere stati le mie radici ed il mio supporto.

Abstract

Italian Version

Il settore edilizio nell'UE rappresenta il 10% delle emissioni totali di CO_2, principalmente a causa dell'età e dell'inefficienza degli edifici. Azioni di riqualificazione energetica sono dunque cruciali, soprattutto considerando che il 75% di questi edifici continuerà a essere utilizzato fino al 2050. Per tali ragioni, l'UE ha sviluppato regolamenti come la Direttiva sulla Prestazione Energetica degli Edifici (EPBD), la quale richiede che, entro il 2021, tutti gli edifici di nuova costruzione siano Zero o Nearly Zero Energy Buildings; ciò implica la selezione di design passivi dell'edificio e di soluzioni impiantistiche che minimizzino, per quanto possibile, la domanda dell'edificio stesso. La progettazione edilizia, in Italia, segue un approccio regolamentato in tre fasi principali (*Preliminare*, *Definitiva*, *Esecutiva*), ma questo può portare a una "Ottimizzazione a Silos", che richiede successive integrazioni e miglioramenti del design a cui corrispondono, quando fattibili, costi rilevanti. Una soluzione a tale criticità è stata fornita dall'AIA, ente virtuoso che ha proposto una metodologia di progettazione definita integrata, che richiede di anticipare la maggior parte delle decisioni di design alle fasi iniziali dello stesso. Ciò causa non poche difficoltà, soprattutto a seguito della necessità di effettuare una modellazione energetica degli edifici progettati nelle fasi iniziali di progettazione con un numero molto ridotto di input. Per affrontare questa sfida, il presente lavoro di tesi si propone di valutare le alternative progettuali nelle prime fasi di un processo di progettazione e selezionare quelle che garantiscano prestazioni ottimali degli edifici, in linea con gli obiettivi di decarbonizzazione ed efficienza energetica delineati dall'Unione Europea. Si è deciso dunque di implementare un Simulation Based Optimization Method sfruttando una ottimizzazione multi-obiettivo con l'algoritmo evolutivo NSGA-II per identificare alternative progettuali che ottimizzino un set di funzioni obiettivo opportunamente selezionate. Sulla base del caso di studio fornito da GET Consulting s.r.l. e seguendo l'Appendix G dell' ASHRAE 90.1-2016 si è definito il modello dell'edificio di riferimento, considerato come il benchmark rispetto cui valutare l'ottimalità delle prestazioni dell'edificio progettato su un anno tipico di operazione simulato mediante un approccio di simulazione dinamica tramite il motore di simulazione EnergyPlus. La procedura punta a massimizzare la riduzione percentuale di emissioni di CO_2 del proposed design rispetto al baseline building, garantendo il soddisfaci-

mento dei setpoint di temperatura estiva ed invernale. L'ottimizzazione è stata affrontata con due diversi approcci: il primo, quello sequenziale, è composto da due fasi successive di ottimizzazione prima dell'involucro edilizio e poi degli impianti HVAC e fotovoltaico; il secondo approccio, quello integrato, consiste invece nell'ottimizzare contemporaneamente sia le variabili passive che quelle attive impiantistiche in modo da tenere conto delle loro interdipendenze.

English Version

The building sector in the EU accounts for 10% of total CO_2 emissions, primarily due to the age and inefficiency of buildings. Energy retrofit actions are therefore crucial, especially considering that 75% of these buildings will continue to be used until 2050. For these reasons, the EU has developed regulations such as the Energy Performance of Buildings Directive (EPBD), which requires that by 2021 all new buildings be Zero or Nearly Zero Energy Buildings; this implies the selection of passive building designs and technical solutions that minimize as much as possible the building's demand. Building design in Italy follows a regulated approach in three main phases (*Preliminary*, *Definitive*, *Executive*), but this can lead to a "Silo Optimization," which requires subsequent integrations and design improvements that correspond, when feasible, to significant costs. A solution to this issue has been provided by the AIA, a virtuous entity that proposed an integrated design methodology, which requires anticipating most design decisions to the initial stages. This causes considerable difficulties, especially due to the need to perform energy modeling of the designed buildings in the initial design stages with very limited inputs. To address this challenge, this thesis aims to evaluate design alternatives in the early stages and select those that ensure optimal building performance, in line with the decarbonization and energy efficiency goals outlined by the European Union. Therefore, it was decided to implement a Simulation Based Optimization Method by leveraging a multi-objective optimization using the NSGA-II evolutionary algorithm to identify design alternatives that optimize a set of appropriately selected objective functions. Based on the case study provided by GET Consulting s.r.l. and following Appendix G of ASHRAE 90.1-2016, the reference building model was defined, considered as the benchmark against which to evaluate the optimality of the designed building's performance over a typical year of operation simulated through a dynamic simulation approach using the *EnergyPlus* simulation engine. The procedure aims to maximize the

percentage reduction of CO_2 emissions of the proposed design compared to the baseline building, ensuring compliance with summer and winter temperature setpoints. The optimization was approached with two different methods: the first, Sequential, consists of two successive optimization phases, first of the building envelope and then of the HVAC and photovoltaic systems; the second approach, Integrated, involves optimizing both passive and active technical variables simultaneously to account for their interdependencies.

Contents

List of Tables

x

List of Figures

Nomenclature

P_{fan}	Fraction of full-load fan power for a variable speed fan	W
PRL_{fan}	Fan part-load ratio for a variable speed fan	l/sec
R_p	Outdoor Airflow Rate Required per Person	$l/(sec \cdot pers.)$
P_z	Zone Population	$pers./m^2$
R_a	Area Outdoor Air Rate	$l/(sec \cdot m^2)$
A_z	Zone floor area	m^2
E_z	Zone Air Distribution Effectiveness	-
HU_{hour}	Unmet Heating hour	-
CU_{hour}	Unmet Cooling hour	-
Z_j	Inside conduction transfer function coefficient	-
$T_i(\tau - j\delta)$	Internal surface of the ith wall temperature at the $\tau - j\delta$ timestep	°C
Y_i	Cross conduction transfer function coefficient	$W/(m^2 \cdot K)$
$T_{o,i}(\tau - j\delta)$	External surface of the ith wall temperature at the $\tau - j\delta$ timestep	°C
$W_{i,j}$	Inside flux conduction transfer function coefficient	-
$q_i(\tau - j\delta)$	Specific thermal flux on the internal surface of the ith wall	-
C_i	Total Investment Cost for the energy efficiency measure	€
$C_{a,t}(j)$	Annual Cost of the jth element of the energy efficiency measure at the year t	€/year
$V_{f,n}(i)$	Residual economic value of the jth element of the energy efficiency measure at the last year n	€/year

Chapter 1

Introduction

Throughout the entire evolutionary history of planet Earth, long geological eras characterized by extreme and opposing temperatures have occurred as a result of natural phenomena that have manifested over time; these have profoundly marked the environment, influencing the evolution of life on Earth. During the period when humans appeared on the scene, these natural phenomena continued to occur, albeit in less extreme forms than in the past; however, human presence introduced a new dynamic: humans developed a considerable capacity for adaptation and actively influenced the surrounding environment; this anthropogenic influence has also been reflected in global temperatures, which have continued to rise in recent times due to the effects of human activities on the planet. In 1899, T.C. Chamberlin, an American geologist, published *A Working Hypothesis of the Cause of Glacial Periods on an Atmospheric Basis* at the University of Chicago: this work marked the birth of climatological science as it demonstrated that climate change is closely linked to the concentration of carbon dioxide in our planet's atmosphere; confirmation of this is also provided by G.S. Callendar who, in 1938, confirmed Chamberlin's theories by demonstrating that, as a result of the increased presence of CO_2 in the atmosphere due to the ever-increasing use of fossil fuels to power human industrial activities, global temperatures were already increasing. However, all calculations and research concerning the relationship between human activities and climate change have always been refuted and forgotten[1], until the manifestations of such correlations became so significant as to be inevitably evident. Concerns about global climate, in fact, are nowadays one of the most important issues in society and have aroused the concern of both the population and the most important

national and international institutions. Following the Earth Summit in Rio in 1992, the Intergovernmental Panel on Climate Change (IPCC) was founded: it is a panel of scientists dealing with various aspects of climate change and publishing global reports every seven years; in their 2014 publication [2], they imposed a maximum budget for the increase in temperature of our planet equal to 2°C, corresponding to a concentration in the atmosphere of 530-580 *ppm* of CO_2; reaching this value, in fact, would lead to a point of no return on the consequences for the planet. Therefore, numerous efforts have been made at the political level to try to contain greenhouse gas emissions into the atmosphere through various directives from major institutions, including the European Union. Of fundamental relevance in this process was the Conference of Parties (COP) in 2015 in Paris, during which the Nationally Determined Contributions (NDC) were presented: the list of countries that did so is long, but among the main protagonists are the United States, China, and the countries belonging to the European Union. The latter, in particular, has issued various directives and regulations with the aim of reducing the impact that various sectors, such as transportation, industry, and buildings, have on the environment.

1.1 European Scenario

The European Union's Total Energy Supply (TES), defined as the total energy produced or imported within the EU minus the portion exported or stored, amounted to 81141883 TJ in 2021 [3], representing 13% of the global TES. Considering the share of energy generated from the combustion of fossil fuels, the aforementioned TES corresponds to 7479.8 Mt of CO_2 emissions[1] [4]. The reason behind this substantial volume of emissions associated with European energy demand lies in the Union's energy mix, which is depicted for the year 2021 in Fig.1.1.

---

[1]This value excludes emissions associated with methane leaks from oil and gas operations as they are more complex to quantify.
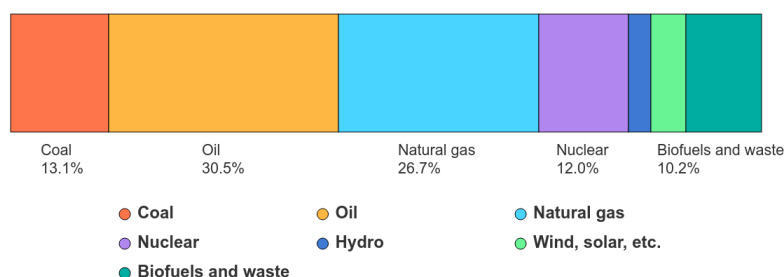
Figure 1.1: Total Energy Supply by sources in Europe, 2021[3].

As evident, the most utilized energy resource is oil, closely followed by natural gas and coal, the latter still holding a significant share despite its well-known environmental impact, akin to that of oil. Conversely, the utilization of renewable sources such as solar or wind energy remains relatively low, trailing behind biofuels and waste. Nevertheless, the share depicted in Fig.1.1 has not remained static over time but has evolved, as illustrated in Fig.1.2:
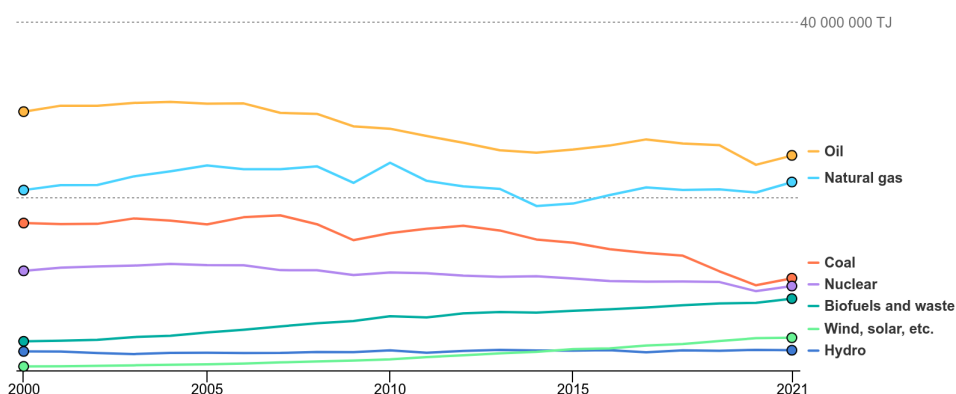
Figure 1.2: Evolution of total energy supply by source in Europe since 2000[3].

In recent years, there has been a noticeable shift in the trend concerning the share of energy produced from fossil sources: there has been a significant reduction in coal and a slight decrease in oil, while the share of energy from natural gas has increased as it has been considered a transitional source due to its lower environmental impact compared to coal and oil. It is worth noting that, in 2020, there is a local minimum point linked to the effect of the COVID-19 pandemic, which resulted in a total halt of activities in Europe and, consequently, a drastic reduction in energy consumption. Concurrent with these changes in trends for fossil sources, there is an increase in the use of renewable sources: the energy produced from renewables has increased of around the 54%

in 2021 with respect to the 2000 level[3]. The reason for these changes in the energy source consumption share is the increasing concern by the European Union about climate change issues, leading to the formulation of energy policies. These policies address four interconnected aspects: environmental security, environmental protection, transition to renewables, and energy access; all four are intertwined, and achieving them allows for a sustainable future. The European Union can be considered one of the leading global institutions committed to mitigating climate change due to numerous policies and initiatives aimed at raising awareness among citizens, reducing greenhouse gas emissions, promoting sustainability not only environmentally but also economically and socially, and implementing climate change adaptation and mitigation policies.

One of the initial actions taken was the European Union's Climate and Energy Package (20-20-20 Package), proposed in 2007 and adopted in 2009[5], which set three targets to be achieved by 2020: a 20% reduction in greenhouse gas emissions compared to 1990, a 20% increase in the share of energy consumed in the European Union from renewable sources, and a 20% improvement in European energy efficiency. Additionally, there is a sectorial sub-target that mandates the use of biofuels for at least 10% of consumption in the transport sector. The package also includes other legislative acts, including the Renewable Energy Directive (RED), first edition in 2009[6]. The RED pursues various objectives, including reducing greenhouse gas emissions to meet the targets set in the 1997 Kyoto Protocol, promoting energy security and technological innovation, and creating job opportunities and regional development. This directive incorporates the three goals of the 20-20-20 package and was replaced in 2018 by the RED II Directive 2018/2001[7], which set a binding target to use 32% renewable energy by 2030 and required each member state to develop a National Integrated Energy and Climate Plan for the period 2021-2030.

Another key action aimed at achieving climate neutrality is the European Green Deal[8], which lays the groundwork for a sustainable future for Europe by ensuring that all citizens and nations are on the same page. This will be achieved through an inclusive approach and ambitious targets leading to climate neutrality by 2050, including net-zero greenhouse gas emissions by 2050 and decoupling European economic growth from resource use. Among the initiatives within this pact, the Fit-for-55[9] is of fundamental importance; it is the latest sustainability package in discussion by the European Union and aims to reduce the EU's net greenhouse gas emissions by at least 55% by 2030, based on 1990

levels. This will be reached through the combined action on different sectors and introducing, as an improvement in the Carbon Pricing policy of the European Union, the Carbon Border Adjustment Mechanism (CBAM), which fits perfectly within the Union's carbon pricing system. The latter is a direct consequence of the European taxonomy on greenhouse gas emissions, developed to ensure that investment directions are towards economic activities that facilitate and expedite the transition, thus being sustainable and enabling the achievement of the European Green Deal goals. It provides a common definition of sustainable economic activities for financial and non-financial activities to provide investors with certainty, protecting them from greenwashing activities and ensuring that companies are climate-responsible. The regulation of the taxonomy came into force in July 2020[10] and is supported by the Carbon Pricing system, defined by the United Nations Climate Change as a system aimed at mitigating greenhouse gas emissions through *imposing a tax on emissions* or *providing an incentive to emit less*[11]. There are several carbon pricing mechanisms that can be classified into two main categories: *carbon tax* and *carbon trade*. The former corresponds to a flat tax based on the amount of emitted CO_2, which corresponds to defining a price for it. The latter, instead, corresponds to defining a market mechanism that allows for the taxation of emissions, called *Cap & Trade*: certificates corresponding to permits to emit a given quantity of climate-altering gas emissions are defined, the total sum of which cannot exceed a certain cap. These certificates must be purchased by various companies, which must ensure that they emit less climate-altering gas than the corresponding permit purchased; to achieve this, they can reduce emissions associated with their production activities or purchase certificate quotas that have not yet been acquired on the market. The system implemented in the European Union is based on this logic and is called the *Emission Trading System* (ETS)[12], which is the world's first major carbon market and remains the largest. Starting from 2005, the ETS applies to all EU member states and focuses on emissions that are measurable with a high degree of precision and refer to CO_2, N_2O, and $PFCs$ produced by sectors defined as carbon-intensive, including electricity and heat production, high-energy-intensive industrial sectors, aviation, maritime, aluminum production, and chemicals such as nitric acid, adipic acid, glyoxal, and glyoxylic acid. In this way, it allowed to reduce of the 37% the industrial and electrical plant related emissions.

The main difficulty encountered in implementing this policy is relocation: companies may relocate their production abroad to avoid purchasing credits, the prices of which continue to rise; however, the goods produced by them continue to be consumed within the Union. As a result, although emissions are associated with goods used in areas where the ETS system is valid, they are accounted for in countries where emissions taxation is more lenient, avoiding the overall benefit on the whole global environment. To reduce this phenomenon as much as possible, the EU has developed the CBAM[13]: it is a tool used by the EU to assign a fair price to emissions associated with the production of high-carbon-intensive goods entering the Union, thereby imposing taxation on them and encouraging more sustainable production, even in non-EU countries. As of 2023, the ETS has been revised and updated to the ETS2 version in order to define a new emissions trading system; the latter allows for covering CO_2 emissions resulting from fuel combustion in buildings, road transport, and all sectors of small industry not previously covered by the ETS system [12]. This system will be operational by 2027 and will not be applied to final consumers, such as households or car owners, but to fuel suppliers, who will have to purchase credit quotas defined based on a cap that will ensure a 42% reduction in emissions by 2030 compared to 2005 levels.

Chapter 2

State of the Art: the Building Sector

The application of a carbon pricing mechanism such as *Cap & Trade* to the building sector helps to understand the Union's concern about it; the reasons for this can be understood by observing Fig.2.1, which allows evaluating how much different sectors impact the Union's CO_2 equivalent emissions.
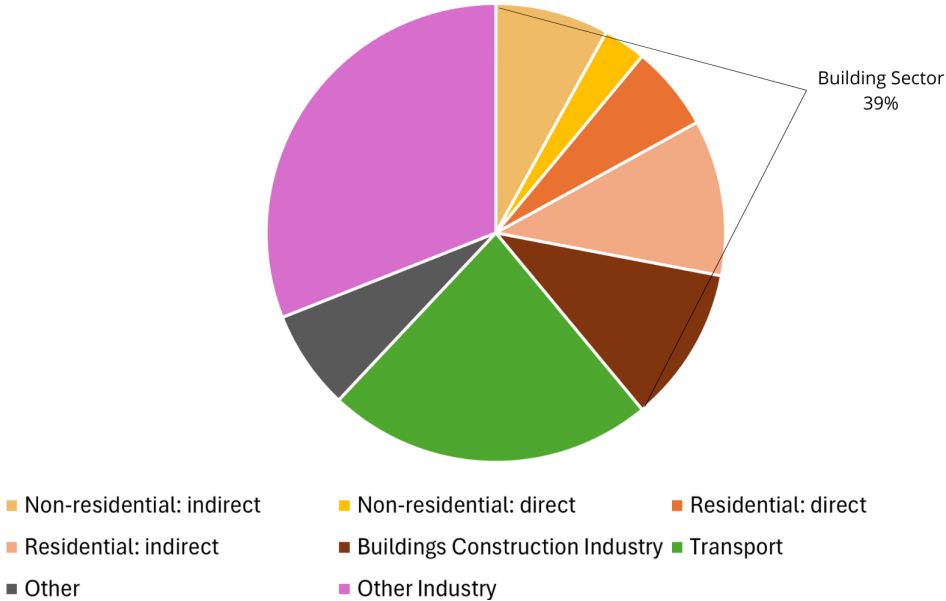
Figure 2.1: Global share of buildings and construction final energy and emissions, 2018[14].

As highlighted in Fig.2.1, the total emissions associated with the building sector account for approximately 39%, encompassing both the residential and

non-residential sectors, as well as the construction industry. An important distinction concerns the division between direct and indirect emissions: the former pertains to internal building consumption, such as heating, cooling, lighting, and hot water, while the latter relates to the building's operations but occurs externally. These indirect emissions are linked to the production of the energy used to meet the energy demands of the occupants. It is noteworthy that the proportion of the latter is always greater than that of the former, underscoring the significance of external energy sources in the overall emission balance of buildings. The main reasons for the big impact that this sector has on the whole emissions of the EU can be found in the characteristics of the European building stock: the volume of new building projects represents only 10% per year of the total constructions in Europe, implying that the majority of buildings are of old age[15]; in particular, according to the European Commission, 75% of the total European building stock is inefficient, and 85% - 95% of the currently existing buildings will still be present in 2050[16]. Considering the historical relevance of a significant part of the European building stock, but also the impact associated with the demolition of old buildings and the reconstruction of new, albeit more efficient structures, the only way to reduce the environmental impact that this sector has is to act on energy efficiency actions, which allow reducing emissions associated with the operation of the buildings themselves. The latter, in fact, accounts for 30% of the global final energy consumption and 26% of the global-energy related emissions. Currently, the global population is growing, so there will be an increase in purchases and installations of equipment associated with building occupancy: since the lifespan of such components is long, the design and purchasing decisions made today, through energy retrofitting of existing buildings and energy efficient design of new buildings, are crucial and will have an impact on both present and future energy consumption[17].

There are numerous new technologies that allow for significant savings in the energy consumption associated with building use; however, their widespread adoption depends heavily on the presence of regulations that mandate their installation and make their selection economically viable compared to the more competitive alternatives that have been on the market for years. For these reasons, among the proposals of the Fit-for-55, there is a section dedicated to the energy performance of buildings, within which the revision of directives on building energy performance is considered to increase their quality by 2030. This revision must be guided by two objectives: the first concerns

new buildings, which should all be zero-emission by 2030; the second concerns existing buildings, which should all be zero-emission by 2050 [9]. This is ensured through the adoption, in all member countries, of European Union directives on building energy performance: as anticipated in Section 1.1, the EU is strongly committed to defining policies for mitigating and adapting to climate change and, over time, has established increasingly specific regulations in the building sector. For example, as of 2011, reference is made to the CPD - Construction Product Regulation (EU) 395/2011 of 9 March 2011, which outlines seven classes of fundamental requirements that must be met by each material and component of a building, including Hygiene, Health and Environment, Energy Economy and Heat Retention, and Suitable Use of Natural Resources. However, the latest European directive regulating sustainability in the building sector is the Energy Performance of Buildings Directive (EPBD) 2002/91 and its subsequent amendments up to the latest (2018/844) [18]. This directive provides a common definition of building energy performance, according to which energy performance is *the amount of energy, normalized to the floor area of the building, calculated or measured and required by the building to meet the various types of energy demand of all energy services associated with the typical use of the building.* The assessment of this parameter is carried out using a detailed procedure described in the directive itself, which also requires EU countries to establish minimum energy performance requirements for new buildings or existing buildings undergoing major renovation or replacement or upgrade of building elements, such as heating and cooling systems, roofs, and walls. Furthermore, it mandates that, from 2021, all new buildings must be Zero Energy Buildings (ZEB) or Nearly Zero Energy Buildings (nZEB), meaning buildings with very high energy performance, with the very low amount of energy still required being fully covered by renewable energy and with no on-site carbon emissions from fossil fuels [19].

2.1 Italian Legislation on Building Energy Performance

It is mandatory for all Member States of the European Union to incorporate into their national legislation the provisions and requirements established by the directives and regulations of the European Union. For this reason,

Italy has legislation concerning the use of energy and the sustainability of buildings; worth mentioning is Legislative Decree 192/2005 [20] regarding energy performance certificates, which defines their scope of application, validity period, and required contents. The methodology for drafting energy performance certificates is described in Ministerial Decree of 26/06/2015 [21]; in it, of fundamental importance for the construction phases of new buildings or major renovations of existing buildings is its Appendix A of Annex 1, which contains the definition of the "reference building": it represents an identical building in terms of geometry, orientation, geographical location, use, and boundary conditions to the building whose energy performance needs to be assessed, but with thermal characteristics and energy parameters described in the same Appendix. To ensure that a newly constructed building or one undergoing major renovation performs better than the reference building and complies with the law, the building envelope and the systems characteristics must meet the requirements defined in Appendix A of Annex 1 of the Ministerial Decree, which are a function of the climate zone in which the building is located.

The Legislative Decree No. 192/2005 was subsequently supplemented and amended in certain parts by Legislative Decree No. 311/2006[22], which introduced additional provisions concerning the energy efficiency of buildings. Among these provisions were the obligation to carry out an energy audit for public buildings and the introduction of technical regulations to enhance the energy efficiency of existing and new buildings.

In Italy, the promotion of building energy efficiency also occurs through a series of fiscal incentive programs, among which the *Superbonus 110%* is noteworthy. Regulated by Art. 119 of Decree Law No. 34/2020 (*Decreto Rilancio*), it entails a tax deduction of 110% of expenses incurred from 1st July 2020 for all energy efficiency improvement interventions, installation of photovoltaic systems, electric vehicle charging infrastructure, as well as structural consolidation or reduction of systemic risk of buildings. It is supplemented by:

- *Ecobonus*, which provides fiscal benefits for energy retrofitting interventions in buildings;
- *Sismabonus*, concerning the recovery of the building heritage.

The eligibility for this bonus is valid until 31st December 2025, with varying percentages over time, namely:

- 110% for expenses incurred until 31st December 2023;
- 70% for expenses incurred in 2024;

- 65% for expenses incurred in 2025 for condominiums and individuals, excluding those engaged in business, art, and profession activities, for interventions on buildings consisting of two to four distinctively catasto units, even if owned by a single owner or co-owned by multiple individuals [23].

2.2 Zero and Nearly Zero Energy Buildings

It can be affirmed that the goals of Zero and Nearly Zero Energy Buildings are operational and their achievement strongly depends on the building's energy demand, which must be minimized as much as possible. This occurs only if, during the design phases, the goal of maximizing performance is considered in order to carry out a design that allows, during the building's annual operation taking into account all seasonal variations it undergoes, to have the minimum energy demand that has to be met by renewable sources. To reach this objective, the first step is definitely to implement an efficient passive architecture: there are no rules valid for all buildings, but in general passive strategies are strongly influenced by various specific project parameters, such as climate, microclimate, site, and building use. Depending on these, the building must be designed so that thermal and visual comfort are always guaranteed without the use of external energy resources to power traditional active systems [24]. Among such strategies, natural ventilation can certainly be mentioned, which allows cooling of rooms using outdoor climatic conditions, when favorable, and the presence of a pressure difference between two areas of the building in order to ensure the movement of air masses inside; another possibility is to exploit the solar radiation typical of the site where the building is located to maximize its use for internal room lighting. For both strategies, it will be necessary to properly orient the building and define its geometry, so that the use of natural resources is maximized. However, since the nature of such solutions is highly dynamic, the use of internal systems that allow for appropriate use of the building by occupants is inevitable [24]. Among the most relevant consumption associated with building operation and, therefore, responsible for their emissions, heating and cooling certainly stand out. Regarding the former, despite the presence of a wide variety of alternatives for hot water production and room heating,

the market is currently dominated by systems based on the use of fossil fuels, predominantly natural gas, such as boilers and furnaces. A better alternative, both in terms of reducing consumption and the reduce the impact of the type of energy source used for its operation, are heat pumps, which are currently at the center of the global energy transition for sustainable heating. As for cooling indoor environments, following the progressive increase in global temperatures that has occurred in recent years, since 1990 the energy consumption associated with this end use has more than tripled, and it is expected that this trend will continue in the coming years: with the planet's warming, it is necessary to ensure better construction of buildings, in order to reduce the need for cooling as much as possible, but also a modification of the operation and properties of these systems: not only must cooling setpoint temperatures around 24-26°C be imposed, but the installation of systems with significant efficiency must also be provided for, such as, once again, heat pumps [17].

A significant support in achieving the goals of zero energy consumption within the building is provided by energy modeling, which indeed enables informed decision-making throughout all phases of the building project by simulating the impact each of them has on its annual performance. With conventional buildings and installations, simulations are often unnecessary because standard methods and data provide sufficient information for design. In the case of complex installations or involvement of building physics phenomena, simulations are indispensable; furthermore, the drive towards designing ZEBs or NZEBs necessitates the early creation of energy models; despite the fact that it would be necessary to leverage such tools from the early design stages, during which, for example, decisions ensuring optimal implementation of passive strategies or suitable selection of installations need to be made, most energy simulations occur too late in the design process. Traditionally, energy simulations serve for the sizing of installations or to assess whether the building complies with previously described regulations only after the architectural design has been completed [25]. A departure from this approach is advocated by replacing the traditional design process with one that can be described as the Integrative Process Delivery, which will be introduced later, in Section 2.3.

2.3 Different Building Design Stages

The methodology for designing and delivering the built environment today is based on a series of steps, which are presented schematically in Fig. 2.2.
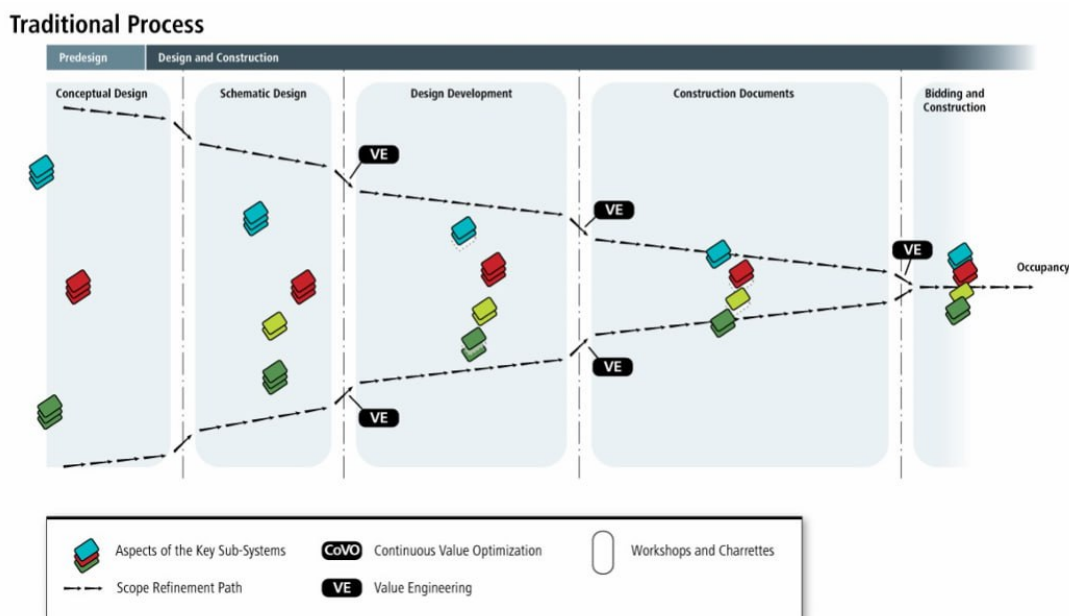
Figure 2.2: Traditional building design stages.[26]

Once the client has discussed with the designer regarding the type of building they want to create, outlining its spaces and functions, the *Pre-design* phase begins. During this phase, the architect proceeds with creating sketches, which are iteratively presented to the owner until they are satisfied. Once this is done, the *Schematic Design*, as defined in Fig.2.2, is ready and delivered to the team of engineers who will handle the design of load-bearing structures, envelope features, HVAC systems, electrical systems, and so on during the *Design Development* phase. At this point, the set of construction documents (the *Construction Documents* phase) is prepared, and construction proceeds, culminating in the delivery and occupancy of the building.

In relation to the Italian context, the previously described design procedure is organized schematically and step-by-step. It begins with the drafting of the Preliminary Design Document (Documento Preliminare alla Progettazione) by the RUP (Responsabile Unico del Procedimento). This document follows the feasibility study and constitutes a refinement of it, as it outlines the general objectives to be pursued in the execution of the work, along with the

technical standards, constraints to be adhered to, and spending limits not to be exceeded[27]. It contains the guidelines within which the subsequent design procedure must operate. For the latter, Art. 93 of Legislative Decree N. 163 of April 12, 2006[28] describes three successive levels of technical detail that must be followed to ensure not only compliance with environmental and urban planning regulations, at both the national and community levels, but also the quality of the work and its adherence to the intended purposes. These three phases can be described as follows:

1. *Preliminary Design*: it defines the requirements to be met and the specific performances that the object of the study must guarantee; this is done through an illustrative report of the selected solution, taking into account the various possible alternatives. Additionally, it provides graphical diagrams for the location and description of the spatial characteristics of the work, along with a preliminary cost estimate for its realization.

2. *Definitive Design*: in this phase, the works to be carried out are identified, based on the requirements highlighted during the preliminary phase; taking into account the elements necessary for obtaining the necessary authorizations and approvals for the realization of the work, a descriptive report is prepared outlining the criteria followed to make the design choices, accompanied by general drawings of the main features of the works and their architectural solutions; furthermore, where required, an environmental impact study is also carried out. The execution of this phase is only possible based on geognostic, hydrological, seismic, and biological studies and investigations, which allow for the preliminary calculations of the structures and systems and the development of the estimate metric computation[1].

3. *Executive Design*: it allows for the specification of the works to be carried out and their corresponding estimated cost; its level of detail must be such that each element can be identified in terms of form, type, quality, size, and price. It consists of reports, executive calculations of structures and systems, and scale graphic elaborations. Additionally, it must be accompanied by a maintenance plan for the whole wotk and its parts.

---

[1]The It is the document prepared to estimate the cost of carrying out the construction works of a building. It is a mandatory elaboration of the final and executive project in the field of public works (Procurement Code, Legislative Decree 18 April 2016, n. 50) but it is also widely used in private works as a contractual tool for regulating the relationship between the client and the executing company[29].

In each of the design phases just described, the drafting of specific documents is mandatory, which are briefly summarized in Tab.2.1:

Table 2.1: Required documentation for each of the three design stages according to DPR 554/99.

PRELIMINARY DESIGN	DEFINITIVE DESIGN	EXECUTIVE DESIGN
Relazione Illustrativa del Progetto	Relazione Descrittiva del Progetto	Elaborati Grafici
Relazione Tecnica	Relazione Geologica e Geotecnica	Calcoli Esecutivi delle Strutture e Impianti
Studio di Prefattibilità Ambientale	Studio di Impatto Ambientale e Studio di Fattibilità Ambientale	Piano di Manutenzione
Schemi Grafici	Elaborati Grafici	Cronogramma delle Lavorazioni
	Calcoli Preliminari delle Strutture e degli Impianti	Computo Metrico Estimativo e Quadro Economico
	Disciplinare Descrittivo e Prestazionale degli Elementi Tecnici del Progetto	Capitolato Speciale d'Appalto
(DPR 554/99, art. 19-22)	(DPR 554/99, art. 26-32)	(DPR 554/99, art. 38-44)

As can be seen from Tab.2.1, the central phase of the design process is richer in documentation compared to the preliminary phase, which it encompasses just the necessary preliminary studies and investigations, which vary depending on the type of work. Regarding the Executive project, the documents presented in Tab.2.1 can be grouped into three categories: technical, economic, and contractual. The technical documents include general and specialized reports, graphic elaborations, executive calculations for structures and systems, the safety and maintenance plan, and the work schedule. The economic documents report the unit prices of components, along with the final detailed cost estimate and the overall economic framework of the project. The contractual documents include the draft contract and the special contract specifications[27]. Thus, it can be stated that as one progresses from one design phase to the next, the level of detail in the design components increases, reaching its maximum level necessary to proceed to the subsequent procurement phases in the executive design. Following these phases, the client, whether private or public, goes through a bidding process to identify the construction company that will be entrusted with the execution of the work. The company, together with its designers, will carry out the two subsequent design phases: the *Construction Design* and the *As-built Design*. The Construction Design phase corresponds to the highest level of detail of the work to be carried out, while the As-built phase corresponds to the completed and constructed building. The latter may differ in minor details from the construction design phase and represents the

description of the completed building, which will be used as input for the testing phases.

The design phases previously described and presented within Legislative Decree No. 163 of April 12, 2006, are valid for the public procurement sector. Over time, however, this division of design phases has also been applied to the private sector.

The fundamental problem associated with the type of approach summarized in Fig.2.2 and related to the Italian context lies in the fact that it leads to a "Siloed Optimization". Each design component that will make up the final building is optimized, at least initially, in isolation from the others, based on the standards pertinent to each element. This implies that, at the end of the design phases, further intervention by an expert will be necessary to integrate the various components, ensuring that the final design fits within the budget required by the owner and is still feasible. Over time, it has become evident that this procedure is costly, both in terms of money and time. As a result, new process design methodologies have been developed, including the "Integrative Process". This approach requires a change in both the process and the mindset regarding the design of the work: the building must be considered as a system composed of various parts, each interacting with and impacting the others[26]. In this way, it is possible to integrate the previously defined "silos" of responsibility and expertise described in the traditional design approach, fostering cooperation among all participants and ensuring alignment between their success and the project's success[30]. The significant energy efficiency and sustainability goals defined by the European Union, as presented in Section 1.1, can only be achieved through a collaborative process. Virtuous organizations like the AIA define this as Integrative Project Delivery (IPD)[30]. Among the main characteristics of IPD are Collaborative Innovation and Decision Making and Open Communication, representing the emphasis on the need to improve collaboration among design participants, including the owner, designer, consultants, builders, and agency. As shown in Fig.2.3, IPD requires their involvement in all design phases to ensure greater ease in collectively achieving project effectiveness.
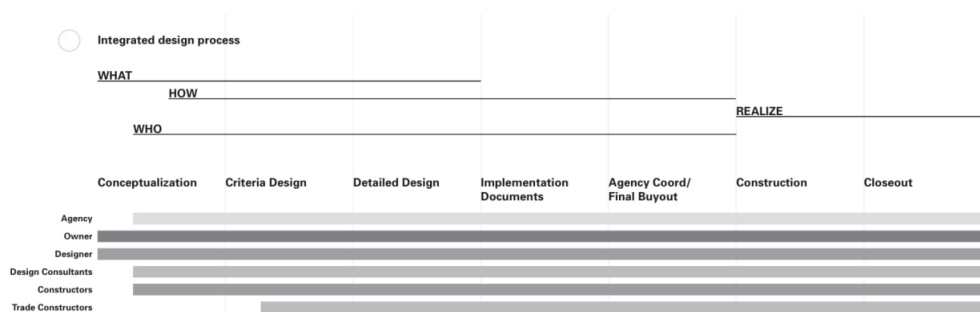
Figure 2.3: Project partecipants' involvment in the IPD.[30]

To facilitate such collaboration, one of the best alternatives is certainly Building Information Modeling (BIM). BIM corresponds to a digital 3D model connected to a project information database that provides significant support for the implementation of IPD. BIM can combine information associated with the different phases of building design and include the management of information concerning the building after its construction and during its use. This allows for verifying the fulfillment of performance requirements that were initially defined during the design phases. As shown in Fig.2.3, the design phases are defined differently in IPD compared to the traditional process: the *Conceptualization* phase, corresponding to the previous *Pre-Design*, determines what needs to be built and how it will be done. This is followed by the *Criteria Design* phase, during which the main options are evaluated, tested, and selected, leading to a *Detailed Design* phase that finalizes all key decisions. The *Implementation Documents* phase completes the necessary documentation to describe how the design will be implemented without making any changes to it, contrary to what happens in the traditional process. In the *Construction Documents* phase of the latter, the designer had to assemble the different design components from the team of experts into a single project, which often required modifying some decisions to make the project feasible. Finally, the agency conducts a review, which is expedited through the use of BIM technology, and especially by the presence of this entity from the early design stages.

Other fundamental features described by the AIA for the IPD include Early Involvement of Key Participants and Early Goal Definition: the objective of the IPD is indeed to move the project decisions as upstream as possible, as in the early design stages, they have a greater impact on the final building performance, and furthermore, their implementation entails lower costs. A clear representation of the advantage of shifting decision-making phases to the

early design stages is provided by the Macleamy curve, depicted in Fig.2.4:
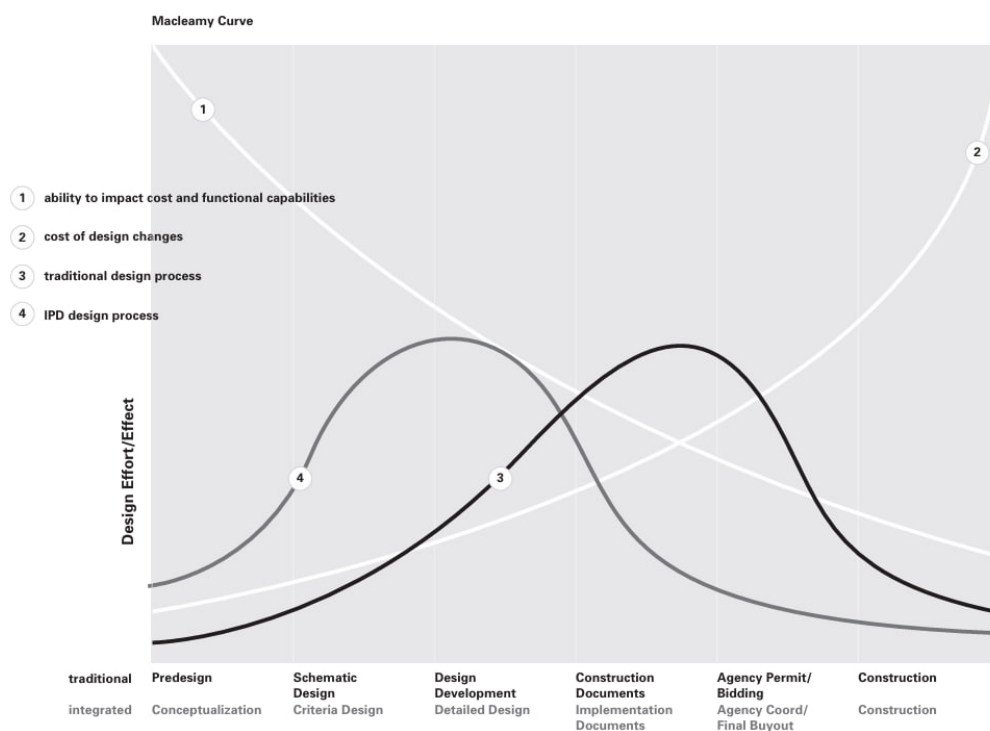
Figure 2.4: Macleamy Curve.[30]

Clearly, it can be observed that during the phases corresponding to the Pre-design in the traditional process, and the Conceptualization in the integrated process, the ability to influence costs and functional capabilities is at its maximum, thus making it more advantageous to act during these stages. However, while in the traditional process, the effort is greater later on, where the cost of design changes is higher, the IPD promotes an increase in effort upfront, to act before design changes can have too significant an impact.

Considering the national Italian context, a marked division of design phases into Preliminary, Definitive, and Executive can sometimes lead to reconsidering decisions made during the preliminary phase in the later design stages. This is because the former has a reduced level of detail, leaving some aspects unclear or unstudied. As shown in Fig.2.4, this can result in not only considerable costs but also, in some cases, the infeasibility of such modifications. The description of IPD presented by the AIA emphasizes the importance of developing a more detailed project from the early design stages, so that only a few specifics need to be added in the later stages, minimizing the costs of these changes. However, within the Italian context, this is rarely applicable, primarily due to budget

allocation constraints of a project. Referring to the division of design phases according to Legislative Decree No. 163, the cost and time associated with the three phases increase from the preliminary to the executive phase, due to the need for more work hours to define the detailed documentation in Tab.2.1.

In general, it can be said that the increasing use of BIM has certainly helped reduce the stark division between these design phases. When creating the model, it is indeed necessary to define the Owner Project Requirement, which allows for understanding the client's expectations and requirements for the project and serves as a guideline for all phases of the project lifecycle, from design to implementation. By doing so, it references all the information required not only for the preliminary design phases but also for the subsequent ones, avoiding the need to start the model from scratch and thus incurring higher design costs. While this provides a broader view of the requirements the project must meet from the early design stages, it still cannot be considered an application of IPD as described by the AIA.

In recent years, the European Union's increased focus on climate change issues has led to the definition of new types of funding, necessitating inevitable modifications to the national design procedures. One example of this is the PNRR (National Recovery and Resilience Plan) funds[31]. These funds amount to 194.4 billion of euros and were approved on July 13, 2021, accompanied by an annex that outlines specific objectives and milestones for each investment and reform. Notably, the disbursement of funds by the European Commission occurs semi-annually from the second half of 2021 until December 31, 2026, following the verification of predefined targets and goals. Given the time constraints associated with fund disbursement, changes to the bureaucratic foundation of the design process were necessary. Consequently, the Nuovo Codice Appalti (Legislative Decree 36/2023[32]) came into effect on July 1, 2023, altering the division of previously outlined design phases. This decree specifically applies to public contracts and defines objectives for their design, including not only compliance with environmental and urban regulations, architectural quality requirements, and technical functionality but also:

- Energy efficiency and minimizing the use of non-renewable materials throughout the life cycle of the projects.
- Adherence to principles of economic, environmental, territorial, and social sustainability.

To streamline the design process while still achieving the aforementioned objectives, Art. 41 of the decree defines two successive levels of technical depth for public works design: the *Progetto di Fattibilità Tecnico Economica* (PFTE) and the *Executive Project.* It can be said that the first of these combines what was previously known as preliminary and final design in a single step, simplifying and expediting the overall process. The main characteristics of these two design steps under the *Nuovo Codice Appalti* are summarized in Tab.2.2.

Table 2.2: PFTE and Executive design content, D. Lgs. 36/2023 [32]

PFTE	Executive design
Identify, among the solutions suggested in the DOCFAP, the alternative that corresponds to the best cost-benefit ratio based on the requirements to be met and the performance to be provided.	Develop a level of definition for the elements that comprehensively identifies their function, requirements, quality, and list price.
It contains references to the methods and tools of digital construction information management that were used.	It is accompanied by a maintenance plan for the work over its entire lifecycle, detailing the tasks to be performed, along with their associated costs and timelines.
Develop the necessary investigations and studies for defining the geometric and spatial configuration, the functional aspects of the work, the mitigation and compensation measures for the environmental impact on archaeological contexts, and an estimate of the expenses related to the work itself.	In the event that digital construction information management methods and tools are utilized, develop a level of definition of the objects in accordance with what is specified in the informational specification accompanying the project.
Identify the dimensional, typological, functional, and technological characteristics of the work to be carried out.	It is drafted by the same entity that prepared the PFTE. However, in cases where, for valid reasons, it is entrusted to a different entity, the latter must unreservedly accept the previous design activity.
It allows, if necessary, the initiation of the expropriation procedure.	It contains the final definition of all works, detailing every architectural, structural, and system related aspect of the interventions to be carried out.
It contains the necessary elements for the issuance of the required authorizations and approvals.	It does not include construction operational plans, procurement plans, or calculations and charts related to provisional works.
It includes a preliminary maintenance plan for the entire work and its components.	

As shown in Tab.2.2, the technical and economic feasibility project encompasses all the necessary verifications for the specific work being carried out, ensuring that the executive design phase is just an extension of these studies with a greater level of detail. This new approach introduced in Italy for public procurement stems from the direction in which European Union funding has moved in recent years. This is also evident in the European Taxonomy[10] previously presented in Section 1.1: within this framework, the necessity to ensure that new buildings can contribute to climate change mitigation and adaptation is defined, as schematically shown in Fig.2.5.
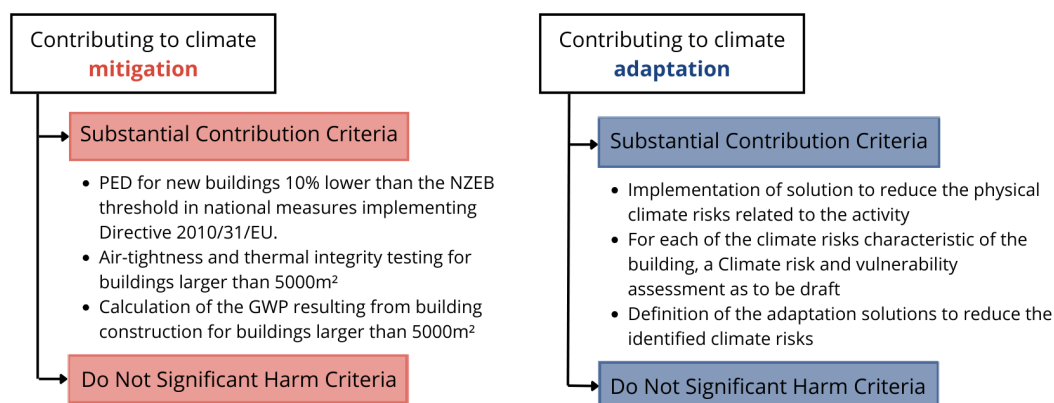
Figure 2.5: Construction of new buildings contribution in EU Taxonomy[33].

Of particular relevance is what is defined in Fig.2.5 as the *Do Not Significant Harm Criteria* (DNSHC): according to Art. 17 of the Taxonomy, considering the six environmental objectives it contemplates, an activity is considered to cause significant harm if it[34]:

1. causes non-negligible greenhouse gas emissions, thus harming *climate change mitigation*;

2. leads to a worsening of the negative effects of current and future climate conditions, thus harming *climate change adaptation*;

3. harms the sustainable use and protection of *water and marine resources*;

4. leads to significant inefficiencies in material use or an excessive increase in waste production, incineration, or disposal, thus harming the *circular economy*;

5. causes a significant increase in the emission of pollutants into the environment, thus harming *pollution prevention and reduction*;

6. harms the protection and restoration of *biodiversity and ecosystems.*

During the design of a building, it is necessary to conduct preliminary analyses to ensure compliance with the DNSHC, so that the completed work can contribute both to climate change mitigation and adaptation. Furthermore, focusing on the building's contribution to the latter, Fig.2.5 highlights the need to analyze the physical climate risks related to the activity under study and, based on these, to conduct a *Climate Risk and Vulnerability Assessment.* This analysis involves examining the expected climate conditions of the location where the building will be constructed over a period proportional to its expected useful life, so that:

- If the building is expected to have a useful life of less than 10 years, the analysis should be conducted using projections at the smallest appropriate climatic scale[35];
- For all other activities, the analysis should be conducted with the highest available resolution, considering the state-of-the-art projections of future climate scenarios, including at least those at 10 and 30 years for major investments. This should be done with reference to the Representative Concentration Pathways RCO2.6, RCP4.5, RCP6.0, and RCP8.5[35] developed by the IPCC.

In identifying the physical risks to which the proposed project will be subjected in future climatic scenarios, it becomes apparent that during the preliminary design phases, merely meeting the general requirements set by the client based on the building's intended use will not suffice. Rather, it becomes imperative to supplement these requirements with interventions aimed at ensuring the building can withstand all anticipated climate risks throughout its useful life. This ensures that the building is truly resilient and contributes to the community's climate adaptation efforts.

Although regulations implemented by the European Union compel designers to conduct specific analyses on the building from the preliminary design phases onwards, which are now more comprehensive compared to the past, and despite the modifications introduced by the N*uovo Codice Appalti*, it is far from accurate to claim that the design process in Italy aligns with an integrated approach akin to that described by the AIA. Despite the advantages associated with the latter are significant, the challenge in implementing such an approach lies not only in the procedures imposed by national regulations but also in the limited availability of information typical of the initial design stages. This misalignment with the demands of numerous input requirements posed by most energy modeling and simulation software currently available on the market further complicates matters. As will be elaborated in Chapter 3, numerous studies have been conducted on the development of calculation methodologies aimed at facilitating the use of energy modeling software from the early design stages. These studies evaluate various software characteristics and approaches, seeking to bridge the gap between the available software capabilities and the demands of early-stage design.

2.4   Research Objective

The following thesis work aims to address the challenge of evaluating design alternatives in the early stages of an integrated design process to ensure optimal building performance aligned with the decarbonization and energy efficiency objectives outlined by the European Union in response to the growing concerns regarding climate issues. To achieve this, the software tools *Rhino* with Visual Programming Interface *Grasshopper3D*, along with its plug-ins *Ladybug*, *Honeybee*, *Ironbug*, and *Wallacei*, will be utilized. Specifically, the latter will enable multi-objective optimization using evolutionary algorithms to identify design alternatives that optimize a set of appropriately selected objective functions.

A workflow to support designers will be developed based on a case study provided by GET Consulting s.r.l. described in Chapter 4. Assuming knowledge of the information typically available in the early design stages of a building, a baseline building will be defined following the procedure in Appendix G of the ASHRAE Standard 90.1-2016, which will serve as a benchmark for evaluating the optimal performance of the designed building over a typical year of operation. The workflow will be developed with two approaches, both tested to evaluate which is more appropriate for application in the early design stages, considering the quality of the solution they provide and the time required for their execution. The first approach involves *Sequential Optimization*, composed of two phases: the first phase will optimize the passive performance of the building by varying selected building parameters as optimization variables, while the second phase will identify the optimal HVAC system type for the modeled building, considering the building envelope characteristics obtained from the previous optimization phase as fixed. In both phases, the evaluation of the installation of a photovoltaic system for self-consumption will also be included, aiming to minimize the building's use of external resources so that it can be considered as an nZEB. The second approach involves *Integrated Optimization*, where both the building variables and HVAC system variables for the building will be optimized simultaneously, again considering the installation of a photovoltaic system for self-generated electricity.

Once the optimal results from both approaches are obtained, they will be presented in Chapter 5 and compared to determine which procedure is superior in terms of delivering the building's energy and environmental performance.

Following this, Chapter 6 will conduct a critical analysis of the two approaches, evaluating how their performance, in terms of the quality of the optimal energy-environmental solution and computational cost, varies with changes in one of the NSGA-II algorithm's setting parameters, such as Population Size. Additionally, a sensitivity analysis will be conducted on the design parameters considered as optimization variables in both approaches to identify those with the greatest impact on specific end uses and to evaluate the consistency of the proposed design model with typical trends of buildings located in the climatic zone of the case study. Based on the results of this analysis, conducted separately for the two approaches, post-processing of the optimization variable values will identify those that ensure maximum performance for the case study, regardless of whether they were identified by the two optimization approaches. These solutions will be defined as Best Case Solutions and can provide useful guidance to the GET Consulting team in the initial design of the studied building.

As mentioned in 2.3, in describing the design stages provided by D.Lgs. 163/2006 and 36/2023, one of the studies to be developed in the early analysis stages of the project is the economic impact associated with the designed work. Consequently, it was deemed appropriate to conduct a cost analysis of the design alternatives suggested by the two optimization approaches. Particular attention will be given to those alternatives selected by Sequential and Integrated Optimization that correspond to the maximum differential global cost, as well as to those optimal results obtained from them. Finally, to provide a preliminary economic analysis of the Best Case Solutions, their global cost will also be evaluated to assess the economic impact of each and, ultimately, select the one that represents the best trade-off between minimum global costs and maximum building performance for the case study.

Chapter 3

Building Performance Simulation and Optimization

As anticipated in Chapter 1, over time, increasing environmental awareness has led to a growing demand for energy efficiency across all sectors involving human activities. This has resulted in the development of always more stringent regulations promoted by international and national governments, aimed at encouraging the adoption of innovative technologies or new design and construction methodologies with the goal of reducing the environmental impact of various sectors. Regarding the building sector, this has led to a growing development of energy modeling, both in terms of usage and available tools; indeed, their use helps to select the alternatives aimed to reduce emissions associated with the buildings they are applied to and allows for a reduction in energy consumption; typically, for conventional buildings, energy modeling or simulations are not necessary, unlike more complex installations that cannot be achieved without the support of simulation tools. However, the increasing push towards the need to create ZEB or nZEB, often driven by legal obligations as shown in Chapter 2, has led to an increasingly widespread use of energy models, for both simple and more complex applications [25], particularly during the early design stages. During these stages, in fact, the design alternatives on which energy performance depends are selected and the degree of freedom is high; by exploiting the features of these stages, starting from the limited inputs available, it is possible to select alternatives that, from the beginning of the design process, guarantee optimal building performance, ensuring that they are not modified in subsequent stages, during which the cost of such changes would

be excessively high, as demonstrated in Section2.3. From this perspective, one possible alternative may be to combine building energy modeling and simulation tools with optimization algorithms.

3.1   Building Energy Modelling

In the past, energy assessments of buildings often relied on approximate methods or empirical rules; however, due to advancements in technology, powerful softwares have been developed, enabling increasingly sophisticated and accurate energy modeling. This development is driven by the growing diversity of buildings, each with specific performance requirements that depend not only on user needs but also on regulatory constraints, as described in Chapter 2. Such modeling is multidisciplinary and complex, involving various fields such as physics, mathematics, materials science, biophysics, human behavior studies, and computational and environmental sciences; it is essential to harness these disciplines appropriately to ensure the realization of robust buildings capable of meeting future needs in terms of energy performance, environmental impact, and occupants comfort[15]. This necessitates an integrated approach to the various subsystems comprising a building, as summarized in Fig.3.1, which outlines the fundamental components that must be considered during building modeling: they cannot be treated separately if a realistic representation of the building's actual energy performance following simulation is desired.
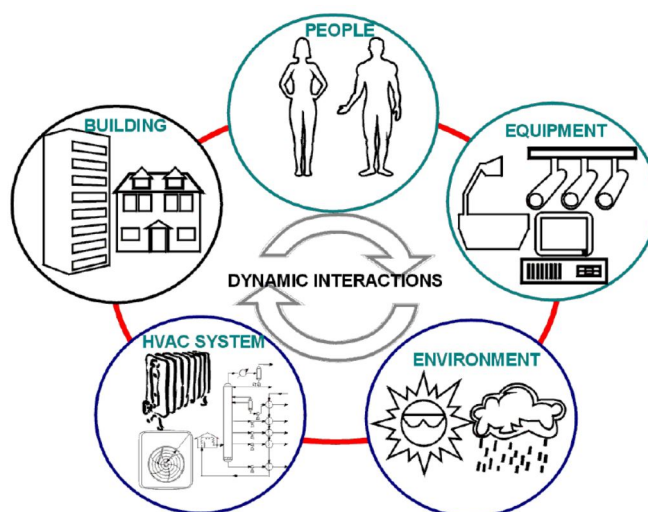
Figure 3.1: Main interacting building subsystems[36].

Two macro-categories of software are used in the field of building energy modeling: *design tools*, used for sizing the building's system components, and *simulation tools*, which predict the building's performance annually. Due to the different purposes of these two groups of tools, in the former one, calculations are based on the worst-case scenario, considering both the summer and winter seasons. In the latter, on the other hand, the typical conditions in which the building is located are considered in order to evaluate its response[37]. The use of this type of software has allowed, over time, to predict the behavior of designed buildings in advance, so that modifications can be made to the decisions taken during the design phase, even before they are actually implemented in the existing building. This capability enables significant economic savings and also allows for the evaluation of the best alternatives that can be selected to achieve a specific performance goal.

These days, there is an extensive variety of Building Performance Simulation Tools available, each with different characteristics in terms of thermodynamic models, graphical user interfaces, usage scenarios, and data exchange capabilities with other software[37], particularly with Computer Aided Design (CAD) programs, required to give a geometrical representation of the building under-study. However, it is possible to define a common data workflow for all of them, as depicted in Fig.3.2:
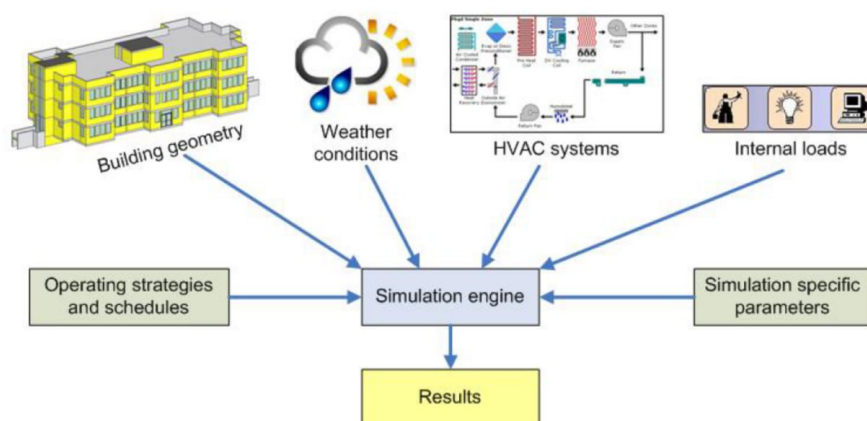
Figure 3.2: Main workflow schema of BPS tools[37].

In Fig.3.2, the fundamental information required as input for creating an energy model of a building for simulation purposes is highlighted. The geometry of the building is crucial, which can either be that of the existing building or the designed geometric project and can be represented directly in the simulation

software used, or imported from a CAD software, depending on the cases. Regarding weather conditions, these are represented by a weather file: there are various types of weather files, but the two most commonly used ones are the *Typical Meteorological Year* (TMY) and the *eXtreme Meteorological Year* (XMY), which are derived from climate data measurements over a historical period of at least 10 years. The difference between TMY and XMY lies in the fact that while TMY corresponds to a set of 12 months where each month selected from all those in the historical period corresponds to the one closest to the 50th percentile calculated from the historical data, the XMY file consists of 12 months where each selected month corresponds to the one closest to the 90th percentile calculated from the available historical data. Therefore, while TMY can be considered a set of "typical months", corresponding to average climatic data over the historical period, XMY represents "extreme months", corresponding to the most extreme climatic data of the considered historical period. Because of this difference, it is possible to asses that if the aim is to analyze how a building performs under normal operating conditions, it will be necessary to use TMY; instead, if the reaction of the building to extreme climatic conditions, typical of the considered location, is to be evaluated, XMY should be used [38]. Additionally, among the inputs, HVAC (Heating, Ventilating, and Air Conditioning) systems are also included: they consist of a group of components that work together to provide/remove heat to/from conditioned spaces and, when properly designed, installed, and maintained, represent a key element in ensuring occupant comfort and good indoor air quality while keeping costs down. Finally, it is necessary to include information about internal loads within the models: this category refers to all components within the building related to its occupants' use and that have an impact on the building's energy balance. Among these, it is necessary to consider the sensible and latent loads of occupants, who, with their metabolic activity, heat the spaces and alter pollutant contents, due to the presence of Volatile Organic Compounds (VOCs), bioeffluents and all the compounds coming from the outdoor environment, and relative humidity; furthermore, all electrical and non-electrical equipment, such as computers or gas stoves, and artificial lighting systems, represent internal contributions that, in summer, increase the thermal load, while in winter, reduce it. However, most of the internal loads in a building are not continuously present but only for certain periods of the day and year: to represent this, it is necessary to use schedules within the

building energy models, representing the fractions of thermal load to be applied at different times in the internal spaces of the building. While such inputs are common to all types of BPS tools, there are specific parameters required by the simulation software and its capabilities; for example, it is necessary to specify the simulation timestep, its running period, which can be a whole year or shorter, and so on.

From Fig.3.2, it is evident that all the described inputs are entered into the so-called *simulation engine*: it allows for detailed thermal simulations based on the previously described inputs provided in text-format using mathematical and thermodynamic algorithms. Since these algorithms are extremely complex and not accessible to all users, a fundamental component that has enabled the widespread adoption of such software is the *Graphic User Interface* (GUI), which facilitates the generation and input of data into the simulation engine and allows for a much faster analysis of the outputs generated by the algorithms. However, it is essential to note that, to ensure proper use of such tools, one must be aware of both the limitations of the program being used and the thermal processes and main equations underlying the energy balance of a building, in order to enable an understanding of the processes and results obtained [37]. Over time, the usage of these software tools has evolved: in the past, they were predominantly used during the design phases of the building's lifecycle. The ever-increasing demand for sharing and multidisciplinary storage of information with a virtual representation has led to the integration of these tools with CAD applications and the development of Building Information Modeling (BIM); the latter is of paramount importance today and represents a model-based technology connected to a project information database [39].

It is possible to define two different macro-categories of approaches used in energy modeling: dynamic and static, with quasi-static approach representing an intermediate path between the two. The static approach is based on conducting simulations over design days, particularly one for the summer season and one for the winter season. It allows for designing building components but cannot be considered an accurate approach for evaluating energy performance as it does not account for all the dynamic phenomena occurring within the building, such as thermal inertia of building envelope components, which allows shifting the peaks of heat demand required by the building over time. The second approach, the dynamic one, allows for a more detailed representation of the building's behavior as it is based on transfer functions: these are functions

that characterize the behavior of a dynamic system in the frequency domain, relating input to output. The family of transfer functions includes the method of Radiant Time Series (RTS), a simplified procedure derived from the direct thermal balance, where the radiant fraction of the instantaneous thermal input due to building envelope components and radiative gains is converted into the corresponding thermal load required by the building using weighting coefficients (Radiant Time Factors). These coefficients allow determining the thermal load at the present moment based on current and past thermal inputs and are defined based on the thermo-physical characteristics of building envelope components and the thermal inertia of the environment as a whole.

In this way, the RTS method quantifies the typical dynamic effects of a building related to:

- Delay and damping of thermal inputs through opaque envelope components;
- Delay and damping of the radiative portion of thermal inputs from endogenous sources;
- Delay and damping of solar-origin thermal gain transmitted through transparent envelope components and, therefore, absorbed by the indoor surfaces.

The elements considered in the case of applying a dynamic simulation approach are:

1. Thermal balance on indoor air, related to infiltration and ventilation and convection from internal sources;
2. Thermal balance on the wall, considering its internal and external surfaces.

These elements are interconnected, especially the thermal balance on indoor air influences the thermal balance on the internal surface of the wall, and vice versa, through the convective heat flow associated with air. In turn, the thermal balance on the external surface of the wall influences the thermal balance on the internal surface of the same wall, and this influence is due to conduction through the envelope. Considering the dynamic regime, this corresponds to the most difficult element to model; for these reasons, its numerical modeling is exploited through the transfer function presented below in equation 3.1.

$$q_i(\tau) = -\sum_{j=0}^{z} Z_j \cdot T_i(\tau - j\delta) + \sum_{j=0}^{z} Y_j \cdot T_{o,i}(\tau - j\delta) + \sum_{j=0}^{w} W_{i,j} \cdot q_i(\tau - j\delta) \quad (3.1)$$

The definition of the elements within equation 3.1 is provided in the Nomenclature. Regarding Z_j, Y_j, and $W_{i,j}$, they are evaluated by solving the balance equation; furthermore, their quantity depends on the wall thickness and the calculation timestep δ. It should be noted that in the case where the transfer function method is applied in steady-state regime, the response factors Z_j, Y_j, and $W_{i,j}$ will simply represent the definitions of thermal transmittance U.

The quasi-steady-state method, on the other hand, is based on the definition of heating and cooling degree days and is not able to represent the dynamic response of buildings. For these reasons, its use is limited both in the design and in the analysis of building performance.

For the present thesis work, it has been decided to work on dynamic models, in order to have the possibility to accurately study the dynamic behavior of the building, taking into account all the complications it entails and which will be presented later.

3.1.1 Main Building Performance Simulation Softwares

As anticipated, all BPS tools consist of two elements: the simulation engines, containing all the algorithms and routines to be performed, and the GUI, which instead simplifies the input insertion and result representation. Within the workflow, therefore, the simulation engine utilizes an input file containing the information associated with the previously described elements and, based on them, performs a simulation and writes the outputs to output files, which also contain information about the simulation itself, like warnings, error messages or simulation time [37].

To date, the most widely used simulation engine is EnergyPlus: it is a simulation program for energy analysis and thermal loads and, therefore, can be used to calculate the winter and summer thermal loads required in the modeled building to maintain internal thermal setpoints; it can also be used to evaluate the resulting HVAC system operating conditions, on both hot and cold coils. The main characteristics of this simulation engine have been inherited from two of its predecessors, namely BLAST (BLAST - Building Loads Analysis and System Thermodynamics) and DOE-2: they were developed and released between the late 1970s and early 1980s as energy simulation software, the

former by the University of Illinois at Urbana-Champaign, the latter by the Lawrence Berkeley National Laboratory, founded by the U.S. Department of Energy (DOE). The latter became particularly relevant over time, as several GUIs were developed for it, enabling its widespread use. It is capable of providing energy analyses of the entire building, even considering complex multi-zone configurations. However, it has not been further developed as DOE funding was redirected towards EnergyPlus, which is capable of providing more detailed simulation results on advanced building technologies [40]. In fact, both BLAST and DOE-2 were written in older versions of FORTRAN and used components that have become obsolete in newer compilers; in particular, the main issue is associated with their limited ability to properly handle feedback from HVAC systems to zone conditions. As a replacement, DOE proceeded with the development of EnergyPlus: based on input and output files written in ASCII text, it can perform energy simulations with sub-hourly timesteps, defined by the user, ensuring the possibility of analyzing interactions between thermal zones and the environment. The simulations, indeed, are dynamic based on the Transfer Heat Conduction Function previously defined in equation 3.1[41]. The main drawback of this simulation engine is its slowness, due to the high level of physical modeling detail, which acts as a barrier to iterative and interactive modeling [40]. The data flow within EnergyPlus is depicted in Fig.3.3:
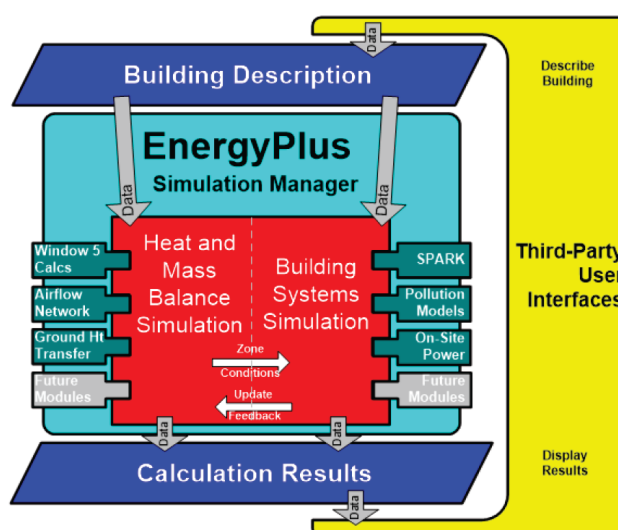
Figure 3.3: Data flow in the EnergyPlus simulation engine[41].

The thermal and heat mass balance simulations are integrated into the building system simulation, so that their outcome is independent of whether the thermal loads of the spaces are met or not. Additionally, within this system, modules such as COMIS, SPARK, and TRNSYS are incorporated to combine various aspects of building energy simulation. Specifically, COMIS (Conjunction Of Multizone Infiltration Specialists) is a component that calculates airflow patterns within the building due to pressure differences; SPARK (Simulation Problem Analysis and Research Kernel), on the other hand, is a generic simulation environment used to find solutions to differential and algebraic equations. TRNSYS (TRaNsient SYstem Simulation Program), instead, is primarily used for HVAC system simulation[37]. As shown in Fig.3.3, a modular approach is adopted, which represents the fundamental advantage of this simulation engine: this facilitates the incorporation of additional modules in the future, to guarantee the continuous improvement and updates.

Over time, several GUIs have been developed to support EnergyPlus, with DesignBuilder and OpenStudio being among the most notable. The former provides a user-friendly modeling environment capable of accommodating data related to energy consumption, occupant comfort, and HVAC sizing. Following simulations, DesignBuilder can generate a set of outputs and reports useful for comparing different design alternatives; its modeling capability enables it to handle complex buildings as well. Additionally, it can interface with existing design data, both BIM and CAD data [42]. The latter, developed by NREL (National Renewable Energy Laboratory), is essentially an interface that provides users with access to various building analysis engines but is typically used in conjunction with EnergyPlus. It includes geometric modeling capabilities akin to SketchUp, allowing users to create geometries, space types, and thermal and lighting zones in a 3D model similar to what can be achieved with a 3D architectural modeling program. It includes easy-to-apply templates containing data on building envelope and activity, considering various building types and climate zones[40].

An alternative to EnergyPlus is TRNSYS [43], a commercially available Building Energy Modeling program characterized by a modular approach that makes it much more flexible than other tools. It includes not only the simulation engine but also a GUI and a library of components that encompass various building models featuring standard HVAC components, renewable energy sources, and emerging technologies. Additionally, it enables the creation of routines

for manipulating meteorological data to alter simulation results. Essentially, it functions as a programming language, primarily used in universities and research endeavors[40]. One of the significant advantages of this software lies in its high flexibility, derived from its ability to share components among multiple users without the need for recompilation, thanks to the use of Dynamic Link Library (DLL) technology, and the possibility of incorporating components developed in software tools such as Matlab, Excel, or similar ones [44].

The simulation software tool IES provides a wide range of variables in building simulation analysis, allowing interaction with other energy simulation tools. Its simulation engine is APACHE[45], providing an environment for detailed building systems analysis, enabling optimization in terms of comfort and energy performance. It also conducts dynamic simulations and includes various blocks that handle different parts of the simulation; for instance, the dynamic tool Macro FLO is structured for natural ventilation modeling, while Apache HVAC is for analyzing air leakage, natural lighting, and solar protection. Results are expected to be exported automatically [44].

3.2 Building Energy Simulation in Early Design Stages

In Section 2.3, the advantages associated with shifting the decision-making phase regarding the fundamental design components of a building to the early stages of the process were highlighted. This approach also ensures integration among the various actors operating within the design process itself to minimize changes to the building design in the advanced phase, where they would be more costly and sometimes unfeasible. The main obstacle to this procedure is related to the applicability of the energy modeling software discussed in Section 3.1 to the initial design phases. These software tools require numerous inputs, often very specific, which are not available during the conceptual design phase, during which, it is necessary to evaluate various possible alternatives to achieve a specific objective, such as maximizing the building's performance. Over time, these challenges have been the subject of various studies, in which authors subsequently sought to propose solutions.

Among the studies conducted on the initial design phases, M. Picco et al.'s work *Towards energy performance evaluation in early stage building design: A simplification methodology for commercial building models* [25] is notable. Indeed, it analyzes the benefits associated with applying energy analysis in the early design stages, focusing on large commercial buildings, to assess the main barriers to integrating this type of analysis in the early design phases. Additionally, it provides a methodology developed to optimize energy efficiency in the early design stages. The procedure is based on a case study of a 1954 office building located in Bolzano, Italy, with a heated area of 2841 m^2. A detailed initial model was created using EnergyPlus software and its GUI OpenStudio, considering a total of 35 thermal zones, including all conditioned and non-conditioned volumes, 23 construction types, 198 fenestration components, and three different HVAC systems. Seven simplification steps were then applied to the model: the first one involved reducing the construction types from 23 to only 6, with only 4 considered as input (exterior walls, exterior roof, exterior floor, and glazing components); subsequently, external shading components were removed, as they represented a level of detail too advanced for the initial design phases. Numerous simplifications were made to reduce the number of thermal zones: initially, each floor was assigned a single thermal zone with a standardized floor area to represent the entire building with a single floor element; finally, each floor was represented as a rectangular box. These simplifications were primarily due to the lack of knowledge about internal partitions during the initial design phases and aimed to minimize the number of inputs required to model the building within the simulation software. Similarly, simplifications were made to the glazing components, where the sum of all transparent surfaces for each floor and each cardinal direction was represented with only four transparent surfaces, one for each cardinal direction, as typically defined in the initial design phases. After defining the fenestration area for each floor and cardinal direction, the total was divided by the number of floors to ensure the same area for each, further reducing the number of inputs. Further simplification was made to the number of modeled floors. Regardless of the actual number of floors in the real building, a fixed number was defined, with the actual number reproduced using zone multipliers. Once all simplification steps were defined, annual simulations were conducted for each simplification step and each of the three identified HVAC system types (Unitary system with relative humidity control and VAV system with and without relative

humidity control) to assess which simplification step resulted in the greatest deviation from the detailed model. Comparing building energy consumption for heating and cooling between each simplification step, and following the entire simplification process, it was observed that, in the worst-case scenario and considering the entire process, the percentage differences were 15.6% for the heating regime and 14.6% for the cooling regime. From the analysis of peak loads, the maximum percentage differences obtained were -4% and -9% for heating and cooling, respectively, compared to the complete model. Despite of this, it can be concluded that, due to the lack of information and its uncertainty during the initial design phases, differences between the detailed and simplified models within a 20% range are acceptable and ensure that the simplified model is indeed providing useful information for the early design stages.

Demonstrating that it is possible to simplify the energy modeling of the buildings in order to adapt it to the information typical of the early design stages, over time various simplified energy performance simulation tools have been developed, providing a simple and effective performance analysis and assisting architects in considering different design alternatives. These tools, not requiring detailed information as input, are perfectly suited for application in the early design stages [46]. The study by Liwei Wen and Kyosuke Hiyama presents ten different simple tools classified into three categories which are schematically represented in Tab.3.1.

Table 3.1: Classification of early design stages energy performance simulation tools according to [46].

CATEGORY	DESCRIPTION	EXAMPLES
Design Index Tools	Use envelope performance to indicate approximate building energy performance	C_f PAL ERED
Simple analysis program tools	Provide specific calculation results according to user requirements but require a greater number of inputs	WinSim TEMMI/MCI CooLVent
BIM relevant programs	Combine a simple tool with BIM software capable of automatically generating the energy model	DPV EcoDesigner

3.2.1 Parametric Energy Simulation in Early Design

One possible implementation of energy simulation software in the early design stages is certainly the use of visualized parametric energy analysis as it allows modifying the building's energy model parametrically, making it easier to evaluate various design alternatives. One of the most commonly used programs for parametric analysis, both in terms of geometry and building energy simulation models, is *Rhino*, with support from *Grasshopper 3D* and its plugins. In [47], for example, these tools are utilized to develop a workflow to simplify modeling and simulation tasks while enabling iterative design processes and monitoring changes during them. Additionally, the *Rhino/Grasshopper* system allows for high interoperability, both among different plugins and with other software. Moreover, for the study in [47], not only plugins related to building energy simulation were used in *Grasshopper*, such as *Honeybee* and *Ladybug*, but also plugins that enable the implementation of optimization algorithms, including *Octopus* for conducting multi-objective genetic algorithm optimization to minimize the shape coefficient, maximize space efficiency, and increase solar radiation incident on the building, and *Galapagos*, which performs single-objective optimization with genetic algorithms to minimize energy consumption by optimizing building openings. The geometry of the building area to be simulated is thus defined parametrically, creating an experimental box representative of a single residential building. From this, variables for parametric energy analysis are identified to assess the impact of different locations, climate data, construction types, and glass properties. Each combination of variables presented so far is simulated using the EnergyPlus simulation engine, generating various scenarios with defined variables and their respective ranges of variation. Metrics for annual and monthly consumption for electric heating, cooling, lighting, and equipment are selected as relevant outputs for the process. In conclusion, it can be stated that this type of study allows for significant accuracy in energy analysis processes, as demonstrated by the sensitivity analysis conducted in the document. Furthermore, considering the large number of alternatives and combinations tested by the genetic optimization algorithm, defining an adequate visualization of the results is crucial. Therefore, the decision was made to use the Parallel Coordinate Plot, which enables the visualization of individual data elements

across many dimensions, each corresponding to a vertical axis of the plot. Each generated solution corresponds to a polyline connecting the various values of the variables corresponding to a solution [47].

As presented in Section 2.2,the integration of building energy simulation and optimization algorithms is driven by the definition of the concept of nZEB. This concept is strongly linked to the notion of the cost-optimal level of energy performance, evaluated over a certain period of time under specific boundary conditions. This translates perfectly into a complex optimization problem, where the optimization variables are various design alternatives that impact the energy performance of the building. These alternatives must be selected by the optimization algorithm to satisfy a defined objective function. Thus, simulation-based optimization methods (SBOM) are employed to explore a vast search space and identify, among the evaluated solutions, the one that meets the objective function [48].

The main difficulty associated with SBOM lies in its extreme multidimensionality due to the high number of variables typical of an energy model that indeed affect the building's performance. Moreover, as mentioned in Section 3.1, the calculation methodology that ensures the best representation of all factors contributing to the building's energy performance is dynamic simulation, implemented, for example, by simulation engines like EnergyPlus and TRNSYS, which increase the complexity of the equations typical of these problems. The multidimensionality and computational cost characterizing this type of study require:

1. Choosing an appropriate optimization algorithm based on the available computational power and the study's requirements;
2. Making a suitable selection of the model variables to be optimized.

For these reasons, the application of this approach is interesting in the early design stages, as during these stages, the level of detail used is lower. Thus, assumptions and simplifications, similar to those mentioned in reference to [25], can be made to reduce the complexity of SBOM.

3.3 Optimization Algorithms and Building Performance

Optimization refers to a technology capable of ensuring that user-defined objectives are achieved using the available resources in the system as efficiently as possible [49]. It plays a fundamental role in research and industry, as numerous real-world problems can be modeled as optimization problems [50]. As early as the 18th century, Newton and Lagrange made significant developments in the field of optimization, allowing the distinction of two fundamental components within it: Modeling and Analysis. The former provides a mathematical expression of the real problem, while the latter aims to find the best solution for the problem itself. To date, various analysis methods have been defined and evolved into what are known as optimization algorithms. Among the first optimization algorithms developed are the Gradient Descent Method and the Newton's method, which focus on searching for stationary points (minima and maxima) of differential functions. A classification of existing optimization algorithms is provided in Fig.3.4 [49]:
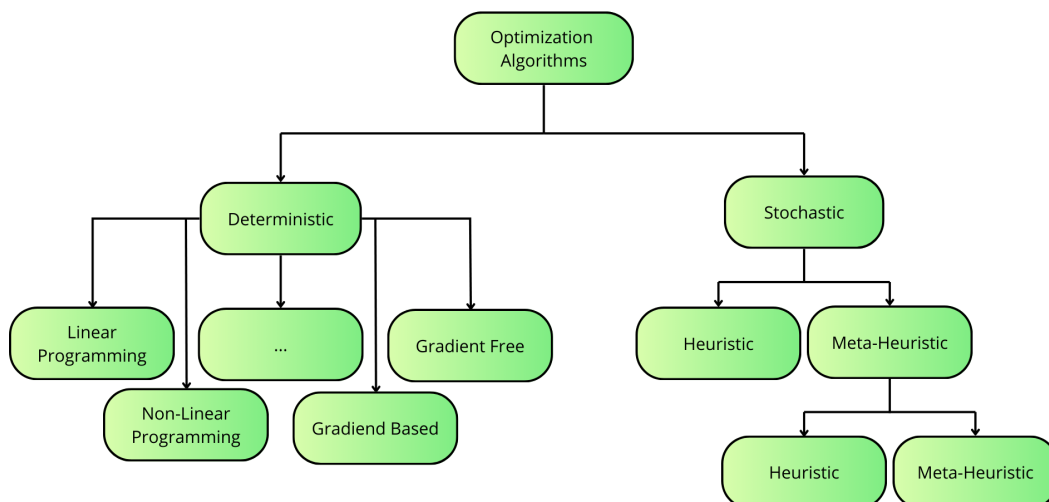
Figure 3.4: Classification of Optimization Algorithms[49].

In particular, the two main families are deterministic and stochastic algorithms: the former are defined in such a way that the same precise sequence of actions is always followed, therefore, at equal input variable values, the obtained objective function will be the same; the latter, instead, are characterized by randomness [49] and are of particular interest as they allow connecting process

simulators containing materials and energy balances, characterized by highly nonlinear equations [51]. For these reasons, they are more commonly used when integrating with energy simulation processes. Among stochastic optimization algorithms, those based on populations are particularly relevant: they do not operate on individual solutions, but on a population of them, and then make a selection using criteria that vary depending on the specific type of algorithm considered.

3.3.1 Population-based optimization algorithms

Among stochastic optimization algorithms, Population-based Algorithms (POA) have been the subject of numerous studies over the last 30 years: being that current real-world optimization problems are characterized by multi-modality, discontinuity, and noise, POAs provide a range of advantages to overcome these difficulties, including the ability to avoid falling into local optima during solution evaluation, the capability to be used for multi-objective optimizations, and the handling of linear and nonlinear equalities and inequalities [50][52]. As a result, their application has spread across various fields, starting with engineering and thus the design of electronic circuits, structures, vehicles, followed by medicine, for defining treatment protocols or optimizing drug dosages. They are also used in the energy and environmental sectors to optimize energy distribution in the power grid or to optimize the operation of energy production plants, both renewable and non-renewable.

The operating logic of this category of optimization algorithms is based on defining different individuals that explore the solution space cooperatively, utilizing mechanisms such as mutation, crossover, selection, and learning. Additionally, an element of randomness is introduced to avoid local optima and improve the exploration of the solution space. According to Wu et al. [50], three main characteristics distinguish POAs from other optimization algorithms:

1. Solutions are searched for in the solution space through multiple points simultaneously.
2. POAs have mechanisms for sharing information and interactive learning among individuals with different search behaviors.
3. They are stochastic, as randomness is an integral part of the algorithm.

In all cases, when the optimization being performed is multi-objective, conflicting objectives often make it impossible to guarantee the existence of a

single solution that optimizes all required objective functions simultaneously. For this reason, non-dominated solutions are sought, meaning solutions for which none of the objective functions can be improved without degrading some of the other objective values. In this type of real-world problems, it is necessary to identify a representative set of Pareto optimal solutions to find compromises satisfying various objectives, thereby finding a single solution that, according to an external decision maker, can be considered of good quality for real-world application [53].

POAs can further be classified into Evolutionary Algorithms (EAs) and swarm intelligence algorithms (SIAs); notable examples of the former include Genetic Algorithms (GAs), while Practical Swarm Optimization (PSO) is an example of the latter [50].

PSO is inspired by the movement of groups of animals, such as flocks of birds or schools of fish, which migrate to advantageous regions based on their adaptability to the environment [54]. It is a metaheuristic because the number of assumptions made about the optimization problem is reduced, so the candidate solution space in which the search takes place is very large, although this type of algorithm does not guarantee finding an optimal solution. EAs, instead, employ mechanisms based on biological evolution, such as reproduction, mutation, recombination, and selection: candidate solutions in the optimization process represent individuals within a population, while the fitness function determines solution quality. One of the main challenges in applying this type of algorithm is computational complexity, which depends on evaluating the fitness function. Moreover, they can be defined as methods for solving constrained and unconstrained problems based on natural selection [55].

In the following thesis work, utilizing the *Wallacei* plugin, the type of genetic optimization algorithm to be used will be the Non-dominated Sorting Genetic Algorithm-II (NSGA-II) which is an elitist evolutionary algorithm equipped with a fast non-dominated sorting algorithm and a crowding distance parameter to obtain a differentiated set of solutions. It represents the current state of the art in evolutionary multi-objective optimization algorithms as it solves the fundamental problem of this category of algorithms, namely the inability to distinguish between solutions based on their trade-offs and distribution [56]. In the case of the NSGA-II algorithm, the relative distances between data points and the Pareto Front are used to sort or classify solutions for pairing and reproduction[57]. Like all genetic algorithms, its operational workflow can

be represented as shown in Fig.3.5.
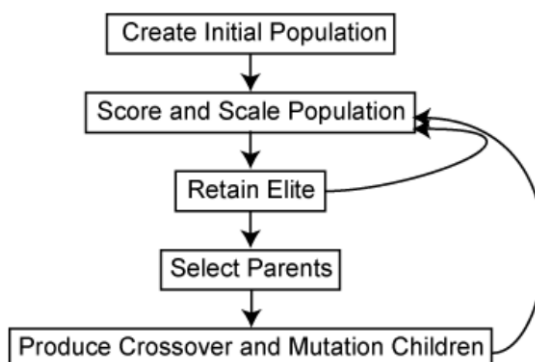
Figure 3.5: Genetic Algorithms logic[55].

From the initial population, each component is evaluated through a score that defines a scale; subsequently, a selection based on specific rules occurs, where the selected solutions become the *parents*, contributing to the formation of the next generation of the population. These are then combined to create the solutions of the next generation using crossover rules; mutation rules are used to make random modifications to the *parent* solutions, giving rise to the *offspring* solutions. This process continues until a specific number of generations is reached, or until an optimization convergence criterion is satisfied[57].

As will be shown below, several studies on SBOM are conducted by incorporating EAs into the energy simulation process due to their properties; however, some studies have also been conducted on the evaluation of the implementation of PSO with energy simulation.

3.3.2 Literature review on SBOM

Once the logic behind optimization algorithms is understood and those best suited to managing the typical complexity of building energy performance simulations, namely stochastic ones, are identified, the numerous advantages that this approach could provide during the early design stages can be inferred. The implementation of SBOM could ensure the evaluation of only optimal alternatives for building design, thus avoiding the need to revise them in later stages of the design process. The risk associated with the application of this working methodology is related to the loss of influence of the designer in guiding the creative process: machine automation is difficult to combine with quality-defined objectives; this can be avoided, according to Negendahl K. et. al. [58],

if the optimization methodology developed is able to assist experts during the design stages, facilitating the generation of integrated solutions to support the decision on the most suitable design alternatives for the specific case study. In fact, in the application of a multi-objective optimization algorithm, as would be required during the initial design stages, various competitive objectives are analyzed, but among all the selected solutions, only one must be optimal, and the evaluation of this cannot be detached from the presence of a decision maker, whose responsibility is the one of select a subset of solutions from those generated and find the one that is most suitable for the application considered[52]. With the aim of combining qualitative analysis, carried out by an expert downstream of the optimization process, and quantitative analysis, typical of the application of optimization algorithms in the early design stages, a simplified method for the energy optimization of an entire building is defined in [58]. The main features of the study are summarized in Tab.3.2:

Table 3.2: Main features of the [58] study.

Tools	Objective
Grasshopper3D's plugins Ladybug/Honeybee Termite	Evaluation of daylight
	Evaluation of building energy consumption
Hourly quasi-steady-state method developed in Python and based on ISO 13790	Evaluation of thermal overheating
Semplifications	
Reduction of the number of simulation steps carrying out simulations only during hours in which direct solar irradiance affects a given area	
Number of annual hourly sun vectors reduced to avoid to use the ones corresponding to all hours of the year	
Division of internal spaces in proxy zones rather than using the real internal division	

Once the model with the simplifications described above has been created, four different objective functions are defined, including building energy use, facade capital cost, daylight availability, and thermal requirements of the building. A multivariate optimization procedure was then developed, with a population size of 300 runs over 32 generations of SPEA2, which is a strong Pareto evolutionary algorithm: it uses an external archive that includes non-dominated solutions and is updated after each generation; for each solution, a strength value is evaluated, and based on this, the fitness function is evaluated for each individual [59]. This algorithm allows obtaining a set of solutions that are graphically represented, in order to identify the values of the previously defined fitness functions for each solution and obtain a Pareto front, to be used

as support for the evaluation of different valid design alternatives; the final goal of the study is not to consider the optimization method as a process defined for identifying the shape of the building, but simply as a support for extracting valid information from an open-ended design problem, thus emphasizing the importance of the presence of a decision maker who ultimately selects the best solution.

The same objective is pursued in the study by T. M. Echenagucia [60], which instead uses an NSGA-II algorithm, appropriately modified to exchange information with the *EnergyPlus* building energy simulation tool. In this case, the multi-objective optimization aims to minimize the energy demand of the building for heating, cooling, and lighting of a case study, i.e., an open-space office building, considering variables such as the number, position, shape, and type of windows, and the thickness of masonry walls. The same analysis was repeated for four different locations, namely Palermo, Turin, Frankfurt, and Oslo, in order to evaluate how the climate impacts the selection of alternatives that optimize the aforementioned objectives. From the results, it was possible to demonstrate that the shape of the Pareto front for all climates is similar, while a high level of contrast between heating and cooling requirements, and between cooling and lighting, is characteristic of all locations considered; on the contrary, there is little contrast between heating and lighting. Of particular interest is the analysis carried out to evaluate the statistical variation of the values that the input variables assume in all non-dominated solutions, which allows providing important information about the design variables in the early design stages of a building; the authors, therefore, selected a box plot representation for the investigation of the statistical variation of the inputs for the non-dominated solutions. This allows understanding the properties of the optimal solution set, and considering a broader knowledge of the optimal set itself, it could be useful for carrying out a true post-Pareto analysis by an expert: the set of optimal solutions could represent a pre-processed material to be used as a starting point for project development [60].

When considering various scenarios for the energy efficiency improvement of a building, it is necessary to evaluate the effects that these scenarios generate on the building and the related community in terms of direct and indirect benefits, such as energy savings, reduction of CO_2 emissions, indoor environmental quality, as well as macroeconomic benefits. A vast framework of international standards addresses the economic aspects related to building efficiency and

includes reference standards depending on whether the environmental, social, and economic performance of the building is considered. An example is EN 15643:2021, *Sustainability of construction works - Framework for assessment of buildings and civil engineering works*, which refers to all three types of performance that can be used to characterize a building. One of the most commonly used methods for conducting a cost-optimal analysis for the energy efficiency improvements of a building involves evaluating, for each of the energy efficiency alternatives that can be applied to the studied building, a parameter representing the building's energy performance following the application of each alternative and the overall investment cost associated with it, in order to graphically represent the results for each retrofit solution and define a front of solutions that can be considered cost-effective. Considering the exploration of alternatives that can be considered cost-optimal already in the initial design stages to ensure the realization of nZEB, it is possible to consider implementing an optimization algorithm that, by varying the parameters of different design variables for specific energy efficiency measures, returns the set of most valid ones, in order to support the final choice and ensure that it occurs as soon as possible during the building project. This study was developed by Ferrara M. et al. [48] and utilizes the Practical Swarm Optimization (PSO) algorithm previously presented in Section 3.3.1. Considering the high number of possible variables associated with the cost-optimal design problem, it is necessary to make an adequate selection of these, taking into account their availability and variability on the market. Furthermore, it is essential to consider the uncertainty of the variables due to manufacturing and construction processes. Based on this, it is necessary to consider that the analyzed problem will have to deal with discrete variables; the ones selected for this study are summarized below in Tab.3.3, together with the resulting size of the search space:

Table 3.3: Optimization variables and search space size for the Ferrara M. et al. [48] study.

Optimization Variables	Results
Opaque envelope insulation thickess Type of windows Type of energy systems	Total number of variables: 9 Order of magnitude of the search space: 10^8

The implementation of PSO is applied to a case study of a single-family house in France, from which the calculation of energy demand and related

operating costs is performed through a multi-zone energy simulation on a model of the same created on TRNSYS. It is important to note that, in this study, the need for problem reduction is emphasized, as the time required for its resolution would not be reasonable in any way: therefore, the number of points for each variable is reduced by 30% or 50% compared to the original problem, and the algorithm is then started. This allows us to note that one of the fundamental problems in this type of applications is undoubtedly that of time, which is the main constraint for researchers and professionals, and which must be considered as one of the necessary elements for evaluating the quality of the algorithm's performance.

Chapter 4

Matherials and Methods

As anticipated in Section 2.4, the aim of the developed study is to analyze the building design issues in the early stages of the process, taking into account the need to comply with European and national directives to reduce the environmental impacts of the building sector and the difficulty to take the most important decisions in this direction, in a design phase in which the info about the building are limited. Therefore, a workflow process was developed to guide designers in creating an integrated design that, through the implementation of a multi-objective evolutionary optimization algorithm, identifies a set of solutions that can be considered as the best alternatives in terms of maximizing the performance of the studied building compared to a baseline. This baseline was developed in this work following the procedures outlined in Appendix G of ASHRAE Standard 90.1-2016. The selection of the optimization algorithm to use was driven by the fact that, as demonstrated in the literature review presented in Chapter 3, stochastic POA algorithms are best suited to the typical complexity of an energy simulation problem.

Following a comparison with the GET Consulting team, a selection was made of the information usually available in the early design stages, and based on this, the parameters that impact the building's energy performance and that must be defined during conceptual design in order to maximize it were selected. These variables will be the ones the optimization process must evaluate to identify optimal design alternatives in terms of energy performance.

The literature review done in Chapter 3 also suggests that developing a parametric modeling of a building is often considered adequate for implementing an optimization algorithm within the workflow process: tools enabling

this type of design not only ensure simplification of modeling but also automate and ensure interoperability of simulation tasks for various alternatives. For these reasons, *Rhino Grasshopper* was chosen as the modeling support, through which the multi-objective optimization plug-in *Wallacei*, along with *Ladybug*, *Honeybee*, and *Ironbug*, can be used. The former, *Ladybug*, integrates standard *EnergyPlus* weather files (in *.epw* format) into the design environment through a user-friendly interface that speeds up the calculation process. Moreover, it is used to create graphical representations of simulation outputs, which are essential for decision support. The second, *Honeybee*, is employed to create and visualize simulation results for natural lighting using Radiance and energy simulation using *EnergyPlus* and *OpenStudio* through a connection between *Rhino Grasshopper*'s CAD environment and the simulation engine. The *Ironbug* plug-in allows detailed modeling of HVAC systems in the building, containing various blocks representing typical elements of building services solutions used in the residential and non-residential sectors, along with pre-made models for specific types of systems, provided within a rich library.

The study begins with the analysis of a case study provided by GET Consulting s.r.l.; using a real case for developing a working methodology rather than a box representing a simplified geometry, without any reference to a location or specific application, may lead to identifying the real difficulties encountered during a real design process. Therefore, considering the need to design the initial case study from scratch, the model of the baseline building will be defined following the Appendix G guidelines of ASHRAE 90.1-2016, as described in Section 4.2. Subsequently, the proposed design model will be developed as described in Section 4.3; in doing so, the limited information characteristic of the early design stages will be considered, and modeling will proceed with all the solutions currently used to minimize the building's energy demand, both with passive strategies and with the choice of energy generation systems and HVAC systems with high efficiencies and reduced environmental impacts.

Once the models of the baseline building and proposed design are created, the optimization process will be defined. For the case study, it was decided to test the effectiveness of two different approaches to the problem: the first involves dividing the optimization procedure into two phases (*Sequential Optimization*). During the first phase, the design of the building's passive components, such as the extension of glazed components or the properties of shading components,

will be evaluated. Once the user selects the optimal alternative from those evaluated by the optimization process, the second phase will proceed to optimize the properties of the photovoltaic system, whose location was identified in the previous phase, and to select the type of HVAC system best suited to meet the building's needs while minimizing its environmental impact. The second approach (*Integrated Optimization*), instead, involves considering both the variables related to the building's passive components and those of the building services components in a single optimization phase, to assess the possibility of identifying trade-off solutions for all building components, which often have interdependencies.

Both optimization procedures are based on selecting appropriate ranges of variation for the selected variables, as well as defining one or more objective functions to represent the objectives typically pursued in the design stages, i.e., minimizing environmental impact while complying with current regulations.

4.1 Case Study

The case study provided by GET Consulting s.r.l. pertains to an office building located in Turin; it is an existing building but will undergo renovation in the coming months and consists in one conditioned basement level and three conditioned above-ground floors. In the Appendix, the floor plans and sections of the real building under study can be found.

Consistently with what was done in [25], a series of simplifications were made starting from the case study, in order to facilitate modeling and consider typical conditions of the early design stages. Therefore, a simplified geometry of the building was considered, while still ensuring the preservation of the conditioned surfaces and volumes of the actual building. In doing so, the actual dimensions of the basement level and all above-ground floors were taken into account except the attic, for which the total volume was calculated in order to represent it in a geometrically simpler manner, associating it with the average height and the floor area of the respective floor. From Fig.4.1 to Fig.4.4, the geometry of the building, created using *Rhino Grasshopper*, is presented, while the geometrical dimensions considered for the model are summarized in Tab.4.1. The fundamental geometric features for the energy modelling and simulation of the building model are presented in Tab.4.2.
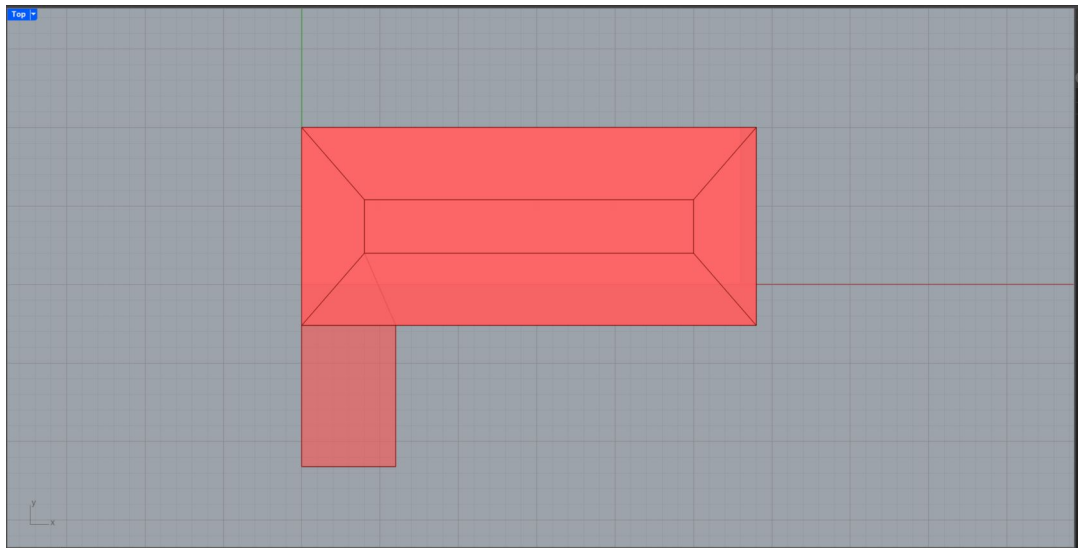
Figure 4.1: Top view of the Geometrical model of the case study.
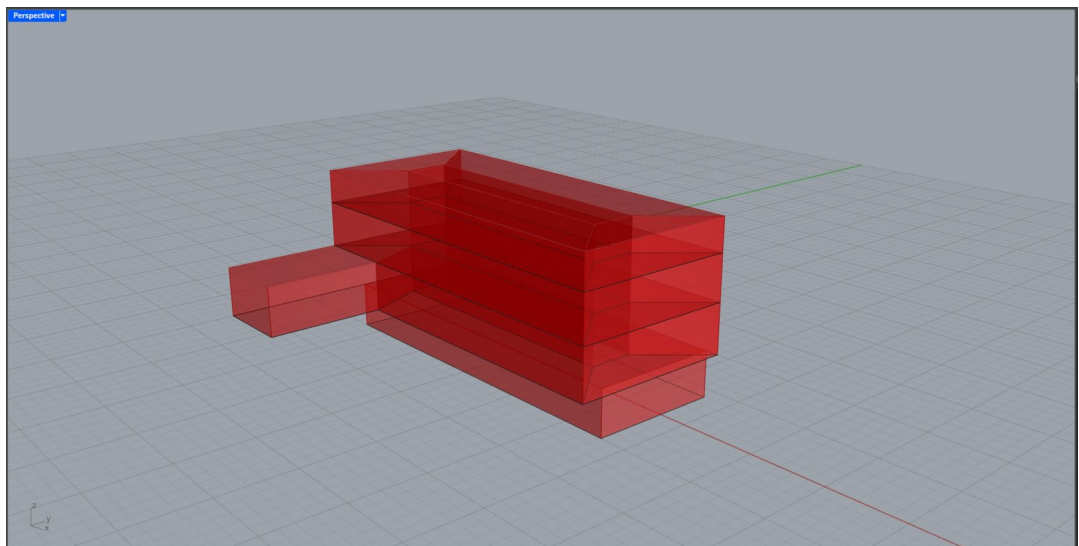
Figure 4.2: Perspective view of the Geometrical model of the case study.
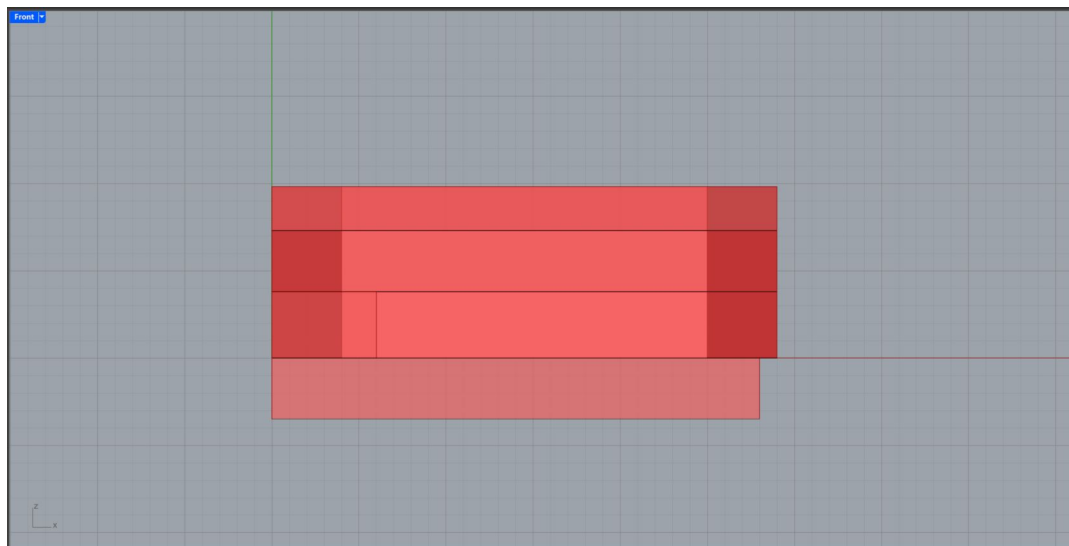
Figure 4.3: Front view of the Geometrical model of the case study.
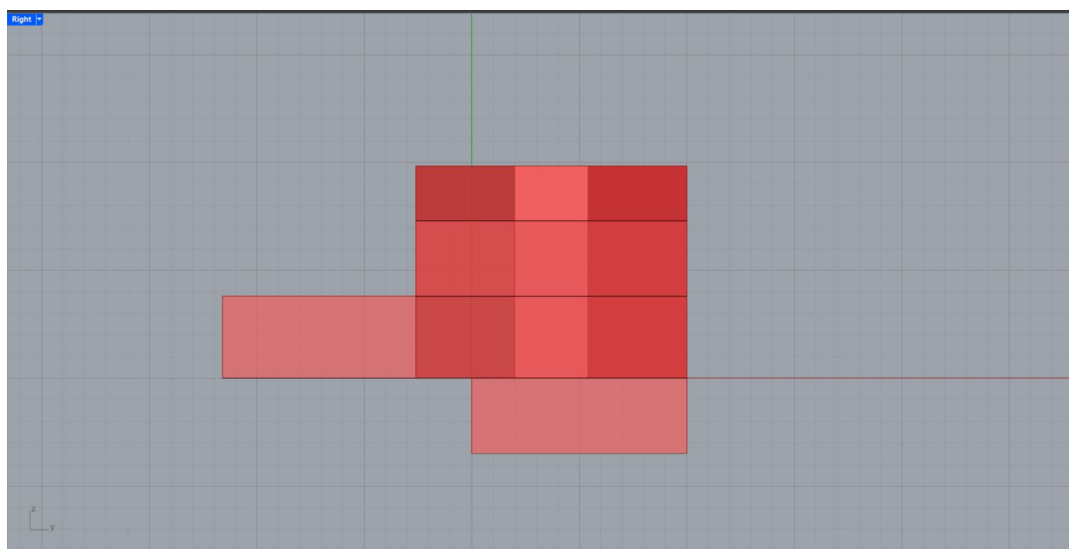
Figure 4.4: Right view of the Geometrical model of the case study.

Table 4.1: Main Geometrical Dimensions of the floors composing the building understudy.

Below-Grade Floor Height	3.50 m
Ground Floor Height	3.80 m
First Floor Height	3.50 m
Second Floor Height	2.54 m
Below-Grade Floor Lenght	28.00 m
Ground Floor Lenght - Eastern Facade	29.00 m
First Floor Lenght	29.00 m
Second Floor Lenght	29.00 m
Below-Grade Floor Width	10.00 m
Ground Floor Width - Southern Facade	12.60 m
Ground Floor Width - Northern Facade	21.60 m
First Floor Width	12.60 m
Second Floor Width	12.60 m

Table 4.2: Geometrical Properties of the Case Study Building models.

Gross Floor Area	1430.2 m^2
Above-grade Floors External Surface Area	2317.3 m^2
Conditioned Volume	4780.7m^3

For the purpose of this study, it is considered to use the case study building simply in terms of its geometric properties, location, and intended use, which represent the information typically available to a designer in the initial design phases; all other characteristics, such as components of the building envelope, window dimensions, and systems, will need to be obtained from the developed workflow to ensure optimization of energy performance compared to that of the baseline building. The assumption of the available information is crucial for considering the requirements with which the baseline building and the proposed design must align in their definition, following ASHRAE regulations.

4.1.1   Location and Climate data

The building location, Turin, corresponds to a number of degree days of 2617 and, therefore, according to DPR 412/93, to a Climatic Zone E. For the assessment of the ASHRAE Zone, the *Ladybug* plug-in can be utilized: it allows obtaining the *.url* of the climate file[1], converting it into a *.stat* file, and calculating the ASHRAE Zone, which in this case is 4A. The information regarding the climatic zone and the ASHRAE Zone will be crucial for applying, respectively, the limits stipulated by Italian regulations and ASHRAE regulations in the development of the baseline building and proposed design model.

The building under study is located in a densely urbanized area, surrounded by several other buildings whose shading effect on the studied building needs to be considered. This effect depends not only on the height and position of the surrounding elements but also on the orientation of the studied building and the path of the sun in the sky, which varies according to the latitude of the area where the building is situated; to account for this shading, a simplified representation of the surrounding buildings is utilized, as depicted in Fig.4.5, where the solar diagram obtained through the *Ladybug* tool is also visible.
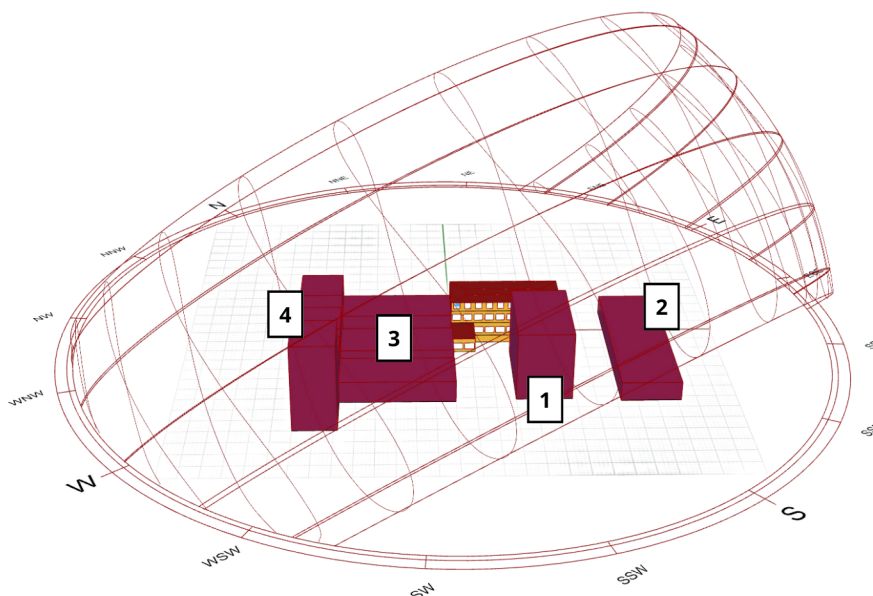
Figure 4.5: Sun Path of the case study location.

---

[1] `https://energyplus-weather.s3.amazonaws.com/europe_wmo_region_6/ITA/ITA_Torino-Caselle.160590_IGDG/ITA_Torino-Caselle.160590_IGDG.zip`

Fig.4.5 was obtained using the corresponding *.url* link for the building's location and its orientation, given by a 40° counterclockwise rotation relative to the y-axis reference. It is evident that during most hours of the year, the building's facades most exposed to solar radiation are those with the greatest extension, namely those facing South-West and North-East. However, for the first orientation, it is possible to notice the presence of building 1 with an height of 18 m[61], which casts significant shading on it, probably reducing solar gains in the summer season but also leading to an increased demand for artificial lighting. As for the other buildings within 20 m of the case study, for the ones named as 2 and 3, an height of 5.7 m is considered, as they are residential buildings with a maximum of two floors. Regarding buildings 4, which are further away and characterized by an height of 12 m with the exception of the one on the westernmost location, corresponding to 23 m of height, the shading effect they will have on the studied building is more limited, almost negligible.

The minimum and maximum dry bulb temperatures of the location, along with its latitude, longitude, and elevation, are reported in Tab.4.3.

Table 4.3: Case study site info.

Dry Bulb Temperature Info	
Maximum Dry Bulb Temperature	31°C
Minimum Dry Bulb Temperature	- 6°C
Location Info	
Latitude	45.18° North
Longitude	7.65° East
Elevation	282

Starting from the *.epw* file corresponding to the studied location and the geometry of the building and its surrounding context, it is possible to derive information regarding the solar radiation incident on the building itself, as shown in Fig.4.6:
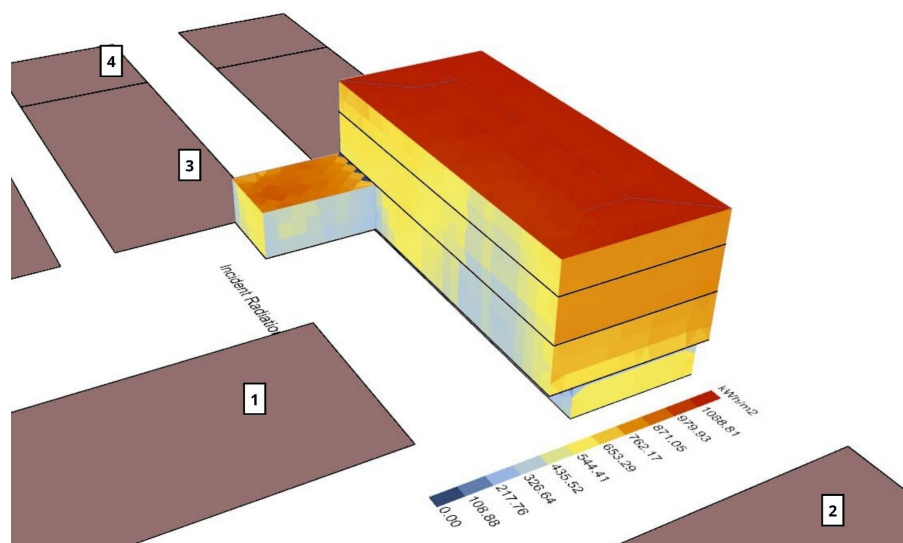
Figure 4.6: Solar radiation incident on the understudy building.

This representation can be useful to gain insight into the energy incident on the various surfaces of the building due to solar radiation and, therefore, can be a valuable tool for evaluating the placement of a photovoltaic system for on-site electricity generation. Naturally, the surface with the highest solar energy reception is the roof; additionally, a significant proportion is observed on the terrace; the facade corresponding to the latter receives a greatly reduced energy share, possibly due to the presence of the building 1, which casts obvious shading even on the southwest-facing facade.

Additional information regarding the trends of dry bulb temperatures, relative humidity, and direct, diffuse, and global solar radiation are presented in Appendix.

4.2   Baseline Building Model

In defining design alternatives aimed at improving a building's performance, it is imperative to reference a specific benchmark which must be defined to account for the typical boundary conditions of the considered building, considering both the climatic conditions of the location and the building's intended use, as well as the state of the art of the building stock in the considered context. For instance, imagine optimizing the energy performance of a school in a rapidly developing city like Nairobi: in such a context, where the building stock generally exhibits lower energy performance compared to that of a typical

European country, it would be nonsensical to use a similar type of building as a benchmark for evaluating the performance improvement resulting from energy efficiency measures. Because of this, the definition of a baseline building has always to be performed using a reference standard.

Currently, there is no globally shared methodology for defining a reference building, and various entities have provided different approaches; within Annex III of the EPBD, for instance, reference buildings are described as *buildings characterized by and representative of their functionality and geographic location, including indoor and outdoor climate conditions* [62]. Generally, it can be stated that the definition of a reference building depends on the purpose of the study. In Appendix G of ASHRAE 90.1-2016, for example, the *Performance Rating Method* is described, which allows defining how much a building outperforms a benchmark, called the baseline building, and the methodology to define the latter is provided. In evaluating the LEED EAp Minimum Energy Performance score, reference is made to these guidelines, and considering that the workflow under development may be used for these kinds of voluntary certifications, it was decided to follow the same ASHRAE standard in this study. Specifically, according to its Appendix G, the Baseline Building must have the same number of floors and the same conditioned floor area as the proposed design, and all simplifications made to the proposed design must also be reflected in the baseline. For these reasons, the same geometric model presented in Figs. from 4.1 to 4.4 is considered for both models.

4.2.1 Baseline Building Envelope

Considering the assumption made regarding the information from the case study used in the development of the energy models for the baseline building and the proposed design, it is possible to assume the building's footprint is known, thus its orientation is given, while information about the dimensions of transparent components is unavailable. This results in two significant consequences:

1. The area of transparent surfaces for the baseline building is fixed and defined by regulations based on the building's intended use and gross conditioned floor area. For the case study, this area falls between 465 and 4650 m^2 (ASHRAE thresholds) as shown in Tab.4.2, resulting in a percentage of exterior wall surface area corresponding to transparent components of 31%.

2. The baseline building performance should not be defined by rotating the model by 90°, 270°, and 360° relative to the initial orientation, as the vertical surface of window components varies by less than 5% for different orientations, given that a windowed area of 31% is associated, as stated at the previous point, to be evenly distributed across the facades of the four orientations.

Regarding shading components, in ASHRAE 90.1 Appendix G it is specified that these should not be considered for the baseline building, therefore they are not represented its model.

Constructions of opaque and transparent components must adhere to the requirements provided by ASHRAE 90.1 standard based on the ASHRAE Zone and whether the building is residential, non-residential, or semi-heated[2]. The selection of construction is made from those available in the *Honeybee* plug-in library: first, it is necessary to select the basic construction set from those available, by choosing the corresponding ASHRAE zone of the building. Once this is done, modifications are made to the construction of the various components of the envelope so that they have thermal properties compliant with the values specified in the standard for Zone 4A and Non-Residential buildings. Tab.4.4 presents the construction associated with each component of the building envelope selected for the baseline building model.

---

[2]ASHRAE Standard 90.1-2016 from Tab. 3.4-1 to Tab. 3.4-8.

Table 4.4: Baseline Building Envelope Constructions.

Building Envelope Component	Construction	U $[W/m^2K]$	SHGC [-]
Roof	Typical IEAD Roof - Highly Reflective - R16	0.329	
External Walls	Typical Insulated Steel Framed Exterior Wall-R12	0.428	
Below-Grade Walls	09J908-3::EPS insulated wall_15p::K0.22	0.221	
Slab-on-Grade Floors	Adiabatic GroundContactFloor	0.001	
Exterior Doors	Generic Exterior Door	1.002	
Below-Grade Floor	Typical Insulated Carpeted 8in Slab Floor-R5	0.853	
Window	ASHRAE 189.1-2009 ExtWindow ClimateZone 4-5	2.568	0.363

Within Table G3.4-4 of the standard, certain types of building components do not have a defined limit value for transmittance. This occurs for Below-grade walls and Slab on Grade Floors, for which the following are provided, respectively:

- C-factor, which is the time rate of steady-state heat flow through unit area of the construction, induced by a unit temperature difference between the body surfaces w without including soil or air films. It is measured in W/m^2K [63].

- F-factor, which represents the heat transfer through the floor, induced by a unit temperature difference between the outside and inside air temperature, on the per linear length of the exposed perimeter of the floor. It is measured in W/mK [63].

Since the C-factor value is not available in the plug-in libraries, it was decided to approximate its value with that of transmittance. Regarding the F-factor, its evaluation was possible following the calculation of the perimeter of the basement floor in contact with the ground: this latter has a width of 28 m and a depth of 10 m, resulting in a perimeter of 76 m. By multiplying the transmittance values of the available floor constructions in the plug-in libraries by the calculated perimeter, it was possible to make a selection of the Slab on Grade Floor component in accordance with the ASHRAE limit. The thermal transmittance value reported in Tab.4.4 corresponds to an F-factor of 0.043 W/mK.

Please note that the construction associated with the Below-Grade floor has been selected retaining the default alternative provided by the *Honeybee* plug-in in the construction set defined based on the climatic zone of the building itself.

4.2.2   Baseline Building Thermal Zones Definition

In whole-building energy simulation programs, the division of the building into thermal zones is a crucial required input; during the history, different terms associated to the same fundamental concept have been defined from different istitutions, like the ones of Thermal Blocks, Thermal Zones, and HVAC Zones. Despite the importance of this definition, to date, there is no universally recognized methodology for performing this division, so various organizations provide guidelines that can support designers[64]. For example, according to ASHRAE 90.1-2016, an HVAC zone is defined as *a space or group of spaces within a building with heating and cooling requirements sufficiently similar to maintain desired conditions throughout using a single sensor*. The Appendix G of the same standard provides basic rules for the division into thermal zones, which have been applied to the case study to divide the baseline building and proposed design models as follows:

- Each above-ground floor was divided into perimeter and core zones; perimeter zones are those within 4.6 m from the external walls of the building, while core zones are beyond that distance. For the particular case of the basement floor, it was considered as a single thermal zone.
- Rooms on different floors were assigned to different thermal zones.
- Perimeter zones were further subdivided based on their major orientation.

Thermal zones obtained are represented in Fig.4.7.
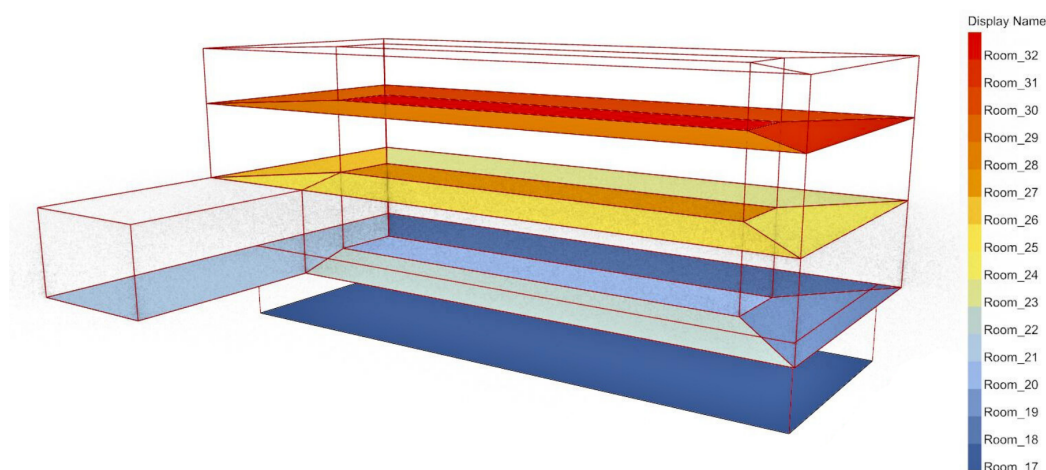
Figure 4.7: Thermal Zones Subdivision of the case study building.

As can be seen, the basement floor is treated as a single thermal zone (*Room_17*), while the perimeter zones of all floors are divided by orientation. Taking into account that the actual building is rotated 40° counter-clockwise from north, the four facades of the building are considered oriented in the four different directions, obtaining the perimeter thermal zones division summarized in Tab.4.5. The remaining *Room_20*, *Room_27* and *Room_32* correspond, instead, to the core zones of the ground, first and second floor, respectively.

Table 4.5: Perimeter Zones Subdivision by Orientation.

SOUTH-ORIENTED ZONES	*Room_19, Room_25, Room_31*
NORTH-ORIENTED ZONES	*Room_21, Room_26, Room_29*
EAST-ORIENTED ZONES	*Room_18, Room_23, Room_30*
WEST-ORIENTED ZONES	*Room_22, Room_24, Room_28*

4.2.3 Baseline Building Schedules

The energy performance of a building must be assessed taking into account its operation during the simulation period. In building performance simulation programs, this is done through *schedules*, which represent the values assumed during the simulation period from occupancy frequency, equipment usage, and other variables reflecting the building's temporal use, also considering differences between working and non-working days or other specifications related to the building's intended use.

In the *Honeybee* modeling plug-in, the operation of the building is modeled through the definition of the program type: by setting the building's use type (*LargeOffice* for the case study), all default schedules related to the selected occupancy type are provided, obtained from the ASHRAE standards that govern each operational component of the building. For modeling the baseline building, therefore, it has been decided to utilize these default schedules and adjust the numerical parameters associated with the lighting system power density and infiltration rate to ensure compliance with ASHRAE 90.1 Appendix G. Additionally, as for the consumption of Domestic Hot Water (DHW), considering that the building is intended for office use, it was decided to set this consumption to 0. As long as it concerns the power density related to the electric equipment, this is set, by default, equal to 16.55 W/m^2, while for the occupancy, the plug-in considers a population density of 0.061 people per square meter of floor area.

Regarding the power density of the *lighting system equipment*, it has been chosen to utilize the surface-based definition method, where the power density is determined based on the building's occupancy type: for offices, it should be set at[3] 11.06 W/m^2.

As for the infiltration rate, Appendix G of ASHRAE 90.1 mandates it to be 2.03 $L/(s \cdot m^2)$ when the imposed difference of pressure is 75 Pa, and it delineates how to convert this rate based on how the building performance simulation program calculates it. In the particular case of the *Honeybee* plug-in, the infiltration rate is defined in m^3/s per m^2 of external facade area, thus requiring the application of the conversion equation 4.1

$$I_{AGW} = 0.112 \cdot I_{75Pa} \cdot \frac{S}{A_{GW}} \tag{4.1}$$

where:

- I_{75Pa} is the air leakage rate of the building at a difference of pressure of 75 Pa, equal to 2.03 $l/(sec \cdot m^2)$;
- S is the external surface of the building envelope, equal to 2317.3 m^2 for the case study considered;
- A_{GW} is the surface of the external facade, equal to 887.1 m^2 for the case study considered.

---

[3]ASHRAE Standard 90.1-2016 Appendix G, Table G3.8

The obtained value is equal to $5.94 \cdot 10^{-4} \ m^3/sec$ per m^2 of external facade area.

As for the powers and schedules of the electrical equipment used within the building, default values are considered, which the *Honeybee* plug-in automatically selects based on the chosen building type (*LargeOffice*).

A key element in ensuring the thermal comfort of building occupants is the determination of setpoint and setback temperatures, which must be maintained through the use of a properly sized HVAC system. In the case study, schedules have been defined to indicate the internal temperatures to be maintained, which vary depending on the occupancy of the building. As indicated in the ASHRAE 90.1 Appendix G standard, these schedules are the same for both the baseline building and the proposed design. The details of the schedules are summarized in Tab.4.6.

Table 4.6: Winter and Summer setpoint and setback temperatures.

Winter Setpoint Temperature	20.0°C
Summer Setpoint Temperature	26.0°C
Winter Setback Temperature	14.4°C
Summer Setback Temperature	28.8°C

Note that:

- the winter setback temperature is obtained by subtracting 5.6°C from the setpoint temperature for the same season, while the summer setback temperature is obtained by adding 2.8°C to the setpoint temperature for the same season. These values have been selected as indicated in the above standard for the sizing of HVAC systems.

- setpoint temperatures are maintained within the indoor environment during its occupancy period, which runs from 9:00 A.M. to 5:00 P.M. on all weekdays (Monday to Friday), while setback temperatures are those maintained during periods when the indoor environment is unoccupied, from 5:00 P.M. to 9:00 A.M. and during all weekend and holiday days.

The temperature setpoint and setback schedules for the winter season are shown in Fig.8.10, while those for the summer season are depicted in Fig.8.11 of the Appendix.

In the definition of setpoints, the *Honeybee* plug-in also provides the option to include information about the cut-out temperature, defined as *An optional positive number for the temperature difference between the cutout temperature*

and the setpoint temperature. Therefore, this parameter allows defining a range within which it is acceptable for the room to be slightly over-heated or over-cooled compared to the setpoint temperature, in order to prevent the HVAC system from turning on for just a few minutes, thus extending the lifecycle of its components. In this study, it was decided to set this value to 2°C.

Finally, following the specifications of ASHRAE 62.1, it has been stipulated that within the indoor environment, a setpoint value of relative humidity must be ensured, in order to guarantee not only thermal comfort but also the hygrometric comfort of the occupants: this value is set at 65%, both for the summer and winter seasons, meaning that the humidification and dehumidification setpoints coincide. However, this setpoint will be inserted into the model only after the modeling of the HVAC system, as it can't be reached without it, taking into account just the passive strategies implemented into the building.

4.2.4   Baseline Building HVAC System

According to Appendix G of the ASHRAE 90.1 standard, the HVAC system associated with the baseline building must be selected considering specific characteristics of the building, which are summarized in the Tab.4.7 with the correspondent values related to the case study.

Table 4.7: HVAC system selection elements for the baseline building.

Building Type	Large Office
Number of Floors	4 floors, 3 above-grade and 1 below-grade
Gross Conditioned Floor Area	1430.2 m^2
Climate Zone	ASHRAE Zone 4A

Based on the values presented above, it is possible to affirm that the building under study refers to a non-residential building, with a total of 4 floors (3 above ground and 1 below ground) with a floor area of less than 2300 m^2, for which the system to be installed corresponds to that defined in the ASHRAE 90.1 Appendix G as *System 5*[4]. In it, hot water generation is ensured by a condensing boiler powered by fossil fuels, particularly natural gas, while cold water generation is provided by a DX (Direct Expansion) compressor with

---

[4]ASHRAE 90.1-2016 Appendix G, Table G3.1.1-3 and Table G3.1.1-4

a variable speed. The fan used to take air from the outdoor environment is a variable volume model, as are the air terminals, which also have reheat capability. The hot water produced by the boiler feeds the heating coil of the AHU and the re-heat coils of the VAV air terminals, while the cooled water produced by the compressor supplies the cooling coil of the AHU. The system thus appears to be an all-air system, without water terminals: both winter and summer thermal loads are entirely satisfied by the AHU. The modelling of the components of the system was done using the *Grasshopper* plug-in called *Ironbug*, which has in its libraries different HVAC systems already modeled, among which the *System* 5 required for the baseline building.

The Appendix G of the standard specifies that it is necessary to consider different HVAC systems for each floor composing the building, but in cases where the floors are characterized by identical thermal blocks, these can be grouped together to simplify the modeling. Based on this statement, for the baseline building, it was considered to install three different HVAC systems, characterized by the same components as mentioned above. Referring to the subdivision of the building into thermal zones described in Section 4.2.2, Tab.4.8 presents the zones to which each HVAC system refers.

Table 4.8: Rooms of the model assigned to each HVAC system.

HVAC System, Below-Grade floor	*Room_17*
HVAC System, Ground floor	*Room_18, Room_19, Room_20, Room_21, Room_22*
HVAC System, First and Second floor	*Room_23, Room_24, Room_25, Room_26, Room_27, Room_28, Room_29, Room_30, Room_31, Room_32*

Despite the fact that a general schematization of the *System 5* is already provided by the *Ironbug* plug-in, it was necessary to apply some changes to it in order to guarantee a modelling compliant with the ASHRAE 90.1 Standard. In order to do so, the steps described below were followed.

Appendix G of the ASHRAE standard used for the creation of the baseline building model stipulates that, for systems characterized by Variable Air Volume (VAV) terminals, the fans that draw in outside air for use within the spaces must be variable speed; furthermore, it is necessary to ensure their operation during all hours when the building is occupied. Therefore, considering the

occupancy conditions referenced in the definition of setpoint temperatures in paragraph 4.2.3, operating schedules for the outside air intake fan are defined as shown in Fig.8.12 in the Appendix. The part-load behavior of the fan has been modeled for the purposes of this study by defining the coefficients of the fan part-load power equation, which is presented in Table G3.1.3.15 of the standard itself and summarized below 4.2:

$$P_{fan} = 0.0013 + 0.1470 \cdot PLR_{fan} + 0.9506 \cdot (PRL_{fan})^2 - 0.0998 \cdot (PRL_{fan})^3 \ (4.2)$$

the terms of which are specified in the Nomenclature. The numerical coefficients specified in equation 4.2 have thus been used within the model to ensure compliance with the standard.

Regarding VAV air terminals, the minimum air volume to be enforced is defined as 30% of the maximum between:

- maximum air flow rate of the zone;
- minimum outdoor air flow rate;
- air flow rate required by standards.

The regulation specifies the need to add or omit certain components from the system, depending on the boundary conditions of the analyzed building and the type of system installed in the building for which it was necessary to generate the baseline model. Given that it is assumed a scenario where the proposed building does not yet exist, only the boundary conditions will need to be referenced to assess the need for component installation. For these reasons, considering that the standard requires the installation of an Economizer for all ASHRAE zones except 0A, 0B, 1A, 1B, 2A, 3A, and 4A, this component has not been modeled for the HVAC systems of the baseline model.

Regarding the water system, as previously mentioned, it is characterized solely by a hot water generation system represented by a boiler fed by natural gas, which supplies hot water to the hot water coil of the air handling system and the heating coils of the VAV air terminals. In this case, the regulations require the enforcement of the following:

1. Hot water supply temperature set to 82°C under design conditions;
2. Hot water return temperature set to 54°C, defined in the model by imposing a temperature difference between supply and return water of 28°C under design conditions;

3. A reset rule for water temperature based on outdoor dry-bulb temperature as summarized in Tab.4.9.

Table 4.9: Hot Water supply reset temperature rule for the baseline building model.

Outdoor Temperature	Hot Water Supply Temperature Setpoint
≤ -7°C	82°C
≥ 10°C	66°C
Between -7°C and 10°C	Linear Variation

For the pipes comprising the water system, it is also unnecessary to define pressure drops.

Finally, it is necessary to properly size the natural gas-fired boilers and determine the minimum air flow rate that must be drawn by the outdoor air fan for each system. As long as it concerns the sizing of the boilers of each HVAC of the building previously described and the selection of the corresponding minimum efficiencies required by the standard, the process involves incorporating, into the baseline model, the option for sizing the active building components, specifying the sizing factors provided by the standard, which are 1.25 for heating and 1.15 for cooling. Once the simulation is initiated, it is possible to read the sizes of the generation components. The capacity results obtained from the aforementioned simulation are presented in Tab.4.10 and they all correspond to the minimum efficiency of the 80% obtained from ASHRAE 90.1-2016 Appendix G.

Table 4.10: Boiler capacities of the HVAC Systems for the baseline model.

Below-Grade Floor Boiler Size	Ground Floor Boiler Size	First and Second Floor Boiler Size
6252.92 W	33039.66 W	65830.5 W

These results were obtained by considering the assessment of the air flow rate drawn by the external fans which results from imposing a difference between:

- the setpoint temperature of the indoor spaces
- the temperature of the outdoor air

equal to 11°C in design conditions. This was achieved in the model by considering a design supply air temperature of 31°C and 15°C respectively in

the winter and summer seasons. Additionally, the standard mandates an equal split of the total capacity previously acquired into two distinct boilers, aiming to alleviate the load on each if the floor area served by the HVAC system is higher than 1400 m^2; in the case study, however, it has been proceeded by dividing the whole building into three different groups of rooms served by different HVAC systems, and because of this to each of them an area lower than the aforementioned limit corresponds. Due to this, only one boiler for each system is maintained.

The calculation of the minimum airflows that each AHU fan must draw from the outdoor environment is performed following ASHRAE 62.1-2016 standard, which requires calculating this value using three different methodologies:

- *Method 1*: By imposing, as done for the boiler sizing, a temperature difference of 11°C between indoor setpoint temperatures and supply air temperature.
- *Method 2*: Following the ventilation rate procedure, which aims to calculate the outdoor air intake flow V_{ot} based on space type, occupancy level, and floor area.
- *Method 3*: Evaluating the outdoor air flow rate that ensures adequate Indoor Air Quality (IAQ) within the spaces.

The first approach is the same as described earlier for calculating the capacities of the HVAC system generators in the building based on the imposition of a difference of temperature of 11°C between the supply air and the indoor temperature setpoints, as done before for the generators sizing. The second approach, instead, requires executing the calculation of a series of intermediate parameters presented in the standard that ultimately allow deriving V_{ot}; these steps are presented below.

1. Outdoor airflow rate in the breathing zone V_{bz} calculation through 4.3:

$$V_{bz} = R_p \cdot P_z + R_a \cdot A_z \qquad (4.3)$$

where R_p and R_a values are given in Table 6.2.2.1 of the ASHRAE 62.1-2016 standard, while P_z is considered equal to the value given by default from the *Honeybee* plug-in and so 0.061 $pers./m^2$

2. Zone outdoor airflow V_{oz} defined as in 4.4:

$$V_{oz} = \frac{V_{bz}}{E_z} \qquad (4.4)$$

The E_z value is chosen among the ones available for different air distribution terminals in Table 6.2.2.2 of the ASHRAE 62.1-2016 standard; considering a ceiling supply of warm air with a temperature of 8°C or more above space temperature and ceiling return, E_z is equal to 0.8.

3. Total outdoor air flow rate for an AHU serving more thermal zones V_{ot} given by the equation 4.5:

$$V_{ot} = \sum_{zones} V_{oz} \tag{4.5}$$

Definitions of all the parameters used from equation 4.3 to 4.5 are presented in the Nomenclature. For the case study, it was decided to separately consider the perimeter zones and the interior zones for calculating the outdoor air flow rate taken by the fan of each HVAC system, computing V_{bz} for each and then summing V_{ot} over them.

Regarding the third calculation methodology, it was decided to consider the procedure indicated for evaluating minimum IAQ flow rate provided by the Italian standard UNI 10339, which stipulates that for open space offices, a ventilation outdoor air flow rate of $Q_{op} = 0.011 \ m^3/pers.$ must be ensured.

Once the calculations described above are performed, the results reported in Tab.4.11 are obtained for each method and each HVAC system, and therefore, the value used ultimately in the model. The intermediate results obtained for each HVAC system are presented in Appendix from Tab.8.1 to Tab.8.6.

Table 4.11: Summary results of the Outdoor Ventilation Airflow Rate for each HVAC System - Baseline Building.

	Below Grade Floor HVAC $[l/sec]$	Ground Floor HVAC $[l/sec]$	First and Second Floors HVAC $[l/sec]$
Method 1	858.41	2736.29	7105.48
Method 2	158.68	237.69	414.17
Method 3	188.97	283.05	493.21
Max. Value	858.41	2736.29	7105.48

As can be observed from Tab.4.11, for all HVAC systems, the maximum airflow is the one obtained by imposing a temperature difference between the supply air temperature of the system and the setpoint temperature of the spaces equal to 11°C. This is because, with no water terminals present, winter

and summer loads must be satisfied through the air terminals. Therefore, the required outdoor airflow is greater compared to, for example, that for IAQ, which is defined solely to ensure sufficient air exchange for an adequate removal of pollutants.

After determining the required outdoor air quantity for the building, it is imperative to adjust the performance of the AHU fan to ensure the fulfillment of the air demand, notwithstanding pressure losses incurred by the AHU components themselves. To achieve this, the procedure outlined in ASHRAE 90.1-2016 is followed, which involves evaluating:

- The pressure drop adjustment (PD), which represents the pressure losses associated with air passage through system components. It is evaluated using the Table 6.5.3.1-2 of the standard, in which a differend pressure drop is associated to different possible components foundable into an HVAC system.

- The design airflow rate through each device through which air passes in the system (L/s_D).

Known them, the coefficient A is calculated as per the equation 4.6:

$$A = \sum_{components} PD \cdot L/s_D/65,0000 \tag{4.6}$$

At this point, the coefficient A can be used to calculate the power of the fan to be installed in each HVAC system of the baseline using the equation 4.7.

$$kW_i \leq L/s_D \cdot 0.0015 + A \tag{4.7}$$

The components that can generate a pressure drop in the baseline building's air system are:

- Return and/or exhaust airflow control devices: corresponding to a PD of 125 Pa[5].

- Particulate Filtration Credit: considering that the building's intended use is office space, it is possible to plan for the installation of an F7 type filter, which, according to ISO 16890 standards, must guarantee a filtration efficiency for PM10 greater than 80% and for PM2.5 greater than 70%. ASHRAE standards classify filters with an efficiency defined as MERV (Minimum Efficiency Reporting Value). Therefore, the efficiency of 80%

---

[5]From Table 6.5.3.1-2 of the ASHRAE 90.1-2016.

for ePM10 and 70% for ePM2.5 is converted to a MERV 13 efficiency, corresponding to a PD of 225 Pa [5] [65].

At this stage, the evaluation proceeded by assessing the airflow rates passing through the two previously mentioned components. To perform this, it is necessary to remember that, in practical application, ventilation systems are never assumed to have precisely balanced airflow rates between intake and exhaust: the difference between them depends on the climate of the area where the system is to be installed. In general, it can be stated that in Italy and all countries in Central-Southern Europe, where winters are not characterized by extremely cold temperatures, it is necessary to ensure that the intake airflow is 10-20% higher than the exhaust airflow, ensuring that the indoor environment is always slightly pressurized. The excess airflow introduced compared to the extracted airflow ensures that there are exfiltrations to the outside, whose presence indeed ensures the absence of infiltrations and, therefore, provides complete control in terms of IAQ and thermo-hygrometry (temperature and humidity) over the airflow rates entering the building. For these reasons, concerning the return and/or exhaust airflow control device, it can be stated that the extraction airflow rate equals the design supply airflow rate divided by 1.1-1.2. Being V_{ot} the required supply airflow rate for the rooms during the design phase, it follows that $L/s_D = \frac{V_{ot}}{1.2}$. Regarding the filters, however, they are installed in the AHU to filter the incoming air and, therefore, the airflow rate passing through them under design conditions is equal to V_{ot}.

The results obtained for the three HVAC systems of the baseline building model are summarized in Appendix from Tab.8.7 to Tab.8.9, while the values of coefficient A and fan motor power kW_i, calculated respectively using equations 4.6 and 4.7, are reported in Tab.4.12, along with the corresponding fan motor efficiencies $\eta_{FanMotor}$.

Table 4.12: Fan Motor Power and Efficiency Calculation Results - Baseline Building Model.

	Below-Grade Floor HVAC	Ground Floor HVAC	First and Second Floor HVAC
A	0.435	1.386	3.598
kW_i	2.2 kW	1.4 kW	3.6 kW
$\eta_{FanMotor}$	87.5%	84.0%	87.5%

Please note that the fan motor efficiencies are derived from Table G3.9.1 of the ASHRAE 90.1-2016 Standard Appendix G; specifically, in the case of obtained power values intermediate to those reported in the standard's table, a linear interpolation between the extreme values has been performed to obtain the exact value.

4.3 Proposed Design Model

The proposed design model is a concept developed, along with that of the baseline building model, in the *Performance Rating Method* of the ASHRAE 90.1-2016 standard, Appendix G: while the baseline model allows obtaining information regarding a reference performance against which to evaluate the performance of the studied building, the proposed design model allows evaluating the performance of the studied building itself and, therefore, assessing possible modifications to improve such performance and, eventually, reach a specified objective of efficiency.

For the study undertaken in this thesis work, it is assumed to be in a situation of complete design freedom of the building, in order to represent the actual conditions in which designers find themselves in the initial stages of design; for these reasons, choices will be made on design variables that already represent an optimization compared to the baseline model features defined in Section 4.2 in order to be compliant with the aforementioned standard. Furthermore, a model will be developed that can indeed be considered as parametric: many of the design variables chosen by a designer are defined in terms of ranges of variation; it will then be the optimization phase described in the following Section 4.5 that will allow the selection of optimal alternatives, in terms of maximizing performance compared to the baseline.

In this Section, therefore, the parametric model of the proposed design that has been developed is described. In doing so, it is necessary to note that, due to regulatory constraints specified in the ASHRAE 90.1-2016 Appendix G standard, the proposed design model has common elements with those of the previously described baseline building model; these are listed below:

- Geometric properties: the two energy models will share the same geometric model described in the Section 4.1;

- Division into thermal zones in function of the floor of the building to which they refer, and further more in perimeter and core zones and by orientation as depicted in Fig.4.8 and Tab.4.5;

- Air infiltration rate, imposed by the standard equal to 2.03 $l/(sec \cdot m^2)$ at a difference of pressure of 75 Pa and corresponding to $5.94 \cdot 10^{-4}$ m^3/sec per m^2 of external facade area, obtained through the conversion equation 4.1;

- Winter and Summer temperature setpoints, defined as in Tab.4.6 and with schedules imposing the setpoint to be maintained from 9:00 A.M. to 5:00 P.M. in working days (occupancy time of the office building) and the setbacks in unoccupied periods, going from 5:00 P.M. to 9:00 A.M. in working days and the whole day for non-working days; it is possible to consider Figs.8.10 and 8.11 of Appendix as reference.

- Winter and Summer humidity ratio setpoint value of 65%, implemented after the modelling of the HVAC systems;

- Operational schedules of the building, considering the ones of default given by *Honeybee* plug-in, as specified in 4.2.3.

Below, the characteristics of the proposed design that will instead differ from the baseline are specified.

4.3.1 Proposed Design Envelope

Considering that the location of the building under study is in Italy, it has been decided to perform the selection of the construction for each component of the building envelope from the *Honeybee* plug-in library, ensuring compliance with the limits set by the Ministerial Decree Minimum Requirements of June 26, 2015, Appendix A, for Climatic Zone E. Tab.4.13 summarizes the constructions associated with each component of the building envelope selected for the proposed design model, along with the corresponding parameter values that were decisive for their selection. Specifically, the latter was conducted among the constructions that refer to the Construction Type indicated in the *Honeybee* plugin as "Mass".

Table 4.13: Proposed Design Building Envelope Constructions.

Building Envelope Component	Construction	U $[W/m^2K]$	SHGC [-]
Roof	Typical IEAD Roof - Highly Reflective - R26	0.208	
External Walls	Typical Insulated Exterior Mass Wall-R22	0.252	
Below-Grade Walls	Typical Insulated Exterior Mass Wall-R22	0.252	
Slab-on-Grade Floors	Typical Insulated Exterior Mass Floor-R27	0.207	
Exterior Door	Typical Insulated Metal Door-R3	1.445	
Below-Grade Floor	Typical Insulated Exterior Mass Floor-R24	0.223	
Window	U 0.19 SHGC 0.20 Trp LoE Film (55) Bronze 6mm/13mm Air	1.223	0.220

Comparing Tab.4.4 and Tab.4.13, two observations can be made:

1. The thermal transmittance values for the baseline building are higher compared to those used for the proposed design for the majority of the building envelope components. This implies that heat losses through the building envelope towards the outdoor environment will be significantly reduced in the case of the proposed design, resulting in lower energy demand compared to that of the baseline building, as will be demonstrated later in the results Chapter 5.

2. The construction associated with the exterior door was not manually selected, but rather the default one provided by the *Honeybee* plug-in for external doors in the construction set corresponding to ASHRAE Zone 4A was adopted.

4.3.2 Window-to-Wall Ratio of the Facades for the Proposed Design

One of the fundamental differences between the baseline building and the proposed design models lies in how the extension of the transparent components relative to the external facade of the building, known as the WWR, is defined. For the baseline building model, the ASHRAE 90.1-2016 standard defines a fixed value of 31%, uniform for all building orientations, determined based

on its intended use, as mentioned in Section 4.2.1. Taking into account the freedom of choice in the initial phases of design, however, it is possible to consider a wider range of alternatives for this parameter. In doing so, it is necessary to consider that the extension of glazed components has however a significant impact on the building's energy balance for two reasons:

- From a thermal point of view, incoming solar radiation represents a thermal gain that in the winter season, reduces the energy demand for heating; however, in the summer season, it adds to other sources of heat gains, increasing the cooling load and thus the energy consumption required for building cooling. At the same time, windows are often cause of thermal losses from the indoor environment towards the outdoor, causing the necessity to compensate them with an higher amount of energy consumption for heating in the winter season.

- From an electrical energy consumption point of view, incoming solar radiation reduces the need for artificial lighting to provide adequate illumination in spaces, which depends on the type of activities conducted within them. Therefore, ensuring an adequate extent of glazed components can reduce energy consumption associated with internal lighting.

For these reasons, it is essential to identify the WWR value that achieves a trade-off between the positive and negative effects of incoming solar radiation on the building's energy demand. Identifying this compromise is not straightforward, as the impact of windows on the energy balance of a building can vary along with other design factors, among which it is possible to highlight the effectiveness of external envelope components insulation, the occupancy patterns of the building, and the presence of window shading devices, along with their respective light transmittance and reflectance characteristics. Several studies in this field are discussed in the article from Chiesa et. al. [66], of which some examples are provided below. One of the initial studies on this topic dates back to 1996 and allowed the development of the LT 3.0 Method, funded by the European Community[67]; it demonstrated that, to decrease the annual energy consumption of a residential building, the optimal window area varies according to the building's orientation and depends on the presence of shading systems. However, this study did not consider the actual space occupancy or the effects of passive cooling strategies or insulation levels of the building envelope. Another more recent study from 2010[68] examined the relationship between window area and thermal energy demand for large office

buildings in Shanghai, highlighting a positive correlation between increased window area and environmental impact reduction, albeit without accounting for internal heat gains and passive cooling strategies. It is possible to conclude that the article [66] from Chiesa et. al. underscores, through a critical analysis of various studies on the definition of WWR, the necessity of adopting a broader approach to the relationships among design variables: merely focusing on the optimal value of WWR without considering other design variables is inadequate. Consequently, it was concluded that including WWR among the variables evaluated in the optimization process is appropriate for achieving the objective function which will be described, along with the general characteristics of the optimization algorithm, in Section 4.5.

To define the ranges of WWR to be considered in the analysis, the results of the research presented in [66] were taken into account, demonstrating that the optimal WWR values hover around 30% for the two locations examined in the study (Turin and Helsinki), while keeping the building occupancy rate constant. Furthermore, consideration was given to the recommendation arising from the paper of Kamal [69] about the shading components: in it, it is suggested to limit the extension of glazed surfaces in the East and West orientations due to the challenges of shading the sun in the morning and evening respectively. On the other hand, considering the abundant natural sunlight typical of the South orientation of the building, it might be advantageous to increase the extent of glazed surfaces to minimize the use of artificial lighting during most hours of the day. These considerations guided the selection of a range of variation for the WWR in the proposed design's parametric model, which goes from 30% to 80%. Additionally, since the optimal WWR value is expected to differ for different orientations, it is considered to associate each orientation with a WWR variable that varies within the previously specified range independently of the others.

In the *HB Apertures By Ratio* component used in *Honeybee* for modeling window components based on the WWR, it is necessary to define additional inputs, including:

- Number of windows to be created on each facade: the component allows to choose whether to model a single window in the center of the facade or more than one rectangular window based on the inputs provided later. It is decided to keep the default value and, so, the second option.

- Horizontal distance between the centers of individual apertures: if this distance is greater than the length of the parent face, only one aperture will be created. It is decided to consider the default value of 3 m.
- Vertical separation of windows: it is assumed that there is no separation, and thus the window is composed of a single component, leaving the default option.
- Window operability: windows are considered operable to promote natural ventilation, as will be discussed in Section 4.3.5.

4.3.3 Shading Objects for the Proposed Design

As anticipated in the preceding Section 4.3.2, the presence of transparent components in the building facade positively impacts the reduction of energy demand required for space heating and artificial lighting, but it leads to an increase in consumption to meet summer loads due to incident solar radiation and winter loads due to thermal losses if their design is not adequately executed. To minimize this adverse effect on the thermal balance, one may consider installing solar shading components: these allow for the modification of window and facade properties according to climatic conditions and, consequently, the characteristic sun path of the area under consideration depicted in Fig.4.5. Various design alternatives for shading components exist, which can be classified as either movable or fixed, for instance; proper management of movable components enables the maximization of solar gains during the winter season and the minimization of the same loads in summer, while still ensuring occupant visual and thermal comfort maintenance[70]. For these reasons, solar shading objects can be regarded as passive components of building design, along with, for example, natural ventilation, which will be discussed subsequently in Section 4.3.5.

When solar radiation strikes the components of the transparent envelope, the latter behaves like all other materials existing on Earth, namely causing the radiation itself to divide into three parts:

- transmitted solar radiation, represented by the transmission coefficient τ;
- reflected solar radiation, represented by the reflection coefficient ρ;
- absorbed solar radiation, represented by the absorption coefficient α.

The sum of the three coefficients is equal to 1 since each of them is defined as the ratio between the part of the incident radiation component it represents and the total incident radiation itself [70]. The three components can be schematically represented as shown in Fig.4.8. Additionally, the transmission component can be further divided into direct transmission, in the case where the radiation is not altered by the material, and diffuse transmission, which corresponds to the scattering of radiation in all directions.
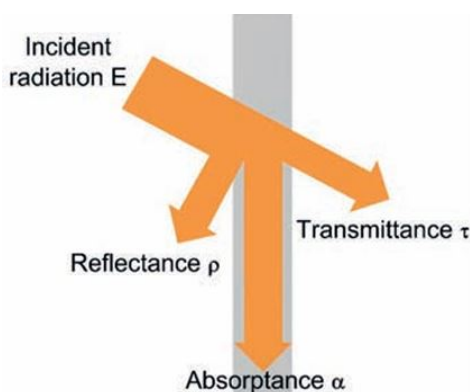
Figure 4.8: Composition of the solar radiation incident on a material[70].

One of the fundamental properties of window components is represented by the total solar energy transmittance coefficient g_{tot}, which denotes the portion of energy of the incident flux transmitted into a room. It encompasses both the solar heat gain coefficient (SHGC) of the transparent element itself and the transmission properties of the shading component. Up to now, in defining the properties of envelope components for both baseline building and proposed design model (see Section 4.2.1 and 4.3.1), reference has been made to the SHGC, which solely accounts for the transparent component behaviour. While ASHRAE 90.1, Appendix G requires windows to have, for the case study properties, an SHGC below 0.39, which is adhered to by the selected construction in Tab.4.4, Ministerial Decree 26/06/15 refers to g_{tot}: for the case study, a construction has been chosen with an SHGC below the g_{tot} limit specified in the decree (equal to 0.8), regardless of the presence of shading components. This ensures that, once the shading component is added, the value of g_{tot} remains below the selected SHGC, guaranteeing full freedom in the selection of the properties of the shading object.

Exploring the capabilities of the plug-ins employed in the study for the modelling of the shading object properties, the alternatives allowing the repre-

sentation of their actual impact on the building energy balance were selected; this allowed to have the possibility to define these properties in therms of ranges, from which the optimization algorithm could select the best alternative in order to maximize the building energy performance with respect to the baseline building. In the initial design phase, there is considerable freedom in defining the geometric properties of shading components. However, it was decided to simplify these choices for two reasons:

1. Despite the design freedom, the primary objective remains to ensure a design that positively influences the building's energy balance, resulting in reduced energy consumption, improved comfort, or lower CO_2 emissions. Therefore, the selection of one geometry over another is only relevant in terms of aesthetic design if they have the same impact on the performance of the building.

2. Although the *Honeybee* plug-in offers the possibility of designing shading component geometric properties in detail, incorporating them into an optimization process would require a high level of detail which could result in longer optimization times, not suitable for the initial design phases where it is necessary to quickly select the best alternatives.

These reasons have led to the decision to consider external shading components for windows that can be approximated as representatives of Venetian blinds with an horizontal orientation, with the geometric characteristics summarized in Tab.4.14.

Table 4.14: Shading objects geometrical properties.

Nr. of shading objects per window	5
Depth of each shading object	0.10 m
Distance from the facade	0.10 m
Inclination of each shading object	30°

A representation of the result of this modelling can be observed in Fig.4.9:
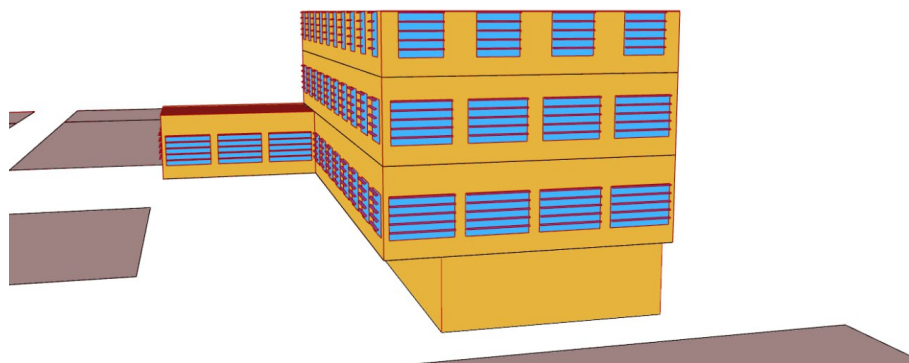
Figure 4.9: Focus on shading objects applied on window components.

It is necessary to mention that the distance between the five shading elements is obtained by equally dividing the height of the glazing component on which they are applied. It would be possible to establish the optimal geometric properties to maximize the performance of the proposed design compared to the baseline using the optimization algorithm; however, for the case study, it is decided to hold these constant and thus not consider them as variables in the optimization procedure as iterations involving the modification of the geometry of these building components are computationally expensive and would therefore result in an excessive increase in the time required to search for optimal solutions. It is therefore decided to vary the solar transmittance value associated with each shading element; the reason for this is linked to the fact that, in general, different types of shading that can be applied to a fenestration component have different solar transmittance values: by introducing this as a variable in the optimization algorithm, it is as if the algorithm selects the transmittance corresponding to the optimal shading type for the studied building. Based on these considerations and the information contained in [70], values of solar transmittance are selected from which the algorithm will identify the optimal one. These are listed in Tab. 4.15.

Table 4.15: Shading objects solar transmittance ranges of variation.

Shading Objects Solar Transmittance	0.01 - 0.05 - 0.10 and from 0.2 a 0.8

It can be stated that the first three values correspond to curtains in pearl white, gray white, and gray, while the others are defined to represent the effect

of various construction types, such as shutters, solar screens, thermal drapes, and shading films.

4.3.4 Proposed Design Lighting Control

One of the main sources of energy consumption within a building is the use of electrical energy, which can be attributed to various factors, including the use of equipment typical of the building's intended use and artificial lighting.

Electrical equipment, in particular, represents a significant component of electrical consumption in an office building, where various devices such as computers, printers, monitors, and photocopiers are common, characterized by different power consumptions depending on the type of usage (continuous or standby): the *ASHRAE Handbook of Fundamentals* suggests several alternative values that can be used in energy modeling. The use of such equipment not only generates electrical energy consumption required for their operation but also serves as a heat source, which has negative implications for the energy demand required for cooling the spaces. However, given the necessity of using these components due to the activities performed in the spaces, there is no possibility of reducing their negative impacts on the energy performance of the building. Because of this, not just for the baseline building model as mentioned in Section 4.2.3 but also for the proposed design one, it was decided to use the default power values and usage schedules of the program.

As for the consumption associated with the lighting system, these can be reduced through various means, including the use of highly efficient luminaires, such as LED lamps, or maximizing the use of natural light while minimizing artificial lighting to ensure adequate visual comfort for occupants. For this type of consumption as well, the *ASHRAE Handbook of Fundamentals* suggests example values; based on the installed electrical power, therefore, it is possible to evaluate the electrical power consumption, but also the thermal energy emitted by these terminals considering two factors:

- Utilization factor, representing the electrical power actually used for lighting compared to the installed electrical power for the same purpose;
- Correction factor, which takes into account the different types of light sources and their efficiency.

By the product of these two factors and the installed power, it is possible to have an idea of the increase in energy demand for cooling the building

associated with the heat gains generated by the light sources. Considering the double negative impact that these components have on the building's energy balance, it is crucial to minimize the demand for power for artificial lighting, which can be achieved through appropriate passive building design, ensuring that the WWR selected by the optimization process maximizes the use of available solar radiation at the building's location, thereby reducing the use of artificial lighting to guarantee the satisfaction of a specific visual comfort for occupants. To ensure this in the proposed design, rather than setting a fixed value for the power density associated with lighting consumption as done for the baseline building, a dimmable lighting control is modeled; this control varies the use of artificial light based on the availability of natural light, ensuring that the combination of these sources allows to achieve a lighting value equal to a well-defined setpoint: if there is sufficient natural light to reach this setpoint, internal light sources will not be used; as soon as natural light is no longer sufficient, artificial lights are used proportionally to the amount of natural light lacking.

The definition of this type of control was made possible using a tool available in the *Honeybee* plug-in, called *HB Apply Daylight Control*. It requires the following inputs:

- The thermal zones where the lighting control should be applied;
- The height above the floor at which the sensor for controlling the available light in the room is considered to be placed and the position of the sensor itself into the zone;
- The control fraction, representing the fraction of artificial light controlled based on the availability of natural light;
- The illuminance setpoint that needs to be satisfied.

In the case study, it was decided to set a value of 800 *lux* to be ensured at the center of the room and at a vertical distance from the floor of 0.80 *m*, considered as the typical height of a desk. As for the control factor, this was considered different for perimeter zones and internal zones; in particular, keeping the position of the control system and the illuminance setpoint fixed, it is assumed that:

- For perimeter zones the control of artificial light based on natural light is higher and set at 0.9;
- For internal zones the control of artificial light based on natural light is not considered as the sunlight's availability in internal spaces is limited.

Once this is done, the control has been defined and will allow for a reduction in energy demand for internal lighting and cooling of the spaces, as will be discussed in Chapter 5.

4.3.5 Passive Strategies for the Proposed Design: Natural Ventilation

As anticipated, one of the primary objectives in the design of new buildings and major renovations today is to ensure a design that makes the building nZEB or, if possible, ZEB. To achieve this goal, it is necessary first and foremost to seek to reduce energy demand as much as possible, which will then need to be met by renewable energy sources, whether on-site or purchased from third parties, depending on the boundary against which the building's associated emissions are evaluated.

In previous Sections, some design alternatives have already been presented as passive design strategies, such as the appropriate use of shading components and the evaluation of the extension of window components on different orientations, to optimize the use of natural light for illumination while minimizing its negative impact on cooling energy demand. However, today there are also well-developed passive cooling techniques, among which it is possible to mention the natural ventilation, which requires the design of buildings characterized by a simple, elongated, and properly oriented narrow geometry in order to maximize the available prevailing winds of the building's location. If achieving narrowness through other means is not feasible, it is possible to define multiple narrow and elongated wings oriented along the east-west axis and connect them via a central spine. Wind speeds may vary, but general trends are predictable; to ensure the possibility of harnessing natural ventilation, it would be advisable to arrange the narrower sections of the building for cross-ventilation by aligning the long facade with the prevailing wind direction. This allows for the utilization of cross ventilation, which utilizes pressure differences to move air and requires positive pressure on the windward facade and negative pressure on the leeward facade[63].

In the case under consideration, the orientation of the building is known and fixed, but the decision is made to evaluate the impact that the implementation of a natural ventilation technique would have on its performance: to gain an

effective advantage in terms of reducing energy demand, it is necessary to ensure that the incoming outdoor air enters the building when it is not too hot during the summer season or too cold during the winter season: in both cases, this would represent an increase in the thermal load on the building and, therefore, would have the opposite effect to that of reducing energy demand. For these reasons, in defining this type of strategy in the energy model, the controls for outdoor and indoor temperature within the building have been defined as summarized in the Tab.4.16:

Table 4.16: Temperature Controls for the Natural Ventilation Strategy.

Minimum Indoor Temperature	22°C
Maximum Indoor Temperature	26°C
Minimum Outdoor Temperature	18°C
Maximum Indoor Temperature	28°C
Delta Temperature	2°C

Referring to Tab.4.16, the variables used are defined as follows:

- *Minimum Indoor Temperature* is the minimum indoor temperature at which to ventilate, so it is used to initiate ventilation with values around room temperature above which the windows will open;

- *Maximum Indoor Temperature* is the maximum temperature at which ventilate, so above it the natural ventilation process stops and the cooling system is turned on in order to guarantee the thermal comfort;

- *Minimum Outdoor Temperature* is the minimum outdoor temperature at which it is possible to ventilate, so if the outdoor temperature is higher than this value, it is possible to start the natural ventilation process in order to cool the indoor environment;

- *Maximum Indoor Temperature* is the maximum outdoor temperature at which to ventilate, so it is the upper limit representing when it is too hot outside to cool the indoor environment through natural ventilation and so the cooling system has to be turned on.

- *Delta Temperature* is the difference of temperature between indoor and outdoor environment below which the natural ventilation stops and it is defined to guarantee that the process happens only when the outdoor is cooler than the indoor.

The *Honeybee* plug-in object used to model natural ventilation is called *HB Ventilation Control* and, in addition to requiring the inputs defined as in

Tab.4.16, it also requires the definition of a schedule representing the periods during which natural ventilation is permissible, otherwise the default option of *Always On* is selected by default from the plug-in. For the case study, therefore, a schedule has been defined that activates the natural ventilation process for cooling the building from 7:00 PM to 9:00 AM, ensuring that:

- Before the occupants enter the building, at 9:00 AM, if necessary, the indoor environment is cooled, ensuring comfortable conditions from the early hours of the day without the need to turn on the cooling system, if outdoor conditions are favourable;

- After the building's closing hours, when occupants leave, in order to cool the spaces, where internal loads related to occupants themselves, electrical equipment, or lighting are expected.

At this stage, the definition of natural ventilation as described so far must be coupled with the involved thermal zones and, consequently, also with the window components present within them. To accomplish this, the *HB Window Opening* block is utilized, for which all default parameters are considered, as summarized below:

- The fraction of window area that can be considered operable is set to 0.5, typical of sliding windows;

- The fraction of the distance from bottom to top that is operable is set to 1 in order to represent windows sliding horizontally;

- The discharge coefficient allows to represent the effect of friction due to the geometry of the windows or the presence of other additional obstacles like insect screens; considering that, into an office, these kind of systems are not present, it is used the default value of 0.45.

- It is required to specify weather or not there are windows with the same area on two opposite facades so that the wind-driven cross ventilation is favoured. Being that the area extension on the different facades is set from the optimization algorithm, it is maintained the default value, through which normal vectors of the operable aperturs of the thermal zones will be analyzed: if window normals of a given room are found to have an angle difference greater than 90°, cross ventilation will be considered possible, otherwise not.

4.3.6 Proposed Design Renewable Energy Production

As described in Section2.2, one of the mandatory features for newly constructed buildings is to have access to a share of self-generated energy from renewable sources. In Italy, this is implemented through Legislative Decree no. 199 of November 8, 2021: in its Article 26, the obligation to use energy from renewable resources is defined in order to improve the energy performance of buildings, thereby ensuring the use of clean energy, mostly solar, to produce electricity and thermal energy[71]. There are several technologies available today that allow for this: the most commonly used in the building sector are of two types, namely solar thermal and photovoltaic. The former harnesses solar radiation to produce thermal energy: through the panel, mounted in areas of the building characterized by adequate exposure, the incident solar radiation reaches the absorber, which heats up transferring heat to the heat transfer fluid used; the latter then transfers the energy to the water of the utilities, whether they are related to sanitary use or heating system terminals, usually at low temperatures[72]. The latter, instead, harnesses solar radiation to produce electricity directly, without the need to pass through thermal and mechanical energy, through the photovoltaic effect, discovered in 1839 by the French physicist Alexandre-Edmond Becquerel; this physical phenomenon, linked to the interaction between light radiation and matter, is due to the presence within light of *photons*, particles devoid of matter, but charged with energy, which allow the passage of electrons from the valence band to the conduction band of semiconductor materials. Among these, the most commonly used for the realization of solar cells used for this application is silicon, which is suitably subjected to the doping phenomenon in order to modify its prevailing charge, thus generating P-type silicon when doped with trivalent substances such as boron, to obtain excess positive charges (holes), and N-type silicon when doped with pentavalent substances such as phosphorus, to obtain excess negative charges (electrons). From the positioning of these two components thus realized adjacent to each other, the so-called P-N junction is created: when this is hit by the photons of solar radiation, these cause an electron shift between the atoms of the semiconductors, until an equilibrium is reached; as a result, an electric field is created that prevents the passage of further electrons through

the junction itself. In Fig.4.10, a schematic representation of the previously described photovoltaic effect is provided.
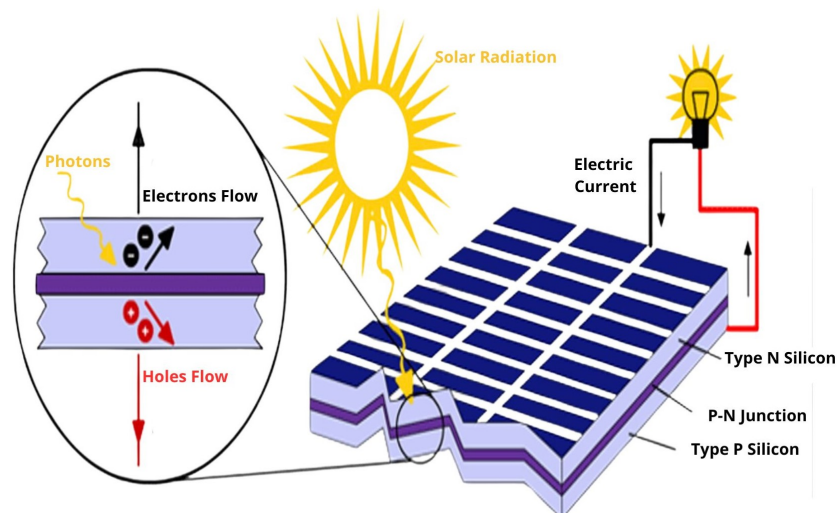
Figure 4.10: Schematic explaination of the Photovoltaic effect[73].

Considering the capabilities of the modeling software being used, it has been decided to evaluate the installation of a photovoltaic system for the proposed design, so that it can be used to offset the electrical energy consumed by the building, at least in part. Taking into account the typical conditions of the initial design phases and the sequential optimization procedure, the assessment of the installation of such a system in the building has been divided into two phases:

1. Phase 1: Four different potential positions of the photovoltaic system are evaluated, and the effect of their shading on the energy performance of the building is considered;

2. Phase 2: Once the optimal location for the installation of the system is identified, the sizing properties of the system are evaluated to define their optimal values. In particular, the tilt of the panels and the optimal percentage of active surface area will be determined.

Regarding the type of panels that are considered for installation, this is kept fixed for all the analyzed locations and is characterized by the properties listed in Tab.4.17:

Table 4.17: Photovoltaic modules features.

Module Type	Monocristalline
Efficiency	17%
Installation Type	Fixed Roof Mounted

In particular, the Fixed Roof Mounted installation type corresponds to a rooftop integrated installation, which may not guarantee optimal airflow but has been decided upon to ensure compliance of the system with local legislations about, for example, preservation of local heritage, regardless of the building's location. As for the technical characteristics of the inverter, default values provided by the *Honeybee* plug-in are considered, hence an efficiency of 96% and a ratio between the DC rated power and the AC rated power of the inverter equal to 1.1.

The possible locations evaluated for this system are synthetically represented in Fig.4.11.
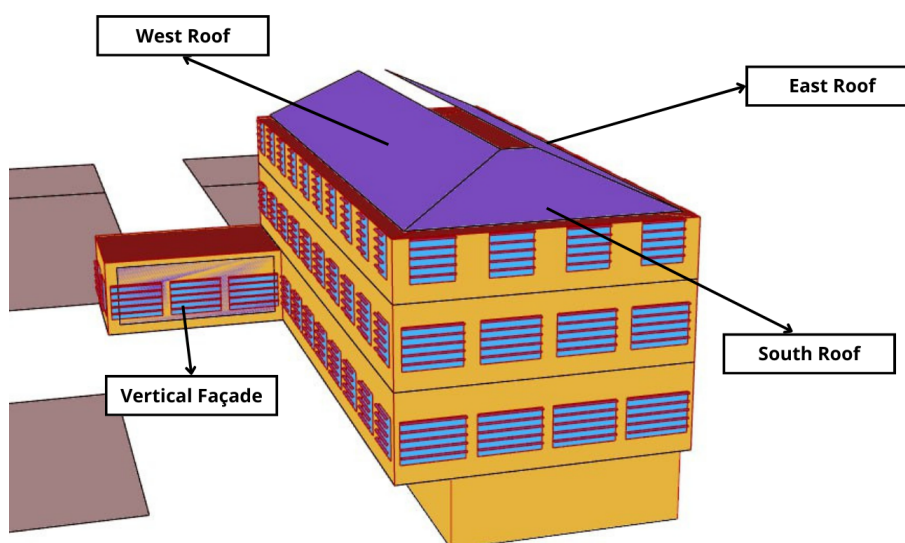
Figure 4.11: Locations of the PV plant analyzed during the Optimization Process.

Considering the sequential optimization procedure, once the optimal location is selected during the first phase, in the second phase, the variables that need to be properly selected by the algorithm to optimize the building performance will be, as aforementioned, the fraction of active surface area dedicated to the photovoltaic system and its tilt angle. These will vary as in Tab.4.18.

Table 4.18: Optimization variables for the photovoltaic panels installation.

Active Fraction	Range: 0.5 - 0.9, step 0.1
Inclination	10°, 22°, 30°, 40°

Note that the variable referring to the tilt angle has been selected because, as will be shown in the results in Chapter 5, the optimal location will not be the one on the Vertical Facade in Fig.4.11, but rather one of those on the roof. Therefore, it is worthwhile to consider the impact of the panel tilt angle on their annual production. Additionally, the tilt angle of 22° is considered as the initial value for this variable and for all the photovoltaic panels locations on the building because it corresponds to the tilt of the roof currently planned in the design of the real building used as a case study for the purposes of this thesis.

Regarding integrated optimization, the procedure involves evaluating, as alternatives, the four locations indicated in Fig.4.11, but for all those referring to the roof, the different inclinations presented in Tab.4.18 will be considered, together with the active fraction also for the Vertical Facade alternative.

4.3.7   Proposed Design: HVAC Systems

The maintenance of indoor air quality in terms of thermal comfort and pollutant presence within buildings is ensured by HVAC systems. However, in commercial or office buildings, these systems account for between 30% and 50% of energy consumption, depending on the type of system considered[74]. Such reasons underscore the need to select the components comprising the system to be installed so that they exhibit significant efficiency, not only in terms of machine performance but also in terms of system solutions. To achieve this, it is necessary to take into account the type of building on which the system will be installed, thereby ensuring compliance with the thermal-hygrometric comfort and air quality requirements that characterize it, and thus selecting the most suitable alternative, taking into account energy efficiency, maintenance requirements, and system cost. To guide designers in this design phase, given the high demand for sustainable HVAC systems, several regulatory bodies have been established, among which it is worth mentioning the Building Research Establishment Environmental Assessment Methodology (BREEAM) and the Leadership in Energy and Environmental Design (LEED).

BREEAM was established by the BRE Group (Building Research Establishment), a British organization involved in research, consultancy, and certification in the field of construction, founded in 1921 and funded by the British government, which then developed into a global profit-for-purpose business[75]. BREEAM certifications were launched in 1990 to improve the performance of the built environment, from its design to its construction. LEED, on the other hand, is the most widely used green building classification system[76] and was founded by the U.S. Green Building Council with the aim of providing a framework for "*healthy, efficient, and cost-effective buildings that offer social, environmental, and governance benefits*". It can be applied to all types of residential and commercial buildings and leads to improved building performance in terms of energy and water savings and environmental impact, ensuring the reduction of CO_2 emissions and the ecological quality of interiors, resources used, and site selection where the building is located[77]. This sustainability-oriented approach increases the property value of the building, ensuring a better assessment on the market; furthermore, it improves a company's reputation by demonstrating its concrete commitment to environmental sustainability, thereby attracting the attention of customers, investors, and stakeholders.

Currently, there are multiple types of HVAC systems suitable for installation in buildings, especially those intended for non-residential use as in the case at hand; however, selecting the optimal solution is not a simple task for designers and requires a thorough evaluation of the various options available on the market in order to maximize building performance. To facilitate designers in this decision and thus reduce the analysis time that evaluating different alternatives would require, it is proposed to include the type of HVAC system as a variable within the optimization process, in order to select the best alternative based on maximizing the objective function, which will be further presented in Section 4.5.

Although it is possible to perform detailed modeling of HVAC systems using the *Ironbug* plug-in in *Grasshopper*, it has been chosen to employ the HVAC types available in the *Honeybee* plug-in library so that they can be included as variables in the optimization process and their sizing can be automatically performed during the energy simulation, based on the heating, cooling, and ventilation needs of the building. Detailed modeling of HVAC systems, indeed, increases the complexity of the model and makes it difficult to use the *Wallacei* plug-in to execute the NSGA-II evolutionary optimization algorithm.

As mentioned earlier, the software and plug-ins used in this work have been developed in an American context, so the HVAC library includes some types not common in Italy, due to cultural differences and the state of the art. In order to prevent the algorithm from selecting systems unsuitable for the Italian context, a preliminary evaluation of the models available in the library has been carried out, after which the following types of HVAC systems have been selected:

1. *DOAS with fan coil chiller with central air source heat pump*;
2. *DOAS with fan coil chiller with baseboard electric*;
3. *DOAS with fan coil air-cooled chiller with central air source heat pump*;
4. *DOAS with fan coil air-cooled chiller with baseboard electric*;
5. *DOAS with VRF*;
6. *DOAS with low temperature radiant chiller with air source heat pump.*

For all systems, there is a component called DOAS (Dedicated Outdoor Air System), which manages the outdoor air taken from the outdoor environment in a dedicated manner and introduces it into the indoor spaces to provide fresh air, so free from pollutants, at defined inlet conditions through precise control over its quality, temperature, and humidity. Considering that the goal of an HVAC system is not only to ensure thermal comfort indoors but also to achieve an IAQ suitable for the intended use of the spaces, the presence of a system that handles the treatment of outdoor air is indispensable. In particular, through the DOAS, before being introduced into the indoor spaces via appropriate terminals, the air is treated by filters that remove impurities; additionally, it is pre-heated or pre-cooled by heating and cooling coils to reduce the thermal load on other components of the HVAC system dedicated to meeting the winter and summer thermal loads. In cases where the conditions of thermal air treatment are appropriate, indeed, these allow for a reduction in the load on the rest of the terminals and, thus, an overall improvement in system efficiency, while maintaining thermal-hygrometric comfort in indoor spaces.

The block enabling the integration of DOAS HVAC systems into the *Honeybee* plug-in (*HB DOAS HVAC*) allows for the selection of some fundamental characteristics of the DOAS, including:

- the sensible and latent thermal recovery efficiency of the system, which has been set at 80% for both;

- the implementation of *Demand Control Ventilation* (DCV), which represents a logic for controlling the airflow within the spaces that adjusts its intake based on the occupancy of those spaces. Considering that this allows for the use of outdoor air and, therefore, all its treatment components only when necessary, it has been decided to consider its presence to reduce the building's energy demand associated with such uses.

- the definition of the *Availability Manager*, meaning predefined schedules regulating the activation and deactivation of systems within the building. For these, it is considered that the system is activated during office hours, considered, for the case study, from 9:00 A.M. to 5:00 P.M. on weekdays (Monday to Friday), while it is deactivated for the remaining hours of the day and during weekends and holidays; schedules representing this behaviour are represented in Fig.8.12 in Appendix.

In evaluating the types of systems among which the optimization algorithm will need to make a selection, care has been taken not to consider systems that involve the use of fossil fuels at their generation. As presented in Section 4.3.6, indeed, it has been decided to assess the inclusion of various possible configurations of photovoltaic systems, ensuring the maximum production of electricity from renewable sources possible and utilizing this to offset the internal electrical energy consumption of the building. By avoiding the use of fossil fuels such as natural gas, the focus is primarily on self-consumption of self-generated electricity, reducing not only the operational cost of the building associated with the purchase of fossil fuel but also the emissions associated with the energy consumed within the premises. It is noted, therefore, that the generation systems used are all powered by electricity and include heat pumps and chillers.

The heat pump can be defined as a reversible thermal machine capable of producing thermal power for both heating and cooling of spaces. By utilizing vapor compression cycles, it enables extremely efficient heat exchange between two different temperatures: this occurs in four stages, namely evaporation, compression, condensation, and expansion, as depicted in Fig.4.12.
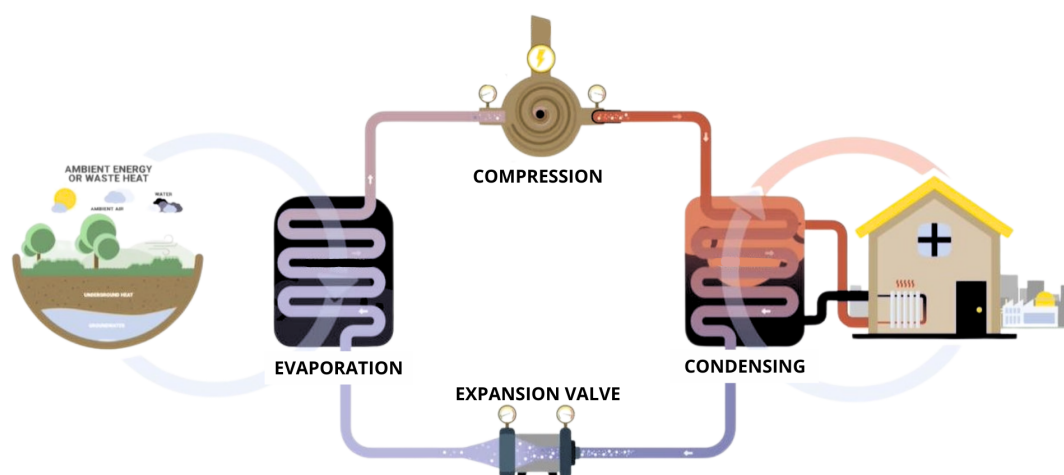
Figure 4.12: Schematic representation of the operating cycle of a heat pump[78].

Referring to the winter season, these stages can be described as follows:

- *Evaporation*: The machine utilizes this stage to extract thermal energy from the first temperature well, indicated as the outdoor environment in Fig.4.12. This energy is then used to evaporate the refrigerant fluid within the cycle.

- *Compression*: The refrigerant fluid is compressed to increase its temperature. This requires the use of energy, which can be electric energy drawn from the grid or generated by a photovoltaic system installed in the building, or other energy sources such as fuels or thermal energy.

- *Condensation*: The pressurized and superheated vapor passes through the condenser, which is essentially a heat exchanger that allows the release of thermal energy contained in the refrigerant fluid to the thermal fluid flowing through the building's terminals to heat the indoor spaces.

- *Expansion*: It occurs within an expansion valve that allows the refrigerant fluid to return to a liquid state and resume the operating cycle.

The operating scheme remains the same for the summer season, during which, however, evaporation occurs in contact with the indoor environment to extract heat from the spaces to be cooled, while condensation occurs in contact with the outdoor environment to release the accumulated heat from the indoor spaces. The real advantage of this process lies in the fact that heat exchanges occur at relatively low temperatures, between 30 and 45°C: this implies that the energy demand for powering the machine itself is contained

and is lower compared to the energy it provides to or draws from the system it serves, resulting in a Coefficient of Performance (COP) for the winter season and an Energy Efficiency Ratio (EER) for the summer season always greater than one.

Heat pumps can be classified based on the type of external thermal well from which heat is extracted or to which it is released during the evaporation and expansion stages. According to [79], they are distinguished as follows:

- *Air Source Heat Pumps (ASHP)*: These use the energy contained in the outdoor air or in ventilation system air to heat or cool the thermal fluid of the system installed in the building.
- *Water Source Heat Pumps (WSHP)*: In this case, the source of thermal energy is represented by groundwater, surface water, or seawater. These heat pumps are particularly efficient due to the high efficiency of water as an energy carrier.
- *Geothermal Heat Pumps* or *Ground Source Heat Pumps (GSHP)*: These exploit the energy stored in the ground at adequate depths, where the temperature is constant, as a source of thermal energy in winter and as a destination for thermal energy in the summer season.

In applications similar to those of the case study, therefore, buildings located in urban areas, far from where it is not possible to carry out excavations at high depths for exchange with the ground, the ideal solution is that of ASHPs. Therefore, in the analysis of the library of the *Honeybee* plug-in, only types with this generation system have been selected.

The second type of generator presented is that of the chiller, used for the production of chilled water distributed within the building's systems through an appropriate distribution system. The operating scheme of the chiller can be represented in Fig.4.13:
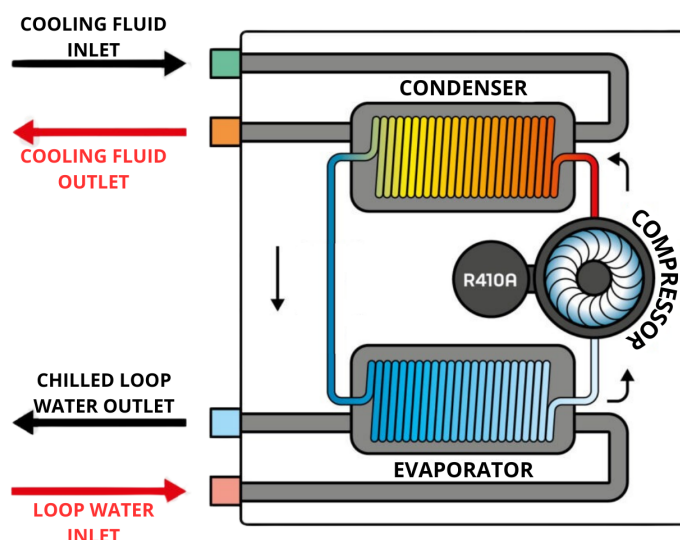
Figure 4.13: Schematic representation of chiller components[80].

In this case as well, the operating phases are four and are identical to those performed by the heat pump, with the difference that, in the case of the chiller, the cycle is only reversed, and therefore, this machine can only be used for the production of chilled water. A fundamental element of this system is the evaporator's Entering Dewpoint temperature (EED); it is monitored and controlled to ensure that the machine operates efficiently.

Analyzing the selected system alternatives, it is noted that where the heat pump is present, the chiller is actually present too, despite the fact that, as anticipated, the first machine can handle both chilled water and hot water production. The reason for this lies in the fact that within the library, an ASHP refers to a machine that only produces hot water, thus not operating a reversible cycle; for these reasons, the production of chilled water is performed by a machine that separately operates the reverse cycle. It is also noticeable that while some chillers are *air-cooled*, the type is not specified for others. This depends on the fact that what is indicated as "Cooling Fluid" in Fig.4.13 can be of different types; in particular, there are two main categories of chillers:

1. *Air-cooled chillers*: These utilize outdoor air to condense the high-pressure system fluid; in this case, the condenser is appropriately designed to dissipate heat into the outdoor air, through fans or other ventilation devices.

2. *Liquid-cooled chillers*: These utilize a liquid to condense the high-pressure system fluid. The liquid, in this case, circulates through a heat exchanger in the condenser, where the condensation of the refrigerant fluid of the machine itself occurs again. There are different types of liquids that can be used for these purposes; however, in the case of non-residential buildings such as those in the case study, water is used. In this case, the addition of another component called a *Cooling Tower* is required, used to dissipate the heat that the water has absorbed inside the chiller by coming into contact with the condenser. The incoming cold and dry air from the outdoor environment is used to cool the water exiting the chiller; at this point, the vapor part contained in it turns into water and is collected and removed from the machine with an appropriate system, while the now heated air is re-introduced into the environment. This type of system can be defined as Closed-loop because the cooling water is inserted into a closed hydraulic system, which prevents its exposure to external contaminants and reduces sediment accumulation. A schematic representation of such a system is provided in Fig.4.14.
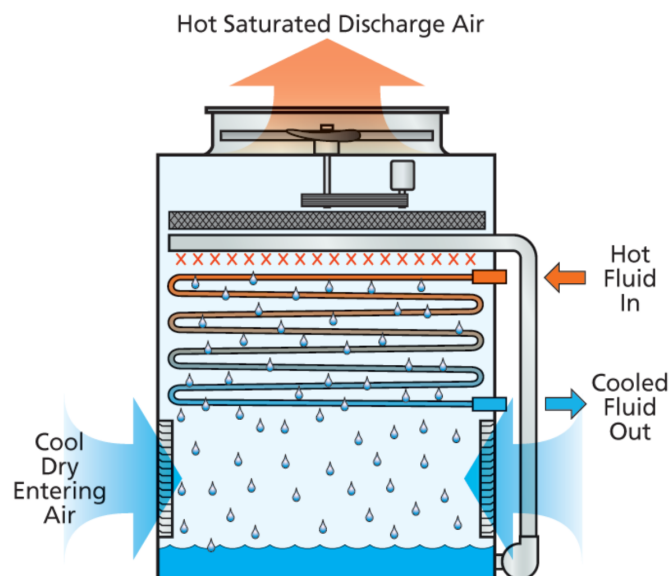
Figure 4.14: Schematic representation of a cooling tower[81].

Note that an alternative is an Open-loop system, where the cooling water is taken from an external water source, such as a river or the sea, and used directly in the cooling cycle. In the case study, this type of system is not feasible as the building is located in a city, far from such sources.

Another particular type of system that has been decided to evaluate is the Variable Refrigerant Flow (VRF) system, representing an efficient and flexible solution for heating and cooling buildings, ensuring precision in controlling the required temperature in different areas and optimal thermal comfort for occupants. This is achieved through the use of refrigerant fluid: the flow of it reaching each terminal and thus each room is regulated based on the thermal load of the latter, in order to simultaneously meet different loads and avoid energy waste. This is done by using an external unit connected to various internal terminals through specific piping: the cycle that occurs is identical to that described earlier for the heat pump, except that, in this case, the outdoor unit contains only a compressor, condenser, and expansion valves; the evaporator, on the other hand, is contained in the indoor units, which absorb heat from the indoor environment or from the refrigerant fluid, depending on whether heating or cooling is required in the specific indoor space. These operations can occur simultaneously in different rooms, making the design of this type of system modular and allowing for high energy efficiency.

Taking into account that heat generation is carried out by a heat pump for all the analyzed HVACs, it is necessary to work with lower temperatures for heating, and thus, the terminals coupled with this type of machines must be appropriately selected. Among those available, it is necessary to highlight:

- *Fan coil units*: This type of terminal can operate at both high temperatures, in case they are paired with boiler-type generation systems, and at low temperatures, in the case of models paired with heat pumps. An example is provided by Daikin, particularly the *Daikin Altherma HPC* line[82]: it uses the principle of convection for heating or cooling a space, achieved by utilizing a fan that facilitates heat exchange between the room air and the coils through which hot water flows in the heating season or cold water flows in the cooling season. Fig.4.15 shows a schematic representation of the heat exchange process within the terminal for the winter season just described. It is worth noting that this type of terminal is also used in the VRF system described earlier.
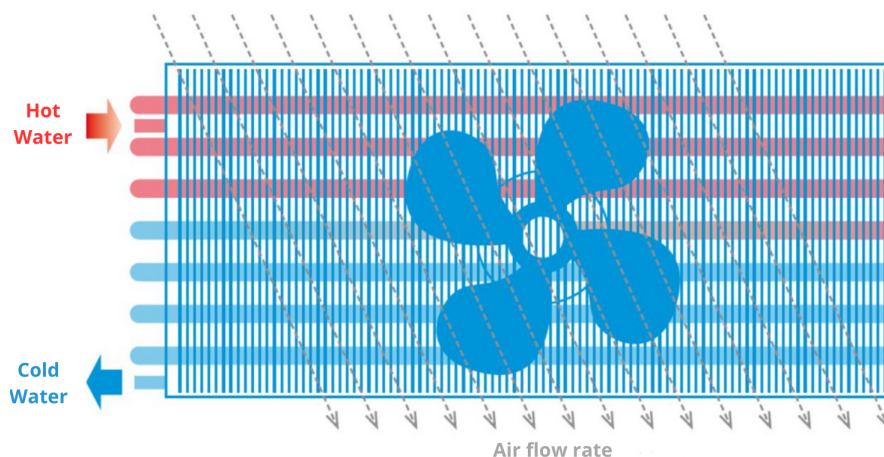
Figure 4.15: Schematic representation of the FanCoil operation [82].

- *Radiant panels*: The use of this type of terminal provides numerous advantages; in fact, besides being perfectly compatible with heat pumps as they are designed as low-temperature terminals, they ensure high occupant comfort since temperature distribution within the rooms is uniform. Additionally, the absence of forced convective heat exchange by fans minimizes the creation of convective currents, avoiding the dispersal of any dust deposited on the floor into the air, thereby reducing occupants' inhalation. Like fan coil units, they can be used for both heating and cooling, and today there are various types depending on their integrated position within the building envelope. They are often installed in the floor, with the floor structure designed to accommodate them, minimizing insulation between them and the indoor environment and maximizing it in the opposite direction, thus avoiding heat dispersion from these terminals. However, in office spaces, they are often also used in the ceiling. Modeling this type of terminal requires the use of a specific block from the *Honeybee* plug-in, such as *HB Radiant HVAC Properties*: it is necessary to specify the type of radiant panel to be installed, as well as the minimum number of operating hours before it turns off and the minimum number of hours after which the system can switch from heating to cooling mode. While the default values were retained for the latter two, so one hour and 24 hours respectively, the *Ceiling Metal Panel* type was manually selected for the first, as the roof and floor constructions were modified as indicated in Tab.4.19 to allow modeling of such terminals:

Table 4.19: Horizontal envelope components construction for Ceiling Metal Radiant Panels

8 in. Normalweight Concrete Floor
Roof Insulation [18]
Metal Surface
Internal source
Metal Surface

The combination of these materials corresponds to a thermal transmittance of the horizontal components of $0.20 W/m^2 K$, which, therefore, complies with the limit defined in Appendix A of the Minimum Requirements Ministerial Decree for climate zone E. Note that, in Tab.4.19, "Internal Source" refers to the heat source provided by the radiant panel; it is surrounded by two metallic panels to facilitate its integration within the building envelope component. However, while there are no additional components on the side facing the interior space, on the opposite side, after the metallic surface, there is an insulation layer that prevents heat dispersion and, therefore, unnecessary consumption of the system for maintaining occupant comfort.

The final type of terminal among those selected for the HVAC systems is the baseboard, commonly used in residential and commercial buildings. It consists of a heating element represented by an electric resistance enclosed in a protective casing mounted along its entire length. Therefore, it can only be used for heating, and indeed in HVAC systems 2. and 4., it is paired with fan coils, which will solely handle cooling in these specific cases. It has been decided to evaluate this type of system as it is powered by electricity, for the reasons previously mentioned; however, considering that high-quality energy, such as electricity, is used to produce low-quality energy, such as heat, and given the reduced efficiencies of this process, it is expected that the optimization algorithm will not select systems where baseboards are present.

To minimize variability compared to the baseline building, the proposed design will also involve grouping the building zones into the three groups presented in Tab.4.8, assigning an HVAC system to each group separately. The optimization procedure, therefore, involves evaluating the six types of systems previously presented for each of the three groups so that, depending on the heating, cooling, and ventilation demand characteristics, the algorithm assigns

the most suitable one to each of them to minimize the overall energy demand of the building and its environmental impact.

It should be noted that, as will be presented in Section 4.5, the incorporation of the HVAC system and its optimization within the model of the proposed design will be repeated twice, but differently, taking into account the two alternatives of the optimization process to be evaluated. Initially, the HVAC systems for the three groups of rooms in the proposed design will be added to a model of the proposed design whose envelope characteristics have already been optimized in a preliminary phase of the NSGA-II algorithm application, during which the constructions of the building envelope components correspond to the ones reported in Tab.4.13. Then, the constructions will be modified to enable the installation of radiant ceiling heating and cooling systems as showed in Tab.4.19, and proceeding with the optimization of the HVAC system type and the producibility characteristics of the building's photovoltaic system. Once done so, the results obtained will be compared with those obtained by optimizing both the envelope components and systems in a single phase represented by the integrated optimization procedure, in which the constructions of the envelope will be the ones modified for the radiant panels installation. This will allow for a comparison of the performance and, therefore, the quality of the optimal solutions obtained from sequential optimization and integrated optimization.

4.4   Energy Simulation

The energy simulation was performed using the *EnergyPlus* calculation engine, utilizing the *HB Model to OSM* component of the *Honeybee* plugin. The fundamental inputs required from this component are the model of the building, obtained as described in Sections 4.2 and 4.3 respectively for the baseline building and the proposed design building, and the *.epw* file corresponding to the building location. Additionaly, it is possible to set specific simulation options, as described below:

- *North Position*: A 40° counterclockwise difference between the North direction and the y-axis is imposed to represent the current orientation of the modeled building.
- *Simulation Outputs*: For optimization purposes, it is considered to use only the default available outputs provided in the *.sql* file produced from

the simulation, while considering system energy use and comfort metrics outputs in the HVAC component sizing phase of the two models.

- *Run Period*: The simulation period is the entire year represented in the climatic file corresponding to the building location.
- *Daylight Saving*: Periods where daylight calculation is avoided are not considered.
- *Holidays*: Building non-occupancy periods are not manually defined as they are implicitly defined in the occupancy schedules provided by the *Honeybee* plug-in.
- No specific day of the week is imposed for simulation initiation, rather the default day present in the climatic file is considered.
- *Timestep*: Number of calculation steps per hour, set to 1; using smaller timesteps in the initial design analysis phase considered would provide only marginally better detail than that obtained with hourly calculation, and would not be useful for evaluating design alternatives in the early project stages.
- *Terrain*: The type of terrain on which the building stands is specified, maintaining the default option "City"; no specific temperature for it is set, as the one present in the climatic file is used.
- *Simulation Control*: Calculation types that the simulation must perform are defined here; for the sequential optimization, the sizing option is set to true only during Phase 2, while for the integrated optimization it is always imposed equal to true.
- *Sizing*: This option allows defining sizing factors, which represent multiplicative factors to apply to heating and cooling energy demand for component size calculations. Therefore, 1.25 and 1.15 are imposed, respectively for heating and cooling systems as suggested from the ASHRAE 90.1-2016 Standard.

4.5   Optimization Process

As previously illustrated, decisions made in the early stages of building design have a greater impact on their performance compared to alternatives selected in later design stages or during operational phases[25]; therefore, selecting the optimal design during these early stages is crucial to ensure that the building

achieves optimal performance, in terms of energy consumption or environmental impact. Additionally, modifying decisions made in the early design stages later in the process is complex and costly. Since years, fundamental aids for designers undoubtedly include energy simulation softwares, which enable the comparison of the impact that various design solutions have on building performance; however, modeling different solutions and subsequently simulating them entails considerable time and computational costs. With the aim of attaining valid design solutions efficiently and in short time, numerous studies have sought to integrate energy simulation with optimization algorithms, as defined in Section 3.3.2, developing the so-called Simulation-based Optimization Methods. In the process devised for this thesis work, the objective is to assess the quality of design solutions suggested by the NSGA-II algorithm implemented in the *Wallacei Grasshopper* plug-in, based on modeling and energy simulation using *EnergyPlus*.

4.5.1   Wallacei Plug-in

The plug-in chosen for this optimization is *Wallacei*, an evolutionary engine able to run evolutionary simulations through a detailed analytic tool allowing users to better understand the evolutionary runs conduced and supporting them in making informed decisions about the problem understudy. Through this plug-in, it is possible to analyze the results obtained during the optimization process and, therefore, select the optimal solution; furthermore, the possibility is provided to select, reconstruct, and extract any phenotype of the population once the simulation is completed[83]. As previously defined, *WallaceiX* employs the NSGA-II algorithm[84] as the primary evolutionary algorithm and utilizes the K-means method as the clustering algorithm. In Fig.4.16, the block used to start the optimization process is depicted.
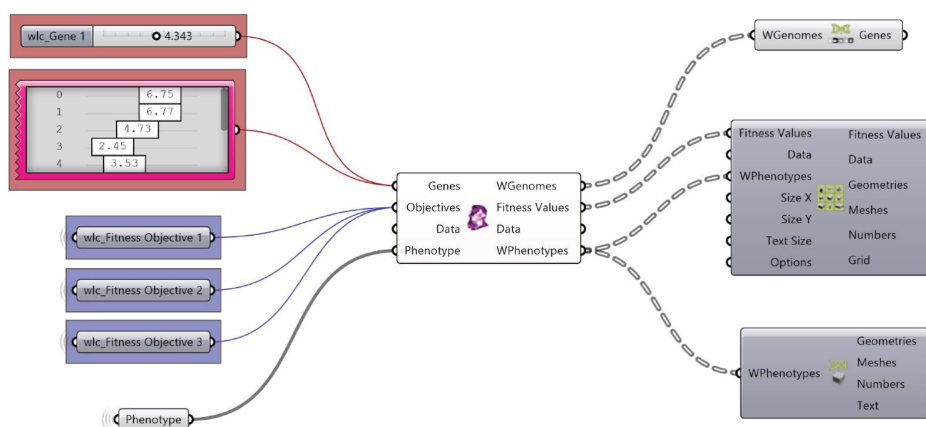
Figure 4.16: *WallaceiX* block used to run the evolutionary algorithm[56].

The inputs required for this block, and those actually utilized in the optimization process conducted on the case study, are as follows:

- *Genes*: representing the variables of the optimization algorithm, so the parameters that are varied at each iteration of the algorithm to evaluate successive offspring solutions.
- *Fitness objectives*: representing the objective functions that need to be optimized by appropriately selecting the values of the genes.

Regarding the input and output *Data* and *Phenotype*, as they allow saving some data for each solution of the population and selecting phenotypes to be exported, respectively, they are not used in the optimization process to streamline it as much as possible. Only the *WGenomes*, which are all the solutions generated in the population produced by the *WallaceiX* block, and the *Fitness Values*, so the objective function values associated with each solution corresponding to a genome, will be utilized.

4.5.2 Application of the Evolutionary Algorithm

To initiate the optimization process with the evolutionary algorithm, it is necessary to appropriately set the optimization parameters from the *Wallacei Settings* page. For the case study, the parameters listed in Tab.4.20 have been decided for use.

Table 4.20: Wallacei Setting parameters values used for the optimization process.

Generation size	10
Generation Count	10
Crossover Probability	0.8
Mutation Probability	$\frac{1}{n}$
Crossover Distribution Index	10
Mutation Distribution Index	10
Random Seed	1

The parameters of *Generation Size* (number of individuals per generation) and *Generation Count* (number of generations) allow defining the population size and have a significant impact on the quality of the obtained solutions; indeed, the larger the population size, the wider the set of solutions examined by the algorithm in search of the best one. However, if the population size is excessively large, this results in a very high optimization time, which can be reduced by using a smaller population; nevertheless, the latter may exclude some solutions, risking the selection of a solution that is not actually the best possible. It is therefore necessary to find a compromise between solution quality and optimization time; because of these reasons, a sensitivity analysis will be conducted with different population sizes. For the other parameters listed in Tab.4.20, the selected values were chosen starting from the default values of *WallaceiX*. In particular, the *Crossover Probability* (the percentage of solutions in the generation that will reproduce for the next generation) was reduced from 0.9 to 0.8 in order to decrease simulation time without excessively negative impact on the solution. Regarding the *Mutation Probability*, representing the percentage of mutations occurring in the generation, the default value is maintained, where n is the number of optimization variables. Additionally, both the *Crossover* and *Mutation Distribution Indexes* are slightly reduced compared to the default program value of 20 in order to decrease optimization time: low values of these parameters allow distant solutions from parent ones to be selected as child solutions.

At this point, the objective function that the algorithm will optimize has to be defined. Considering the aim of selecting design alternatives that make the proposed design more efficient compared to the fixed baseline building, two objectives for optimization can be considered:

- the primary energy consumption of the proposed design compared to the baseline;
- the CO_2 emissions of the proposed design compared to the baseline.

Implementing both objectives in a multi-objective optimization framework would be redundant and would not lead to a better result compared to utilizing only one of the two. The challenge in analyzing primary energy consumption lies in selecting the conversion factors for the various energy sources used as resources in the building. To overcome this issue, it is decided to consider the variation in CO_2 emissions as the optimization objective. In particular, it is beneficial to work in terms of percentage variation, obtaining the objective function 4.8.

$$min \quad \frac{kgCO_{2PD} - kgCO_{2BB}}{kgCO_{2BB}} \tag{4.8}$$

Please note that the minimization of the relative difference between the CO_2 emissions from the proposed design ($kgCO_{2PD}$) and those from the baseline building ($kgCO_{2BB}$) is considered, as the *Wallacei* plug-in can only perform optimizations in terms of minimization. Furthermore, these emissions are referenced to the building's floor area and are automatically calculated by the *Honeybee* plug-in as output from the energy simulation via the *HB Carbon Emission Intensity* block; the latter requires as input the *.sql* file obtained from the energy simulation and the CO_2 emissions associated with the electricity grid of the location where the studied building is located. By default, some values are provided that can be selected considering various location alternatives within the territory of the United States, where such plug-ins have been developed. However, to account for the emissions associated with Italian electrical energy production, it was decided to rely on analyses conducted by the IEA[85], which indicate that in 2021, electricity production generated 93 million tons of CO_2. Since the *Honeybee* block requires emissions in kg of CO_2 per MWh of generated energy, it has been considered the electricity production in 2021, amounting to 1051915 TJ[85]: the data obtained allow for the calculation of emissions equal to 318 $kgCO_2/MWh$ for the Italian grid.

It is possible to approach this problem in two different ways: the first consists of carrying out a *Sequential Optimization*, in which two successive optimization phases are conducted, one for the building's construction parameters and one for its system components; the second, instead, consists of performing an

Integrated Optimization, in which building parameters and system components are considered in the same step. Once this is done, it is possible to evaluate which of the two yields the best result, or whether the two approaches are interchangeable as they allow obtaining the same optimal result.

Considering the first of the two approaches, following is presented the description of the two optimization phases that will be implemented sequentially: the first aims to identify the optimal values of some of the characteristics of the building envelope previously selected in Section 4.3.2, 4.3.3, and 4.3.6, which are the WWR, the solar transmittance of shading components, and the location of the photovoltaic system, taking into account its shading on the building, for the proposed design. The second phase focuses, instead, on the selection of the type of system to be installed inside the building among those presented in Section 4.3.7 and the sizing parameters for the photovoltaic plant.

Below, the optimization variables and their respective ranges of variation are summarized, reported respectively in Tabs.4.21 and 4.22 for Phase 1 and Phase 2 of the optimization:

Table 4.21: Phase 1 optimization variables range definition.

WWR - North Facade	From 0.3 to 0.8, step size: 0.1
WWR - East Facade	From 0.3 to 0.8, step size: 0.1
WWR - South Facade	From 0.3 to 0.8, step size: 0.1
WWR - West Facade	From 0.3 to 0.8, step size: 0.1
Shading Objects Solar Transmittance	0.01, 0.05, 0.10, From 0.2 to 0.8, step size: 0.05
PV Panels Location	Vertical Façade, East Roof West Roof, South Roof

Table 4.22: Phase 2 optimization variables range definition.

HVAC Type	DOAS with fan coil chiller with central ASHP
	DOAS with fan coil chiller with baseboard electric
	DOAS with fan coil air-cooled chiller with central ASHP
	DOAS with fan coil air-cooled chiller with baseboard electric
	DOAS with VRF
	DOAS with low temp. radiant chiller with ASHP
PV Panels Active Fraction	From 0.5 to 0.9, step size: 0.1
PV Panels Tilt Angle	10°, 22°, 30°, 40°

The types of systems referenced in the second optimization phase, summarized in Tab.4.22 were selected from the *Honeybee* plug-in library, taking into account which of these are commonly used in Italy. As for the WWR presented in Tab. 4.21, they were selected based on the results of the energy simulation of the proposed design model, which was carried out with sample values for the design variables presented later in Tab.4.23, the results of which will be described in Chapter 5. Regarding the solar transmittance values of shading components in Tab.4.21, the first three values correspond to different shading objects type, as described in Section 4.3.3. The alternatives for the installation of the photovoltaic system in the same table, instead, are dictated by the considerations made in Section 4.3.6.

The two optimization phases are distinct and successive, ensuring that the HVAC system components are sized by the energy simulation software on a building with well-known and optimal envelope characteristics. The subsequent steps characteristic for this optimization approach are listed below:

1. Step 1: The CO_2 emissions associated with the operation of the baseline building are calculated using the model generated in Section 4.2, which does not include an HVAC system and therefore operates in free running mode.

2. Step 2: The CO_2 emissions associated with the operation of the proposed design are calculated using the model generated in Section 4.3, which, once again, does not include an HVAC system, thereby operating in free running mode. Initial values for optimization variables are selected, as

shown in Tab.4.23. For both Step 1 and Step 2, the energy simulation settings are configured to exclude HVAC system sizing and focus solely on thermal zone sizing.

Table 4.23: Initial values of the Phase 1 Optimization variables.

OPTIMIZATION VARIABLES - Before Phase 1 Optimization	
WWR - North Facade	0.4
WWR - East Facade	0.3
WWR - South Facade	0.4
WWR - West Facade	0.3
Shading Objects Solar Transmittance	0.01
PV Panels Location	South Roof

3. Step 3: Keeping constant the CO_2 emissions associated with the baseline building model, the first optimization phase (Phase 1) is initiated using the evolutionary algorithm parameters specified in Tab.4.20, obtaining all generated alternatives by varying the variables listed in Tab.4.21 within their defined ranges.

4. Step 4: Known the values of the variables obtained in Phase 1 of the optimization to minimize CO_2 emissions of the proposed design compared to the baseline building, both lacking HVAC systems, the models of the respective two buildings including the HVAC systems as described in Sections 4.3.7 and 4.2.4 are considered. In particular, the CO_2 emissions of the baseline building model, which includes the three HVAC systems sized appropriately as reported in Tab.4.10, are evaluated.

5. Step 5: Keeping constant the CO_2 emissions of the baseline building with HVAC systems and the building envelope features obtained as an output from the Phase 1 optimization, it has been proceeded by evaluating the emissions of the proposed design with the complete set of three HVAC systems , using the initial HVAC Types for the three HVAC systems included in the building presented in Tab.4.24, together with the initial active fraction and tilt angle of the PV panels installed in the optimal location obtained from the previous optimization phase.

Table 4.24: Initial values of the Phase 2 Optimization variables.

OPTIMIZATION VARIABLES - Before Phase 2 Optimization	
HVAC Type - Below Grade Floor	DOAS with fan coil chiller with central ASHP
HVAC Type - Ground Floor	DOAS with fan coil chiller with central ASHP
HVAC Type - First and Second Floor	DOAS with fan coil chiller with central ASHP
PV Panels Acrive Fraction	0.5
PV Panels Tilt Angle	22°

6. Step 6: While keeping constant the emissions calculated through the complete model of the baseline building with the three HVAC systems in Step 4, the Phase 2 optimization is initiated. During this phase, the evolutionary algorithm selects the optimal values within the defined ranges of the optimization variables listed in Tab.4.22. The parameters of the evolutionary algorithm remain as those indicated in Tab.4.20.

The two phases of the optimization process proceed almost identically, except for the objective function used. Indeed, while in the Phase 1 optimization it was sufficient to optimize considering a single objective function, namely the 4.8 one, it has been observed that by varying the variables listed in Tab.4.22 within the selected ranges, there is not only a variation in the CO_2 emissions associated with the building's operation over the course of a year, but also a variation in the number of hours during which the summer and winter setpoint temperatures indicated in Tab.4.6 are not reached despite the operation of the HVAC systems. For this reason, the evolutionary algorithm optimization in Phase 2 becomes a multi-objective optimization, in which the objective function for minimizing the relative increase in CO_2 emissions of the proposed design compared to the baseline is supplemented by equation 4.9.

$$min \quad \sum_{hour=1}^{8761} HU_{hour} + CU_{hour} \tag{4.9}$$

A schematic representation of the logic of the *Sequential Optimization* approach is given in Fig.4.17.
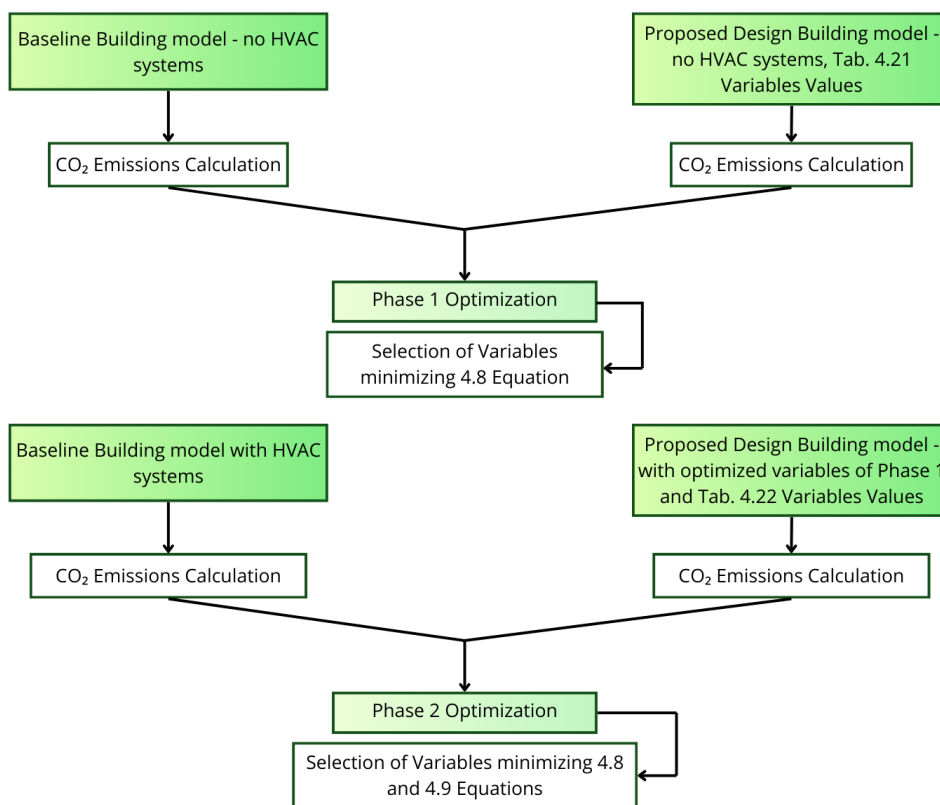
Figure 4.17: Sequential Optimization approach logic.

The second approach is the *Integrated Optimization* one: during it, multi-objective optimization will be carried out with the two equations 4.8 and 4.9, taking into account, in a single procedure, all the variables from Tab.4.21 and Tab.4.22. Also in this case, this will be preceded by the calculation of CO_2 emissions and energy consumption for the proposed design before starting the optimization procedure, considering the initial values of the variables presented in Tab.4.23 and Tab.4.24. In this way, it is possible to take into account any trade-off solutions between conflicting objectives, such as heating and cooling. The previously presented Sequential Optimization procedure, in fact, could lead to a reduction in energy demand for a certain end use, but at the same time, an increase for others, preventing the achievement of an optimum on the overall building performance[86]. A schematic representation of the logic of this optimization approach is given in Fig.4.18:
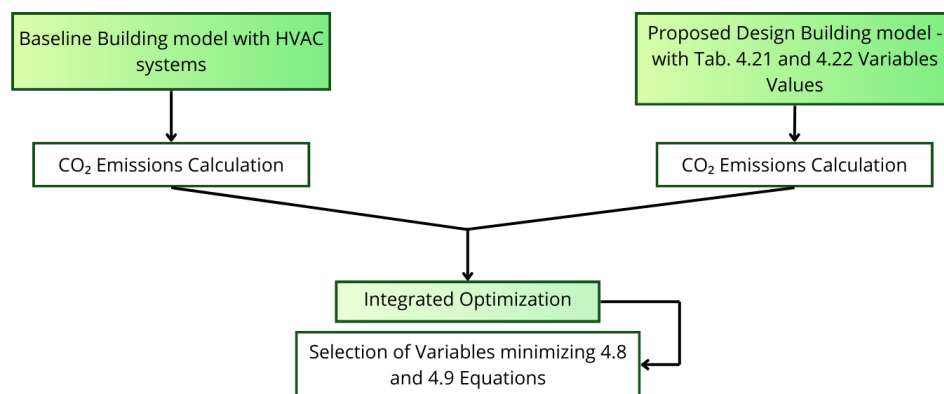
Figure 4.18: Integrated Optimization approach logic.

In both types of approaches, the procedure followed by the optimization algorithm is the same, beginning with the definition of a set of values k_i assigned to the optimization variables, which is input into the model to initiate energy simulation using the *EnergyPlus* engine, thus calculating the objective functions. Based on these, the algorithm selects a subsequent set of values according to the typical evolutionary logics of the POA described in Section 3.3.1, and repeats the energy simulation using *EnergyPlus*. The procedure continues until the entire solution space has been explored, taking into account the number of generations to be realized, dependent on the parameters set forth in Tab.4.20. A schematic representation of this operational logic is presented in Fig. 4.19.
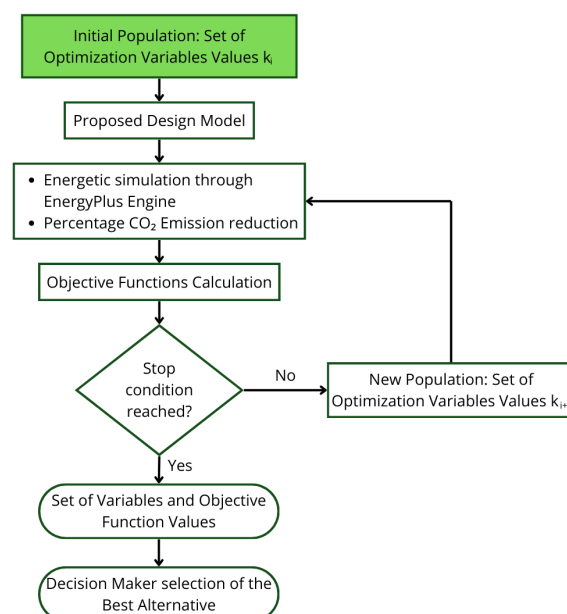
Figure 4.19: Optimization process logic.

Chapter 5

Optimization Analysis

After implementing both the Sequential and Integrated optimizations described in Section 4.5, the results are presented. Specifically, the aim of this chapter is to assess how useful the application of the optimization procedure via the NSGA-II evolutionary algorithm can be considered in evaluating design alternatives, with a focus on application in the early stages of building design. To achieve this, the performance of the baseline building will be firstly described; relative to this, the performance of the proposed design will be evaluated both before and after the application of the optimization procedure, both in Sequential and Integrated modes.

5.1 Baseline Building Performance

Considering the baseline building model, devoid of HVAC systems and thus employing an Ideal load, it can be affirmed that the associated energy consumption is solely attributed to heating and cooling of the indoor environment, as well as to the use of electrical energy for internal lighting and electrical equipment. The emissions associated with each of these and their corresponding consumptions are reported in Tab.5.1. It is noteworthy that both the CO_2 emission results and the energy consumption for each End Use are normalized to the heated surface area of the building, which is 1430.2 m^2.

Table 5.1: Baseline Building model simulation results, Ideal Load.

	Baseline Building	
End Uses	CO_2 Emissions $[kgCO_2/m^2]$	Energy Consumption $[kWh/m^2]$
Heating	14.76	39.92
Cooling	1.92	21.08
Interior Lighting	9.41	29.59
Electric Equipment	24.20	76.10
TOTAL	50.29	166.70

As evident, the most significant portion of energy consumption and thus CO_2 emissions is associated with the use of electrical appliances, which aligns with the office purposes of the building understudy, where, as mentioned in Section 4.2.3, the use of computers or printers is substantial. Additionally, in Fig.5.1, the energy balance of the building is presented, evaluated directly utilizing the capabilities provided by *Honeybee* plug-ins for calculation and *Ladybug* for graphical representation:
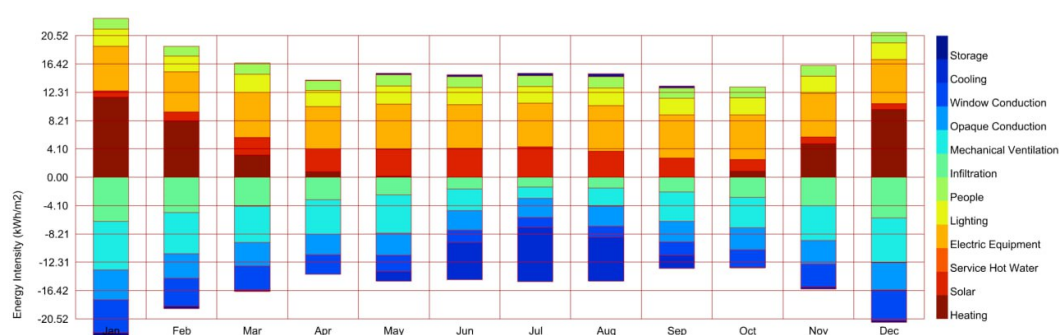
Figure 5.1: Normalized energy balance for the passive performance of the Baseline Building.

It is noticeable how the consumption related to electric equipment, occupants, and lighting remains constant throughout all seasons; the reason for this can be attributed to the fact that this type of usage is not tied to the seasonal variations occurring throughout the year and, therefore, to the climate of the location where the building is considered. Instead, it solely depends on the utilization of the building by its occupants, which, for an office, remains relatively constant in the long term and, in this case, depends on the default schedules provided by the *Honeybee* plug-in and the corresponding power density values. As for the use of hot water for services, although it is included in the legend, it

has no impact on the balance as, as mentioned in Section 4.2.3, its absence has been assumed for the case study.

In the balance, a significant variability in the impact of solar heat gains is observed: these are highest during the central months, particularly in summer, while they tend to decrease during the winter season. The reasons for this variability stem from the fact that, during colder months, the weather is typically characterized by cloudiness or precipitation. The infiltration rate is also dependent on seasonality: notably, the increased significance of this component during winter months is attributed to the fact that they are characterized by colder outdoor air temperatures compared to those maintained indoors; this temperature difference tends to facilitate the entry of cold air through cracks, crevices, or voids in the building into the internal spaces, where it is then heated and, becoming less dense, rises upward.

At this point, the trends of losses through the building envelope components can be analyzed: the conduction through opaque components remains almost constant throughout the year, while that related to transparent components tends to decrease during summer months due to the effect of solar radiation on them. During the winter season, these losses are compensated by the heating system, which has evidently higher consumption compared to the cooling required during the summer season. Consequently, it is observed that overall, during summer months, the energy balance concludes with lower energy shares, around 15 kWh/m^2 compared to over 20 kWh/m^2 during the winter season.

It should be noted that the balance includes a portion for mechanical ventilation: its presence is due to considering an Ideal Load system for the building, which is an idealized system responsible for meeting the building's energy demand. Mechanical ventilation is a component of this system and is thus included in the balance. Furthermore, especially during the hottest and coldest months, there is a portion labeled "Storage", representing in the *Honeybee* plug-in the small energy per m^2 that is not perfectly balanced.

At this point, the performance evaluation of the baseline building with the addition of the HVAC system described in Section 4.2.4 is undertaken. The emission and energy consumption results are reported in Tab. 5.2:

Table 5.2: Baseline Building model simulation results, HVAC systems.

Baseline Building		
End Uses	CO_2 Emissions $[kgCO_2/m^2]$	Energy Consumption $[kWh/m^2]$
Heating	18.80	67.80
Cooling	12.44	39.11
Interior Lighting	9.41	29.59
Electric Equipment	24.20	76.10
Fans	3.91	12.29
Pumps	0.03	0.10
TOTAL	68.80	225.00

As can be observed, there is an increase in the building's energy demand related to heating and cooling. This is attributed to the presence of a system like the one modeled, which ensures the fulfillment of the winter and summer temperature setpoints as specified in Tab. 4.6, as well as a relative humidity setpoint of 65%. Furthermore, it is important to note that the inclusion of such a system results in additional consumption associated with fans, such as those for outdoor air intake of the AHU, and pumps necessary for water movement within the system's ducts, which convey hot water produced by the boiler to VAV terminals with re-heat and to the hot coils of the AHU, as well as cold water produced by the direct expansion compressor with variable speed. It is worth noting that while these consumptions have minimal impact on the total, they are nonetheless essential for the proper functioning of the system.

5.2 Sequential Optimization

The first optimization approach chosen to be tested on the proposed design, aiming to select the best building and system variables for minimizing the environmental impact of the building, is the *Sequential Optimization*. As detailed in Section 4.5, it consists of two phases: in the first one, only variables related to the passive behavior of the building are considered for optimization, as listed in Tab.4.21. Once the algorithm has selected the optimal variables, these are held constant, and the second phase of optimization takes place, where only the variables listed in Tab.4.22 are optimized. In both phases, the same optimization algorithm settings, represented in Tab.4.20, will be maintained.

5.2.1   Passive Proposed Design Performance

Initially, the energy performance of the building associated with the proposed design model described in Section 4.3 is evaluated, once again considering it with an Ideal Load and thus devoid of an HVAC system. Considering the initial values of the variables for Phase 1 optimization as listed in Tab.4.23, the emission and energy consumption results for each end use are summarized in Tab.5.3. Additionally, the energy balance of the building is depicted in Fig.5.2.

Table 5.3: Proposed Design model simulation results, Ideal Load before Phase 1 optimization.

Proposed Design - Before Phase 1 Optimization		
End Uses	CO_2 Emissions $[kgCO_2/m^2]$	Energy Consumption $[kWh/m^2]$
Heating	14.54	39.31
Cooling	1.42	15.63
Interior Lighting	4.31	13.55
Electric Equipment	24.20	76.10
TOTAL	44.47	144.6
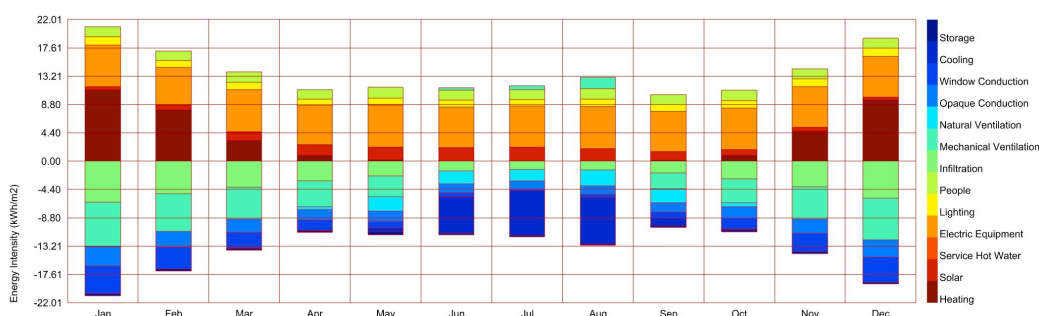
Figure 5.2: Normalized energy balance for the passive performance of the proposed design, Before Phase 1 Optimization.

From the analysis of the energy balance depicted in Fig.5.2, similar observations can be made as those made for the balance shown in Fig.5.1 of the baseline building regarding the end uses of lighting, occupants, electrical equipment, and hot water for services. However, concerning the conduction components through the building envelope, it is noted that both opaque and trasmparent envelope components are reduced, demonstrating an improved insulation performance for both. On the other hand, the solar load component

of the balance is slightly reduced in winter months, while this reduction is much more pronounced in the summer season. The reasons for these results are undoubtedly attributed to the presence of solar shading devices modeled as venetian blinds: the initial solar transmittance value is currently set to 0.01, significantly reducing the impact of incident radiation on the building's energy balance, leading to lower solar heat gains, especially in the summer season.

Of particular interest is the natural ventilation: it is completely absent during winter months, unlike in the summer months. The reason for this trend lies in the appropriate selection of temperature limit values from Tab.4.16, which have been used to regulate the operation of the system to prevent it from generating an undesirable effect, namely increasing both winter and summer loads. The mechanical ventilation, present for the same reasons defined for the baseline building in Section 5.1, is in this case reduced, indicating that indeed the passive behavior of the proposed design building is more efficient than that of the baseline building. This is evident also from the fact that the energy demand for heating and cooling, for the same month considered, is lower in the case of the proposed design, thanks to both the improved characteristics of the building envelope and the application of shading components on windows and natural ventilation, not provided in the baseline building.

Utilizing, in this initial phase, Equation 4.8 and considering the value of $kgCO_{2_{BB}}$ as the total emissions from Tab.5.1 and $kgCO_{2_{PD}}$ as the total emissions from Tab.5.3, a -11.58% reduction in CO_2 emissions of the proposed design compared to the baseline building is calculated, prior to the optimization procedure itself. This result is due to the fact that, as anticipated, in the development of the proposed design model, alternatives that ensure a reduction in the building's energy demand were selected, considering all end uses. To facilitate the comparison between the emissions associated with each End Use between the two models it is possible to use the histogram of Fig.5.3.
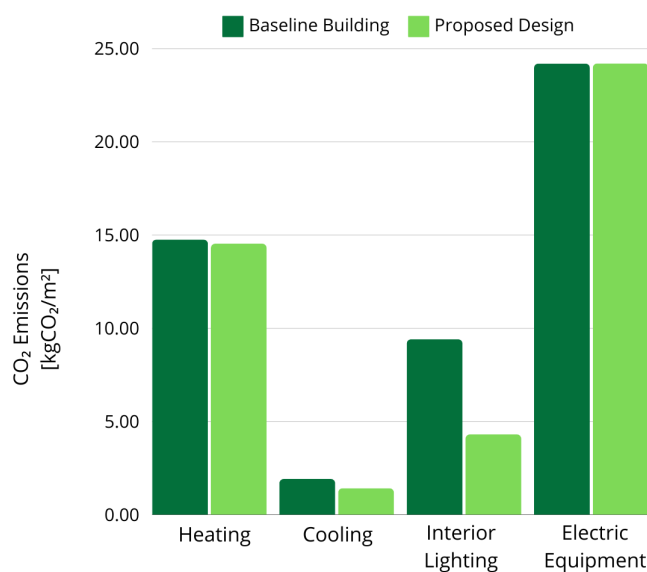
Figure 5.3: Comparison of CO_2 emissions per end use between Baseline Building and Proposed Design, before optimization.

It is immediately noticeable that the emissions related to electrical equipment are identical for both models. This is because they share the same geometry and occupancy type, thus having the same power associated with this End Use, defined as default by the *Honeybee* plug-in. Furthermore, this type of consumption and emissions cannot be modified simply by altering the building design, as is done considering both envelope and HVAC system properties: only a change in operational conditions can impact this type of end use. Considering these constants in the conducted study, the energy consumption and CO_2 emissions associated with electrical equipment will remain unchanged for all cases analyzed.

For each of the remaining end uses, it can be stated that:

- The reduction in heating-associated emissions, albeit minimal, is undoubtedly attributed to the selection of building envelope components that are more efficient for the proposed design compared to those chosen for the baseline building. These components are characterized by lower thermal transmittance, minimizing thermal energy losses to the external environment. This can also be asserted for the reduced cooling emissions, which is also influenced by the application of shading components on the facades' windows. Indeed, the implementation of solar shading devices reduces the incoming solar radiation, consequently lowering solar gains and thus the demand for cooling energy.

- The reduction in cooling emissions for the proposed design compared to the baseline building can also be linked to the implementation of natural ventilation techniques in the building. By allowing nighttime cooling, the demand for energy to maintain the setpoint temperature of 26°C during occupancy hours is reduced.

- The most significant reduction in emissions for the proposed design compared to the baseline is recorded for internal lighting. This is because, while according to Appendix G of ASHRAE 90.1-2016, a constant lighting power density must be applied on the baseline building based on the building's occupancy type, the proposed design implements artificial lighting control based on incoming natural light from windows, as described in Section 4.3.4. This allows for maximizing the use of available natural light on-site and minimizing the need for electrical energy consumption to ensure occupants' visual comfort.

Furthermore, Fig.5.3 provides crucial information regarding the building's performance as realized by the proposed design model: excluding the consumption associated with electrical equipment, for the reasons presented above, the most significant energy consumption and, thus, CO_2 emissions, characterizing the building is for heating. The reasons for this can be attributed to:

- Building envelope characteristics, which are assumed to be non-variable during the optimization procedure.

- Boundary conditions, particularly the climate of the site where the building is located, which is one of the constants during the building design phases.

- Extent of fenestration components: these are indeed a source of heat loss to the outdoor, thus optimizing them in the early design phases is crucial. This observation was fundamental for defining the range of variation of the WWR applied in the optimization procedure. Considering that lower WWR values correspond to reduced heat losses to the outdoor and thus lower heating consumption, the algorithm tends to associate the smallest available value with these variables, taking into account the trade-off with internal lighting consumption. To prevent this and ensure that the selected WWR has a value consistent with those required for adequate visual comfort of occupants, it was imposed that the lowest value that can be associated with this variable, for all orientations, is set to 0.3.

At this point, considering the optimization parameter values reported in Tab.4.20, and using the total $kgCO_{2_{BB}}$ value from Tab.5.1, the optimization procedure is initiated to ensure the selection of Phase 1 optimization variables within the ranges specified in Tab.4.21. It should be noted that all simulations and optimization procedures were performed on a computer with the following specifications: Intel® Core™ i7-860 – 2.80 GHz, 8 MB cache, 4 cores. Based on this, there is a certain time required to complete the optimization procedure, which can be reduced using a computer with more powerful specifications.

In this initial phase of the optimization procedure, the NSGA-II algorithm worked with a search space size of $2.10 \cdot 10^4$, a number of genes equal to 5, and a number of values to test equal to 40. With a Population Size of 100, the optimization time was 14 hours and 50 minutes. The optimal values of the variables are reported in Tab.5.4, while the CO_2 emissions values and associated energy consumptions are summarized in Tab.5.5:

Table 5.4: Optimal value for the Phase 1 optimization variables, Population Size: 100.

Phase 1 Optimization, Population Size: 100	
WWR N	0.3
WWR E	0.4
WWR S	0.3
WWR O	0.4
Solar Transmittance Shading Components	0.8
PV Plant Location	West Roof

Table 5.5: Proposed Design model optimization Phase 1 results, Population Size: 100.

Proposed Design - After phase 1 optimization, Population size:100		
End Uses	CO_2 Emissions $[kgCO_2/m^2]$	Energy Consumption $[kWh/m^2]$
Heating	13.87	37.50
Cooling	1.50	16.54
Interior Lighting	4.30	13.51
Electric Equipment	24.20	76.10
TOTAL	43.87	143.67

These results correspond to a 12.77% reduction in CO_2 emissions compared to the baseline building: the optimization procedure thus allows for an improvement in performance compared to manual insertion of building parameter values, considering that the percentage reduction in emissions is higher, in absolute terms, compared to what was achieved before applying the optimization algorithm (11.58%). From the comparison between the results in Tab.5.3 and Tab.5.5, a slight reduction in heating energy demand is observed. This is because the algorithm associated higher solar transmittance values with all shading components and made changes to the photovoltaic panels shading surface. A higher solar transmittance value increases the portion of solar heat gain entering the spaces, thus reducing the need for heating. This is also consistent with the higher energy consumption and emissions associated with cooling the building: greater solar heat gains in the summer season lead to heating of the spaces, which must be offset by increased cooling from the cooling system. Regarding the impact of different in WWR on the energy balance, this will be discussed in the sensitivity analysis phase conducted subsequently, along with the impact of different shading locations associated with the photovoltaic system. As for internal lighting, the demand remains nearly identical, and any minimal variation could be attributed to inherent uncertainties characteristic of energy simulations.

The energy balance of the building obtained from the *Honeybee* plug-in is therefore reported in Fig.5.4:
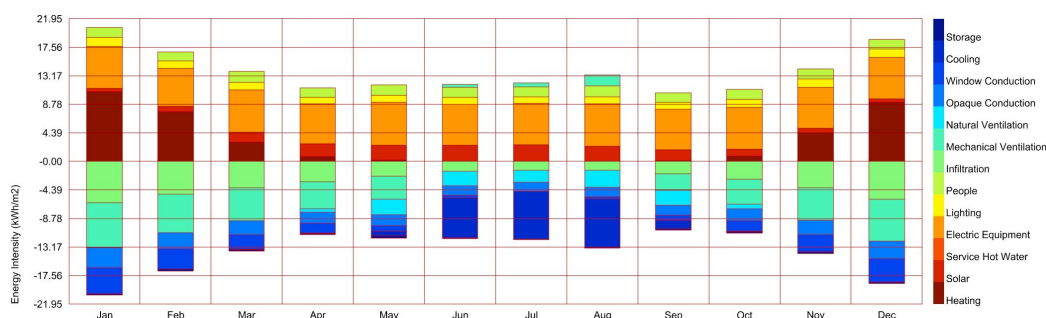
Figure 5.4: Normalized energy balance for the passive performance of the proposed design, After Phase 1 Optimization.

To assess the impact of the optimization procedure on the energy balance of the proposed design building, it is advisable to compare Fig.5.2 with Fig.5.4: they appear almost identical, but it is important to note that the vertical reference of the normalized energy intensity is different: before optimization, the

axis ranges from about -22.01 kWh/m^2 to +22.01 kWh/m^2, while after optimization, it ranges from about -21.95 kWh/m^2 to +21.95 kWh/m^2. Therefore, overall energy consumption is reduced, which is attributed to a lower heating energy demand compared to before the optimization procedure. As anticipated, this is due to increased solar radiation availability resulting from higher solar transmittance of shading components, particularly evident in February, March, and April. For the same reasons, there is a slight increase in cooling demand. As for the other components of the balance, they are very similar to those described for the case before the optimization procedure.

5.2.2 Proposed Design Performance with HVAC

Given the optimal values of the Phase 1 optimization variables reported in Tab.5.4, the behavior of the optimized proposed design is evaluated when HVAC systems are integrated, along with the consideration of electricity production from a photovoltaic system. Starting with the model with the variable values from Tab.5.4, HVAC systems are added to each of the three groups of rooms selected in Tab.4.8, as presented in Tab.4.24, along with the tilt angle and active surface characteristics of the photovoltaic system placed on the South-West facade. As anticipated, the constructions of the horizontal components of the building envelope are also modified, as shown in Tab.4.19, to allow for the potential subsequent installation of radiant ceiling panels.

The results of CO_2 emissions and energy consumption obtained from the annual simulation, considering the self-sizing of the components of the three HVAC systems with factors of 1.25 for heating and 1.15 for cooling, are reported in Tab.5.6:

Table 5.6: Proposed Design model simulation results with HVAC systems before Phase 2 optimization.

Proposed Design - Before Phase 2 Optimization		
End Uses	CO_2 Emissions $[kgCO_2/m^2]$	Energy Consumption $[kWh/m^2]$
Heating	2.23	7.00
Cooling	3.44	10.83
Interior Lighting	4.31	13.55
Electric Equipment	24.20	76.11
DOAS Fans	0.52	1.63
Fcu Fans	1.07	3.35
Pumps	1.37	4.32
Heat Rejection	0.14	0.45
Humidification	0.10	0.31
TOTAL	37.38	117.54

As observed in Tab.5.6, the end uses related to the HVAC system components chosen for all three groups of rooms are present. Initially, the system is defined as DOAS with fan coil chiller with central ASHP, including the fans of the outdoor air management system and of the fan coils, labeled as DOAS Fans and Fcu Fans, respectively. Additionally, there are energy consumptions associated with Heat Rejection and Humidification: the former corresponds to a process where excess heat in the system is expelled, possibly related to the heat rejected by the cooling tower associated with the chiller in the specific system considered; the latter is a consumption associated with the system's capability to maintain the relative humidity setpoint at 65% in the rooms. All end uses listed in Tab.5.6, as mentioned in Section 4.3.7, involve the use of electrical energy, which can be drawn from the grid or produced by the building's own photovoltaic system. However, the results provided so far only represent the electricity demand for each of the listed end uses, without distinguishing between the portion drawn from the grid and that supplied by the photovoltaic system. Therefore, to understand the positive impact of integrating the photovoltaic system on the building's energy balance, the hourly renewable energy production on-site and the building's hourly consumption are evaluated. The difference between them allows assessing the total amount of electricity that needs to be imported into the system, thus effectively generating emissions as it is purchased from the national grid on an hourly basis.

For the selected case study, the following assumptions were made:

1. Electrical energy self-produced by the photovoltaic system and consumed within the building is characterized by zero kg of CO_2 emissions per kWh.

2. Electrical energy produced by the photovoltaic system and not utilized within the building is the surplus exported to the grid and considered to have zero kg of CO_2 emissions per kWh. This means that the surplus energy production from the system is not considered advantageous in terms of reducing the overall environmental impact of the building.

For the selected case, the breakdown of electrical energy consumed by the building, produced by the photovoltaic system, and purchased from the grid is provided in Tab.5.7.

Table 5.7: Site utils for production and consumption of electrical energy, Proposed Design before Phase 2 Optimization.

Proposed Design - Before Phase 2 Optimization	
On site produced electricity	11054.00 kWh
On site surplus electricity	1.67 kWh
Purchased from grid electricity	157048.89 kWh

As can be observed, the surplus of on-site electricity production injected into the grid is very limited, and the electricity production from the plant consumed directly on-site corresponds to only about 7% of the total building consumption. Nevertheless, since this portion helps reduce grid dependency and thus the building's environmental impact, for the calculation of the objective function 4.8, $kgCO_{2_{PD}}$ will not consider the total value from Tab.5.6, but the sum, over the entire year, of the hourly difference between the building's consumption and the system's production, normalized to the building's heated area. For the proposed design case with optimized building characteristics and HVAC system properties and the photovoltaic system of Tab.4.24, this value is $35.77 kgCO_2/m^2$. Comparing this to the baseline building performance with HVAC systems, summarized by the $kgCO_{2_{BB}}$ Total value from Tab.5.2, a percentage reduction in emissions of -48.01% is calculated. This result is attributed to two factors:

1. Lower energy consumption per m^2 of heated area for the proposed design compared to the baseline building, undoubtedly due to the use of a more efficient HVAC system: the baseline building's HVAC generation system is a condensing boiler with 80% efficiency. This means that only 80% of the energy input into this component, supplied in the form of natural gas, becomes useful energy for the building's hot water production. The heat pump and chiller, as described in Section 4.3.7, have COP and EER greater than 1, meaning the portion of useful energy they produce exceeds what they receive as input, resulting in lower consumption compared to a boiler, for the same amount of energy produced and, thus, demanded from the building.

2. Different energy source: the condensing boiler is fueled by natural gas, which has a higher environmental impact and therefore higher CO_2 emissions per kWh of energy compared to electricity from the grid or, even more so, electricity generated by a photovoltaic system.

At this point, it's necessary to evaluate how much the optimization procedure can further reduce the CO_2 emissions of the proposed design compared to the baseline building, by selecting the best HVAC system alternatives and photovoltaic system properties from those summarized in Tab.4.22. Using the same computer as in the Phase 1 optimization phase, it has been proceeded with the Phase 2, characterized by a solution search space size of $4.30 \cdot 10^3$, resulting from analyzing 5 genes with 27 values in total. The total simulation time is 12 hours and 56 minutes, and the results of the optimized variables obtained are presented in Tab.5.8, while the energy consumption and CO_2 emissions are summarized in Tab.5.9.

Table 5.8: Optimal values for Phase 2 optimization variables, Population Size:100 (Alternative 1).

Phase 2 Optimization, Population Size: 100	
HVAC Type - Below Grade Floor	DOAS with VRF
HVAC Type - Ground Floor	DOAS with fan coil chiller with central ASHP
HVAC Type - First and Second Floor	DOAS with VRF
PV Panels Acrive Fraction	0.9
PV Panels Tilt Angle	40°

Table 5.9: Proposed Design model Integrated Optimization results, Population Size: 100 (Alternative 1).

Proposed Design - After Phase 2 Optimization		
End Uses	CO_2 Emissions $[kgCO_2/m^2]$	Energy Consumption $[kWh/m^2]$
Heating	1.50	4.73
Cooling	1.88	5.91
Interior Lighting	4.31	13.56
Electric Equipment	24.20	76.11
Doas Fans	0.52	1.63
Fans	0.39	1.23
Humidification	0.15	0.49
TOTAL	32.96	103.65

The alternatives selected by the optimization algorithm for the Phase 2 of Sequential Optimization allow achieving net emissions from the building, taking into account the photovoltaic system production, equivalent to -59.86%, thus enabling achieving a performance that is better by almost the 60% compared to the baseline building complete with HVAC systems described in Section 4.2.4. However, in this optimization phase, not only the objective function 4.8 is considered but also the one defined in 4.9 equation, which, for the described solution, has a value of 7754, corresponding to 4052 for the winter season and 3702 for the summer season. To better understand the solution analysis procedure by the algorithm, it's possible to use the representation of the solutions provided by the *Wallacei* plug-in, which is depicted from two different perspectives in Fig.5.5.
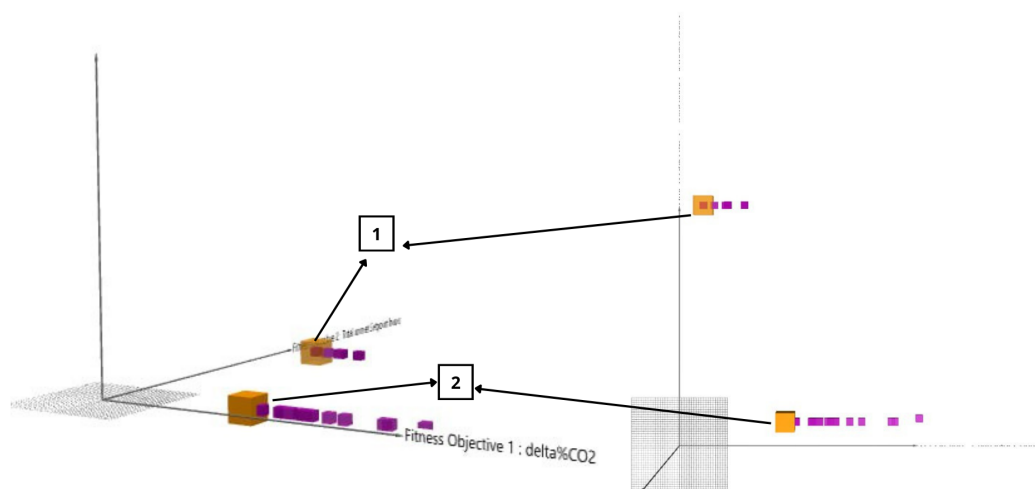
Figure 5.5: Solutions Plot - Phase 2 Optimization, Population Size: 100.

As observed from the representation of solutions obtained after completing the optimization procedure, the alternatives evaluated by the algorithm tend to shift towards higher absolute percentage reductions in CO_2, but there is also a concentration of solutions even at very high values of Unmet Setpoint Hours. In particular, the solution described in Tab.5.8 and Tab.5.9 corresponds to the one with the minimum emissions but with elevated Unmet Setpoint Hours, thus the one indicated by 1 in Fig.5.5. Therefore, the selection process proceeded by choosing the solution indicated by 2, corresponding to zero Unmet Setpoint Hours and minimum emissions, which is described below in Tab.5.10 and Tab.5.11:

Table 5.10: Optimal values for Phase 2 optimization variables, Population Size:100 (Alternative 2).

Phase 2 Optimization, Population Size: 100	
HVAC Type - Below Grade Floor	DOAS with fan coil chiller with baseboard electric
HVAC Type - Ground Floor	DOAS with VRF
HVAC Type - First and Second Floor	DOAS with fan coil chiller with central ASHP
PV Panels Acrive Fraction	0.9
PV Panels Tilt Angle	40°

Table 5.11: Proposed Design model Integrated Optimization results, Population Size: 100 (Alternative 2).

Proposed Design - After Phase 2 Optimization		
End Uses	CO_2 Emissions $[kgCO_2/m^2]$	Energy Consumption $[kWh/m^2]$
Heating	2.23	7.02
Cooling	3.44	10.80
Interior Lighting	4.31	13.56
Electric Equipment	24.20	76.11
Doas Fans	0.52	1.63
Fcu Fans	1.07	3.35
Pumps	1.38	4.33
Heat Rejection	0.14	0.45
Humidification	0.10	0.31
TOTAL	37.38	117.55

Analyzing first the selection of optimal alternatives for the optimization variables as reported in Tab.5.10, it's notable that it only shares the characteristics of the photovoltaic system with the solution in Tab.5.8. This indicates that these variables have no impact on the number of hours where the winter and summer temperature setpoints are not met. Concerning the active fraction of the shading surface associated with the panels, it's set to the maximum value within the range, maximizing the system's productivity: a larger active surface leads to higher electricity production and, consequently, lower emissions associated with the building's use. Additionally, the tilt angle has been selected to its maximum value; observing Fig.4.5, it's evident that a high tilt angle on the South-west-facing slope of the roof allows the photovoltaic system to receive optimal sunlight in the southwest direction, facilitating high production. It's worth noting that this alternative has been selected also because, despite it corresponds to a better exposition to the sun radiation, it doesn't lead to overheating of the panels, which would decrease their productivity.

On the contrary, the selected HVAC systems in this alternative are entirely different from the previous one: considering the starting values from Tab.4.24, the only unchanged value pertains to the first and second floors. As demonstrated later during the sensitivity analysis, the choice of different HVAC systems for the group of rooms corresponding to the first and second floors has the greatest impact on energy consumption and thus on the building's overall

emissions due to the larger floor area covered. Therefore, the emissions and energy consumption results are practically identical to those recorded before the application of the second phase of the Sequential Optimization procedure. Nonetheless, the improved selection of variables associated with the photovoltaic system enhances the building's overall performance; to demonstrate this, a comparison between Tab.5.7 and the following Tab.5.12 can be made:

Table 5.12: Site utils for production and consumption of electrical energy, Proposed Design after Phase 2 Optimization, Population Size: 100 (Alternative 2).

Proposed Design - After Phase 2 Optimization	
On site produced electricity	23379.00 kWh
On site surplus electricity	681.39 kWh
Purchased from grid electricity	145024.82 kWh

From the comparison between Tab.5.7 and Tab.5.12, it's noticeable that the net production has increased. This can be attributed to a higher percentage of active surface area, as well as the greater tilt angle of the panels, which, as anticipated, enhances the reception of solar radiation. Consequently, there is a lower draw from the grid and a greater surplus injected into the grid itself. The emissions associated with the proposed design, net of photovoltaic production and hourly consumption, amount to 32.03 $kgCO_2/m^2$. Using these as $kgCO_{2_{PD}}$, the value of the optimized objective function is -53.44%: the proposed design, complete with envelope components, HVAC systems, and photovoltaic system, leads to a performance that is over 50% better than that of the baseline building. Considering the effect of only the Phase 2 of optimization, compared to the model where a non-optimal choice of HVAC systems was made, there is a further 5% reduction in emissions. In general, therefore, it can be concluded that the Sequential Optimization procedure just presented indeed allows a significant improvement in the building's performance in design. Thus, it could be beneficial to consider its incorporation in the early design stages, providing guidance to designers in selecting alternatives that may be considered optimal, both in terms of reducing environmental impact and complying with current regulations or, potentially, obtaining voluntary certifications such as LEED or BREEAM mentioned in Chapter 4.

5.3 Integrated Optimization

In Section 5.2, the effectiveness of applying an optimization procedure with the evolutionary algorithm NSGA-II to evaluate various design alternatives in the early stages of design was demonstrated, considering a Sequential procedure. However, with a Population Size of 100, the time required for each phase amounts to a total of approximately 14 hours for building components and 13 hours for system components, totaling 27 hours. Additionally, such an approach may not lead to the global optimum as there are, in fact, various interdependencies in complex systems like those of buildings, especially in terms of long-term operability. Hence, it might be more useful to ensure that they are optimized simultaneously. For instance, larger window components may increase winter thermal loads but concurrently reduce the demand for lighting energy; if heat production is carried out by an efficient system, the negative impact on winter loads from larger glazed areas could be well managed, resulting in a lesser overall impact compared to its positive effect on lighting energy demand. To assess the effectiveness of an Integrated Optimization procedure, the results are presented below.

Before the optimization procedure, the performance of the proposed design, complete with HVAC systems and a photovoltaic production system, is evaluated using the optimization variable values listed in Tab.4.23 and Tab.4.24. The results of CO_2 emissions, energy consumption, and those related to the production of electricity from the photovoltaic system are presented in Tab.5.13 and Tab.5.14, respectively.

Table 5.13: Proposed Design model simulation results with HVAC systems before Integrated optimization.

Proposed Design - Before Integrated Optimization		
End Uses	CO_2 Emissions $[kgCO_2/m^2]$	Energy Consumption $[kWh/m^2]$
Heating	2.40	7.54
Cooling	3.28	10.31
Interior Lighting	4.32	13.58
Electric Equipment	24.20	76.11
Doas Fans	0.52	1.63
Fcu Fans	1.03	3.22
Pumps	1.32	4.15
Heat Rejection	0.14	0.42
Humidification	0.15	0.46
TOTAL	37.34	117.43

Table 5.14: Site utils for production and consumption of electrical energy, Proposed Design Before Integrated Optimization.

Proposed Design - Before Integrated Optimization	
On site produced electricity	2053.00 kWh
On site surplus electricity	0.00 kWh
Purchased from grid electricity	165875.00 kWh

Considering the hourly difference between electricity production and consumption in the building over the entire simulation year, the net emissions of the proposed design amount to 36.89 $kgCO_2/m^2$, corresponding to a percentage reduction of -46.38% compared to the baseline building complete with HVAC systems. The percentage reduction achieved before Phase 2 optimization, and thus, by applying HVAC systems and the photovoltaic system to a model with already optimized building envelope, was -48.01%: the difference of approximately 2% between the two values is attributed to the fact that building envelope components, with the same installed systems, have an impact on the building's energy consumption. To understand which End Uses are most influenced by a non-optimized envelope, one can refer to the graphical comparison between the results before Phase 2 optimization and those before integrated optimization shown in Fig.5.6.
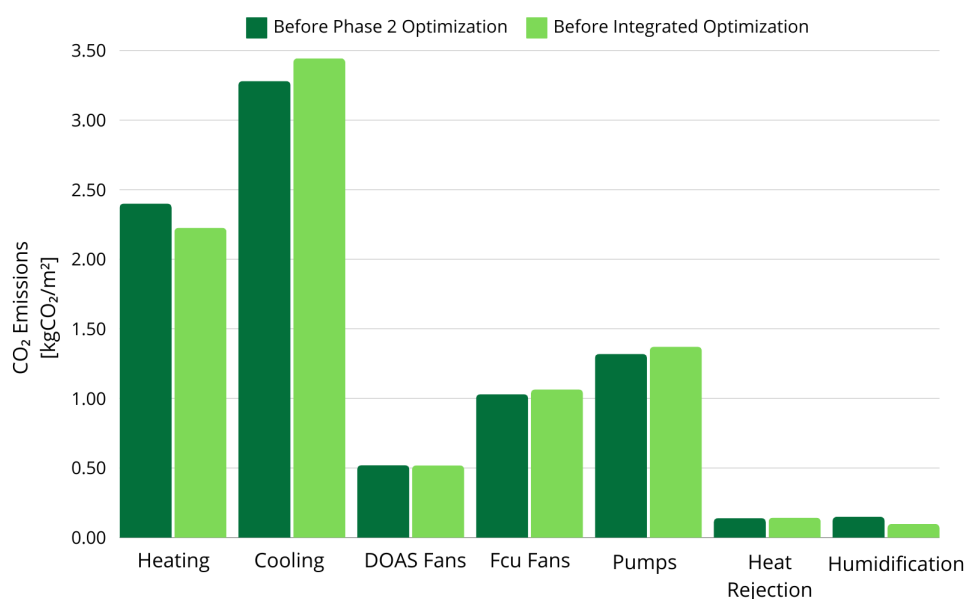
Figure 5.6: Comparison of CO_2 emissions of the Proposed Design before Phase 2 optimization and before Integrated Optimization.

In this case, the representation of emissions associated with Interior Lighting and Electric Equipment has been avoided as they remain practically unchanged between the two analyzed cases. The graph in Fig.5.6 clearly shows that a non-optimized building envelope in terms of WWR and shading systems results in higher energy consumption for cooling, leading to higher consumption of plant components such as pumps and fan coils' fans. Considering the differences in the values associated with the properties of the envelope between the two studied cases, it can be stated that the consumption related to these factors may be due to a different arrangement of window components in the building: higher WWR values in the South and North cardinal directions may lead to excessive solar radiation input during the summer season, increasing the load during that period; at the same time, this would also explain a reduced winter load, as solar radiation contributions partially satisfy the building's heat demand to maintain the required setpoint and setback temperatures.

Regarding Tab.5.14, it is noticeable that the photovoltaic production is significantly lower compared to that reported in Tab.5.7: this results in zero electricity exports to the grid. The causes of this are surely a suboptimal location of the system, both in terms of orientation and tilt angle, which are, in this case, the South roof one with 22° of inclination, as well as too small an active surface, only 0.5 of the available plan area.

Thus, an Integrated Optimization is carried out by varying the optimization variables within the ranges summarized in Tab.4.21 and Tab.4.22. Using the same computer as for the Sequential Optimization to run the NSGA-II optimization algorithm through the *Wallacei* plug-in with the settings in Tab.4.20, the time required for a population size of 100 was 12 hours and 41 minutes, with a search space size of $2.90 \cdot 10^8$, due to a number of genes equal to 10 and a number of values equal to 76. It is worth noting that, as in the case of Phase 2 Sequential Optimization, the algorithm's objective function is not only the one expressed in 4.8, but also 4.9. At the end of the optimization procedure, therefore, the solution minimizing CO_2 emissions compared to the baseline is selected, and then the number of corresponding unmet setpoint hours is evaluated. The values taken by the optimization variables for the solution with the lowest CO_2 emissions are reported in Tab.5.15, while the consumption and emissions, divided by end use, are in Tab.5.16. Information on renewable energy produced by the photovoltaic system and fed into the grid is in Tab.5.17.

Table 5.15: Optimal values for the Integrated Optimization, Population Size: 100 (Alternative 1).

Integrated Optimization, Population Size: 100	
WWR - North Facade	0.8
WWR - East Facade	0.3
WWR - South Facade	0.4
WWR - West Facade	0.3
Shading Objects Solar Transmittance	0.6
PV Panels Location	West Roof, 40° Location
HVAC Type - Below Grade Floor	DOAS with VRF
HVAC Type - Ground Floor	DOAS with fan coil air-cooled chiller with central ASHP
HVAC Type - First and Second Floor	DOAS with VRF
PV Panels Acrive Fraction	0.9

Table 5.16: Proposed Design model simulation results with HVAC systems after Integrated Optimization (Alternative 1).

Proposed Design - After Integrated Optimization		
End Uses	CO_2 Emissions $[kgCO_2/m^2]$	Energy Consumption $[kWh/m^2]$
Heating	3.70	11.64
Cooling	1.90	5.96
Interior Lighting	4.16	13.08
Electric Equipment	24.20	76.11
Doas Fans	0.52	1.63
Fans	0.57	1.79
Humidification	0.16	0.52
TOTAL	35.21	110.73

Table 5.17: Site utils for production and consumption of electrical energy, Proposed Design After Integrated Optimization, Population Size: 100 (Alternative 1).

Proposed Design - After Integrated Optimization	
On site produced electricity	23216 kWh
On site surplus electricity	844.44 kWh
Purchased from grid electricity	133520.28 kWh

Considering the comparison between the optimized photovoltaic system's hourly production and the building's hourly consumption over the entire operational year, the net emissions amount to 29.50 $kgCO_2/m^2$, corresponding to a percentage reduction in CO_2 emissions compared to the baseline of -57.12%. This reduction is comparable to that achieved with the same population size following Phase 2 Optimization, with a difference of less than about 4%. However, the number of unmet setpoint hours, calculated as per equation 4.9, amounts to 9904, comprising 4869 hours for the winter season and 4225 for the summer season. The set of solutions analyzed by the algorithm for integrated optimization is also represented in Fig.5.7.
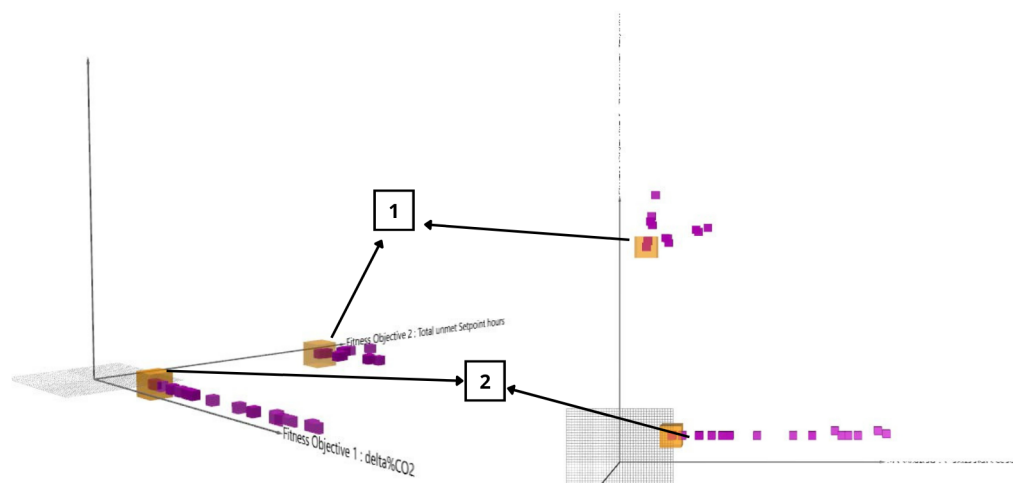
Figure 5.7: Solutions Plot - Integrated Optimization, Population Size: 100.

The observations that can be made are similar to those regarding Phase 2 of Sequential Optimization; in particular, the solution analyzed in Tab.5.15, Tab.5.16, and Tab.5.17 corresponds to the one with minimal emissions but with a high value of unmet setpoint hours, thus corresponding to the one indicated as 1 in Fig.5.7. It has been proceeded to search, among those available, for the one indicated as 2, thus with a number of Unmet Setpoint Hours equal to zero and with minimal emissions. Features of this solution are summarized in Tab.5.18, Tab.5.16, and Tab.5.20:

Table 5.18: Optimal values for the Integrated Optimization, Population Size: 100 (Alternative 2).

Integrated Optimization, Population Size: 100	
WWR - North Facade	0.8
WWR - East Facade	0.3
WWR - South Facade	0.4
WWR - West Facade	0.3
Shading Objects Solar Transmittance	0.65
PV Panels Location	West Roof, 40° Location
HVAC Type - Below Grade Floor	DOAS with VRF
HVAC Type - Ground Floor	DOAS with fan coil chiller with baseboard electric
HVAC Type - First and Second Floor	DOAS with fan coil air cooled chiller with central ASHP
PV Panels Acrive Fraction	0.9

Table 5.19: Proposed Design model simulation results with HVAC systems after Integrated Optimization (Alternative 2).

Proposed Design - After Integrated Optimization		
End Uses	CO_2 Emissions $[kgCO_2/m^2]$	Energy Consumption $[kWh/m^2]$
Heating	2.86	8.99
Cooling	3.06	9.63
Interior Lighting	4.16	13.07
Electric Equipment	24.20	76.11
Doas Fans	0.52	1.63
Fans	0.10	0.32
Pumps	0.69	2.15
Humidification	0.15	0.48
TOTAL	36.66	115.28

Table 5.20: Site utils for production and consumption of electrical energy, Proposed Design After Integrated Optimization, Population Size: 100 (Alternative 2).

Proposed Design - After Integrated Optimization	
On site produced electricity	23343.00 kWh
On site surplus electricity	717.78 kWh
Purchased from grid electricity	141535.00 kWh

The emissions net of photovoltaic production amount to 31.31 $kgCO_2/m^2$, corresponding to a percentage reduction compared to the baseline building model with HVAC systems of -54.49%. This value exceeds the -53.44% obtained following Phase 2 of Sequential Optimization, and ensures not only better performance compared to the baseline case, but also the satisfaction of occupant comfort for all hours of the year considered.

To understand the impact of the two different design alternatives suggested by the two optimization procedures analyzed in this study, namely the Sequential Optimization analyzed in Section 5.2 and the Integrated Optimization described above, one can refer to Fig.5.8.
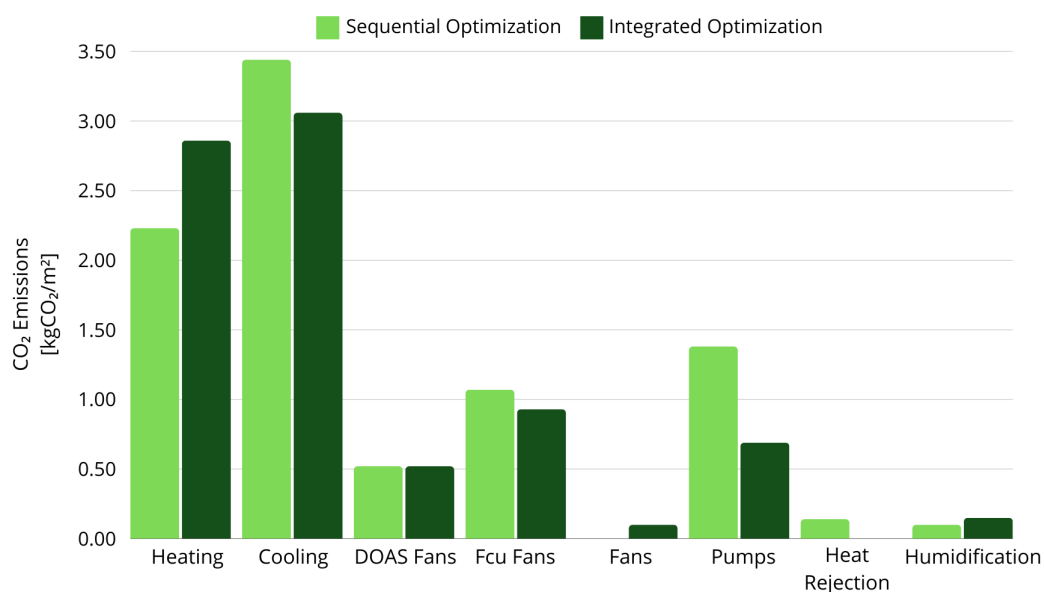
Figure 5.8: Comparison of CO_2 emissions of the Proposed Design after Phase 2 of Sequential Optimization and after Integrated Optimization.

As can be noted, the 1% difference in emissions reduction observed following the two optimization approaches is due to a compensation between the CO_2 emissions related to the different end-uses. Firstly, examining the ones associated with heating, it is apparent that those resulting from the Integrated Optimization are higher than those from the Sequential Optimization; the reason for this can be understood by comparing Tabs.5.18 and 5.4:

- The share of solar gains entering through fenestration components is lower in the alternative suggested as optimal by the Integrated Optimization compared to the Sequential Optimization one due to the lower solar transmittance value of shading objects;

- The share of energy dissipated during the winter season to the outdoor environment is higher in the solution suggested as optimal by the Integrated Optimization compared to the one of Sequential Optimization due to the higher WWR of the North orientation.

However, the first reason can be considered also the primary cause of the reduced cooling demand and, consequently, the associated emissions for the building in the solution suggested by the Integrated Optimization as can be noted form Fig.5.8.

Then, analyzing the system components, from the comparison between Tab.5.18 and Tab.5.10, it can be observed that the HVAC types DOAS with

VRF and the one with baseboard terminals are present in both solutions; however, their arrangement within the building differs. Specifically, the solution of Phase 2 of Sequential Optimization assigns the former to the Ground floor and the latter to the Below-Grade Floor, whereas the Integrated Optimization solution does the opposite. In general, it can be stated that the HVAC system characterized by baseboard terminals, as mentioned in Section 4.3.7, cannot be considered highly efficient since heat production is carried out via the Joule effect. However, of particular relevance is the HVAC system assigned to the First and Second floors, which has the greatest impact on the overall energy balance as will be demonstrated in Section 5.2.2. It would be advisable, therefore, to evaluate what happens if another type of system is associated with the group of rooms on the first and second floors. This will be done and discussed during the Sensitivity Analysis phase in Chapter 6. Regarding Fig. 5.8, some observations can be made:

1. For the DOAS Fans, there is no difference between the two design alternatives, as for both of them, the Proposed Design requires a minimum amount of external air flow to ensure adequate IAQ;

2. The fans of the fan-coils have slightly lower emissions for the alternative suggested by the Integrated Optimization, probably due to the reduced cooling energy demand;

3. For the same reasons, the energy demand and, consequently, the corresponding emissions for pumps are much lower for the Integrated Optimization alternative compared to the Sequential Optimization;

4. As for the remaining end-uses, the differences are minimal and could also be related to the uncertainty associated with energy simulation.

At this point, it seems that an Integrated Optimization procedure could be the best way to obtain the best design alternative for the analyzed proposed design. Indeed, although the difference compared to the results of Phase 2 of Sequential Optimization is only +1%, it is necessary to assess the simulation time as well: as anticipated, for Sequential Optimization with a Population Size of 100, it is about 27 hours, compared to just 13 with Integrated Optimization. It could therefore be interesting to evaluate how the solution varies with both optimization approaches when trying to reduce the optimization time in order to check if, through the application of Sequential Optimization with a lower Population Size, it is possible to obtain an optimal solution with a quality comparable with the one previously presented for the Integrated Optimization,

but with a lower optimization time. To do this, in the following Chapter 6, different population sizes will be evaluated as inputs to both procedures in order to assess:

1. The impact on the quality of the solution;
2. The impact on optimization times.

Additionally, a sensitivity analysis on the optimization variables will be carried out in order to check for the environmental and energy behaviour of the proposed design.

Chapter 6

Sensitivity Analysis

As anticipated, one of the key parameters affecting the quality of solutions obtained from the evolutionary optimization algorithm is the Population Size: the higher it is, the greater the number of evaluated generations, thus increasing the probability of finding the global optimum. However, this comes at the cost of simulation time, which grows exponentially with this value. For these reasons, at least initially, it was decided to set both the Sequential Optimization and the Integrated Optimization phases to a fixed value of Population Size equal to 100. However, it is interesting to evaluate how the quality of solutions varies by increasing or decreasing the Population Size, taking into account also its effect on optimization time. For these reasons, the optimization procedures described in Section 4.5 were run again, considering all the settings summarized in Tab.4.20, except for the population size, which was set to 80 and 200. Below are the results divided into Sequential and Integrated Optimization, which are also used to assess the impact of varying optimization variables on the building's energy performance, to understand if the optimization algorithm used has indeed moved towards minimizing the building's environmental impact compared to the baseline building model.

6.1 Sequential Optimization

The first step is to repeat Phase 1 of Sequential Optimization for the three population sizes considered: Tab.6.1 reports the optimal values of the optimization variables of Tab.4.21 obtained with the three analyzed population sizes, while Fig.6.1 graphically shows the percentage reduction in emissions compared to

the baseline building for each case.

Table 6.1: Optimal values of Phase 1 of Sequential Optimization variables with different Population Size.

Phase 1 Optimization Variables	Population Size: 80	Population Size: 100	Population Size: 200
WWR N	0.3	0.3	0.3
WWR E	0.3	0.4	0.3
WWR S	0.3	0.3	0.3
WWR O	0.4	0.4	0.4
Shading Objects Solar Transmittance	0.6	0.8	0.8
PV position	West roof	West roof	East roof
OPTIM. TIME	12 hours, 10 mins.	14 hours, 50 mins.	18 hours, 15 mins.
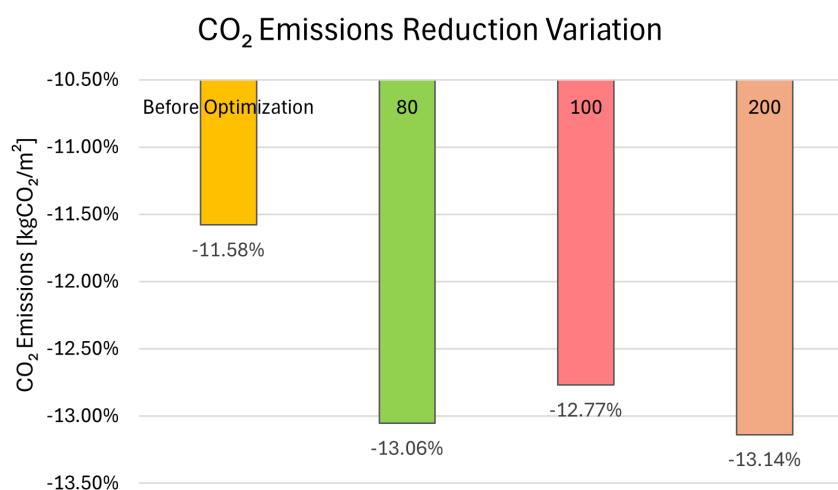
Figure 6.1: Percentage CO_2 emissions reduction, Phase 1 of Sequential Optimization with different Population Sizes.

The analysis of optimization times immediately reveals an increase in simulation time, ranging however from a minimum of about 12 hours to a maximum of about 18 hours; thus, if a higher population size leads to a better optimization result as it happens in this case, the time required to execute the optimization algorithm would not be considered a significant obstacle, as it does not increase significantly with the increase of the Population Size.

As evident from Tab.6.1, the WWRs for the North, South, and West orientations selected by the algorithm are identical for all three population sizes, while there is a change for the East orientation, which was selected as

0.4 only for the Population Size of 100. Considering that, as noted in Fig. 5.3, the most significant component of the energy balance of the building is related to heating, linked to WWRs for a constant solar transmittance of shading components, the reason for a lower percentage reduction in emissions compared to the baseline for this population size could be precisely related to the selection of a higher WWR for the East orientation for this Population Size compared to that made in the case of the other two. Regarding the solar transmittance of shading components, it is 0.8 for both population sizes of 100 and 200, while it is slightly lower for a population size of 80. The position of the photovoltaic system for a Population Size of 200 is different from that of the other two cases, respectively East Roof for the former and West Roof for the latter. The consequences of these selections are evident in Fig.6.1, which shows that the alternative with a population size of 200 returns the maximum percentage reduction in CO_2 emissions compared to the others. The reasons for this result could thus be related to the different location of the photovoltaic system, but also to the different WWR for the East orientation and the solar transmittance of the shading objects. To understand this, a sensitivity analysis of these parameters was performed, considering the results of a Population Size of 100 as a reference.

In Fig.6.2, the variations in emissions associated with heating, cooling, and interior lighting are graphically reported for different locations of the photovoltaic system, along with the corresponding reduction in CO_2 emissions compared to the baseline, obtained by keeping the values of WWR and Shading Objects solar transmittance from Tab.5.4 fixed.
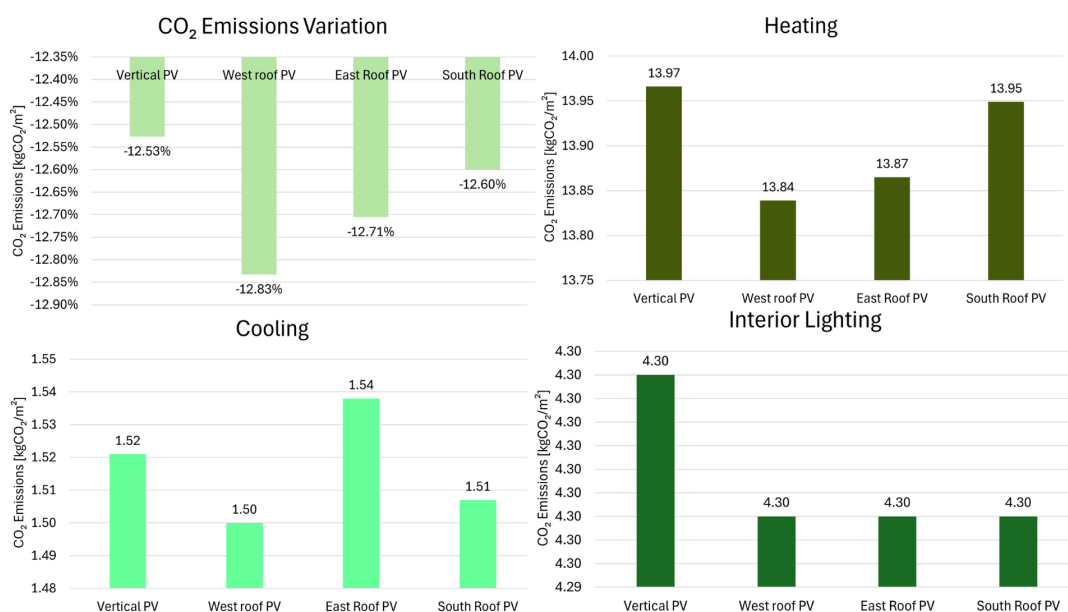
Figure 6.2: End uses emissions and percentage emissions reduction for different PV panels location.

Observing the percentage reduction in emissions associated with different locations of the photovoltaic system in the top left of Fig.6.2, it can be noticed that the one guaranteeing the minimum value, and so the best reduction, is the location called West Roof in Fig.4.11: it can be asserted that this was also clear during the results analysis phase, as for a Population Size of 100, both the Phase 1 of Sequential Optimization and the Integrated Optimization considered it as the optimal alternative for this variable. The reason for this is evident when analyzing the emissions related to heating, cooling, and interior lighting: for all three, the minimum value corresponds to this location. Considering that, during Phase 1 of Sequential Optimization, only the shading effect that the system generates on the building is taken into account, Fig.4.8 immediately allows to notice that positioning a shading structure on the roof, characterized by the maximum incident radiation, allows to reduce the negative impact it has on the building's cooling demand. Furthermore, considering the position of the sun in the early and late periods of the year, represented in Fig.4.5, it is noticed that this location does not generate an increase in energy demand for heating because, in the winter season, the sun is at very low altitudes, so its impact on the South-west part of the roof is minimal; furthermore, during this season, days are shorter, and therefore, this orientation is hit by solar radiation only for a short time. Conversely, the shading generated by the South

and South-East locations, called respectively South and East Roof in Fig.4.11, where the radiation has a greater impact during the early hours of the day, ensures that the effect of reducing the building's winter heat load is lower, and therefore, the emissions and consumption associated with heating are higher. The location indicated as "Vertical Façade" in Fig.4.11 is characterized by the highest emissions related to the building's interior lighting as it replaces window components, greatly limiting the entry of natural light and thus causing higher consumption to ensure the setpoint of 800 *lux* in the adjacent area.

Continuing, therefore, with the assessment of the effects of different WWR values for various orientations on the building's energy balance, the results obtained are graphically presented in Fig.6.3.
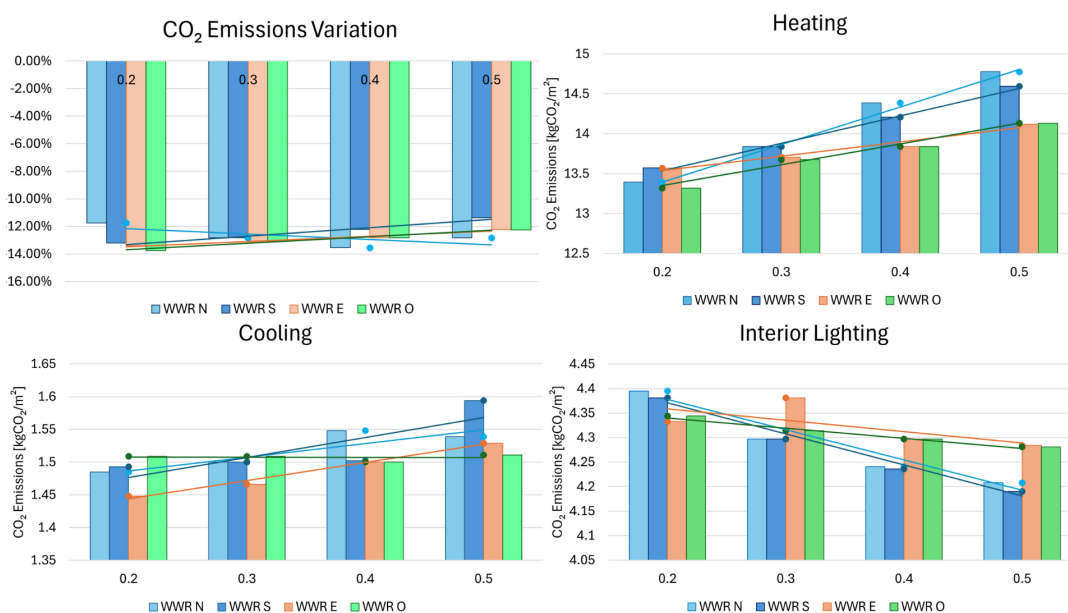
Figure 6.3: End uses CO_2 emissions and percentage CO_2 emissions reduction for different WWR values and different orientations, Phase 1 Sequential Optimization.

Trends concerning the percentage reduction in emissions allow to notice that for all orientations an increase in WWR corresponds to a percentage reduction in CO_2 emissions compared to the baseline lower in absolute value, except for the North orientation. To understand the reasons for this exception, it is simply needed to observe the variation in emissions related to heating and internal lighting: for all orientations, an increase in WWR corresponds to an increase in emissions associated with room heating, but the steepest slope is observed for the North exposure, as it is the most disadvantaged in terms of

solar radiation entering through the window components, thus the negative effect due to the energy losses towards the outdoor environment of increasing their extent prevails. At the same time, this increase is well compensated by the significant reduction in emissions related to internal lighting: the steepest slope is indeed for the South and North orientations, and for the latter, this is because, given the unfavorable exposure to solar radiation, in order to reduce electricity consumption associated with room lighting, a greater extent of window components is necessary. The evolutionary optimization algorithm, for population sizes of 80, 100, and 200, was not able to identify the WWR value that, for the North orientation, manages to balance the positive and negative effects that the extension of window components has on the overall energy balance of the building as it should have been set to 0.4. This can't be affirmed for the West and South orientations: they were set to 0.3, corresponding, as shown in Fig.6.3, to the maximum CO_2 emissions reduction, in absolute value. As long as it concerns the East orientation, in the case of a population size of 100, the WWR value is too high: this can therefore be seen as the main cause of a less pronounced reduction in CO_2 emissions compared to the baseline, as shown in Fig. 6.1.

Finally, it is possible to refer to Fig.6.4 to assess the impact that different values of solar transmittance of shading objects have on heating, cooling, and internal lighting emissions, and therefore on their percentage reduction compared to the baseline building.
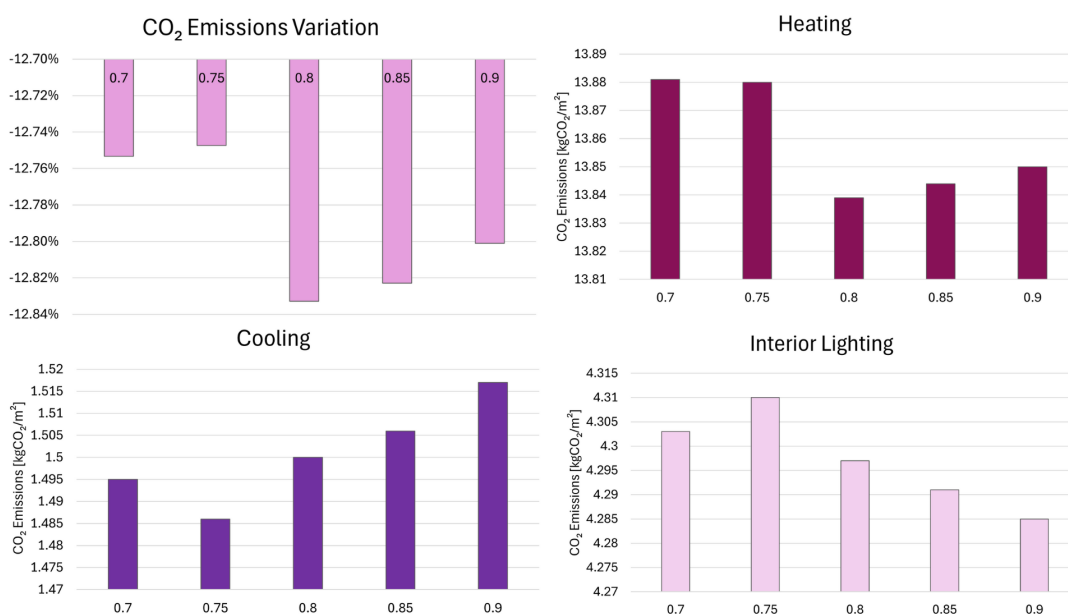
Figure 6.4: End uses CO_2 emissions and percentage CO_2 emissions reduction for different shading objecs solar transmittance values, Phase 1 Sequential Optimization.

Unlike what occurred for the WWR, the emission trends for different end uses and their percentage reduction associated with different values of solar transmittance of shading objects are not linear: generally, it is observed that, consistently with what was selected by the optimization process with a Population Size of 100 and 200, the maximum absolute reduction in CO_2 emissions is recorded for a solar transmittance value of 0.8. This is because the CO_2 emissions for heating associated with this value are the lowest: the 0.8 value allows for a significant entry of solar heat gains into the rooms, which helps reduce the winter thermal load. However, for the same reasons the value that would minimize emissions for cooling is slightly lower, at 0.75, as seen in the graph in the bottom left. Despite of this, observing the values associated with the differences in emissions between solar transmittance values of 0.75 and 0.8, it is noted that for cooling it is 0.0014 $kgCO_2/m^2$, compared to 0.04 $kgCO_2/m^2$ for heating, thus the effect that this parameter has on the energy balance and the environmental impact of the building prevails on the latter. Regarding internal lighting, once again, the emission reduction effect generated by the value of 0.8 compared to the value of 0.75 prevails, thus explaining the reasons why optimization led to the results in Tab.6.1 for population sizes of 100 and 200.

At this point, the evaluation proceeded with the assessment of the differences obtained following the application of Phase 2 of Sequential Optimization with various population sizes: the optimal values of the variables listed in Tab.4.22 are summarized in Tab.6.2 for Population Sizes of 80, 100, and 200, while the corresponding percentage reduction values of emissions compared to the baseline are graphically depicted in Fig.6.5.

Table 6.2: Optimal values of Phase 2 of Sequential Optimization variables with different Population Size.

Phase 2 Optimization Variables	Population Size: 80	Population Size: 100	Population Size: 200
HVAC Type - Below Grade Floor	DOAS with VRF	DOAS with fan coil chiller with baseboard electr.	DOAS with VRF
HVAC Type - Ground Floor	DOAS with fan coil air-cooled chiller with baseboard electr.	DOAS with VRF	DOAS with low temp. radiant chiller with central ASHP
HVAC Type - First and Second Floor	DOAS with fan coil chiller with central ASHP	DOAS with fan coil chiller with central ASHP	DOAS with fan coil chiller with central ASHP
PV Panels Active Fraction	0.8	0.9	0.9
PV Panels Inclination	40°	40°	40°
OPTIM. TIME	11 hours, 40 mins.	12 hours, 56 mins.	20 hours, 15 mins.
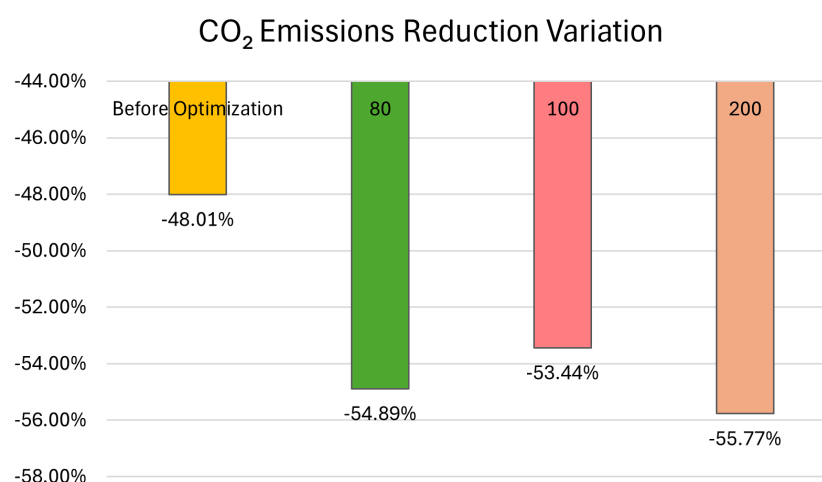
Figure 6.5: Percentage CO_2 emissions reduction, Phase 2 of Sequential Optimization with different Population Sizes.

Tab.6.2 highlights that, in this case, as the Population Size increases, the simulation time experiences a more significant increase compared to that observed in Tab.6.1. The reason for this is that the time associated with each individual energy simulation is higher compared to the time required for simulating the model with only the building components of the proposed design using Ideal Load. Therefore, for the analysis of the HVAC system, it is necessary to carefully evaluate the trade-off between the quality of the optimal alternative and the time required for the optimization procedure.

As can be seen from Fig.6.5, the Population Size that results in the minimum percentage reduction in CO_2 emissions compared to the baseline is, as in Phase 1, equal to 200. The reason why the Phase 2 yields such an high absolute percentage reduction in emissions is primarily due to:

1. the active fraction of the shading surface associated with the photovoltaic plant's productivity;
2. the type of HVAC system assigned to the three groups of rooms.

Regarding the first reason, a lower active fraction at the same location and panel inclination leads to lower electricity production and, consequently, higher electricity withdrawal from the grid to meet the building's demand. Since the electricity drawn from the grid corresponds to an emission of 318 $kgCO_2/MWh$, whereas the electricity produced by the photovoltaic system has zero emissions, if the photovoltaic system produces less and thus allows less self-consumption by the building, the emissions associated with its operation increase. Concerning the second reason, related to the type of HVAC systems installed, the reasons behind this result are more complex and have been evaluated by conducting a sensitivity analysis on these variables. This analysis focused on assessing the impact that different types of HVAC systems have on the three groups of rooms in which the building has been split. For simplicity, the types of systems used for this analysis will be indicated by the indices listed in Tab.6.3, representing the entire group extracted from the *Honeybee* library and used for optimization.

Table 6.3: Indexes used for HVAC systems identification.

1	DOAS with fan coil chiller with central ASHP
2	DOAS with fan coil chiller with baseboard electric
3	DOAS with VRF
4	DOAS with low temp. radiant chiller with central ASHP

Considering the solution obtained with a Population Size of 100 as a reference, each of the HVAC systems indexed in Tab.6.3 is tested one by one in each of the three groups of rooms in which the building understudy has been divided, with the results summarized graphically in Fig.6.6:
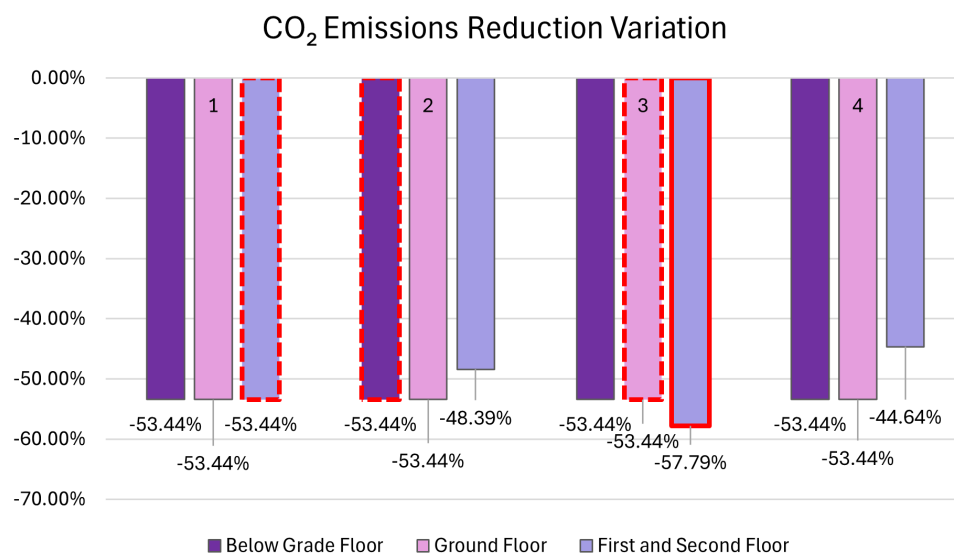
Figure 6.6: Percentage CO_2 emissions reduction, Phase 2 of Sequential Optimization with different HVAC types.

In Fig.6.6, the dashed red columns indicate that the type of HVAC system they refer to is the optimal one for the group of rooms represented by each color, while the column with the continuous red border corresponds to the lowest emissions among all the alternatives considered. The histogram shows that if the HVAC system of either the Below Grade or the Ground floor is varied from the types selected by the optimization algorithm with a Population Size of 100, the percentage reduction in emissions remains the same, at 53.44%. On the other hand, modifying the system for the First and Second floors reveals the actual performance of the tested system and its impact on the energy balance of the proposed design. The reason for this is the larger floor area of the rooms managed by the HVAC system for these zones, and therefore the greater demand that the systems associated with this group of rooms must handle, making the effects of different alternatives on the energy balance and emissions more evident. In particular, it is noted that the alternative corresponding to the greatest percentage reduction in emissions compared to the baseline building is the one that associates each of the three groups of rooms with the types of systems summarized in Tab.6.4:

Table 6.4: HVAC system types combination for maximum CO_2 emissions percentage reduction, sensitivity analysis on Phase 2 of Sequential Optimization optimal solution.

Below Grade Floor	DOAS with fan coil chiller with baseboard electric
Ground Floor	DOAS with VRF
First and Second Floor	DOAS with VRF

Considering that the greatest impact on emissions is given by the selection of the HVAC type for the first and second floors, it can be concluded that the DOAS with VRF system is the one that maximizes the building's performance compared to the baseline. Despite this, such a result was not achieved for any Population Size. This demonstrates the ongoing necessity for a decision maker who, at the end of the optimization procedure, evaluates the solutions and the design alternatives recommended by the algorithm to select the one most suitable for their purposes.

Regarding the system associated with the Below Grade floor, the one present in Tab.6.4 uses baseboard electric terminals, which, as previously mentioned, can be considered one of the least efficient since heat production occurs via the Joule effect. The algorithm's selection of this system can be explained by the fact that the Below Grade floor was evaluated as consisting of a single thermal zone, characterized by a floor area of 280 m^2, the smallest among those associated with each HVAC system. Thus, the selection of any HVAC system for this group of rooms is inconsequential as its weight on overall emissions is negligible compared to that of the other groups of rooms.

To demonstrate this, the building's performance in terms of percentage reduction in emissions compared to the baseline was tested by evaluating, for its entirety, the same type of system, considering those indexed in Tab.6.3. The results obtained are reported in Fig.6.7, presenting these in comparison with those obtained by applying the same type of HVAC systems only to the First and Second floors while leaving those of the Below Grade floor and Ground floor unchanged:

CO$_2$ Emissions Reduction Variation
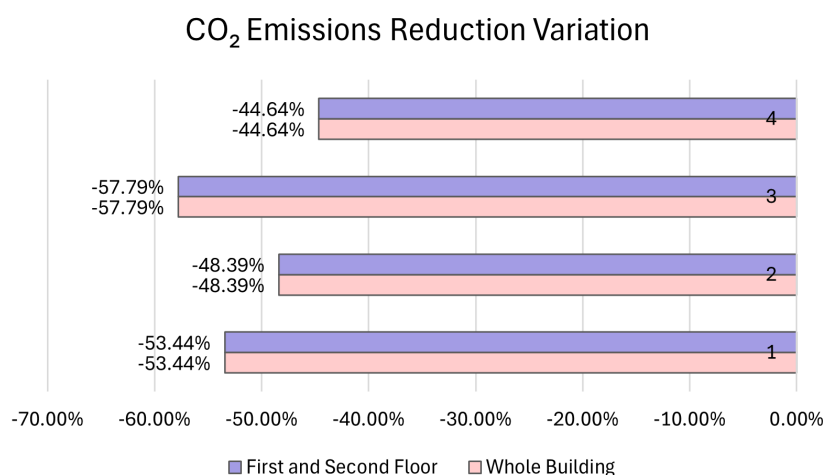
Figure 6.7: Percentage CO_2 emissions reduction, Phase 2 of Sequential Optimization with different HVAC types applied on just First and Second Floors and on the whole building.

Observing Fig.6.7, it is evident that for all system types, the percentage reduction in emissions obtained by implementing a given system only on the First and Second floors or throughout the entire building is the same. This demonstrates that this group of rooms has the greatest overall impact on the building's energy balance. Furthermore, it is noted that the alternative in Tab.6.4 corresponds to a percentage reduction in CO_2 emissions relative to the baseline that is identical to that which would be obtained by applying a DOAS with VRF system to the entire building. This is because the DOAS with VRF system allows for lower emissions even compared to those associated with the implementation of a radiant panel system.

This type of observation allows for the conclusion that, considering the variables of the building envelope as obtained from the output of Phase 1 of the Sequential Optimization, the optimal type of system for the building under study, modeled with the constructions of Tab.4.13, is defined as DOAS with VRF. This system should be applied to the First and Second floors to minimize CO_2 emissions associated with the building's operation. Furthermore, considering that it is usually preferable to use a single type of system whenever possible to leverage, for example, economies of scale or discounts on the quantity of components purchased, it may be optimal to associate this same type of system with the Below Grade floor and Ground Floor as well. Tab.6.5 allows to summarize the optimization variables values associated with the solution guaranteeing the CO_2 emissions reduction of -57.79%:

Table 6.5: Values of the optimization variables used for the case study guaranteeing the best environmental performance of the proposed design (Best Case Solution), Sequential Optimization.

Best Case Solution, Sequential Optimization CO_2 emissions reduction: -57.79%	
WWR - North Facade	0.3
WWR - East Facade	0.4
WWR - South Facade	0.3
WWR - West Facade	0.4
Shading Objects Solar Transmittance	0.8
PV Panels Location	West Roof, 40° Location
HVAC Type - Below Grade Floor	DOAS with VRF
HVAC Type - Ground Floor	DOAS with VRF
HVAC Type - First and Second Floor	DOAS with VRF
PV Panels Acrive Fraction	0.9

6.2 Integrated Optimization

Having completed the sensitivity analysis for the Sequential Optimization approach, it has been evaluated the impact of different Population Sizes on the Integrated Optimization procedure. This evaluation considers the quality of the solution obtained in terms of both percentage reduction in emissions and the time required for the optimization procedure itself. The results, derived from executing the optimization procedure while keeping all parameters from Tab.4.20 constant except for Population Size, which is varied using values of 80, 100, and 200, are reported in Tab.6.6. Furthermore, Fig.6.8 shows the percentage reduction in CO_2 emissions achieved by the best alternative selected by the algorithm with the three Population Size alternatives.

Table 6.6: Optimal values of Integrated optimization variables with different population size.

Phase 2 Optimization Variables	Population Size: 80	Population Size: 100	Population Size: 200
WWR N	0.8	0.8	0.7
WWR E	0.3	0.3	0.4
WWR S	0.4	0.4	0.4
WWR O	0.5	0.3	0.3
Shading Objects Solar Transmittance	0.65	0.65	0.8
PV position and Inclination	West roof, 40°	West roof, 40°	West roof, 40°
HVAC Type - Below Grade Floor	DOAS with VRF	DOAS with VRF	DOAS with VRF
HVAC Type - Ground Floor	DOAS with fan coil air-cooled chiller with central ASHP	DOAS with fan coil chiller with baseboard electr.	DOAS with VRF
HVAC Type - First and Second Floor	DOAS with fan coil chiller with central ASHP	DOAS with fan coil air-cooled chiller with central ASHP	DOAS with fan coil air-cooled chiller with central ASHP
PV Panels Active Fraction	0.9	0.9	0.9
OPTIM. TIME	9 hours, 58 mins.	12 hours, 41 mins.	25 hours, 20 mins.
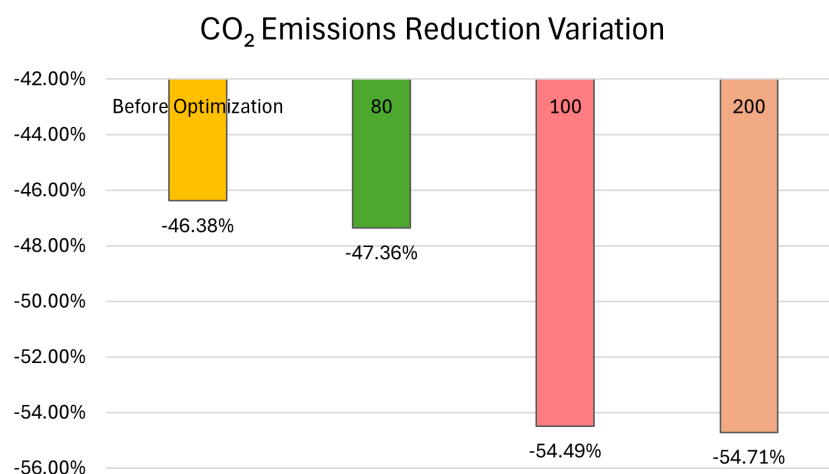
Figure 6.8: Percentage CO_2 emissions reduction, Integrated optimization with different Population Sizes.

As is evident from the graph in Fig.6.8, even in the case of Integrated Optimization, the alternative that allows for the minimization of CO_2 emissions

compared to the baseline building, even if marginally, is achieved using a Population Size of 200. However, in this case, the increase in the algorithm's run time is significantly more substantial, reaching 25 hours. Therefore, the choice between a Population Size of 100 and 200 depends solely on the user's willingness to accept an additional 13 hours of optimization time for only a 0.22% improvement in the solution compared to that obtained with a Population Size of 100.

Analyzing the values of the variables at the completion of the optimization procedures with the three Population Sizes reported in Tab.6.6, it is observed that all the solutions share the following characteristics:

- Position and inclination of the photovoltaic system, with a South-West orientation and a 40° tilt angle;
- Active surface area of the photovoltaic system equal to 0.9;
- HVAC system of the Below Grade floor, which has been assigned the type DOAS with VRF, which, as demonstrated in the sensitivity analysis conducted following Phase 2 of the Sequential Optimization, is the best alternative among those selected from the *Honeybee* library for the studied building.

Regarding the other parameters, there is some variability in the values selected following the three optimization runs. Of particular interest are the values assigned to the WWR for the four orientations and the solar transmittance of the shading objects. It is noted that while the maximum WWR value selected following Phase 1 of Sequential Optimization, with all three population sizes, was 0.4, Integrated Optimization allows for the selection of higher WWR values, especially for the North orientation, where this parameter can reach 0.8. The reason for this is undoubtedly due to the fact that the system types from which the algorithm selects the best option are energy-efficient. Therefore, the additional consumption that may be generated by:

- a) Greater heat loss through windows to the outdoor during winter months;
- b) Greater solar heat gains during summer months;

are actually compensated by the fact that the energy demand is met using systems that, for the same amount of energy produced, require a lower amount of input energy due to high COP and EER. Additionally, this energy comes from renewable sources, with zero CO_2 emissions associated for this case study.

Considering this, it has been decided to conduct a sensitivity analysis while keeping all the values of the Integrated Optimization variables fixed, as selected

following the application of the algorithm with a Population Size of 100, except for the WWR, which will be assigned with the same four values used to perform the sensitivity analysis in Phase 1 of Sequential Optimization. This approach aims to evaluate how the impact of the WWR varies on the energy balance for a building equipped with HVAC systems and photovoltaic production. The results obtained are shown in Fig.6.9:
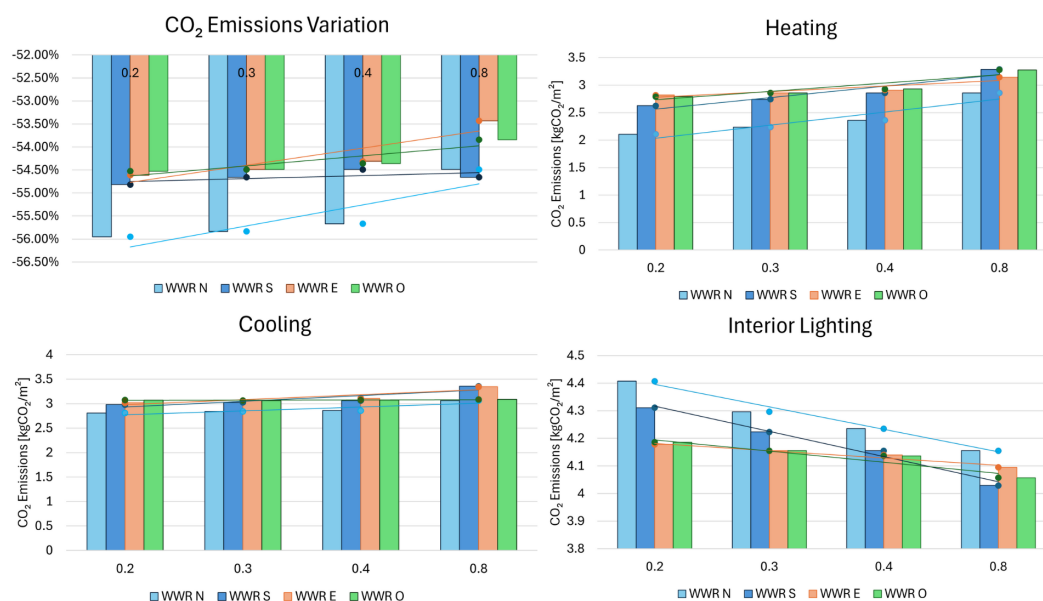
Figure 6.9: End uses CO_2 emissions and percentage CO_2 emissions reduction for different WWR and different orientations, Integrated Optimization.

From the comparison between Fig.6.3 and Fig.6.9, it is evident that, for the same tested WWR values, the general trends remain unchanged; however, the slopes associated with heating emissions for different WWR values for each orientation are significantly lower than those observed in the sensitivity analysis conducted in Phase 1 of Sequential Optimization. Additionally, observing the bottom-left graph related to the building's cooling emissions, it is noted that the North orientation corresponds to the minimum cooling emissions and the smallest increase in these emissions as the WWR value increases; furthermore, also in this case the slope for the variation of the emissions with the variation of the WWR value is reduced compared to the one observed in Fig.6.3. This confirms the previous observation: a well-designed HVAC system manages the negative impacts of higher WWR on the energy balance during both winter and summer with reduced consumption and, therefore, reduced emissions.

The bottom-right graph for indoor lighting shows that the slope associated with the variation in emissions is the highest among the three selected end-uses. The South and North orientations exhibit the greatest reduction in emissions as the WWR value increases, which could explain why the final WWR value for the North orientation is so high after the optimization procedure.

Nevertheless, the representation of the effects of different WWR extensions on the building's façades highlights that, even for Integrated Optimization, in which building and system variables are optimized simultaneously, higher WWR values lead to a smaller absolute reduction in emissions. However, the difference between the minimum reduction value obtained with the minimum WWR and the maximum reduction value with the maximum WWR is much smaller for the Integrated Optimization compared to that observed in the sensitivity analysis conducted for Phase 1 of Sequential Optimization, respectively 0.61% and 1.86%. This demonstrates that, in this case, the impact of these parameters on the overall energy balance is much less significant.

At this point, it was decided to evaluate the impact of different types of HVAC systems on a proposed design characterized by building envelope parameters obtained as output from the Integrated Optimization with a Population Size of 100. Keeping these parameters fixed, the impact of applying the HVAC systems indexed in Tab.6.7 was evaluated one by one on each of the three groups of rooms into which the studied building was divided. The results obtained are reported in Fig.6.10.

Table 6.7: Indexes used for HVAC systems identification, Integrated Optimization.

1	DOAS with fan coil chiller with central ASHP
2	DOAS with fan coil air cooled chiller chiller with central ASHP
3	DOAS with fan coil chiller with baseboard electric
4	DOAS with VRF
5	DOAS with low temp. radiant chiller with central ASHP
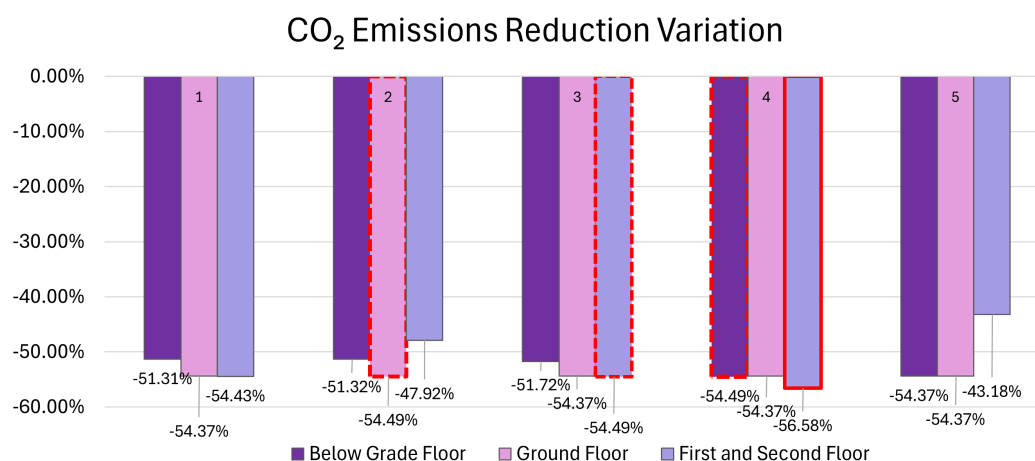
Figure 6.10: Percentage CO_2 emissions reduction, Integrated Optimization with different HVAC types.

As can be observed from the comparison between Fig.6.10 and Fig.6.6, unlike in Phase 2 of Sequential Optimization, for the Integrated Optimization, the variation in different types of HVAC systems is significant not only when applied to the First and Second floors but also for the Below Grade floor and Ground floor. In particular, it is noted that, with the same HVAC systems tested on the three groups of rooms in which the building has been divided, the maximum effect is once again recorded with variations in the system associated with the First and Second Floors due to the larger heated surface area, while the minimal consequences are related to the Ground Floor. This explains why the optimization algorithm assigned to this group of rooms the system indexed as 3 in Tab.6.7, which has baseboard electric terminals. These terminals, as previously mentioned, correspond to the least efficient type since heat production is based on the Joule effect. For this group of rooms, the algorithm assigns the value almost randomly, as its impact on the building's overall emissions is very limited.

The difference between the two optimization approaches can be explained by comparing the values of the building parameters assigned during Phase 1 of the Sequential Optimization and during the integrated optimization. As previously mentioned, for the latter, the WWR values are higher, especially for the North orientation. Additionally, while in the Sequential Optimization the WWR values were very similar for the different orientations, in the integrated optimization there is greater variability. This results in a higher heating demand for the alternative suggested by the Integrated Optimization compared to that provided

by the Sequential Optimization, as demonstrated in Fig.5.8. Consequently, the selection of the HVAC system is crucial to adequately compensate for the negative impact that a larger extent of window components has on the balance, and thus, on the building's energy and environmental performance.

In the output from the Integrated Optimization, the suggested combination provides a percentage reduction of 54.49%. However, Fig.6.10 indicates that with the combination reported in Tab.6.8, a value of 56.68% can be achieved.

Table 6.8: HVAC system types combination for maximum CO_2 emissions percentage reduction, sensitivity analysis on Integrated Optimization optimal solution.

Below Grade Floor	DOAS with VRF
Ground Floor	DOAS with fan coil chiller with baseboard electric
First and Second Floor	DOAS with VRF

At this point, as was done for Phase 2 of Sequential Optimization, it has been proceeded with the comparison of the impact that the installation of an HVAC system has on the First and Second floors and on the entire building, using Fig.6.11.
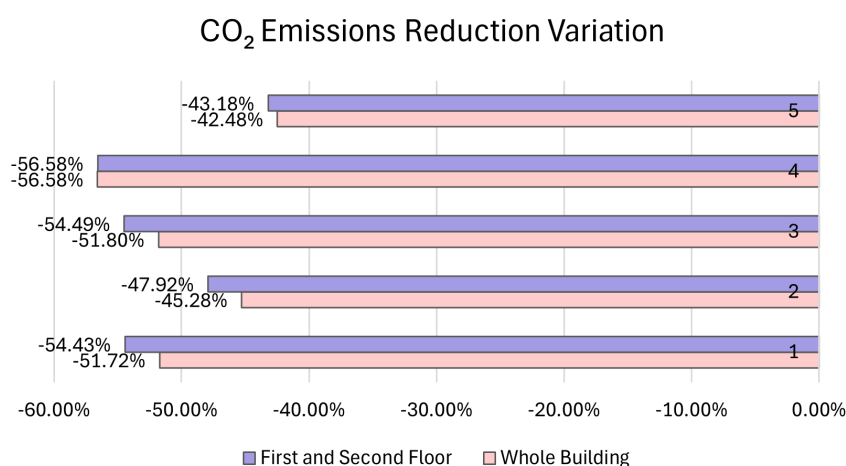
Figure 6.11: Percentage CO_2 emissions reduction, Phase 2 of Integrated Optimization with different HVAC types applied on just First and Second Floors and on the whole building.

Fig.6.11 shows that, unlike with the building envelope parameters associated with Phase 1 of optimization, in the case of Integrated Optimization, applying the same HVAC system to the entire building or only to a part of it has a different

impact. However, even when applying the same system to the entire building, the maximum percentage reduction in emissions is 56.58%, which corresponds, consistently with what was presented in Section 6.1, to the installation of the DOAS with VRF system on the entire building. Tab.6.9 summarizes the values of the optimization variables that result from the sensitivity analysis of the optimal solution in output from the Integrated Optimization corresponding to the lowest environmental impact and thus the maximum percentage reduction in CO_2 emissions.

Table 6.9: Values of the optimization variables used for the case study guaranteeing the best environmental performance of the proposed design (Best Case Solution), Integrated Optimization.

Best Case Solution, Integrated Optimization CO_2 emissions reduction: -56.58%	
WWR - North Facade	0.8
WWR - East Facade	0.3
WWR - South Facade	0.4
WWR - West Facade	0.3
Shading Objects Solar Transmittance	0.65
PV Panels Location	West Roof, 40° Location
HVAC Type - Below Grade Floor	DOAS with VRF
HVAC Type - Ground Floor	DOAS with VRF
HVAC Type - First and Second Floor	DOAS with VRF
PV Panels Acrive Fraction	0.9

The sensitivity analysis conducted on Sequential Optimization and Integrated Optimization allows to conclude that:

- The model created for the proposed design exhibits behavior consistent with typical trends in heating, cooling and lighting demands for buildings, thus demonstrating its correctness.

- In the case of Integrated Optimization, where both building envelope and HVAC variables are optimized, the ability to consider the interdependencies among the various variables typical of a complex system like a building allows for a slightly better solution, albeit only by 1%, compared to that obtained with Sequential Optimization. However, the different impact on optimization time associated with the two approaches should not be overlooked, nor the possibility of obtaining a much better solution with minimal perturbation from the optimal solution in the case

of Integrated Optimization.

6.3 Comparison between Sequential and Integrated Optimization Procedures

The previous comparison of the impact of different Population Sizes on the quality of the solution, given the same optimization procedure, concluded that in both the approaches, a higher value of this parameter ensures a better optimal solution in terms of percentage reduction of CO_2 emissions compared to the baseline building. However, the cost of this improvement is represented by the optimization time, which increases to a varying extent depending on the implemented procedure; specifically, the greatest increase is observed for Integrated Optimization, as the search space is larger compared to that for Sequential Optimization in both phases: it is $2.90 \cdot 10^8$ for Integrated Optimization, while it is $2 \cdot 10^4$ for Phase 1 and $4.30 \cdot 10^3$ for Phase 2 of Sequential Optimization. It is important to note, however, that Sequential Optimization will yield the overall solution only after a time that is the sum of the times required for Phase 1 and Phase 2, which is longer than the time required by Integrated Optimization for all Population Sizes. The optimization times associated with each optimization procedure for each analyzed population size are provided in Tab.6.10 below.

Table 6.10: Summary of search space size and optimization time for both the Optimization Approaches and the three tested Population Sizes.

	Search Space Size	Population Size: 80	Population Size: 100	Population Size: 200
Sequential Opt.: Phase 1	$2 \cdot 10^4$	12 hours, 10 mins.	14 hours, 50 mins.	18 hours, 15 mins.
Sequential Opt.: Phase 2	$4.30 \cdot 10^3$	11 hours, 40 mins.	12 hours, 56 mins.	20 hours, 15 mins.
Sequential Opt.: Total	-	23 hours, 50 mins.	27 hours, 40 mins.	38 hous, 30 mins.
Integrated Opt.	$2.90 \cdot 10^8$	9 hours, 58 mins.	12 hours, 41 mins.	25 hours, 20 mins.

At this point, if the user is solely interested in obtaining an analysis of different alternatives generated by the NSGA-II algorithm, or any other genetic algorithm, in the shortest possible time, it would be more convenient to directly perform an Integrated Optimization procedure. However, it is worth evaluating

the quality of the optimal solutions obtained at the end of the complete Sequential Optimization procedure and the Integrated Optimization procedure allowing for an analysis of the algorithm's performance when applied to the complex system of a building using two different approaches. To do this, Fig.6.12 shows the percentage reduction in emissions of the proposed design compared to the baseline, which was achieved using the two approaches[1] with the different population sizes analyzed in Sections 6.1 and 6.2:
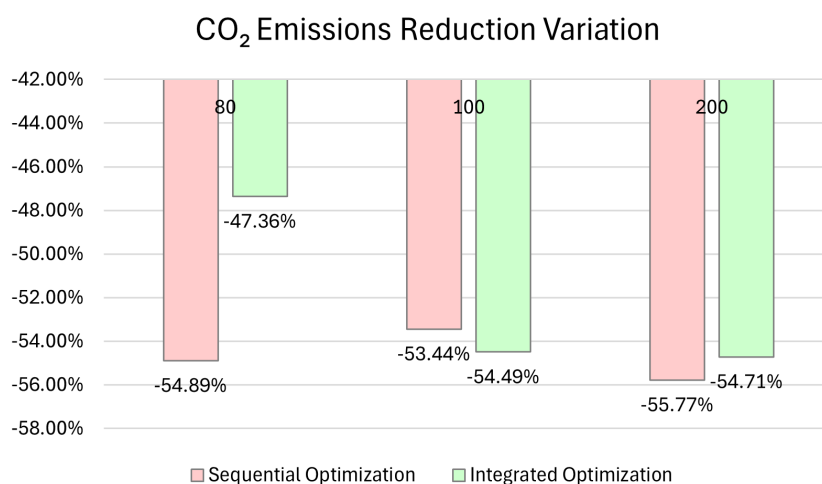
Figure 6.12: Percentage CO_2 emissions reduction, comparison between Integrated and Sequential Optimization for different Population Sizes.

From the graph in Fig.6.12, two observations can be made:

1. The Integrated approach with a Population Size of 80 has the worst performance since the percentage reduction in emissions compared to the baseline is the lowest in absolute value. The reasons for this can be attributed to the fact that such a small population size for such a large solution space does not allow the algorithm to explore a sufficient number of design alternatives, leading it to settle on local optima.

2. With a Population Size of 100, the performance of the Integrated Optimization algorithm is better than that of the Sequential Optimization; indeed, the former provides a percentage reduction approximately 1% higher in absolute terms than the latter. However, the opposite is true for a Population Size of 200, where Sequential Optimization yields a better design alternative, with the same percentage reduction gap as that obtained for a population size of 100.

[1]For the results of Sequential Optimization, only those obtained after Phase 2 are considered.

Therefore, it was decided to evaluate the stability of the solutions obtained with the two procedures to gain a clearer idea of the quality of the optimal solution obtained with a Population Size of 100 and to definitively determine which of the two optimization approaches could be better with an intermediate Population Size and thus a shorter optimization time. To do this, the graphs in Fig.6.13 were first examined:
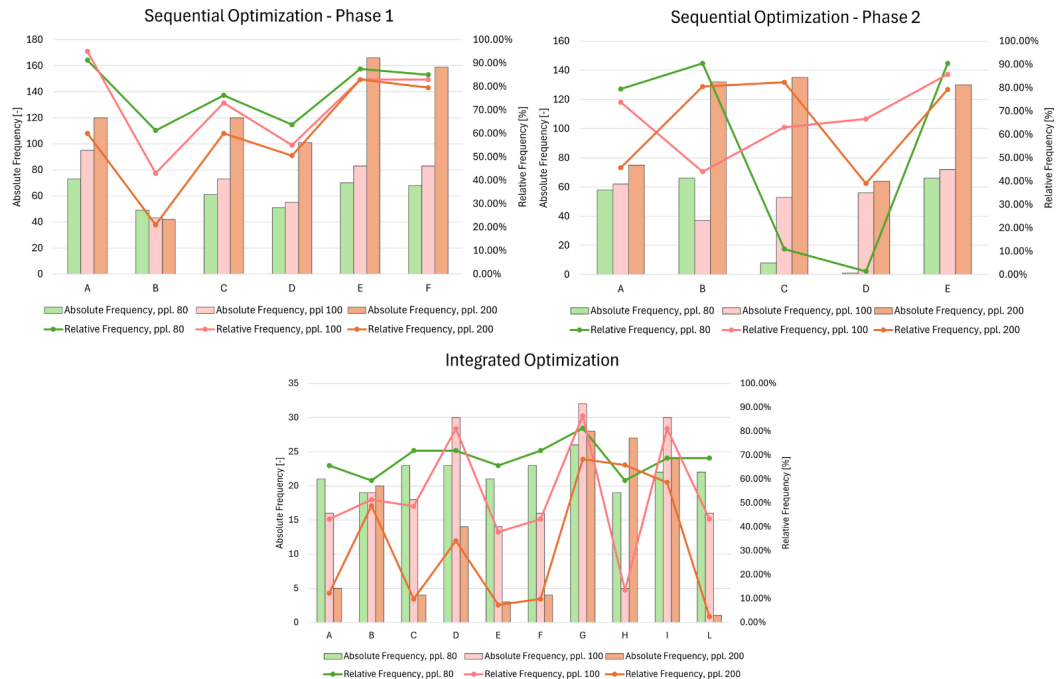
Figure 6.13: Relative and Absolute frequency of optimal values of optimization variables for Sequential Optimization phases and Integrated Optimization.

These results were derived from the calculation of the absolute and relative frequencies with which the optimal value of each variable used in the two phases of Sequential Optimization and the Integrated Optimization appears across the entire population analyzed by the algorithm, for all three population sizes[2].

Analyzing the first optimization approach, it is evident that in Phase 1, the most stable variables are those indicated as E and F for all three Population Sizes, as their relative frequency within the population is the highest. These correspond to the WWR for the South and West orientations respectively; this observation indicates that the algorithm can identify the best alternative for these variables in just a few iterations and then promotes its survival through all

---

[2]Note that for Phase 2 of Sequential Optimization and Integrated Optimization, the set of solutions provided by the optimization algorithm was filtered to exclude those corresponding to unmet hours greater than 300, as they are not acceptable per ASHRAE 90.1-2016.

generations. Conversely, the least stable variable is indicated as B in the same graph, corresponding to the solar transmittance of the shading components; this relative frequency result is due to the fact that this variable has the highest number of possible alternatives to analyze in Phase 1, which should be evauluated into a fixed Population Size causing an higher variability. Ultimately, it can be said that the algorithm performs similarly for all Population Sizes in Phase 1, so the selection of one size over another depends solely on the user's available time.

For Phase 2 of the same approach, it is observed that the stability of the variables varies with different population sizes, and this is most notable for variables B, C, and D, which refer to the HVAC systems of the Below-Grade Floor, First and Second Floors, and Ground Floor, respectively. Analyzing the columns and the line representing the absolute and relative frequency of optimal values for the Population Size of 80, it is noted that these are minimal for the C and D variables, as the algorithm struggles to evaluate them adequately with such a small population size. Indeed, as this parameter increases, it is observed that the optimal value of the C and D variables obtained by the algorithm is evaluated more frequently, demonstrating that the optimization procedure can better recognize their optimal values and promote their survival in the generations with larger population sizes, which are therefore recommended for Phase 2 of the Sequential Optimization approach. Regarding variable D, corresponding to the HVAC system for the Ground Floor, it is noted that the relative frequency is higher with a Population Size of 100 compared to that obtained with a Population Size of 200. The reason for this is linked to the observation made in Section 5.2.2, according to which, among the three groups of rooms into which the building is divided, the overall more significant impact on the energy balance is associated with the HVAC system of the First and Second Floors, corresponding to variable C in the top right graph of Fig.6.13. Based on this, considering that the algorithm's objective is to minimize the overall CO_2 emissions of the building, it will tend to assign the most effective values to this variable. Conversely, for parameters with a lesser impact on the objective function, the values associated will be more random since the selection of one alternative over another has a very limited impact on the overall balance, leading to a reduced relative frequency of the value that has so far been considered as optimal. This phenomenon is more evident with a larger Population Size, such as 200, where the number of alternatives evaluated is

higher, thus increasing the variability of these variables.

Moving on to the analysis of the last graph in Fig.6.13, referring to the Integrated Optimization approach, similar variations in relative frequency for the same variable across different Population Sizes are noted. It is observed that for variables B and C, the values of the relative frequency are high for all three Population Sizes. These again correspond to the WWR for the South and West orientations, for which the algorithm selects very similar, if not identical, optimal values for all Population Sizes, as shown in Tab.6.6. This is consistent with the observations made for Phase 1 of Sequential Optimization. Once again, the greatest variability among the three population sizes is observed for the variables related to the HVAC systems of the Below Grade Floor, Ground Floor, and First and Second Floors, which in this case are G, H, and I, respectively. For the first and last, a Population Size of 100 corresponds to the highest relative frequency, demonstrating that indeed, an intermediate population size provides better survival of optimal values in the generations for these parameters, which instead in the case of an excessively large Population Size, are characterized by greater variability. However, this is not true for the HVAC system associated with the Ground Floor, for which an adequate relative frequency is only obtained with a larger population size. The cause of this phenomenon is related to the observations made during the sensitivity analysis on the types of HVAC systems in Section 5.3, which allowed to conclude that the HVAC system associated with the Ground Floor has the least impact on the building's energy and environmental performance, thus its assignment is almost random during the optimization procedure. However, in this case, the highest relative frequency is associated with a Population Size of 200: once again, this result cannot be considered as a specific rule as it depends on the random assignment of values to this optimization variable.

In conclusion, it is possible to state that when only variables related to the building envelope are considered, the optimization procedure with the NSGA-II genetic algorithm performs well even with small population sizes, allowing the identification and survival of optimal values in a short time. However, when the level of complexity increases by including parameters related to HVAC systems, trade-offs and dependencies between these variables come into play, making the problem more complex. A better performance of the NSGA-II optimization algorithm can only be achieved with a larger population size, which, however, corresponds to a longer optimization time.

The graphs in Fig.6.13 allow for the selection of the most stable variables for each phase of Sequential Optimization and for Integrated Optimization. These are the variables for which, regardless of the values assumed by the other variables, their values remain robust, and any variation from the optimum could make the overall solution, in terms of percentage reduction of CO_2 emissions, no longer optimal. These variables are characterized by the maximum relative and absolute frequency within the set of solutions obtained by the algorithm with different Population Sizes. To evaluate their robustness, it was decided to evaluate the same frequency parameters for these variables as used in Fig.6.13, both in the entire population of solutions and in a subset of solutions extracted to represent the neighborhood of the optimal solution itself. Specifically, for each of the two phases of Sequential Optimization and for Integrated Optimization, known the minimum reduction in CO_2 emissions obtained following the optimization procedures, solutions obtained by the NSGA-II algorithm corresponding to a percentage reduction in emissions within the range represented by the optimum value and the optimum value itself minus 1% were selected.

Using the starting Population Size as reference, so that of 100, the variables considered the most stable and least stable for each phase of Sequential Optimization and for Integrated Optimization were selected, as shown in Tab.6.11, resulting in the respective graphs presented in Fig.6.14, Fig.6.15, and Fig.6.16.

Table 6.11: Most and Least stable variables selection for Sequential Optimization and for Integrated Optimization, Population size: 100.

	Most Stable Variable	Least Stable Variable
Phase 1 - Sequential Opt.	WWR S	Shading Obj. Solar Transmittance
Phase 2 - Sequential Opt.	HVAC Type - Ground Floor	HVAC Type - Below Grade Floor
Integrated Opt.	HVAC Type - Below Grade Floor	HVAC Type First and Second Floor
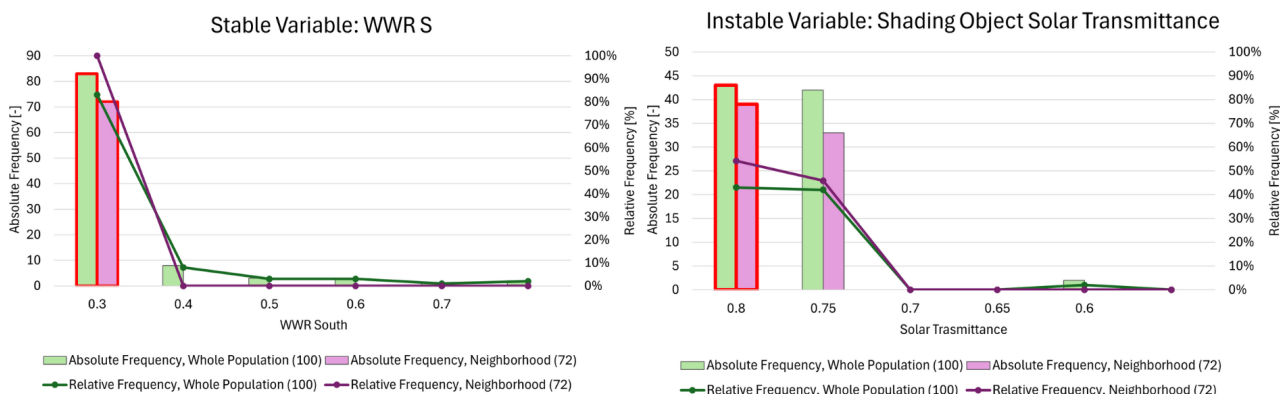
Figure 6.14: Stable (on the left) and unstable (on the right) relative and absolute frequency of the whole population and the optimal neighborhood for Phase 1 Sequential Optimization
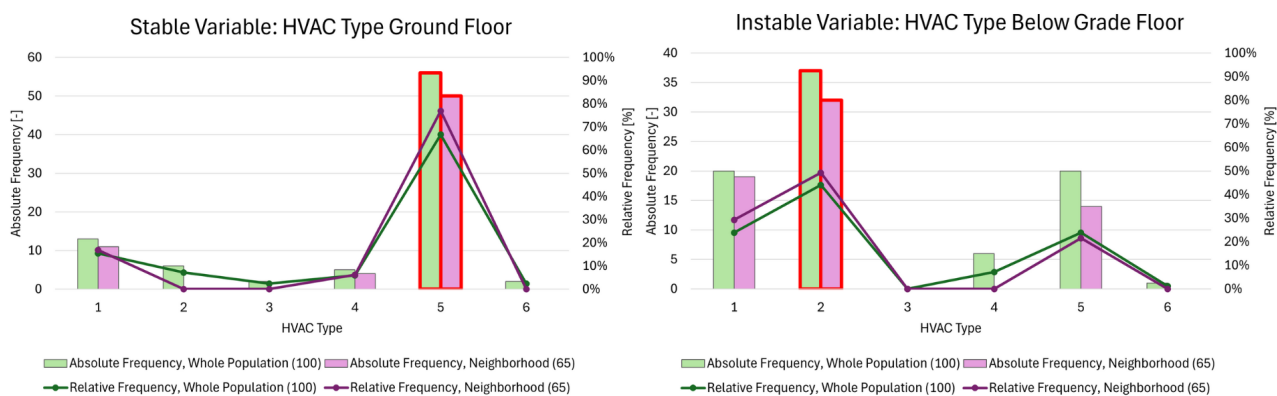
Figure 6.15: Stable (on the left) and unstable (on the right) relative and absolute frequency of the whole population and the optimal neighborhood for Phase 2 Sequential Optimization.
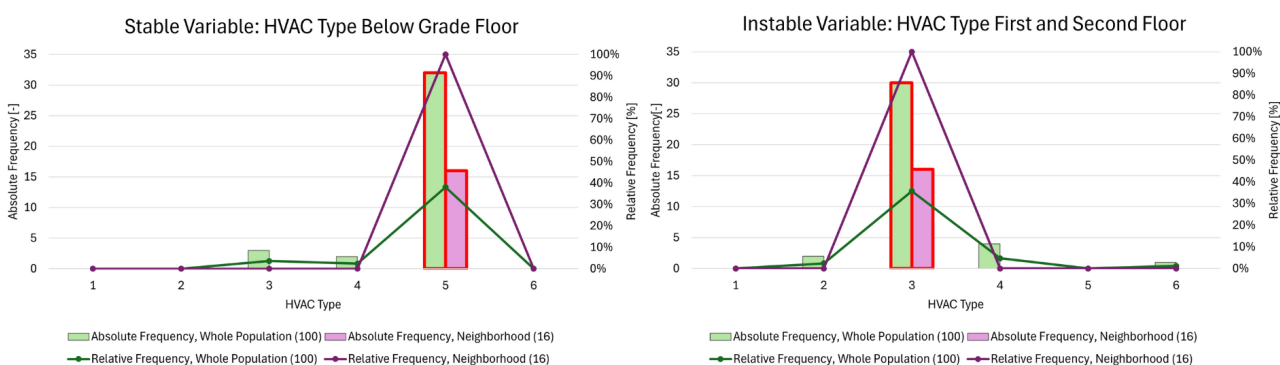
Figure 6.16: Stable (on the left) and unstable (on the right) relative and absolute frequency of the whole population and the optimal neighborhood for Integrated Optimization.

It is necessary to clarify that for Phase 2 of Sequential Optimization and for Integrated Optimization, the most stable variables actually correspond to:

1. Active fraction of the surface dedicated to the photovoltaic system;
2. Position and inclination of the photovoltaic system and active fraction of the surface dedicated to it.

However, it was decided to exclude these variables from the selection because it was considered more useful, for the purposes of the study, to evaluate the behavior of the NSGA-II algorithm regarding the selection of HVAC systems for the three groups of rooms into which the proposed design has been divided, as these showed the most critical aspects in Fig.6.13.

Observing the Figs. from 6.14 to 6.16 and focusing on the graphs referring to stable variables on the left, it is noticeable that for values other than the optimum, indicated in red, both absolute and relative frequency decrease, and this is more evident in the neighborhood of the optimal solution. This means that these variables are indeed recognized by the algorithm as having one of the most significant impacts on the objective function of reducing emissions. Hence, they are kept at the optimal value even when different values are considered for the rest of the optimization variables because any deviation from it would lead to a departure from the optimum itself.

Conversely, referring to the graphs for unstable variables on the right, it can be observed that for values other than the optimum, both absolute and relative frequency are not reduced or nullified. For instance, regarding Fig.6.14, for a value of the shading object solar transmittance very close to the optimum of 0.8, both absolute and relative frequency are significant for both the entire population and the vicinity of the optimum. This suggests that even a value of 0.75 could be considered adequate to minimize the objective function, indicating that the solar transmittance of shading components has a less significant impact than, for example, the WWR for the South-oriented facade.

The same assertion can be made for Fig.6.15, where the variation in absolute and relative frequency is even higher. This is consistent with the observations made in Section 6.1, where it was highlighted that different values of variables associated with the HVAC system for the Below Grade Floor have little impact on the building's balance, given the same values of the other optimization variables. Furthermore, observing the graph related to the same phase of Sequential Optimization but for the variable HVAC Type Ground Floor, selected as stable, despite the variability being less significant compared to that recorded

for the Below Grade floor, it can be noted that for systems other than the optimal ones, the frequency is not zero. As anticipated, the algorithm proceeds by assigning values to this variable almost randomly because its overall impact on CO_2 emissions is minimal. In the same Section, but als in Section 6.2, it was stated that the type of HVAC system assigned to the First and Second floor plant has the greatest importance on the environmental impact of the building, followed by the Basement Floor and, at last, the Ground Floor. Indeed, in Fig.6.16, it is noted that, despite the first being selected as a somewhat unstable variable, both for the entire population and for the neighborhood of the optimum in Integrated Optimization, the absolute and relative frequency values are high.

Chapter 7

Cost Analysis

The sensitivity analysis of Chapter 6 allows to conclude that, in the vicinity of the optimal solution identified by the NSGA-II algorithm, whether in the case of the Sequential or Integrated Optimization, some variables may deviate from the values corresponding to the identified minimum of the objective function, causing only a minor variation in the energy-environmental parameter used to evaluate the performance of the proposed design compared to the reference model. This outcome benefits users who, in the early stages of the design process, need to select the best design alternatives: these not only correspond to a different environmental impact but also to a different economic impact of the building. In the context of applying the Integrative Delivery Process described by the AIA and presented in Section 2.3, it is therefore advantageous to evaluate from the early design stages the consequences of alternatives corresponding to the minimum impact on the investment associated with the proposed building. Thus it may be useful to conduct post-processing of the data, evaluating the cost variation generated by the different combinations of optimization variable values obtained from the algorithm output, relative to a reference; the latter, for this type of analysis, will be the non-optimized proposed design, for which some design elements remain fixed during the application of all optimization procedures. Consequently, in the cost analysis associated with the design solutions, the following variables are considered non-impactful on the costs of the various alternatives:

1. Parameters whose values do not change in the optimization procedure aimed at finding the minimum of the objective function;

2. Variables whose variation does not generate a significant impact on the overall cost of the building.

The total cost for each alternative is thus calculated based on the values assumed by the optimization variables and to all that design components on which their variation has an impact: the variation of these parameters can be associated with different consequences on the investment related to the designed building. This analysis will be repeated for Phase 1 and Phase 2 of the Sequential Optimization and for the Integrated Optimization based on the results obtained with a Population Size of 100. However, considering that, as demonstrated in Section 4.5.2, the optimization variables differ for each of them, the cost analysis will be conducted by considering the variation of different building parameters; specifically, Tab.7.1 defines the variables used for the three cost analyses conducted.

Table 7.1: Optimization variables used for the cost analysis of each of the design alternatives for both Sequential and Integrated Optimization approaches.

Sequential Opt. Phase 1	Sequential Opt. Phase 2	Integrated Opt.
WWR	HVAC Type	WWR
External Walls Extension	PV plant	External Walls Extension
		HVAC Type
		PV Plant

From the analysis of Tab.7.1, it is observed that, for Phase 1 of Sequential Optimization and Integrated Optimization, among the components of the opaque envelope, only the extension of the external facades is present, while the constructions or extensions related to other elements such as roofs or floors are not included. The reason for this is twofold and is illustrated below:

- The materials comprising the opaque envelope have been kept constant, and therefore the suggested design alternatives do not generate any variation in them: the associated cost variation between one alternative and another is zero.

- Although the building geometry has not changed in the optimization procedure, the latter includes an assessment of the impact of different extensions of the window components, which, in the case study, are only present in the vertical facades. This implies that a variation in the WWR corresponds to a variation in the extension of the opaque envelope related

to the external facades, which, therefore, must be considered as having an economic impact on the investment generated by each alternative.

Further observing Tab.7.1, it is also important to note that the solar transmittance of the shading components is not present for either Phase 1 of the Sequential Optimization or the Integrated Optimization, despite this being a variable of optimization in these procedures. The reason for this is that, in general, the economic impact of shading devices on a building is solely related to their geometry. However, for the case study, this has been kept constant and equal to that described in Tab.4.14. Therefore, since the economic impact generated by these components on different design alternatives is null, this will not be taken into account in the cost analysis described below.

7.1 Global Cost Calculation

A cost-benefit analysis of various energy efficiency measures to be applied to a building to improve its performance can be considered effective if it takes into account both the investment cost and the cash flows generated over time associated with each of the design alternatives being evaluated for the analyzed building. These elements, in fact, are used within equations that allow for the calculation of specific economic parameters, which provide an indication of the feasibility of the initial investment. Within EN 15459-1, the cost-effectiveness of a solution is evaluated by calculating the *Global Cost*: it represents the sum of the investment cost and the sum of the present value of the costs generated by the analyzed energy efficiency measure over its useful lifetime. Therefore, the best design alternative will be the one characterized by the minimum global cost. The definition of the latter is given by equation 7.1:

$$GC(n) = C_i + \sum_j \left[\sum_{t=1}^{n} \frac{C_{a,t}(j)}{(1+i)^t} - V_{f,n}(j) \right] \tag{7.1}$$

The definition of the parameters present in equation 7.1 is provided in the Nomenclature. Specifically, for the case study, the following assumptions are made:

- Useful life of the investment n: this is assumed to be 30 years for all design alternatives suggested by the optimization procedures;
- Discount rate i: This takes on different values depending on the investment made. For building interventions, European directives suggest a value of

3%, which will thus be used for the subsequent evaluations;

- $C_{a,t}(j)$: Only the cost associated with the electricity purchased from the grid is considered relevant for the evaluation of this therm. This cost varies depending on the building envelope's performance, the type of HVAC systems installed and the characteristics of the photovoltaic system. Therefore, knowing the building's consumption for the different alternatives in $kWh/year$ obtained as output from the annual energy simulation, this value is considered constant for all 30 years of the investment's useful lifetime, along with the electricity price on the Italian energy market. This price is assumed to be 0.12209 €/kWh[1] [87], and multiplied by the annual consumption, it yields the value of $C_{a,t}(j)$ for each combination of optimization variable values obtained as output from both phases of Sequential Optimization and Integrated Optimization.

- $V_{f,n}(j)$: It is considered that, at the end of the useful life, none of the design alternatives have a residual value. Thus, this parameter will always be assumed to be 0.

For the application of equation 7.1, it is necessary to calculate the investment cost C_i for the different design alternatives. To do this, the steps suggested in Section 7.2 have been followed.

7.2 Prices Definition

Tab.7.1 presented earlier specifies the only four design elements whose variation among the alternatives obtained from the optimization procedures impacts the investment related to the proposed design. These elements are represented by the extent of the window components relative to the facade surface for each orientation and the area of the vertical facade itself, the type of HVAC system installed for each of the three groups of internal spaces into which the building is divided, and the design characteristics of the photovoltaic system's extension and inclination. It was therefore necessary to define costs associated with different values assumed by these variables, and different approaches were taken for each variable.

---

[1]It is important to note that this value only considers the purchase of energy from the grid, excluding fixed costs that make this parameter higher when read in the bill. The reason for this is that a delta cost analysis is being conducted relative to a reference, and since the fixed costs remain unchanged between the reference and the alternatives, their impact on the incremental cost will be null.

7.2.1 Glazing Components Price

Regarding the WWR, Tab.4.13 shows the thermal transmittance value of the window components, which is 1.223 W/m^2K. This represents one of the fundamental cost parameters for the transparent envelope, and the price of the windows varies based on this value. Referring to the pricing data for *Serramenti, Facciate Continue, Schermature Solari Esterne, Partizioni e Protezioni* present in the P*rezzario Opere Edili ed Impintistiche sulla piazza di Torino* published by *Camera di Commercio Industria Artigianato ed Agricoltura di Torino*[88], the reference price for the type of windows hypothesized to be installed in the proposed design was selected. The selected price code is *19.4.10.60.10*, related to aluminum-wood sliding windows/doors with thermal break profiles, open joint, and thermal transmittance $U_w = 1.30 \ W/m^2K$ calculated according to UNI EN ISO 10077-1. The related price is 3311.99 euros for a window with dimensions 160x130 *cm*, which corresponds to 1592.30 €/m^2. This price does not include installation, for which the *Listino Opere Pubbliche Piemonte Anno 2024* was referenced: the price code *01.A18.1319.005* corresponds to an installation cost of 49.51 €/m^2. Therefore, the windows were assigned with a price based on their thermal transmittance, amounting to 1641.8 €/m^2.

Using the building model in *Grasshopper*, the facade areas by orientation were calculated, with the results shown in Tab.7.2:

Table 7.2: External walls extension of the case study for the different orientations.

	Area[m^2]
North Facade	285.36
East Facade	123.98
South Facade	262.56
West Facade	215.18

Therefore, knowing the WWR values associated with each orientation in the different alternatives obtained as output from the optimization procedures, their product with the corresponding external walls extension from Tab.7.2 is calculated to obtain the total area of the window components of the building. Multiplying this area by the previously calculated cost of 1641.8 €/m^2 yields the investment cost associated with this component of the energy efficiency measures ($C_{i,WWR}$).

7.2.2 External Walls Price

To evaluate the price per square meter associated with the selected construction for the external facades, it is necessary to start with the materials that comprise it. These materials are summarized schematically in Tab.7.3, along with their main thermophysical characteristics.

Table 7.3: External Walls Construction Materials.

Material	Thickness [m]	Thermal Conductivity [W/m²K]	Density [kg/m3]	Specific Heat [J/kgK]
Stucco	0.025	0.691	1858	836.46
Cement hw	0.203	1.31	2240	836.26
Typical Insulation		$R_T = 3.522\ m^2K/W$		
Gypsum	0.013	0.1599	784.9	829.49

Table header spanning: **Typical Insulated Exterior Mass Wall-R22**

These details were obtained using the *Honeybee* plug-in by analyzing the characteristic layers of the selected construction for this element of the opaque envelope in the proposed design model, as shown in Tab. 4.13. As can be noted, there is no information about the thickness and type of insulation provided. Therefore, EPS graphite insulating panels with a thickness of 72.5 *mm* and thermal resistance characteristics comparable to those reported in Tab.7.3 were considered. The prices associated with each layer per square meter were derived from the *Prezzario regionale Piemonte Opere Pubbliche 2024* and are summarized in Tab.7.4 along with the associated price codes and the total price of this cost variable, which will be used to calculate the investment cost of each alternative:

Table 7.4: Code prices and square meter prices for each of the layers composing the External Wall construction.

Material	Price Code [-]	Price [€/m²]
Stucco	*01.A10.A45.005*	73.13
Cement hw	*01.P05.A05.010*	14.62
Typical Insulation	*01.P09.A47.015*	26.73
Gypsum	*01.A10.C20.005*	11.95
TOTAL		126.43

In conclusion, the investment cost associated with this component ($C_{i,op.}$) for each alternative will be obtained by multiplying the price per square meter for the entire construction, as reported in Tab.7.4, by the total extension of the external walls across all four orientations. The latter will be equal to the product of the facade areas of Tab.7.2 and the complement to one of the WWR for each facade, corresponding to each alternative selected by the optimization algorithm.

7.2.3 Photovoltaic System Price

The evaluation of the price associated with the photovoltaic system was done by assuming the installation of monocrystalline panels, as described in Section 4.3.6, with a peak power between 310 and 320 W_p. For roof-integrated installations, the corresponding code in the *Listino Opere Pubbliche Piemonte Year 2024* is *03.P14.A06.005*, with a price of 0.82 €/W_p. Considering 310 W_p and a panel size of 1.11x1.65 m [89], the purchase price of this type of system is 138.79 €/m^2, excluding installation. Given that the maximum extension of the photovoltaic system provided in the different alternatives analyzed in the optimization procedure is less than 100 m^2, the installation price from the *Listino Opere Pubbliche Piemonte Year 2024* is 97.77 €/m^2 (price code: *03.A13.A01.010*), for a total of 236.56 €/m^2 of installed photovoltaic surface. It is important to note that the cost analysis did not consider the prices associated with the inverter, as it is assumed that the same model will be used for all photovoltaic system installations analyzed in the optimization procedure, thus not causing any cost variation between them. Moreover, since it was not possible to obtain a reference price for the installation of a photovoltaic system on the facade, it was assumed that the total price per square meter would be the same as that used for roof installation. This type of assumption, however, does not cause significant alterations in the cost values of the alternatives, as the optimization algorithm rarely selects the Vertical Facade as the location for the system. This is due to its negative impact on internal lighting consumption and its low productivity given the reduced solar radiation incident on it, as demonstrated in Fig.4.6.

For each design alternative evaluated by the optimization algorithm, the following were analyzed:

- Alternative location of the system and, therefore, the corresponding extension;
- Percentage of active surface selected.

The product of these factors with the previously calculated price per square meter allows for determining the investment cost associated with this component of the energy efficiency measures $C_{i,PV}$.

7.2.4 HVAC Systems Price

Section 4.3.7, provides the description of the types of HVAC systems considered for installation in the proposed design to compare the performance of the same for different solutions obtained through the application of the NSGA-II algorithm. As described in Chapter 6, the HVAC type among the six tested on each of the three groups of rooms into which the building is divided, that ensures the minimal environmental impact of the building, is the Variable Refrigerant Flow system (i.e. DOAS with VRF) and this result is consistent for both Sequential Optimization and Integrated Optimization. However, while for the first approach, installing the system only on the First and Second Floors was sufficient to achieve an optimal reduction of 57.79% in CO_2 emissions compared to the baseline, for the second approach, it proved more advantageous to install the system throughout the entire building, resulting in a 56.58% reduction in emissions compared to the baseline.

From an economic perspective, however, it is necessary to evaluate the impact of different HVAC systems based on the group of rooms to which they are associated allowing the designer, from the early stages of design, to select the combination that achieves the same energy performance of the optimal design alternative for the proposed design but with the minimum cost. It can be stated that, at such an early stage of design, not all the specific equipment required for each type of HVAC system is known. Additionally, valves, pipes, and ducts have less significance on the overall price of the system compared to the impact exerted by generation systems and terminals. For these reasons, only these components were considered for the investment cost evaluation of the HVAC systems. The first step was to extract from the model created in *Grasshopper* the peak power demand values for heating and cooling for each

of the three groups of rooms in the proposed design, which are summarized in Tab.7.5.

Table 7.5: Cooling and Heating peak power for the three groups of rooms of the case study building.

	Peak Cooling Power [kW]	Peak Heating Power [kW]
Below Grade Floor	9.2	1.8
Ground Floor	28.4	29.0
First and Second Floor	48.3	44.1

These values have allowed for the determination of the capacities and so the sizes of the different generation systems for the six types of HVAC systems analyzed in the study for each of the three groups of rooms. Regarding the terminals, an intermediate power level among those provided by the price lists was chosen for the selection of each unit's price. Therefore, the prices of the generators and terminals in the six systems considered in the analysis, selected from the *Prezzario DEI per Impianti Tecnologici del 2020* [90], are illustrated below. It is necessary to emphasize that for all HVAC systems where both chiller and ASHP are present, generation systems represented by reversible heat pumps, capable of producing both cooling and heating power, were selected from the price list. This is because, in Italy, the state-of-the-art practice is to install a single type of system (a reversible unit) rather than two different components for each type of power.

- *Chiller with central ASHP*: As mentioned in Section 4.3.7, when only "Chiller" is provided in the *Honeybee* library, it implies that it is water-cooled. Therefore, a generation system defined as a chiller/heat pump with a water-cooled condenser operating with R134A refrigerant and a twin-screw compressor was selected from the price list. The corresponding price code in [90] is *035034a*.

- *Cooling Tower*: This component is necessarily present when the HVAC system includes a water-cooled chiller. From [90], an axial cooling tower made of fiberglass was selected, with the price code *033164a*.

- *Chiller*: For the DOAS with fan coil chiller with baseboard electric system, a generation system consisting solely of a water-cooled chiller, which only produces cooling power and is condensed using water, needs to be defined. Since a reference model was not available in [90], the price information

was obtained with support from the team at GET Consulting s.r.l. and is reported for the three groups of rooms in Tab.7.7.

- *Air-cooled chiller with central ASHP*: In this case, the chiller is air-cooled. Therefore, a chiller and heat pump with air-cooled condensation, axial fans, and scroll compressors was used as reference. The price codes in [90] for the models considered for the case study vary according to the cooling and heating power values summarized in Tab.7.5 and are *035027a*, *035027e*, and *035030a* for Below Grade Floor, Ground Floor, and First and Second Floor, respectively.

- *Air-cooled chiller*: For the DOAS with fan coil air-cooled chiller with baseboard electric HVAC system, the installation of an air-cooled chiller is required. Therefore, a chiller model with air-cooled condensation, axial fans, operating with R410A refrigerant, and scroll compressors was considered. Again, the price codes in [90] vary according to the cooling power and are *035025a*, *035025e*, and *035029a* for Below Grade Floor, Ground Floor, and First and Second Floor, respectively.

- *DOAS with VRF*: For this particular type of system, the DEI price list [90] provides the price code for the external unit based on the cooling and heating power. Considering the peak cooling and heating values for the three groups of rooms in the building reported in Tab.7.5, codes *035001a*, *035003c*, and *035003f* were selected for Below Grade Floor, Ground Floor, and First and Second Floor, respectively. For the terminals, the price code is the same for all three groups and is *035012e*.

- *Baseboard Electric*: This type of terminal is not used in Italy, so its price was obtained from [91] and is subsequently reported in Tab.7.7, along with those of the other elements analyzed so far and subsequently.

- *FanCoil*: For all HVAC systems that require fan coils, the model used is characterized by two coils, four pipes, and an electric motor, with the price code *035072d*.

- *Ceiling Metal Panels*: The DOAS with water chiller and radiant panels and central ASHP system is characterized by radiant panels installed on the ceiling. The model selected for the case study consists of PR-R polypropylene pipes with high resistance to high temperatures, with the price code *025242b* and a price of 163.6 euros per m^2. It is necessary to emphasize that in the subsequent calculations of the investment cost associated with these terminals, the price will be multiplied by a surface

area that does not represent the entire ceiling area of each group of rooms served by the system. It is assumed that only 85% of the total surface area is covered, and therefore, the values used are reported in Tab.7.6:

Table 7.6: Total ceiling surface and radiant panels covered ceiling surface for the three groups of rooms of the case study building.

	Total Ceiling Surface $[m^2]$	Covered Ceiling Surface $[m^2]$
Below Grade Floor	280.0	238.0
Ground Floor	419.4	356.5
First and Second Floor	730.8	621.2

In Tab.7.7, the previously described prices are summarized. If a single value is present in each row, it represents the price valid for all three groups of rooms into which the proposed design has been divided. It is important to clarify that all the prices listed include both the cost of materials and components as well as their installation.

Table 7.7: Prices for each HVAC component for the three groups of rooms of the case study building.

	Below Grade Floor	Ground Floor	First and Second Floor
Chiller and Central ASHP [€/unit]		33622.6	
Cooling Tower[€/unit]		2535.0	
Chiller [€/unit]	15000.0	30000.0	45000.0
Air-cooled Chiller with Central ASHP [€/unit]	7449.7	12628.2	21593.5
Air-cooled Chiller [€/unit]	5614.9	10091.8	19755.9
DOAS with VRF - outdoor unit [€/unit]	3800.4	9867.9	14823.9
DOAS with VRF - terminal [€/unit]		1198.3	
Baseboard electric [€/unit]		1501.0	
FanCoil [€/unit]		1472.88	
Ceiling Radiant Panels [€/m^2]		163.6	

The cost associated with each of the six HVAC systems described in Section 4.3.7 was calculated for all three groups of rooms. The results are presented in Tab.7.8. Note that the numbering corresponds to the following list:

1. *DOAS with fan coil chiller with central air source heat pump*;
2. *DOAS with fan coil chiller with baseboard electric*;
3. *DOAS with fan coil air-cooled chiller with central air source heat pump*;
4. *DOAS with fan coil air-cooled chiller with baseboard electric*;
5. *DOAS with VRF*;
6. *DOAS with low temperature radiant chiller with air source heat pump*.

Table 7.8: Total investment cost for each HVAC type and each of the three groups of rooms of the case study building.

	Below Grade Floor $C_{i,BGF}$ [€]	Ground Floor $C_{i,GF}$ [€]	First and Second Floor $C_{i,F\&SF}$ [€]
1	37630.5	43522.0	50886.4
2	19036	40040	62545
3	8922.6	19992.6	36322.3
4	8588.8	24961.2	49494.7
5	4998.6	15859.2	26806.5
6	75082.5	70706.9	118952.9

7.3 Cost Analysis Results

The application of equation 7.1 was carried out starting with the calculation of the investment cost C_i for each alternative identified by the optimization procedure as the sum of the investment costs previously calculated for each selected design component. These components combine differently depending on the optimization approach considered, so the calculation of C_i is carried out differently for the two optimization approaches. Below, in equations 7.2, 7.3, and 7.4, the cost components considered respectively for Phase 1 and Phase 2 of Sequential Optimization and for Integrated Optimization are reported:

$$C_i = C_{i,WWR} + C_{i,op.} \tag{7.2}$$

$$C_i = C^*_{i,Ph1} + C_{i,PV} + C_{i,BGF} + C_{i,GF} + C_{i,F\&SF} \tag{7.3}$$

$$C_i = C_{i,WWR} + C_{i,op.} + C_{i,PV} + C_{i,BGF} + C_{i,GF} + C_{i,F\&SF} \tag{7.4}$$

Please note that in equation 7.3, there is a term indicated as $C^*_{i,Ph1}$: this represents the investment cost associated with the combination of WWR considered optimal in the output from Phase 1 of Sequential Optimization, and thus, the one represented in Tab.5.4. This assumption is made because, as described in Section 5, Phase 2 of Sequential Optimization is carried out based on the optimized building envelope design obtained from Phase 1 of the same; the investment cost of this latter, indicated as $C^*_{i,Ph1}$ and equal to the sum of $C_{i,WWR}$ and $C_{i,op.}$ for the optimal solution, is summed with the investment costs associated with the HVAC variables to obtain the investment that must be sustained for the complete design of the building obtained as an output from Phase 2 of Sequential Optimization, considering both the building envelope and the HVAC systems, as well as the photovoltaic system.

At this point, the results of the Global Cost obtained by implementing equation 7.1 for each of the two optimization approaches are graphically represented in Fig.7.1, where it is plotted for each alternative as a function of the corresponding percentage reduction in emissions. Moreover, to facilitate the understanding of the impact that operational costs (Opex) have on the Global Cost, the individual investment costs (Capex) for each alternative are represented in gray on the graphs.
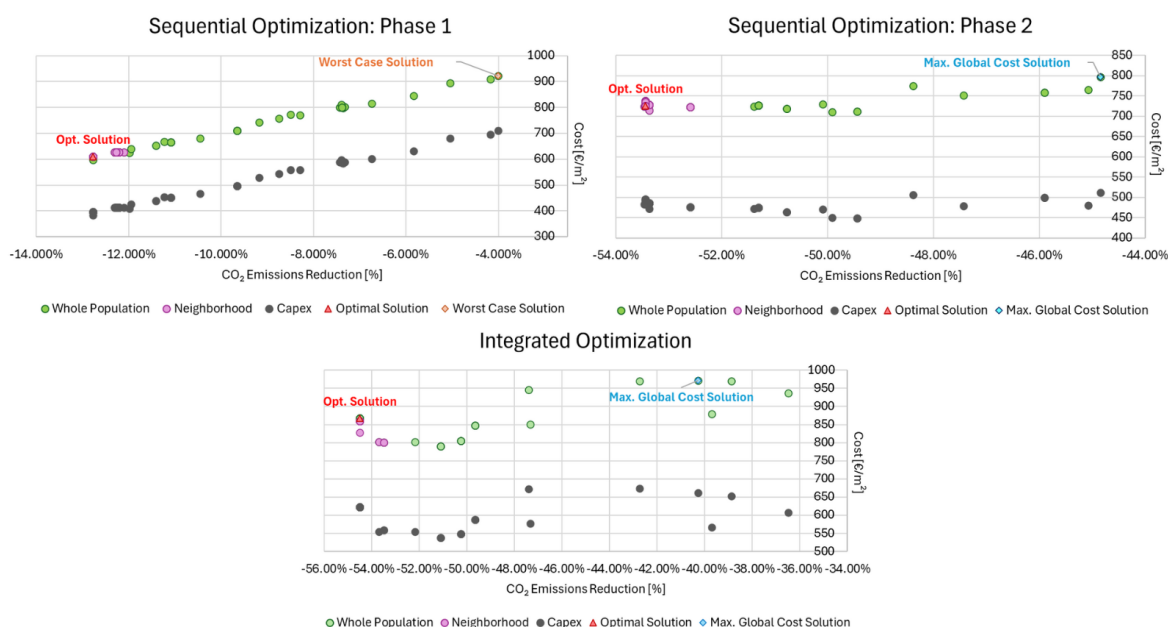

Figure 7.1: Global costs and Capex plot for Phase 1 and Phase 2 of Sequential Optimization and for Integrated Optimization.

Observing Fig.7.1 at the top left, and thus analyzing the trend of the Global Cost per square meter of heated surface for Phase 1 of Sequential Optimization, it is noted that solutions corresponding to higher Global Cost values are also those characterized by a lower absolute value percentage reduction in CO_2 emissions compared to the baseline. The reason for this is linked to the fact that the selection of WWR values, solar transmittance of shading components, and location of the photovoltaic system, which have a positive impact on the building's energy balance, allows for a reduction in the building's energy demand. Since this study considers costs associated not only with the initial investment but also with the building's operation over a 30-year period, the lower the energy demand resulting from the design, the lower the purchase of energy from the grid, and thus the lower the Global Cost of the design alternative. However, observing the Capex, in gray, it can be noted that the difference between these and the Global Cost for each alternative, including the Opex over the 30-year useful life of the investment, remains almost constant. In fact, the initial investment costs associated with the design alternatives obtained from Phase 1 of optimization show the same trend observed for the Global Cost. Two elements can explain these results:

1. Observing the electricity consumption associated with the different design alternatives recorded following the optimization procedure, these vary from a maximum value of 126735.6 $kWh/year$ for the worst-performing alternative to 128562.2 $kWh/year$ for the most performing one. Thus, from this perspective, the different solutions are essentially equivalent to each other, and hence the difference between Global Cost and Capex is practically constant among them, averaging around 200 €$/m^2$.

2. For Phase 1 of Sequential Optimization, the only design components impacting the initial investment are those related to the transparent envelope and the external walls extension. As highlighted in Chapter 5, a higher value assigned to the WWR of the different facades corresponds to a negative impact on the energy balance, linked to a higher heating demand in winter due to losses towards the outdoor environment and a higher cooling demand in summer due to increased solar heat gains entering the internal spaces, resulting in smaller percentage reductions in emissions. It can be asserted, however, that a higher WWR value not only has negative impacts on the energy balance but can also negatively impact the investment costs (Capex): an higher WWR implies a larger window

area and thus an higher $C_{i,WWR}$ and a lower $C_{i,op.}$. In general, it can be assessed that the weight of the latter two components can lead to different values of the total Capex; however being the external walls construction price lower than the one of the windows by an order of magnitude, it prevails the negative effect of the higher cost of the latter rather than the lower one of the former. This is very evident when comparing the Capex values reported in Tab.7.9 associated with the optimal solution and the worst-case solution, with percentage emission reductions of -12.77% and -4.00%, respectively. The same table also shows the values assumed by the optimization variables for the two design alternatives.

Table 7.9: Capex comparison between worst case and optimal solution for Phase 1 Sequential Optimization.

	Worst Case	Opt. Solution
	-4.00%	**-12.77%**
Economic Results		
Capex [€]	710.1	396.3
Global Cost [€]	922.1	610.8
Optimization Variables Values		
WWR N	0.7	0.3
WWR E	0.5	0.4
WWR S	0.7	0.3
WWR O	0.7	0.4
Sh. Objects Solar Transmittance	0.2	0.8
PV location	East Roof	West Roof

It is noticeable that the initial investment associated with the optimal solution is almost halved compared to that corresponding to the worst-performing building performance. The reason for this is clear when observing the WWR values corresponding to the two alternatives: in the case of a percentage reduction of -4.00% (Worst Case Solution), indeed, they are much higher compared to those of the alternative corresponding to -12.77% (Opt. Solution) and despite this should cause a lower cost for the external walls construction, the higher investment cost for glazing components prevails. From an emissions perspective, moreover, the reasons for such a low absolute value of percentage reduction in emissions compared to the baseline could be:

- Higher WWR, corresponding to worse energy performance in both summer and winter seasons for the reasons previously presented;
- Lower solar transmittance of shading components, corresponding to a lesser positive impact on the energy balance in the winter season associated with the entering of solar gains into internal spaces.

The calculation of investment costs and Global Costs for the solutions obtained from Phase 1 of Sequential Optimization thus allows us to conclude that a building with better energy-environmental performance can be achieved with lower investment costs and, consequently, lower Global Cost compared to those that would be incurred in the case of a design with poorer performance. It is necessary to emphasize, however, that this type of result is valid for the analyzed case study and, in general, for all those cases in which the construction characteristics of the building envelope components and the building's location lead to a reduced extension of glazing components corresponding to lower emissions and, consequently, lower costs. More often, however, the opposite occurs: considering, for example, a more efficient opaque and transparent envelope, higher WWR allows for a significant reduction in lighting-related consumption, representing the most significant effect of such intervention on the balance. This, however, entails the need to identify a trade-off solution between reduced emissions and higher investment costs.

In Tab.7.9, the investment cost associated with the optimal solution is reported as 396.3 €/m^2, corresponding to the term $C^*_{i,Ph1}$ in Equation 7.3.

In observing the remaining two graphs in Fig.7.1, once again, there is a clear shift in the Global Cost values compared to the Capex values, with the difference ranging between 200 and 300 €/m^2. In this case, the deviation is more variable compared to the previously analyzed scenario because the electricity consumption varies between a minimum of 144674 $kWh/year$ and a maximum of 170684 $kWh/year$ for Phase 2 of Sequential Optimization, and between 144404 $kWh/year$ and 196481 $kWh/year$ for Integrated Optimization. The wider range of values is due to the fact that for these optimization procedures, the algorithm evaluates different values for the tilt angle of the panels and the extension of their active surface, thus more significantly altering the self-produced energy value and the energy drawn from the grid. This results in a more variable overall impact of Opex on the Global Cost for the different design alternatives analyzed. With this aspect highlighted, to make a better comparison between the final outcome of Sequential Optimization

and Integrated Optimization, the trends of solely the Global Cost have been analyzed, representing them in Fig.7.2.
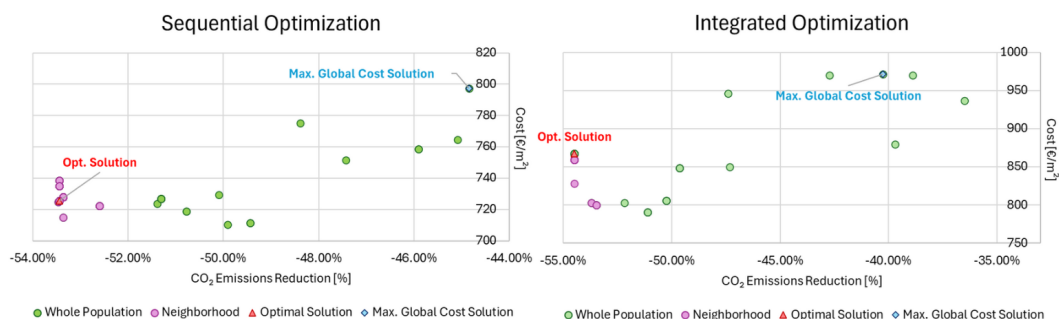
Figure 7.2: Global costs plot for Phase 2 of Sequential Optimization and for Integrated optimization.

The analysis of individual Global Costs reveals that, although less pronounced than in the graph obtained for Phase 1 of Sequential Optimization, there is still a trend where lower absolute values of percentage reduction in emissions correspond to higher Global Costs. In this case, the reason for this could be attributed to the fact that the alternatives corresponding to these results are characterized by either reduced on-site electricity production from photovoltaic systems or higher electricity consumption, depending on the combination of values assumed by the optimization variables, leading to increased purchases from the grid and consequently higher operating costs (Opex). To understand this, it is possible to compare the solutions with the maximum Global Cost for Sequential Optimization and Integrated Optimization: for these solutions, the economic aspects are summarized in Tab.7.10, while the values assumed by the optimization variables are presented in Tab.7.11.

Table 7.10: Economic results of the maximum Global Costs solutions for Sequential and Integrated Optimization.

Maximum Global Cost Solutions				
	CO_2 **Emissions Reduction**	**Global Cost** $[\text{\euro}/m^2]$	**Capex** $[\text{\euro}/m^2]$	**Electrical Energy from Grid** $[kWh]$
Sequent. Opt.	-44.84%	797.3	511.7	170684.2
Integrated Opt.	-40.27%	971.6	662.3	184804.7

Table 7.11: Maximum Global Cost solutions variables values for Sequential and Integrated Optimization.

Maximum Global Cost Solutions		
	Integrated Opt.	**Sequential Opt.**
WWR N	0.4	0.3
WWR E	0.8	0.4
WWR S	0.6	0.3
WWR O	0.5	0.4
Sh. Objects solar Transmittance	0.7	0.8
PV Location	East Roof, 10°	West roof, 22°
HVAC Below Grade Floor	DOAS with fan coil air-cooled chiller with baseboard electric	DOAS with chiller and radiant panels with central ASHP
HVAC Ground Floor	DOAS with fan coil air-cooled chiller with central ASHP	DOAS with fan coil air-cooled chiller with central ASHP
HVAC First and Second Floor	DOAS with fan coil chiller with baseboard electric	DOAS with fan coil air-cooled chiller with baseboard electric
PV Panels Active Fraction	0.6	0.6

Analyzing the results reported in Tab.7.10, it is possible to notice that the solution represented for Integrated Optimization corresponds to:

- the minimum value, in absolute terms, of percentage reduction in CO_2 emissions;
- the maximum value of Global Cost and Capex.

The results related to the percentage reduction in CO_2 emissions and Global Cost can be partly explained by the last result reported in Tab.7.10, i.e., the electricity purchased from the grid: this is higher for Integrated Optimization, implying higher emissions first and then higher operating costs. However, to pinpoint the reasons for these results more precisely, it is necessary to refer to Tab.7.11:

1. Regarding the building envelope components, the WWRs are higher for the solution output from Integrated Optimization compared to those obtained from Sequential Optimization. The latter, indeed, is characterized by passive components that have already been optimized previously during Phase 1, which improves the building's performance and thus reduces energy consumption and CO_2 emissions compared to the solution obtained from Integrated Optimization, but also results in lower invest-

ment costs because the extent of the transparent envelope is smaller and even if the extension of the external walls is more relevant, its complex impact on the Capex is low, as already demonstrated for Phase 1. As for the solar transmittance of shading components, it is similar for the two solutions; however, the lower value for Integrated Optimization leads to worse winter energy performance, as demonstrated by Fig.6.4, and thus to higher emissions, consumption, and operating costs for purchasing electricity from the grid.

2. Analyzing the characteristics of the photovoltaic system, it is possible to asses that the one related to Integrated Optimization not only does not correspond to the optimal location, which is the one indicated as West Roof but is also characterized by an inclination of 10°, which leads to poor reception of solar radiation and thus to reduced production which, with the same active surface as the solution presented for Sequential Optimization, will be lower than that corresponding to the latter, as also demonstrated in Tab.7.10.

3. The HVAC types selected by the two optimization approaches do not correspond to what was considered optimal in Section 6.1 and 6.2, which is the Variable Refrigerant Flow system. This represents the primary cause of a non-optimal result from an energy-environmental perspective.

To assess the economic impact of the HVAC types selections, it was decided to summarize in Tab.7.12 the costs associated with the selected systems for the solutions with maximum Global Cost from the two optimization approaches:

Table 7.12: Investment Cost related to HVAC systems selected for the Maximum Global Cost solution by Integrated and Sequential Optimization.

Maximum Global Cost Solutions		
	Integrated Opt. [€]	Sequential Opt. [€]
HVAC Below Grade Floor	8588.8	75082.5
HVAC Ground Floor	19992.6	19992.6
HVAC First & Second Floor	62545	49494.7
TOTAL	91126.3	144569.8

As evident from the sum of investment costs related to the selected HVAC systems for solutions with maximum Global Cost obtained from Integrated and Sequential Optimization, the HVAC alternatives selected in the case of the latter are actually less advantageous compared to those for the solution identified by the former. However, as shown in Tab.7.10, the Capex for the solution obtained with Sequential Optimization is overall lower. This allows to understand that between the passive and HVAC components of the building, the most significant cost is represented by the former: since these have already been optimized during Phase 1 of optimization, their negative impact on energy balance and investment cost will be lower for Phase 2 Sequential Optimization than what is observed in Integrated Optimization, where the lower investment cost related to HVAC systems is actually worsened by the higher cost associated with higher WWR and inefficient location of the photovoltaic system.

To assess whether this observation can be considered valid for the entire set of available solutions, it was decided to summarize the economic results related to the optimal solutions obtained from Sequential Optimization and Integrated Optimization, as done in Tab.7.14 and 7.15. The values of the optimization variables of the two analyzed solutions are summarized in Tab.7.13.

Table 7.13: Optimal Solutions variables values for Sequential and Integrated Optimization.

Optimal solutions in output from NSGA-II algorithm		
	Integrated Opt. -54.49%	**Sequential Opt. -53.44%**
WWR N	0.8	0.3
WWR E	0.3	0.4
WWR S	0.4	0.3
WWR O	0.3	0.4
Sh. Objects solar Transmittance	0.65	0.8
PV Location	West Roof, 40°	West roof, 40°
HVAC Below Grade Floor	DOAS with VRF	DOAS with fancoil chiller with baseboard electr.
HVAC Ground Floor	DOAS with fancoil chiller with baseboard electr.	DOAS with VRF
HVAC First and Second Floor	DOAS with fancoil air cooled chiller with central ASHP	DOAS with fancoil chiller with central ASHP
PV Panels Active Fraction	0.9	0.9

Table 7.14: Economic results of Optimal Solutions for Sequential and Integrated Optimization.

Optimal solutions in output from NSGA-II algorithm				
	CO_2 **Emissions Reduction**	**Global Cost** $[€/m^2]$	**CAPEX** $[€/m^2]$	**Electrical Energy from Grid** $[kWh]$
Sequential Opt.	-53.44%	673.5	430.9	145025
Integrated Opt.	-54.49%	827.2	582.8	141535

Table 7.15: Investment Costs for Integrated and Sequential Optimization optimal solutions

Optimal solutions in output from NSGA-II algorithm		
	Integrated Opt.	**Sequential Opt.**
HVAC Systems C_i [€]		
HVAC Below Grade Floor	4999	19036
HVAC Ground Floor	40040	15859
HVAC First & Second Floor	36322	50886
TOTAL	81361	85782
Passive Components C_i [€]		
Windows	714287	472254
External Walls	79371	93803
PV Panels	37821	37821
TOTAL	831479	603878

As anticipated in Section 5.3, the difference in terms of percentage reduction in CO_2 emissions between the two optimization procedures is approximately 1% in favor of Integrated Optimization, which could suggest to the user the preference towards this kind of approach, considering also the lower time required with respect to the one of the Sequential Optimization. However, Tab.7.14 suggests that the former returns the solution with the maximum Global Cost, corresponding to higher electricity purchase from the grid, but also to higher initial investment costs. This is composed as presented in Tab.7.15: the most significant portion of initial investment is once again related to passive components, and this holds true for both Integrated Optimization and Sequential Optimization; for the solution suggested by the latter, however, while the costs related to HVAC systems are very similar to those obtained with Integrated Optimization, the portion related to passive components is much lower because the WWR of the North facade in this case is lower than that associated with the optimal solution of Integrated Optimization and despite this leads to an increase of the investment cost for the external walls, its impact is not relevant with respect to the one of the glazing components.

Based on these observations, it is possible to conclude that, considering only and exclusively the optimization of the energy-environmental performance of the building, the two optimization approaches return solutions that are similar as

they differ only by about 1% in terms of percentage reduction in CO_2 emissions compared to the baseline building. However, by performing post-processing of the data from an economic point of view, it is evident that, with such a small difference in building performance, there is a very significant economic impact, leading to a Global Cost that is, for the solution that ensures a more efficient design, higher by approximately 200 €/m^2. In particular, it increases from 1140232 euros for the solution obtained from Sequential Optimization to 1389530 euros for Integrated Optimization.

Once the optimal solutions output by the two optimization approaches were characterized from an economic standpoint, it was decided to do the same for the Best Case Solutions considered following the sensitivity analysis conducted in Chapter 6, as described in Sections 6.1 and 6.2. The values of the optimization variables for these solutions are summarized below in Tab.7.16:

Table 7.16: Maximum CO_2 emissions reduction solutions (Best Case Solutions) for Sequential and Integrated Optimization.

Best Case Solutions		
	Integrated Opt. -56.58%	**Sequential Opt. -57.79%**
WWR N	0.8	0.3
WWR E	0.3	0.4
WWR S	0.4	0.3
WWR O	0.3	0.4
Sh. Objects solar Transmittance	0.65	0.8
PV Location	West Roof, 40°	West roof, 40°
HVAC Below Grade Floor	DOAS with VRF	DOAS with VRF
HVAC Ground Floor	DOAS with VRF	DOAS with VRF
HVAC First and Second Floor	DOAS with VRF	DOAS with VRF
PV Panels Active Fraction	0.9	0.9

The solutions described in Tab.7.16 are the ones obtained after a post-processing of the optimization output alternatives and can be considered as those with the types of HVAC systems that guarantee the maximum percentage reduction in CO_2 emissions compared to the baseline, while keeping the building envelope components fixed at the outputs from the Phase 1 of Sequential Optimization, for the solution corresponding to -57.79%, and at the outputs from Integrated Optimization, for the one corresponding to -56.58%. Once again, the difference between them is approximately 1%, this time in favor of

the Sequential approach. Therefore, it is decided to evaluate:

- Capex;
- Global cost;

for the two alternatives, in order to determine which one adequately represents a trade-off between economic and environmental impact. Tab.7.17 summarizes the results of the economic analysis of the two solutions:

Table 7.17: Economic results of maximum CO_2 emissions reduction (Best Case Solutions) for Integrated and Sequential Optimization.

Best Case Solutions				
	CO_2 **Emissions Reduction**	**Global Cost** $[€/m^2]$	**Capex** $[€/m^2]$	**Electrical Energy from Grid** $[kWh]$
Sequential Opt.	-57.79%	676.2	456.1	131543
Integrated Opt.	-56.58%	825.4	599.2	135238

As evident from the analysis, the economically superior solution among the two examined is the one suggested by Sequential Optimization, which also corresponds to the one with the maximum percentage reduction in CO_2 emissions due to its overall reduced extent of glazing components. However, it is necessary to strike a balance between the lower Global Cost associated with the solution obtained through Sequential Optimization and the higher optimization time associated with it. In cases where the latter incurs a significant cost, both economically and otherwise, it might be more advantageous to select Integrated Optimization, which, with a total time halved compared to the Sequential approach, yields a solution differing by only 1% from the optimal one and although this approach results in a slightly higher global cost of approximately 150 $€/m^2$, it offers considerable time savings.

Chapter 8

Conclusions

Concerns about the global climate are among the most important issues in society today and have attracted the interest of both the public and national and international institutions. The 2°C maximum global temperature increase limit set by the IPCC in 2014 has led to numerous political efforts to contain greenhouse gas emissions. The European Union, in particular, has issued various directives and regulations to reduce the environmental impact of sectors such as transportation, industry, and buildings.

The building sector, in particular, contributes to 10% of the EU's total CO_2 emissions, mainly due to the inefficiency of older buildings, which constitute the majority of the building stock. With 75% of these buildings being inefficient and expected to be in use until 2050, improving energy efficiency is crucial. The EU's commitment to this goal is supported by regulations such as the Energy Performance of Buildings Directive (EPBD), which mandates that new buildings be Zero or nearly Zero Energy Buildings (ZEB/nZEB) by 2021. The directive also requires member countries to set minimum energy performance standards for new constructions and major renovations. Italian government, for example, has incorporated these EU directives into its national legislation: Legislative Decree 192/2005 and its amendments establish the framework for energy performance certificates and the required energy standards for buildings. Additionally, fiscal incentives, such as the *Superbonus 110%*, further promote energy efficiency improvements in buildings by offering tax deductions for expenses related to such interventions.

Achieving the goals of nearly zero-energy buildings involves minimizing energy demand through efficient passive architecture and the use of advanced

technologies such as heat pumps for heating and cooling. Energy modeling is an essential support in this process as it allows for the prediction of building performance based on the model of the understudy building itself. The design approach in Italy is regulated and organized into three main phases of technical detail, according to Legislative Decree No. 163 of April 12, 2006: *Preliminary*, *Definitive*, and *Executive*. One negative aspect of this approach is that it inevitably leads to "Siloed Optimization", where each design component is initially optimized in isolation, requiring subsequent integrations to ensure feasibility and budget compliance. For these reasons, virtuous organizations like the AIA have developed the "Integrative Project Delivery" (IPD), which considers the building as a system of interconnected parts, promoting collaboration among all participants to achieve the sustainability and energy efficiency goals set by the European Union. Despite the directives and regulations issued by the EU forcing designers to anticipate numerous analyses in the early design stages, it is possible to state that the procedure is still far from a definition allowing to implement an integrative design approach as promoted by the AIA. One of the reasons is the difficulty of using modeling and energy simulation tools in the early design stages, as these require a significant number of inputs with a high level of detail, which are not available during the preliminary design phases.

This thesis is thus situated within this context and aims to address the challenge of evaluating design alternatives in the early stages of the design process to ensure optimal building performance, in line with the decarbonization and energy efficiency objectives outlined by the European Union in response to growing concerns about climate issues. To achieve this goal, the software *Rhino* with the visual programming interface *Grasshopper3D* and its plugins *Ladybug*, *Honeybee*, *Ironbug*, and *Wallacei* were utilized. The latter enabled multi-objective optimization using the NSGA-II evolutionary algorithm to identify design alternatives that optimize a selected set of objective functions.

Based on the case study provided by GET Consulting s.r.l., the reference building model was defined following the procedure described in Appendix G of ASHRAE Standard 90.1-2016. This model is considered the benchmark against which the performance optimality of the proposed building design is evaluated over a typical year of operation simulated using a dynamic simulation approach implemented through the *EnergyPlus* software engine. The procedure aims to maximize the percentage reduction in CO_2 emissions of the proposed design compared to the baseline building, ensuring the satisfaction of summer and win-

ter temperature setpoints. It considers two categories of optimization variables: those related to the building envelope, represented by the WWR on the four facades of the building and the solar transmittance of the shading components placed on the windows, and those related to the systems, represented by six different types of HVAC systems tested on three HVAC zone groups into which the building is divided, and the location, extension, and inclination properties of the photovoltaic system, considered made of monocrystalline panels with an efficiency of the 17%. The optimization was approached using two different methods: the Sequential approach and the Integrated approach.

The first approach involves *Sequential Optimization*, which consists of two phases. The first one considers the building envelope variables, including the optimal location of the photovoltaic system to maximize the positive shading effect on the interior spaces. With a Population Size of 100 for the NSGA-II algorithm, the optimal values of the variables resulted in a 12.77% reduction in CO_2 emissions. Keeping these values fixed as shown in Tab.5.4, the second phase of optimization focuses on the active components of the building, such as HVAC systems and the photovoltaic system. After excluding solutions with unmet setpoint hours exceeding 300, the optimization algorithm suggests a solution corresponding to a 53.44% reduction in emissions. This sequential approach, with a Population Size of 100, required a total simulation time of approximately 27 hours. The second approach, *Integrated Optimization*, simultaneously optimizes both passive and active system variables to account for their interdependencies. After a total simulation time of approximately 13 hours, the solution achieved a 54.49% reduction in emissions compared to the baseline. This demonstrates that simultaneously evaluating both building design and system variables yields an energy-environmental performance improvement of only 1% compared to the Sequential approach; however, the true advantage lies in the significantly reduced optimization procedure time, which is nearly halved.

Subsequently, the impact of different population sizes on the computational costs of the optimization and the quality of the obtained solution was evaluated by repeating both approaches with Population Sizes set to 80 and 200. From the comparison of the results, it is evident that the increase in simulation time due to the higher Population Size is much more significant in the case of the sequential approach. However, the sequential approach demonstrates better performance in terms of percentage reduction in emissions when using the

maximum population size, achieving an improvement of 1% over the Integrated approach. Therefore, it can be concluded that for such a minimal improvement in the performance of the proposed design compared to the baseline, the additional 13 hours required to complete the Sequential procedure may not be justified.

Certain optimization variables have a significantly greater impact on the overall performance of the building compared to others. To better understand this phenomenon, the relative and absolute frequencies of some key variables were analyzed in Phases 1 and 2 of the Sequential approach, as well as in the Integrated approach. This analysis was conducted on the entire Population of 100, excluding solutions with unmet setpoint hours exceeding 300, as well as within a 1% neighborhood of the optimal solution. The results demonstrated that the WWR on the four facades, particularly on the South facade, significantly influence the building's energy performance. Consequently, once the algorithm identifies the optimal value for this variable, it maintains it consistently across different generations of solutions. This is evidenced by the high relative frequency both in the whole population and in the vicinity of the optimal solution (75% and 90% respectively for the South facade). In contrast, the solar transmittance of shading elements was found to have a less significant impact on the overall emissions of the building. This is indicated by the non-negligible relative frequency for values different from the optimal ones selected, suggesting a lesser influence on the global energy performance. Indeed, for the entire population, the optimal values of 0.8 and 0.75 for this parameter have relative frequencies of 20%, which increase to 28% and 25%, respectively, within the neighborhood.

An analogous analysis was also conducted on the types of HVAC systems associated with the different groups of rooms in which the building was divided according to ASHRAE 90.1. It was observed that the type of HVAC system adopted on the first and second floors has the greatest impact on the overall emissions of the building, both in the Sequential and Integrated Optimizations. In the latter, the relative frequency of the optimal value is 30% for the entire population and 100% within the neighborhood. However, in this approach, the ground floor's importance was also significant. This is because, by simultaneously considering passive and active parameters, the optimization algorithm seeks to balance the positive and negative effects of these variables, leading to combinations of variable values that minimize overall emissions.

The initial design phases require the designer to be able to select alternatives that maximize the building's performance. Therefore, implementing a Simulation Based Optimization Method that targets an energy-environmental parameter, as done in this thesis, is a valid approach as it allows the generation of a vast range of valid design alternatives and suggests the optimal one. However, it is also necessary to consider the economic impact of the optimal solution since it is a fundamental driver in the designer's decision-making process. This necessity led to a post-processing analysis of the design alternatives suggested by the two NSGA-II algorithm approaches to calculate the Global Cost as defined in equation 7.1. This analysis highlighted that, regarding building envelope variables, lower WWR values correspond not only to better energy performance of the building and, therefore, lower CO_2 emissions compared to the baseline, but also to a reduced global cost due to the lower investment associated with the purchase and installation of fenestration components. For example, the optimal result of Phase 1 of the Sequential Optimization shows a $CO2$ emission reduction of 12.77% compared to the baseline, with an investment cost of 396.3 €/m^2, against 710.1 €/m^2 for the worst case solution provided by the algorithm, which only achieved a 4.00% reduction compared to the baseline. Regarding the economic impact of HVAC systems, each tested system and each of the three selected HVAC zones corresponds to different investment costs and generated consumption. The latter has a more significant impact on the variability of global cost results during the optimization of installed systems since they correspond to different performances. Additionally, these procedures consider photovoltaic production, which varies according to the values assumed by the location and the active fraction of the shading surface. However, the comparison between the solution with the maximum global cost from the Sequential approach and that from the Integrated approach revealed that the most significant impact on this economic parameter is not due to the active components of the HVAC systems or the photovoltaic system but solely to the characteristics of the building envelope considered in the economic analysis, particularly the WWR. Among the two analyzed solutions, the Sequential approach one results in a greater percentage reduction in CO_2 emissions compared to the integrated approach due to the lower WWR values and the more favorable photovoltaic system location. Furthermore, when analyzing the investment costs separately for the building envelope and the plant components, it is noted that the latter has a more significant impact

in the solution derived from the Sequential Optimization compared to the Integrated Optimization. Despite this, the overall Capex is higher for the latter due to higher WWR values, which lead to an overallincrease of about 200 €/m^2 compared to the solution with the maximum global cost derived from the Sequential Optimization.

Finally, the results of the two optimization approaches and the associated sensitivity analysis have identified two optimal combinations of optimization parameters for the building under consideration, as highlighted in Tab.7.16, which are called Best Case Solutions. It is evident from the sensitivity analysis that to maximize the building's performance, it is necessary to install a photovoltaic system on the South-West slope of the roof with an inclination angle of 40° and maximize the active solar collection area. Additionally, the DOAS with VRF HVAC system has proven to be the most suitable for the building's needs, ensuring an optimal balance between heating and cooling demand and thus minimizing emissions. However, certain difference elements have been identified, such as the WWR and the solar transmittance of shading elements, which primarily influence both the percentage reduction in CO_2 emissions compared to the baseline and the overall cost of the building. A comparison between the best case solutions obtained from the post-processing of the optimal solutions obtained from Sequential and Integrated Optimization revealed a difference of approximately 1% in the percentage reduction of emissions in favor of Sequential Optimization (56.58% versus 57.79%). Considering that the HVAC system type and the properties of the photovoltaic system are identical between the two and consistent with those previously defined, this difference is simply attributed to the fact that the output from Phase 2 of Sequential Optimization provides passive building parameter values that were previously optimized during Phase 1 of the same approach. This optimization led to associating lower values with the WWR and a higher value with the solar transmittance with respect to the ones associated with the Integrated Optimization solution. Not only does this result in better energy and environmental performance of the building, but it also leads to a lower global cost compared to the solution suggested by the sensitivity analysis of Integrated Optimization, with values of 825.4 €/m^2 for the latter and 676.2 €/m^2 for Sequential Optimization. This kind of post processing allowing for the identification of the Best Case Solutions demonstrates the additional effectiveness of the SBOM applied on early design stages, as just a simple modification of the values of the optimal

design alternatives suggested by the optimization approaches leads to an additional improvement of the building performance. This observation, additionally, underlines the importance of the presence of a decision maker, whose role is to use its knowledge to make an adequate selection of the best design for the case study considered.

As observed, the most cost-effective approach between the Sequential and the Integrated one varies depending on the aspects considered and the goals of the study. With an intermediate Population Size of 100, the Integrated approach seems more advantageous, offering a solution better by 1% compared to that obtained with the Sequential approach, albeit in half the time. However, by improving the solutions obtained from both approaches with the optimal HVAC system, the DOAS with VRF, the passive components of the building envelope optimized in Phase 1 of Sequential Optimization allow for a reduction in emissions of 57.79%, compared to the 56.58% achieved with the passive components optimized by the Integrated approach. Nevertheless, this higher energy performance and lower global cost of the solution obtained with the Sequential approach entail an optimization time almost twice as long as the Integrated approach. In conclusion, if the designer's goal is to maximize emission reduction, the Sequential approach is preferable. However, if the high computational cost of the Sequential approach is not manageable, for instance, due to time constraints in the initial design phase, it is possible to opt for a solution that deviates by only 1% from the optimum, benefiting from a halved optimization time of 13 hours guaranteed by the integrated approach.

Bibliography

[1] *Cronologia degli eventi rilevanti sui cambiamenti climatici.* URL: `http://www.comitatoscientifico.org/temi%20CG/documents/Cronologia21.pdf`.

[2] *AR5 Synthesis Report: Climate Change 2014.* URL: `https://www.ipcc.ch/report/ar5/syr/`.

[3] *IEA, Europe: Energy Mix.* URL: `https://www.iea.org/regions/europe/energy-mix`.

[4] *IEA, Europe: Emissions.* URL: `https://www.iea.org/regions/europe/emissions`.

[5] *Integrated energy and climate change package, 2007.* URL: `https://ec.europa.eu/commission/presscorner/detail/en/IP_07_29`.

[6] *Directive 2009/28/EC of the European Parliament.* URL: `https://eur-lex.europa.eu/eli/dir/2009/28/oj`.

[7] *Renewable Energy Directive (RED 2018/2001).* URL: `https://energy.ec.europa.eu/topics/renewable-energy/renewable-energy-directive-targets-and-rules/renewable-energy-directive_en`.

[8] *European Green Deal - consilium.europa.eu.* URL: `https://www.consilium.europa.eu/it/policies/green-deal/#:~:text=Il%20Green%20Deal%20europeo%20%C3%A8%20un%20pacchetto%20di%20iniziative%20strategiche,un'economia%20moderna%20e%20competitiva.`.

[9] *Fit For 55%.* URL: `https://www.consilium.europa.eu/it/policies/green-deal/fit-for-55/`.

[10] *EU Taxonomy for sustainable activities.* URL: `https://finance.ec.europa.eu/sustainable-finance/tools-and-standards/eu-taxonomy-sustainable-activities_en`.

[11] *UNCC - Carbon Pricing Information.* URL: https://unfccc.int/about-us/regional-collaboration-centres/the-ciaca/about-carbon-pricing#What-is-Carbon-Pricing?-.

[12] *EU Emissions Trading System (EU ETS).* URL: https://climate.ec.europa.eu/eu-action/eu-emissions-trading-system-eu-ets_en.

[13] *Carbon Border Adjustment Mechanism.* URL: https://taxation-customs.ec.europa.eu/carbon-border-adjustment-mechanism_en.

[14] *2019 Global Status Report for Buildings and Construction, IEA.* URL: https://iea.blob.core.windows.net/assets/3da9daf9-ef75-4a37-b3da-a09224e299dc/2019_Global_Status_Report_for_Buildings_and_Construction.pdf.

[15] Jan L. M. Hensen and Roberto Lamberts. *Building Performance Simulation For Design and Operation.* Spoon Press, 2011.

[16] *Energy Performance of Buildings, 15 December 2021.* URL: https://ec.europa.eu/commission/presscorner/detail/en/fs_21_6691.

[17] *IEA, Energy Systems: Buildings.* URL: https://www.iea.org/energy-system/buildings.

[18] *Energy Performance of Buildings Directive (EPBD 2018/844).* URL: https://energy.ec.europa.eu/topics/energy-efficiency/energy-efficient-buildings/energy-performance-buildings-directive_en.

[19] *Nearly zero-energy buildings.* URL: https://energy.ec.europa.eu/topics/energy-efficiency/energy-efficient-buildings/nearly-zero-energy-buildings_en.

[20] *Decreto legislativo del 19/08/2005 n. 192.* URL: https://def.finanze.it/DocTribFrontend/getAttoNormativoDetail.do?ACTION=getSommario&id=%7B49DF617F-4D10-4BD0-AB5F-E79DFCD2B611%7D.

[21] *Decreto Ministeriale 26 giugno 2015.* URL: https://www.mimit.gov.it/index.php/it/normativa/decreti-interministeriali/decreto-interministeriale-26-giugno-2015-adeguamento-linee-guida-nazionali-per-la-certificazione-energetica-degli-edifici.

[22] *Decreto Legislativo 311/2006.* URL: https://www.bosettiegatti.eu/info/norme/statali/2006_0311.htm.

[23] *Superbonus 110%.* URL: https://www.agenziaentrate.gov.it/portale/superbonus-110%25.

[24] Tom Hootman. *Net Zero Energy Design: A Guide For Commercial Architecture.* John Wiley Sons, Inc., 2013.

[25] Picco Marco, Lollini Roberto, and Merengo Marco. "Towards energy performance evaluation in early design stage building design: A simplification methodology for commercial building models". In: *Energy and Buldings* 76 (2014) (2014), pp. 497–505. DOI: http://dx.doi.org/10.1016/j.enbuild.2014.03.016.

[26] John Boeker et al. *The Integrative Design Guide to Green Building: Redefining the practice of sustainability.* John Wiley Sons, Inc., 2009.

[27] *La progettazione dell'opera pubblica e l'affidamento del relativo incarico.* URL: https://www.studiopetrillo.com/lavori-pubblici/rup/rup-03.pdf.

[28] *Decreto Legislativo. n. 163 del 2006.* URL: https://www.bosettiegatti.eu/info/norme/statali/2006_0163.htm#093.

[29] *Computo Metrico Estimativo.* URL: https://biblus.acca.it/computo-metrico-estimativo/.

[30] AIA National | AIA California Council. *Integrated Project Delivery: A Guide.* 2007.

[31] *Piano Nazionale di Ripresa e Resilienza (PNRR).* URL: https://temi.camera.it/leg19/pnrr.html.

[32] *Nuovo Codice Appalti D. Lgs. 36/2023.* URL: https://www.bosettiegatti.eu/info/norme/statali/2023_0036.htm.

[33] *EU Taxonomy: Climate Risk Assessment.* URL: https://ec.europa.eu/sustainable-finance-taxonomy/activities/activity/350/view.

[34] *Do Not Significant Harm Criteria.* URL: https://eur-lex.europa.eu/legal-content/IT/TXT/PDF/?uri=OJ:C_202300111.

[35] *Representative Concentration Pathway 8.5 (RCP).* URL: https://www.climatewatchdata.org/pathways/scenarios/199#:~:text=In%20order%20to%20investigate%20a,as%20against%20the%20360%20ppm.

[36] Jan L. M. Hensen. "Towards more effective use of building performance simulation in design". English. In: *7th International Conference on Design Decision Support Systems in Architecture and Urban Planning*. Ed. by J.P. Leeuwen, van and H.J.P. Timmermans. 7th International Conference on Design amp; Decision Support Systems in Architecture and Urban Planning, DDSS 2004 ; Conference date: 03-07-2004 Through 05-07-2004. Technische Universiteit Eindhoven, 2004.

[37] Tobias Maile, Martin Fiscer, and Vladimir Bazjanac. "Building Energy Performance Simulation Tools - a Life-CYcle and Interoperable Perspective". In: *CIFE Working Paper* WP107 (2007). DOI: `https://www.researchgate.net/publication/237621385_Building_Energy_Performance_Simulation_Tools_-_a_Life-Cycle_and_Interoperable_Perspective`.

[38] Sébastien Doutreloup et al. "Historical and future weather data for dynamic building simulations in Belgium using the regional climate model MAR: typical and extreme meteorological year and heat waves". In: *Earth System Science Data* 14 (2022), pp. 3039–3051. DOI: `https://doi.org/10.5194/essd-14-3039-2022`.

[39] Shady Attia et al. "Selection criteria for building performance simulation tools: contrasting architects' and engineers' needs". In: *Journal of Building Performance Simulation* (2011), pp. 1–15. DOI: `http://dx.doi.org/10.1080/19401493.2010.549573`.

[40] AIA. *An Architect's Guide to Integrating Energy Modeling in the Design Process.* 2012.

[41] *EnergyPlus Version 22.2.0 Documentation.*

[42] *DesignBuilder.* URL: `https://designbuilder.co.uk/software/product-overview`.

[43] *TRNSYS: Transient System Simulation Tool.* URL: `http://www.trnsys.com/`.

[44] Joana Sousa. "Energy Simulation Software for Buildings: Review and Comparison". In: 14 (1993). DOI: `https://doi.org/10.1177/014362449301400302`.

[45] *APACHE/IES.* URL: `https://www.iesve.com/software/apache`.

[46] Liwei Web and Kyosuke Hiyama. "A reveiw: simple tools for evaluating the energy performance in early design stages". In: *Procedia Engineering* 146 (2016), pp. 32–39. DOI: https://doi.org/10.1016/j.proeng.2016.06.349.

[47] Elbeltagi Emad et al. "Visualized strategy for predicting buildings energy consumption during early design stage using parametric analysis". In: *Journal of Building Engineering* (2017). DOI: http://dx.doi.org/10.1016/j.jobe.2017.07.012.

[48] Maria Ferrara, Fabrizio Dabbene, and Enrico Fabrizio. "Optimization Algorithms Supporting The Cost-Optimal Analysis: The Behavior of PSO". In: *Building Simulation* (2017), pp. 1418–1427. DOI: https://doi.org/10.26868/25222708.2017.357.

[49] Osman Özkaraca. "A Review on Usage of Optimization Methods in Geothermal Power Generation." In: *Mugla Journal of Science and Technology* 80 (2018), pp. 130–136. DOI: http://dx.doi.org/10.22531/muglajsci.437340.

[50] Guohua Wu, Rammohan Mallipeddi, and Ponnuthurai Nagaratnam Suganthan. "Ensemble strategies for population-based optimization algorithms – A survey". In: *Swarm and Evolutionary Computation* 44 (2019), pp. 695–711. DOI: https://doi.org/10.1016/j.swevo.2018.08.015.

[51] Xin-She Yang. *Stochastic Algorithm*. Morgan Kaufmann, 2014.

[52] Ioannis Giagkiozis, Robin C. Purshouse, and Peter J. Fleming. "An overview of population-based algorithms for multi-objective optimisation". In: *International Journal of System Science* (2013). DOI: 10.1080/00207721.2013.823526.

[53] *Multi-objective optimization*. URL: https://en.wikipedia.org/wiki/Multi-objective_optimization.

[54] Zhengxuan Liu et al. "Artificial intelligence powered large-scale renewable integrations in multi-energy systems for carbon neutrality transition: Challenges and future perspectives". In: *Energy and AI* 10 (2022). DOI: https://doi.org/10.1016/j.egyai.2022.100195.

[55] *MathWorks: What is the Genetic Algorithm?* URL: https://www.mathworks.com/help/gads/what-is-the-genetic-algorithm.html.

[56]   Viviane De Buck et al. "Multi-objective optimisation of chemical processes via improved genetic algorithms: A novel trade-off and termination criterion". In: *Computer Aided Chemical Engineering* 46 (2019), pp. 613–618. DOI: https://doi.org/10.1016/B978-0-12-818634-3.50103-X.

[57]   Larry Brackney et al. *Building Energy Modeling with OpenStudio: A Practical Guide for Students and Professionals.* Springer, 2018.

[58]   Negendahl Kristoffer and Rammer Nielsen Toke. "Building energy optimization in early design stages: A simplified method". In: *Energy and Buildings* 105 (2015) (2015), pp. 88–99. DOI: http://dx.doi.org/10.1016/j.enbuild.2015.06.087.

[59]   Bhargav Gadhvi, Vimal Savsani, and Vivek Patel. "Multi-Objective Optimization of Vehicle Passive Suspension System Using NSGA-II, SPEA2 and PESA-II". In: *Procedia Technology* 23 (2016), pp. 361–368. DOI: https://doi.org/10.1016/j.protcy.2016.03.038.

[60]   Tomás Méndez Echenagucia et al. "The early design stage of a building envelope: Multi-objective search through heating, cooling and lighting energy performance analysis". In: *Applied Energy* 154 (2015), pp. 577–591. DOI: http://dx.doi.org/10.1016/j.apenergy.2015.04.090.

[61]   *Geoportale, Comune di Torino.* URL: http://geoportale.comune.torino.it/geocatalogocoto/?sezione=mappa.

[62]   Stefano Paolo Corgnati et al. "Reference buildings for cost optimal analysis: Method of definition and application". In: *Applied Energy* 102 (2013), pp. 983–993. DOI: http://dx.doi.org/10.1016/j.apenergy.2012.06.001.

[63]   *C Factor and F Factor Construction.* URL: https://designbuilder.co.uk/helpv7.0/Content/CFactorFFactor.htm.

[64]   Minjae Shin and Jeff S. Haberl. "Thermal zoning for building HVAC design and energy simulation: A literature review". In: *Elsevier Energy and Buildings* 203 (2019). DOI: https://doi.org//10.1016/j.enbuild.2019.109429.

[65]   *What is a MERV rating? | US EPA.* URL: https://www.epa.gov/indoor-air-quality-iaq/what-merv-rating.

[66] Giacomo Chiesa et al. "Parametric Optimization of Window-to-Wall Ratio for Passive Buildings Adopting A Scripting Methodology to Dynamic-Energy Simulation." In: *MDPI Sustainability Journal* 11 (2019). DOI: https://doi.org/10.3390/su11113078.

[67] Nick Baker and Koen Steemers. "LT Method 3.0- a strategic energy-design tool for Southern Europe". In: *Energy and Buildings* 23 (1993), pp. 251–256. DOI: https://doi.org/10.1016/0378-7788(95)00950-7.

[68] Srijan Didwania, Vishal Gatg, and Jyotirmay Mathur. "Environmental performance optimization of window–wall ratio for different window type in hot summer and cold winter zone in China based on life cycle assessment". In: *Energy and Buildings* 43 (210), pp. 198–202. DOI: https://doi.org/10.1016/j.enbuild.2009.08.015.

[69] Mohammad Arif Kamal. "Shading: A Simple Technique For Passive Cooling And Energy Conservation In Buildings". In: *SUSTAINABLE ENVIRONMENT* (2011), pp. 18–23.

[70] European Solar-Shading Organization. "Solar Shading For Low Energy And Healthy Buildings". In: *ESSO Documentation* (2018).

[71] *Decreto Legislativo 8 Novembre 2021 nr. 199.* URL: https://www.normattiva.it/uri-res/N2Ls?urn:nir:stato:decreto.legislativo:2021-11-08;199.

[72] *Thermal solar plant.* URL: https://www.bosch-homecomfort.com/it/it/residenziale/informazioni/lo-sapevi-che/la-soluzione-ideale/funzionamento-impianto-solare-termico-/.

[73] *Photovoltaic effect.* URL: https://taglialabolletta.it/risparmio-energetico/effetto-fotovoltaico.

[74] Hamza Mohannad, Bafail Omer, and Alidris Hisham. "HVAC Systems Evaluation and Selection for Sustainable Office Buildings: An Integrated MCDM Approach". In: 13 (2023). DOI: https://doi.org/10.3390/buildings13071847.

[75] *About BRE.* URL: https://bregroup.com/about.

[76] *LEED Rating system.* URL: https://www.usgbc.org/leed.

[77] *LEED Certification of a building.* URL: https://www.certificazioneleed.com/edifici/.

[78] Sven Klute et al. "Steam generating heat pumps – Overview, classification, economics, and basic modeling principles". In: *Energy Conversion and Management* 299 (2024). DOI: `https://doi.org/10.1016/j.enconman.2023.117882`.

[79] *Types of Heat pumps.* URL: `https://www.ehpa.org/about-heat-pumps/types-of-heat-pumps/`.

[80] *Chiller schema|Frigomar.* URL: `https://www.frigomar.com/prodotti/chiller-unit-trifase-inverter-bldc/`.

[81] *ATW Closed Circuit Cooler.* URL: `https://www.evapco.eu/it/products/closed-circuit-coolers/atw-closed-circuit-cooler`.

[82] *Daikin Altherma HPC.* URL: `https://www.daikin.it/content/dam/DACI-Internet/Download/Riscaldamento/Altherma%20HP%20Convector.pdf`.

[83] *Wallacei: Evolutionary Engine for Grasshopper3D.* URL: `https://www.wallacei.com`.

[84] Kalyanmoy Deb et al. "A Fast and Elitist Multiobjective Genetic Algorithm: NSGA-II". In: *IEEE TRANSACTIONS ON EVOLUTIONARY COMPUTATION* 6.2 (2002).

[85] *Italy - Countries Regions - IEA.* URL: `https://www.iea.org/countries/italy/efficiency-demand`.

[86] Maria Ferrara et al. "EDeSSOpt – Energy Demand and Supply Simultaneous Optimization for cost-optimized design: Application to a multi-family building". In: *Applied Energy* 236 (2019), pp. 1231–1248. DOI: `https://doi.org/10.1016/j.apenergy.2018.12.043`.

[87] *Prezzi ARERA maggior tutela.* URL: `https://www.facile.it/energia-luce-gas/tag/tariffe-arera.html`.

[88] Camera di Commercio Industria Artigianato E Agricoltura di Torino. *Prezzario delle Opere Edili ed Impiantistiche sulla piazza di Torino Numero 32, Dicembre 2023.* 2023.

[89] DEI - Tipografia del Genio Civile. *Prezzi informativi per l'edilizia Impianti Tecnologici 2° Semestre 2021.* 2021.

[90] DEI - Tipografia del Genio Civile. *Prezzi informativi per l'edilizia Impianti Tecnologici Luglio 2020.* 2020.
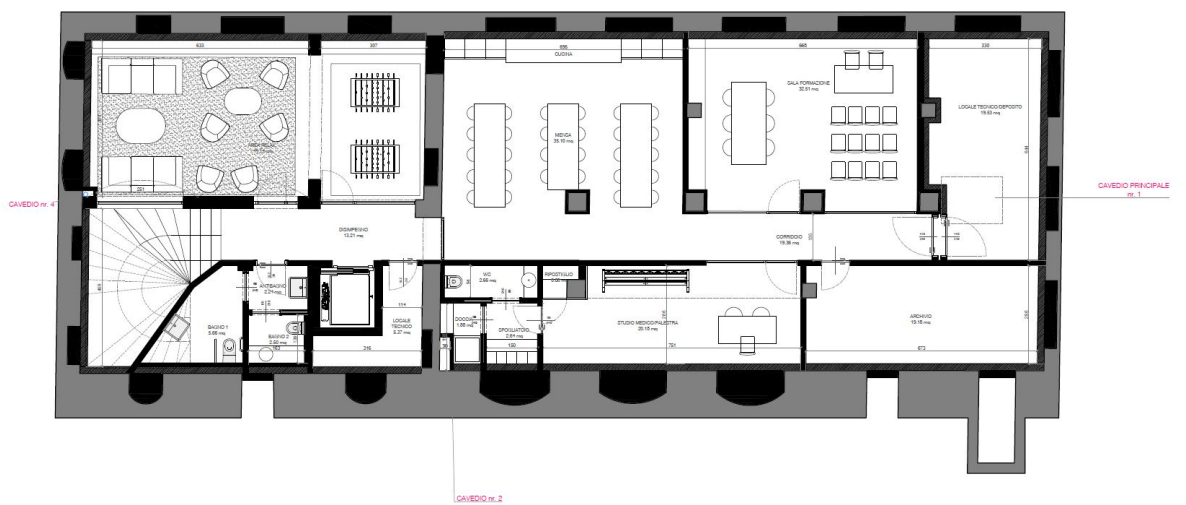
[91]   *Baseboard Electric Price*. URL: https : / / www . angi . com / articles /
        baseboard-heater-cost.htm.

Appendix

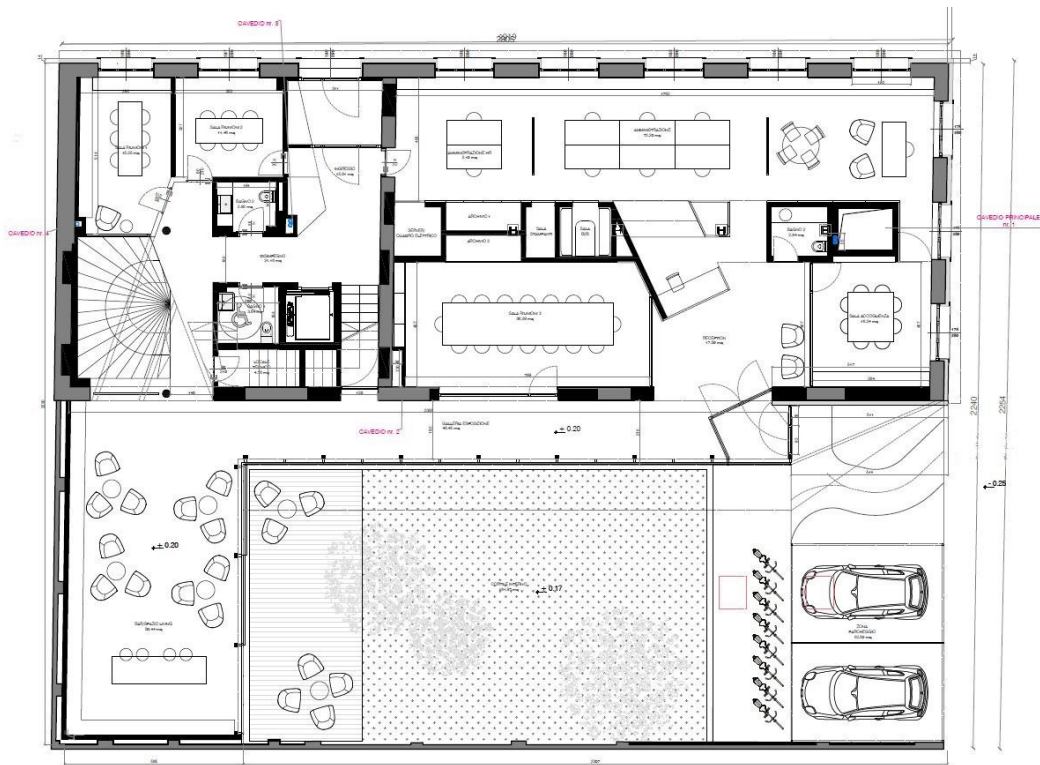

Figure 8.1: Below Ground Floor Plant.

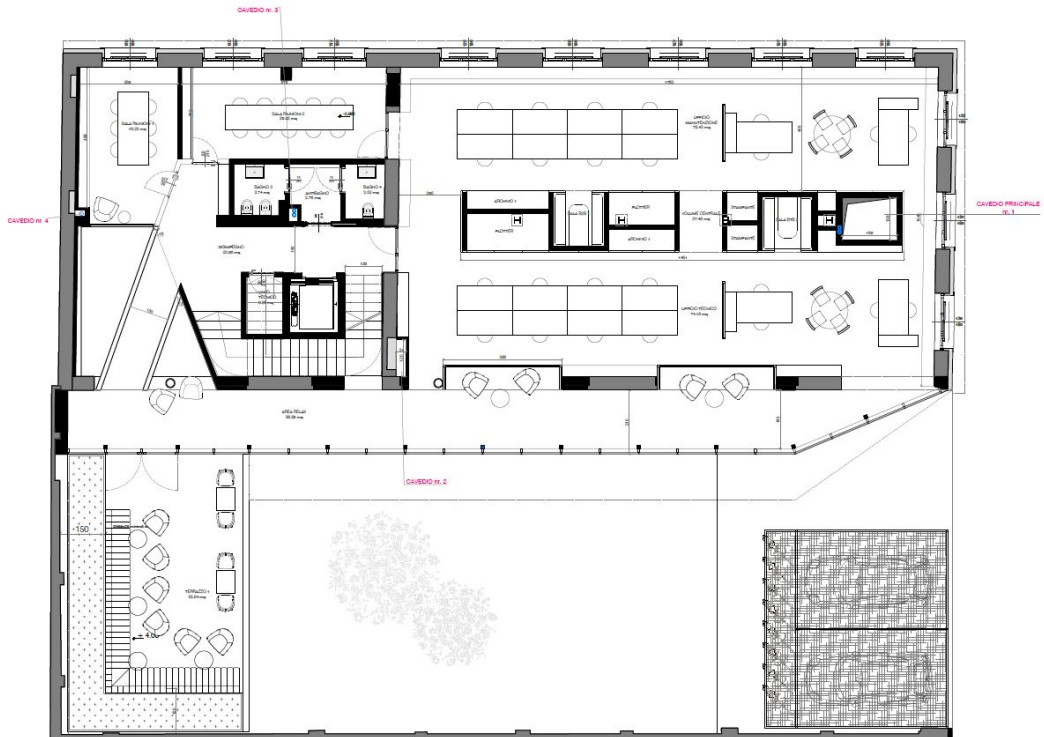**Figure 8.2:** Ground Floor Plant.

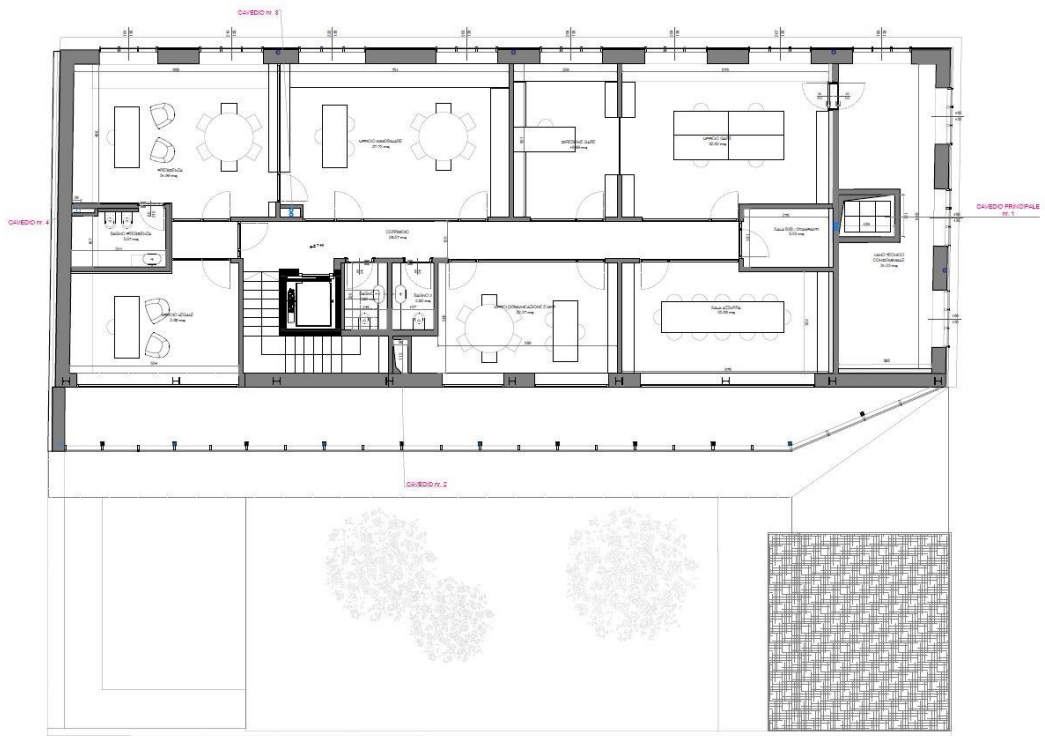**Figure 8.3:** First Above Ground Floor Plant.
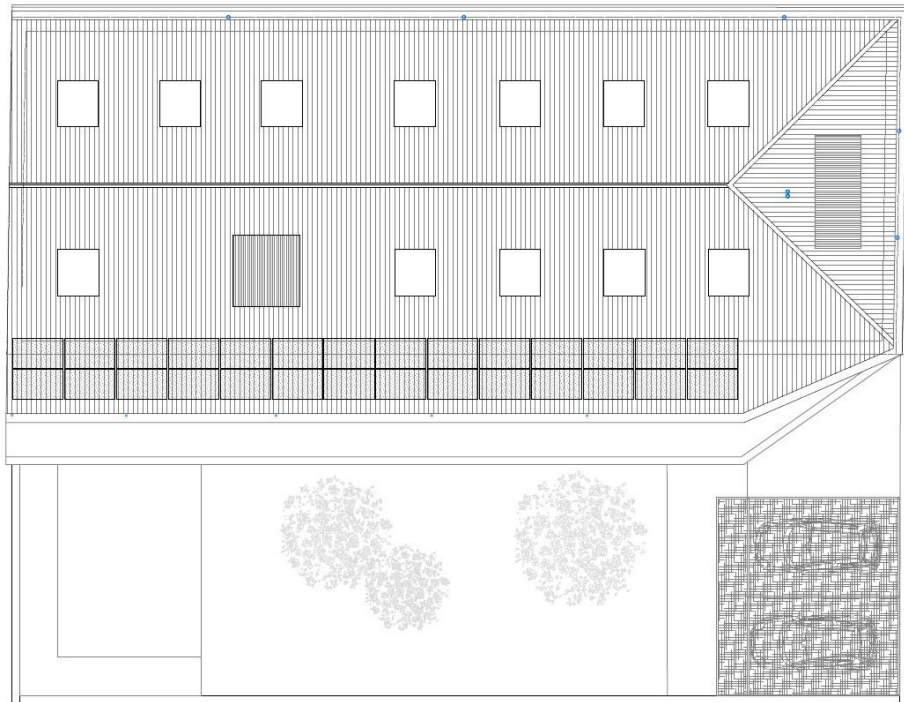
Figure 8.4: Second Above Ground Floor Plant.
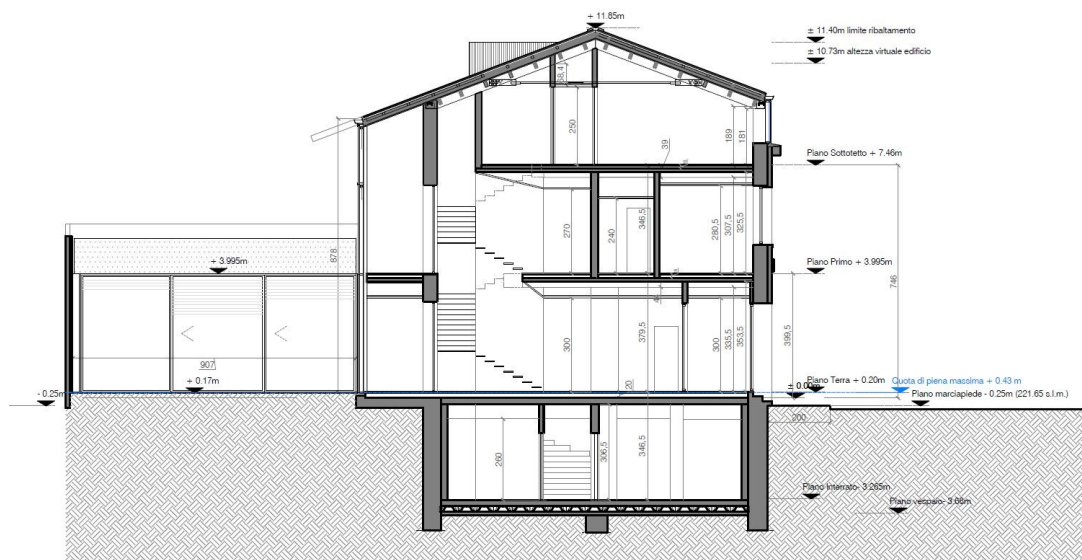
Figure 8.5: Roof.
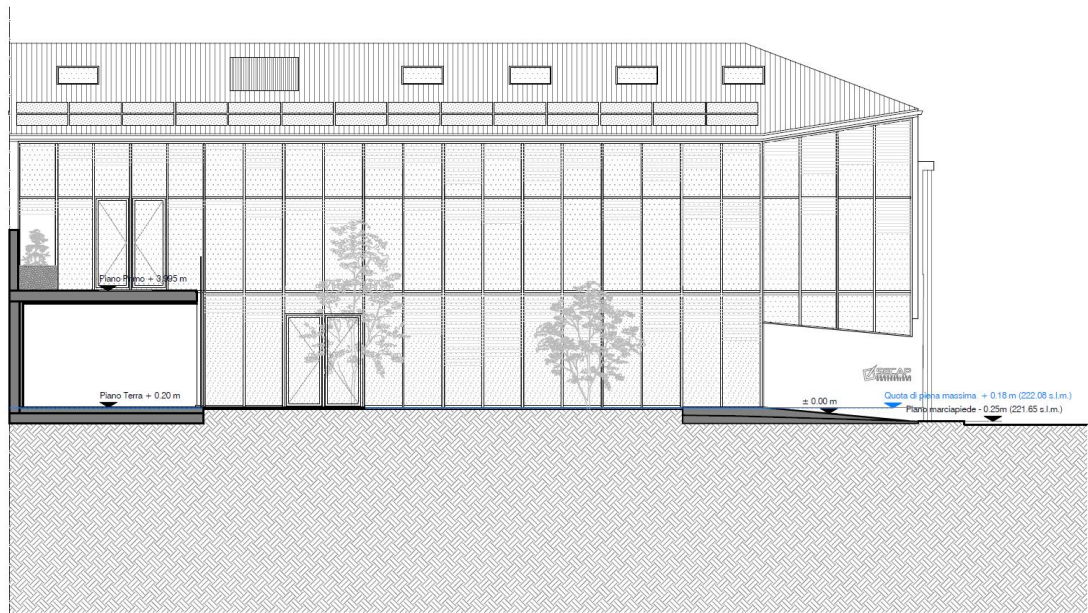

Figure 8.6: Section AA.
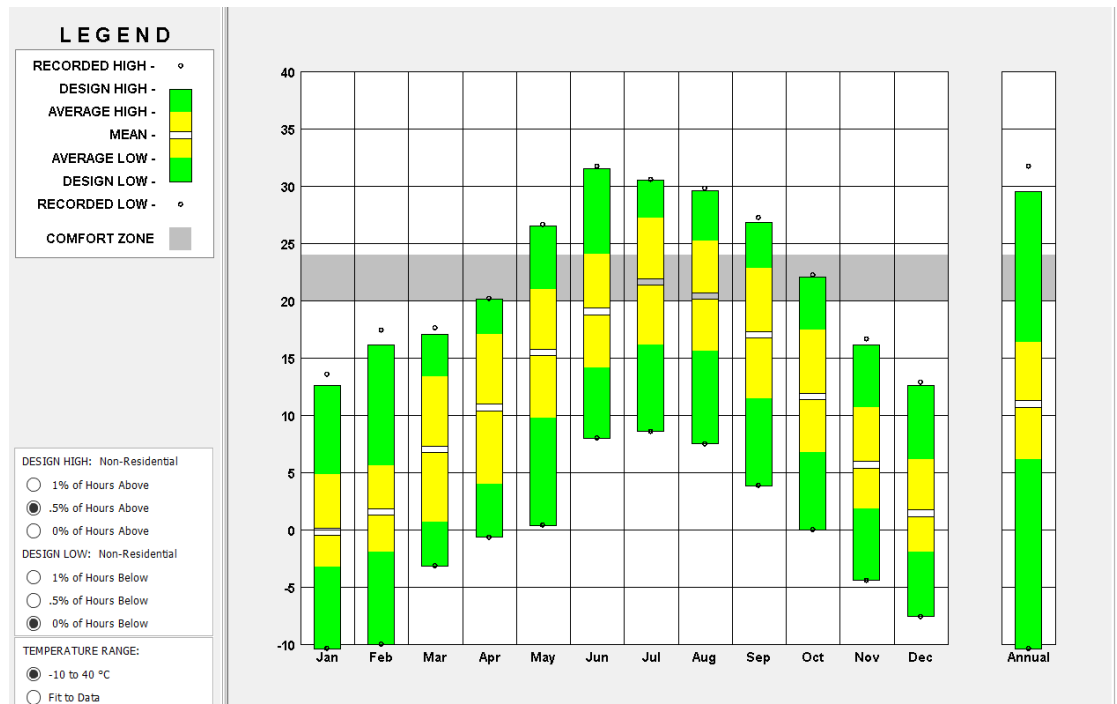
Figure 8.7: Section BB.

Figure 8.8: Temperature ranges for the case study location, Climate Consultant 6.0.
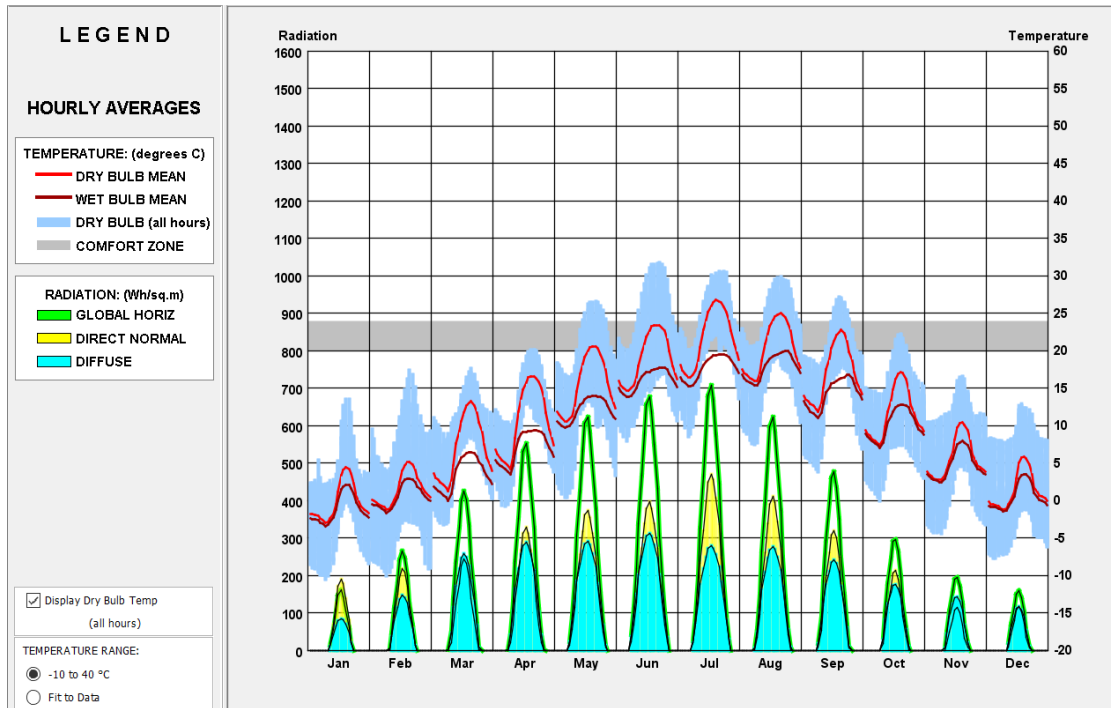
Figure 8.9: Dry bulb temperature and solar radiation component trends, Climate Consultant 6.0.

Table 8.1: Below-Grade floor HVAC system: IAQ Calculation method, baseline building model.

Q_{op}(Open Space Offices)	$0.011 \ m^3/(sec \cdot pers.)$
Occupation rate	$0.061354 \ pers./m^2$
Floor Area	$280 \ m^2$
Outdoor airflow rate - IAQ	$188.97 \ /s$

Table 8.2: Below-Grade floor HVAC system: Ventilation Rate calculation method, baseline building model.

R_p	$2.5 \ l/(sec \cdot pers.)$
P_z	$0.061354 \ pers./m^2$
R_a	$0.3 \ l/(sec \cdot m^2)$
Zone floor area, perimeter zone	$0 \ m^2$
Zone floor area, internal zone	$280 \ m^2$
V_{bz}, perimeter zone	$0 \ l/sec$
V_{bz}, core zone	$126.95 \ l/sec$
E_z	0.8
V_{oz}, perimeter zone	$0 \ l/sec$
V_{oz}, core zone	$158.685 \ l/sec$
V_{ot}	$158.685 \ l/sec$

Table 8.3: Ground floor HVAC system: IAQ Calculation method, baseline building model.

Q_{op} (Open Space Offices)	$0.011\ m^3/(sec \cdot pers.)$
Occupation rate	$0.061354\ pers./m^2$
Floor Area	$419.4\ m^2$
Outdoor airflow rate - IAQ	$283.05\ l/s$

Table 8.4: Ground floor HVAC system: Ventilation Rate calculation method, baseline building model.

R_p	$2.5\ l/(sec \cdot pers.)$
P_z	$0.061354\ pers./m^2$
R_a	$0.3\ l/(sec \cdot m^2)$
Zone floor area, perimeter zone	$348\ m^2$
Zone floor area, internal zone	$71.4\ m^2$
V_{bz}, perimeter zone	$157.78\ l/sec$
V_{bz}, core zone	$32.37\ l/sec$
E_z	0.8
V_{oz}, perimeter zone	$197.22\ l/sec$
V_{oz}, core zone	$40.47\ l/sec$
V_{ot}	$237.69\ l/sec$

Table 8.5: First and Second floor HVAC system: IAQ Calculation method, baseline building model.

Q_{op} (Open Space Offices)	$0.011\ m^3/(sec \cdot pers.)$
Occupation rate	$0.061354\ pers./m^2$
Floor Area	$730.8\ m^2$
Outdoor airflow rate - IAQ	$493.21\ l/s$

Table 8.6: First and Second floor HVAC system: Ventilation Rate calculation method, baseline building model.

R_p	2.5 $l/(sec \cdot pers.)$
P_z	0.061354 $pers./m^2$
R_a	0.3 $l/(sec \cdot m^2)$
Zone floor area, perimeter zone	588 m^2
Zone floor area, internal zone	142.8 m^2
V_{bz}, perimeter zone	266.59 l/sec
V_{bz}, core zone	64.74 l/sec
E_z	0.8
V_{oz}, perimeter zone	333.24 l/sec
V_{oz}, core zone	80.93 l/sec
V_{ot}	414.17 l/sec

Table 8.7: Pressure Drop Adjustment and Design Airflow Rate through devices: Below-Grade Floor, baseline building model.

	Return and/or exhaust airflow control devices	Particulate Filtration Credit: MERV 13
$PD\ [Pa]$	125	225
$L/s_D\ [l/s]$	650.48	780.58

Table 8.8: Pressure Drop Adjustment and Design Airflow Rate through devices: Ground Floor, baseline building model.

	Return and/or exhaust airflow control devices	Particulate Filtration Credit: MERV 13
$PD\ [Pa]$	125	225
$L/s_D\ [l/s]$	2650	3180

Table 8.9: Pressure Drop Adjustment and Design Airflow Rate through devices: First and Second Floor, baseline building model.

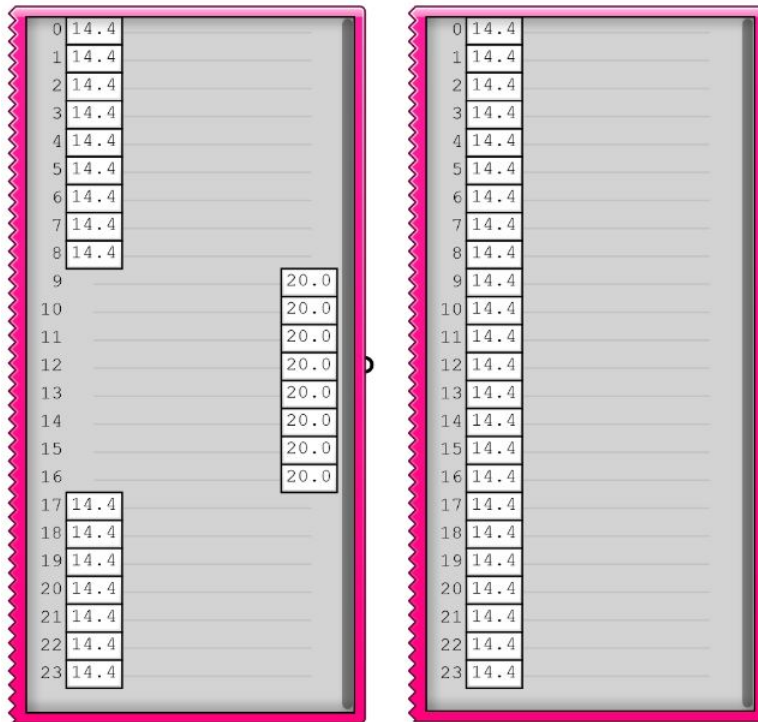|	Return and/or exhaust airflow control devices	Particulate Filtration Credit: MERV 13
$PD\ [Pa]$	125	225
$L/s_D\ [l/s]$	5399.12	6478.94

Figure 8.10: Winter temperature setpoint and setback schedules for working (on the left) and non-working days (on the right).
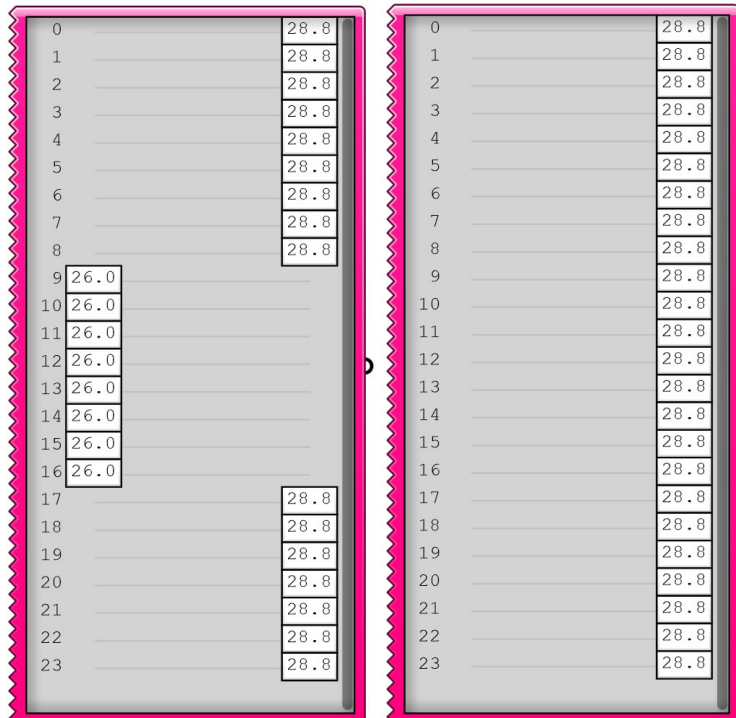

Figure 8.11: Summer temperature setpoint and setback schedules for working (on the left) and non-working days (on the right).
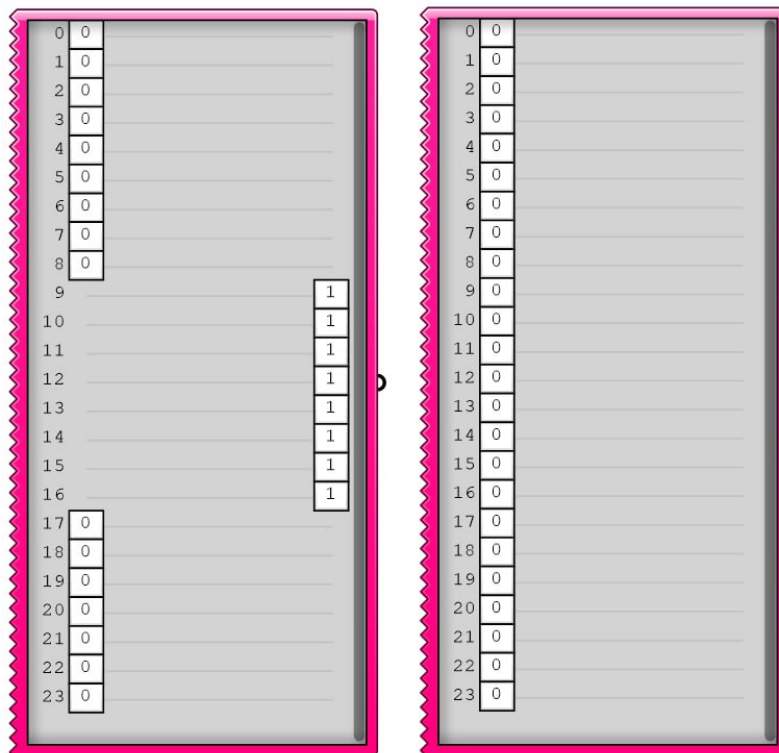
Figure 8.12: Fans availability schedules on working (on the left) and non-working days (on the right).

Ringraziamenti

Al termine del mio percorso di studi, desidero esprimere la mia più sincera gratitudine a tutte le persone che hanno contribuito a rendere possibile questo importante traguardo.

In primo luogo, un sentito ringraziamento va al Prof. Enrico Fabrizio, per il supporto fornito durante questi mesi e per l'opportunità che mi ha dato di essere il mio relatore in questo progetto a conclusione del mio percorso di studi magistrale. La sua guida e i suoi preziosi suggerimenti sono stati fondamentali per la realizzazione di questo lavoro.

Desidero inoltre ringraziare Elisa, Daniele e Teodoro per avermi guidato nella realizzazione del progetto e per la fiducia che avete riposto in me sin dall'inizio. Il vostro incoraggiamento e i vostri consigli sono stati indispensabili per il successo di questo lavoro. Un ringraziamento speciale va anche a tutto il team di GET Consulting per avermi accolta calorosamente e per avermi fatto sentire parte del gruppo da subito. Le nostre pause caffè e pause pranzo sono state momenti preziosi che hanno reso l'esperienza di realizzazione della tesi in azienda più piacevole e arricchente.

Non avrei mai potuto raggiungere questo traguardo senza il sostegno incondizionato della mia famiglia. Nei non pochi momenti complicati degli ultimi mesi siete stati fondamentali, mi avete sempre spronato a resistere ed a completare il lavoro, nonostante tutte le difficoltà. Voglio ringraziarvi per aver sempre creduto in me, per avermi fatto capire cosa significhi la parola sacrificio e di avermi trasmesso il coraggio di raggiungere i miei obiettivi, nonostante questi spesso mi abbiano portato lontana da voi. Mamma e papà, so quanto è stato difficile per voi durante il periodo di erasmus sapere che mi trovassi così distante da casa e sola, in un luogo così lontano da quello che era ormai diventata la nostra città di comfort, Torino. Voglio ringraziarvi perchè nonostante tutte le vostre paure, non mi avete mai fatto sentire sola. Mi scuso perchè so già che in futuro ricapiterà di dover stare lontana da voi, ma spero solo che questo rappresenti un'occasione per voi per viaggiare e sognare assieme a me. Mamma, grazie per essere sempre stata la mia roccia in questi anni e per essere sempre stata presente fisicamente nei momenti più complicati. Papà, grazie per essere stato il primo a spronarmi ad andar via di casa per studiare, nonostante quello che significhi per te. Nico, grazie perchè mi hai sempre accolta a braccia aperte tornata a casa, e grazie perchè mi ricordi

sempre quanto possa essere difficile affrontare l'università e quanto sia bello farcela nonostante tutto. Grazie infinitamente per il sostegno che tutti voi mi avete dato, siete e sarete per sempre la mia casa, la cosa più importante per me, anche a chilometri di distanza.

Durante gli ultimi due anni di laurea magistrale, ho avuto il piacere di incontrare qualcuno che, nonostante inizialmente fosse per me una persona di cui fidarsi solo ed unicamente per i progetti di gruppo, si è pian piano trasformato in qualcosa di più. Emanuele, voglio ringraziarti per essere stato il collega che non ho mai avuto, ed il ragazzo che ho sempre desiderato. Ti ringrazio per avermi fatto capire cosa signifchi sostenersi a vicenda e confrontarsi, non soltanto in ambito accademico. Grazie per aver sempre provato a starmi vicino, anche nei momenti in cui non avrei voluto nessuno con me, e grazie perchè la distanza tra di noi non ha mai contato nulla.

Un ringraziamento importante va a Torino: come per Nietzsche sei stata per me "*Il primo posto dove io sono possibile*", e poi, come si dice, Torino vera capitale. Questa città è stata la mia culla, e mi ha dato l'opportunità di incontrare Tiffany, Francesco e Pia. Siete stati la mia seconda famiglia qui, mamma, papà e sorella. Voglio ringraziare Tiffany perchè, sin dal primo giorno a Casa Montecucco, mi hai guidato e consigliato ed insegnato a vivere da "fuorisede", e grazie perchè so di poter sempre contare sui tuoi consigli da mamma chioccia quando ne ho di bisogno. Grazie a Francesco, per avermi sempre ricordato che l'università non è la vita. E grazie a Pia, sei stata come una sorella e anche se ormai da due anni (sì, due anni) non siamo più coinquiline, tu sarai sempre la mia coinquilina del cuore, e Corso De Gasperi sarà sempre casa nostra.

Infine, voglio ringraziare me stessa, per essere la persona più testarda e più determinata che conosca. Grazie alla versione di me che sono diventata in questi anni: nonostante il voler sempre di più da me stessa sia spesso stato distruttivo, questo mi ha permesso di crescere e di comprendere che se voglio qualcosa e se questa dipende dalle mie sole forze, posso sempre raggiungerla. Mi auguro di non cambiare mai, e nonostante spesso in questo anno io abbia avuto dei momenti di totale apatia, spero di non dovermi mai più sentire così, e di essere per sempre piena di energie e voglia di fare, di mantenere la tenacia che mi ha sempre contraddistinta e che mi ha portato a superare tutte le difficoltà che la vita mi ha messo davanti.